



Stony Brook University



## NASA Student Launch Initiative

2019-2020 Critical Design Review Report

October 31, 2019



Stony Brook University  
113 Light Engineering Building  
Stony Brook, New York 11794-2300



## Table of Contents

1	Summary of CDR Report.....	7
1.1	Team Summary .....	7
1.2	Launch Vehicle Summary.....	7
1.3	Recovery System Summary .....	7
1.4	Payload Summary .....	8
2	Changes Made Since PDR .....	8
2.1	Changes Made to Vehicle Criteria .....	8
2.2	Changes Made to Payload Criteria.....	9
2.3	Changes Made to Project Plan .....	11
3	Vehicle Criteria.....	11
3.1	Design and Verification of Launch Vehicle.....	11
3.1.1	Mission Statement and Mission Success Criteria .....	11
3.1.2	Design Alternatives Chosen.....	11
3.1.2.1.	Nosecone .....	11
3.1.2.1.	Airframe .....	12
3.1.2.1.	On Board Camera System .....	13
3.1.2.1.	Variable Drag System .....	13
3.1.2.1.	Fins .....	14
3.1.3	Qualitative Design Summary & Justification .....	14
3.1.3.1.	Nosecone .....	14
3.1.3.2.	Airframe .....	15
3.1.3.1.	Bulkheads .....	20
3.1.3.1.	Fins .....	21
3.1.3.1.	Motor Retainer .....	22
3.1.3.1.	Centering Rings.....	23
3.1.3.1.	Motor Mount .....	24
3.1.3.1.	Fin Assembly.....	25
3.1.3.1.	Motor .....	26
3.1.3.1.	Camera Bay .....	27
3.1.3.1.	VDS .....	29
3.1.3.1.	VDS Electronics .....	42

3.1.3.2.	Subsystem Integration Overview .....	47
3.1.4	Design Integrity: Quantitative Analysis.....	47
3.1.4.1.	General Deflection Estimates.....	47
3.1.4.1.	Nosecone Shape Calculations .....	48
3.1.4.1.	Bearing calculations .....	49
3.1.4.2.	VDS FEA .....	49
3.1.4.3.	Fin Flutter.....	62
3.1.4.1.	Fin Torque: CFD & FEA .....	65
3.1.4.2.	Center of Pressure CFD.....	72
3.1.4.1.	Drag Coefficient (no VDS) CFD .....	75
3.1.4.1.	Drag Coefficient (VDS) CFD .....	77
3.1.4.1.	Bulkhead FEA .....	80
3.1.4.2.	Centering Ring FEA.....	82
3.1.4.3.	Airframe FEA.....	84
3.1.4.4.	Coupler FEA .....	87
3.1.4.5.	VDS Blades FEA .....	92
3.2	Subscale Flight Results .....	94
3.2.1	Subscale Design.....	94
3.2.1.1.	Scaling Factors .....	94
3.2.1.2.	Material Justification.....	95
3.2.1.3.	Variables Held Constant.....	96
3.2.1.4.	Variables Not Held Constant.....	96
3.2.2	Subscale Manufacturing.....	96
3.2.3	Launch Day Conditions .....	103
3.2.4	Subscale Flight Predictions.....	104
3.2.5	Subscale Flight Analysis.....	108
3.2.5.1.	Raw Flight Data .....	109
3.2.6	Impact of subscale launch on full scale .....	114
3.3	Recovery Subsystem .....	115
3.4	Mission Performance Predictions .....	115
3.4.1	Component Mass Breakdown.....	116
3.4.1.1.	Component Mass Breakdown .....	116

3.4.2	Simulated Motor Thrust Curve .....	118
3.4.3	Altitude Predictions (launch rail at 7.5 deg) .....	118
3.4.4	Simulated Flight Profiles (launch rail at 7.5 deg) .....	119
3.4.5	Altitude Predictions (launch rail at 10 deg) .....	121
3.4.6	Simulated Flight Profiles (launch rail at 10 deg) .....	122
3.4.7	Stability Margin, CP & CG.....	124
3.4.8	RockSim vs. OpenRocket .....	125
3.5	Recovery Subsystem .....	126
3.5.1	Drogue Parachute.....	127
3.5.2	Descent Velocity and Drift .....	127
3.5.3	Shear Pins and Ejection Charges .....	129
3.5.4	Shear Pins.....	129
3.5.5	Black Powder .....	129
3.6	Parachute Deployment .....	131
3.6.1	Pistons .....	131
3.6.2	Recovery Harness .....	132
3.6.3	Avionics Bay Requirements for Deployment .....	133
3.6.4	End Plates.....	134
3.6.5	Fittings .....	134
3.6.6	Ejection .....	135
3.6.7	Altimeters.....	136
3.7	Avionics Electronics .....	136
3.7.1	Altimeter Circuit Configuration.....	136
3.7.2	Arming Switch.....	138
3.7.3	E-Matches .....	139
3.8	Avionics Bay .....	139
3.9	Telemetry Bay .....	149
4	Payload Criteria .....	155
4.1	Tank Overview.....	155
4.2	Tank System Level Design .....	155
4.2.1	Chassis .....	155
4.2.2	Drivetrain .....	157

4.2.3	Sample Collection Scoop.....	162
4.2.4	Sample Collection Unit.....	162
4.3	Tank Electronics Design .....	163
4.3.1	Electrical Schematic and Block Diagram .....	163
4.3.2	Microcontroller .....	165
4.3.3	Motors .....	165
4.3.4	Motor Controller .....	166
4.3.5	Communications .....	166
4.3.6	Power Requirements .....	167
4.4	TEARS Overview .....	168
4.5	Reorientation .....	169
4.5.1	Connecting Rod Assembly .....	169
4.5.2	Reorientation Plate.....	174
4.6	Tank Exiting.....	179
4.6.1	Lead Screw Assembly.....	179
4.6.2	Support Collar.....	184
4.6.3	Lead Screw End Support .....	186
4.7	Tank Retention .....	187
4.8	Launch Vehicle Integration.....	189
4.8.1	Aft bulkhead and Coupler.....	189
4.8.2	Nose Cone Integration .....	193
4.9	TEARS Electronics Design.....	194
4.9.1	Electrical Schematic and Block Diagram .....	194
4.9.2	Motors .....	196
4.9.3	Motor Driver .....	197
4.9.4	Communications Equipment.....	198
4.9.5	Power Requirements .....	198
4.10	DICU Electronics and Software Design .....	199
4.10.1	Software .....	199
4.10.2	Electrical Schematic and Block Diagram .....	202

4.10.3	Microcontroller .....	203
4.10.4	Communications Equipment.....	204
4.10.5	Power Requirements .....	204
4.11	Payload Mass Total .....	205
5	Safety .....	207
5.1	Pre – Field Subsystem Preparation.....	207
5.2	Master Material Checklist .....	207
5.2.1	Structure, Aerodynamics, and Propulsion .....	207
5.2.2	Navigation and Recovery.....	209
5.2.3	Payload .....	210
5.2.4	Miscellaneous. ....	210
6	Project Plan .....	231
6.1	Testing.....	231
6.2	Requirement Compliance.....	234
6.2.1	Vehicle Derived Requirements .....	241
6.2.2	Navigation and Recovery Derived Requirements.....	241
6.3	Budget .....	242
6.4	Funding.....	247
6.5	Timeline .....	248

# 1 Summary of CDR Report

## 1.1 Team Summary

**Team Name:** Stony Brook NASA Student Launch Team

**Mailing Address:**

American Institute of Aeronautics and Astronautics  
College of Engineering and Applied Sciences  
231 Engineering Building  
Stony Brook, NY 11794-2200

**Mentor Name:** George N. George

Phone: (201) 893-0105

Email: georgesquared@yahoo.com

Level 2 Certification: TRA Member #129 | NAR Member #24025

## 1.2 Launch Vehicle Summary

The launch vehicle is made up of main sections consisting of a nose cone with telemetry housing, payload bay, avionics bay and a booster bay which incorporates the motor and fin retention system. The launch vehicle has a diameter of 6.17", length of 107", static stability margin of 2.50 cal and a mass of 47.1 lbm. The finalized motor choice includes the Aerotech L1420R-P which will propel the vehicle to a target apogee of 4500 ft. The launch vehicle will be designed to overshoot the simulated apogee and utilize the on-board variable drag system in order to accurately hit the target apogee.

Table 1: Overall Vehicle Summary

Diameter	Length	Mass	Static Stability	Official Target Apogee	Final Motor Choice
6.17"	107"	47.1 lbs	2.50 cal	4500 ft	L1420R-P

## 1.3 Recovery System Summary

The recovery system is going to be a dual deployment system, in which a drogue parachute will be deployed at apogee (4500 ft) and the main parachute will be deployed at an altitude of 600 ft. Two fully redundant altimeters in the avionics bay will allow for the system to know when to deploy the parachutes, as well as allow for a backup if one fails to function. When the rocket reaches its desired deployment points, the altimeters will produce a signal that results in an electrical match igniting black powder, which will then break the shear pins that keep the parachute bays connected to the rest of the rocket. This will deploy the chutes, which will allow for a safe and controlled descent and touchdown of the rocket.

## 1.4 Payload Summary

The payload is going to be a tank shaped rover, primary function of which is to collect a sample of simulated lunar ice. The rover will be secured inside the launch vehicle via the Tank Exiting and Reorienting System (TEARS) during the flight and recovery portions of the launch. TEARS will act as deployment mechanism to reorient rover right side up after landing and push it out through the nose cone. The entire process will be remotely controlled by our team. Once fully deployed, the rover will drive to one of the recovery areas where a scoop mechanism will be engaged. Once enough material is sampled, the rover will be driven a safe distance from the recovery area.

## 2 Changes Made Since PDR

### 2.1 Changes Made to Vehicle Criteria

Change	Reason
Total mass decreased from 49.3 lbs to 47.1 lbs.	The weight of the booster bay, avionics bay and payload bay were all lowered to have a projected apogee of roughly 5000 ft in order to give the VDS a larger range to be actuated in.
The CG of the rocket was specifically designed to be in between the bulkheads for the booster bay and avionics bay.	This allows the incorporation of ballast bays into the design. Changing out heavier bulkheads in avionics and booster bay will allow the team to more accurately hit target apogee by changing the mass of the rocket while maintaining the same stability margin.
Airframe material changed from fiberglass to carbon fiber.	Switching to carbon fiber allowed for the reduction of the launch vehicle mass by 5 lbs.
Static stability dropped from 2.52 cal to 2.50 cal.	The static stability margin will now be able to be accurately maintained utilizing fore and aft ballast bays.
Coupler sections shortened from 12" to 9"	Allowed for shaving off roughly 1 lb from the launch vehicle while still maintaining a 6" shoulder at the in-flight separation point
Thickness of Fins Changed from 0.1875" to 0.125"	Flutter analysis ensured that 0.125" thick fins are resistant to flutter with a decent margin. Thinner Fins also helped in reducing the mass of the launch vehicle.

Avionic Sled-walls added around 9V battery compartment; deeper indentation of the 9V battery into the sled; increase in sled thickness. Zip tie slot in the longitudinal direction was moved near the ends of the sled.	To better fit and further constrain the 9V battery, and to ensure it doesn't come lose due to vibrations. The zip tie holes were moved to prevent interference with the threaded rods and thus preserve structural integrity.
Piston-changed from plywood to balsa wood; wall thicknesses changed; ends of shock cord hole rounded.	Decreases weight considerably. Rounded hole more accurately depicts how the wood will be cut with a CNC machine.
Telemetry Sled-resized for selected GPS transmitter dimensions; GPS and battery compartments made into one compartment; zip tie slots around sides of sled instead of cut into the middle. Hole made in the middle for threaded rod in the nosecone for attachment. Fillets added to the sides of the sled.	The new dimensions fit the GPS tracker better constrain its movement. Compartments were merged as the transmitter came shipped with the battery strapped to the tracker. Zip tie slots were moved to the outside to preserve structural integrity. Hole was made in the middle for easier implementation inside the nosecone and for interfacing with the payload bay. Fillets were added for structural integrity.
The telemetry plates were removed from the jurisdiction of the Navigation and Recovery Team, which were replaced with a plate to fit inside the nosecone 3D printed as one piece with the telemetry sled.	In order to account for the chance that the telemetry sled could have interfered with the bolts from the Payload, the position of the telemetry sled was moved to the top plate in the nose cone, attached to the lead screw end support mount.
Change in kind of shear pin from #2 to #4	Using larger shear pins to have to drill less holes inside the airframe, and thus use less shear pins.
Avionic tube was made shorter to avoid overhang surrounding the endplates	Not essential to have the overhang.
Quick links added	Added ¼ inch quick links for ease of assembly of subsystem.
Black powder charge size increased.	Increased size to more accurately model the forces required for ejection procedure.
Ematches-Changed to Firewire Mini Initiators	The newly selected matches are pre-dipped in pyrogen and are easier and cheaper to use.
Avionics Bay End Plates-Removed end plate on the Avionic Retention Bulkplate side of the bay. Resized the other end plates.	One of the end plates in the avionics bay was redundant and was therefore removed. The thicknesses of the other wooden plates were increased such that the sum of the thicknesses of the plates remained the same.
Shock Cords-main shock cord length increased from 20 to 30ft; drogue shock cord length changed from 10ft to 20 ft.	Shock cord length was increased by 10ft for each shock cord in order to ensure the cords may withstand large ejection forces.

## 2.2 Changes Made to Payload Criteria

Change:	Justification:
Dual 6mm lead screws for deployment was reduced to a single 8mm screw	After team concerns regarding synchronization between dual lead screws to deploy the rover were supported in design reviews, it was decided to switch to a single screw for deployment. Not only

	did this change remove the need for synchronization between screws but in addition reduced the number of components thus reducing the number of potential failure points and weight of the system. In addition, despite the reduction in quantity, the single screw was changed from a 6mm screw to an 8mm screw to make up for some of the lost strength.
The payload bulk plate was changed to be a separate plate	In an effort to add redundancy to the retention of the payload system, nosecone and contained components, a dedicated payload bulkplate was introduced. This design change allows for a simplification in manufacturing by removing the need for a square hole to be cut in the coupler bulkplate, allows for the supported components to be mechanically attached to both the coupler bulkplate and through the airframe and coupler, simplified the assembly. Additionally, reduces the load supported by the coupler bulkplate as the load is designed to be supported primarily by the airframe bolts with the coupler connection designed to be a part-load bearing connection/redundancy in case of failure of the primary supports.
Support collar was introduced	A support collar was added to bear the load of the rover mass during launch and acceleration as well as during main chute deployment. This design change allows for the load to be transmitted directly to the airframe thus reducing the load supported by the reorientation and bulkplates during these stages, in addition, this design change removes the load experienced by the leadscrew while the rover is being accelerated thus drastically reducing if not removing the likelihood of bulking.
Reorientation plate assembly	In an effort to reduce the length of airframe and increase the structural integrity of the subassembly, components attached to the reorientation plate were through-mounted on the plate, this reduced the number of support components required therefore reducing modes of failure and weight while also increasing the strength.
Telemetry sled in the nosecone is integrated with the lead screw assembly	Telemetry sled now plays a dual role for housing GPS as well as acting as pillow block for the leadscrew to prevent any vibrations and support previously unsupported section of the lead screw during flight.

## 2.3 Changes Made to Project Plan

Change:	Justification:
Testing procedures and checklist have been added	As a part of the CDR requirement and feedback from NASA team, the procedures have been added to project safety and minimize risk
Funding and Budget was updated	Budget was adjusted to keep team on track and new avenues for fund raising was added

## 3 Vehicle Criteria

### 3.1 Design and Verification of Launch Vehicle



#### 3.1.1 Mission Statement and Mission Success Criteria

The SBU Space Wolves launch vehicle will be safely designed to propel the payload to an apogee of 4500 feet while ensuring that all critical subsystem perform as intended. The drogue recovery system will be deployed at apogee and the main recovery system, will be deployed at 600 ft which will allow the vehicle to land safely. The overall mission will be deemed successful if the following criteria are met:

- The launch vehicle avoids any safety risks to students, bystanders or property.
- The launch vehicle achieves the designed length of 107" to within a reasonable tolerance
- The launch vehicle achieves the designed mass of 47.1 lbs to within a reasonable tolerance
- The launch vehicle achieves a stability margin of 2.5 to within a reasonable tolerance
- The launch vehicle reaches the target apogee to within 100 ft with the deployment of the VDS
- The drogue chute will deploy successfully at apogee
- The main chute will deploy successfully at 600 ft
- The launch vehicle will land safely to within a 2,500 ft radius
- The launch vehicle will be undamaged after landing and will allow the TEARS system to safely deploy the payload

#### 3.1.2 Design Alternatives Chosen

##### 3.1.2.1. Nosecone

Conical, Von Karman, and ogive tangent nose cone profiles were heavily considered for the PDR. Since the nose cone profile in the subsonic region does not significantly affect pressure drag, it made sense to pick the profile that is the most readily available. The team also considered 3D

printing the nosecone however due to the lack of reliability, the 4:1 Ogive tangent nosecone was heavily considered for the PDR along with methods of 3D printing it. From the launches of previous years, it was clear that the print quality was not reliable, and the surface finish was questionable at best. On the other hand, the reduced cost of fiberglass nosecone on Black Friday led to team to purchase a 4:1 ogive tangent nosecone with a threaded metal tip. The internal room and the threaded tip will serve as a housing compartment for the telemetry equipment and anchoring point for both the telemetry bay and payload retention method.



Figure 1: 4:1 Ogive Tangent Nosecone

#### 3.1.2.1. Airframe

G12 Fiberglass tubing, phenolic tubing and carbon fiber tubing were considered for the PDR. Due to the tensile strength values of carbon fiber along with its superiority over phenolic and fiberglass in regard to strength to weight ratio, the team chose braided carbon fiber tubing as the primary airframe material. By purchasing the tubing directly from the manufacturer instead of a 3<sup>rd</sup> party vendor, we were able purchase the CF tubing for roughly the same price as fiberglass. Switching to carbon fiber from fiberglass also shaved off around 5 lbs of weight from the rocket.



Figure 2: Braided CF Tubing

#### 3.1.2.1. On Board Camera System

The GoPro Hero7 Silver was heavily considered for the PDR as the primary choice for the primary recording unit. Although the final design for the camera bay is different due to the cameras chosen, the mounting mechanism was heavily inspired by the design of the PDR. The GoPro Hero7 Silver cameras were replaced by the 808 #16 Keychain Cameras which weigh and cost a fraction of that of the GoPro cameras. It can record at 60 fps and take HD still pictures which will more than meet the requirements of the design



Figure 3: 808 Keychain Camera

#### 3.1.2.1. Variable Drag System

Blades actuated by a linkage system was the primary design considered for the PDR. Due to its reliability and resistance to vibrations, a similar method of actuation was chosen for the CDR. Along with inducing the maximum possible amount of drag upon deployment, the chosen design

is very lightweight when compared to its PDR counterpart.

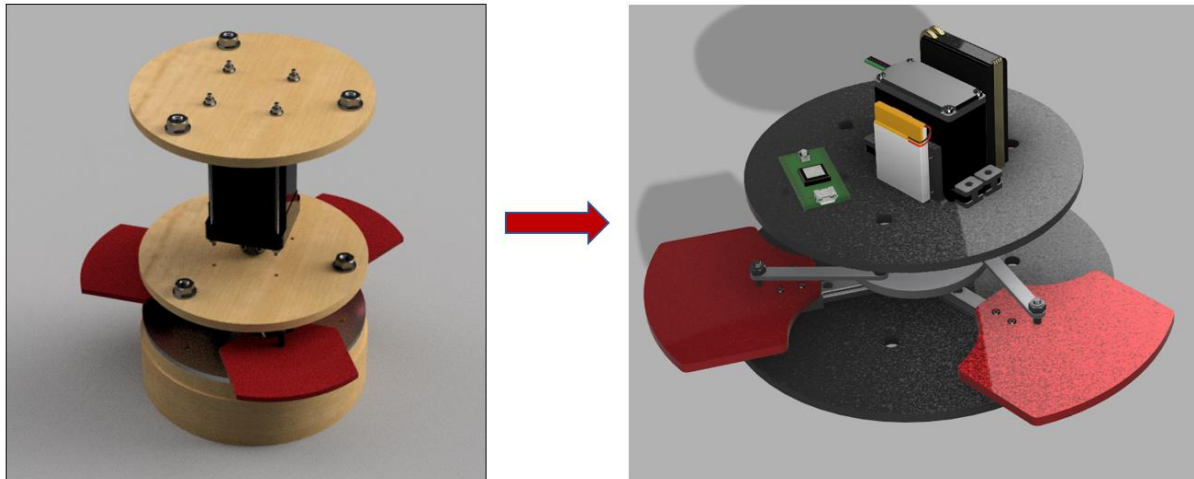


Figure 4: Transition to iterated design for VDS

#### 3.1.2.1. Fins

Various fin shapes were considered for the PDR. The trapezoidal fin profile with a trailing edge was picked due to its resistance to fracture upon landing. The resultant fin dimensions remain the same for the CDR with a change in the fin tang profile:

Table 2: Fin Dimensions

Dimension	Value
Root Chord	14 inches
Tip Chord	4.5 inches
Height	6.5 inches
Sweep Length	7 inches
Sweep Angle	47.1 degrees

### 3.1.3 Qualitative Design Summary & Justification

#### 3.1.3.1. Nosecone

The nose cone design is still the ogive tangent shape, which is a profile generated by a circle which is offset from the origin of the cone. In the subsonic region, pressure drag is negligible, which is why the drag coefficient is heavily influenced by friction drag. In theory, a nose cone which has the least amount of surface area would minimize friction drag and therefore maximize apogee. Profiles such as this exist, and examples would be the Von Karman shape. However, in practicality it is much easier to generate the ogive tangent form which makes it more readily available.

Since the SpaceWolves team does not have access to fiberglass or carbon fiber winding equipment, it makes more sense to pick out a design which minimizes cost, which is exactly what the team did. The final nose cone design was purchased on Black Friday for essentially half the cost of all

the other nose cone. The chosen nose cone also has a metal tip which is slid into the fiberglass and tightened using a nut on the inside. Since the metal tip is machinable, it can also provide for another anchoring point with the telemetry bay using a threaded rod. This means our options for the integration of the telemetry bay with the nosecone is still flexible based on any new changes.

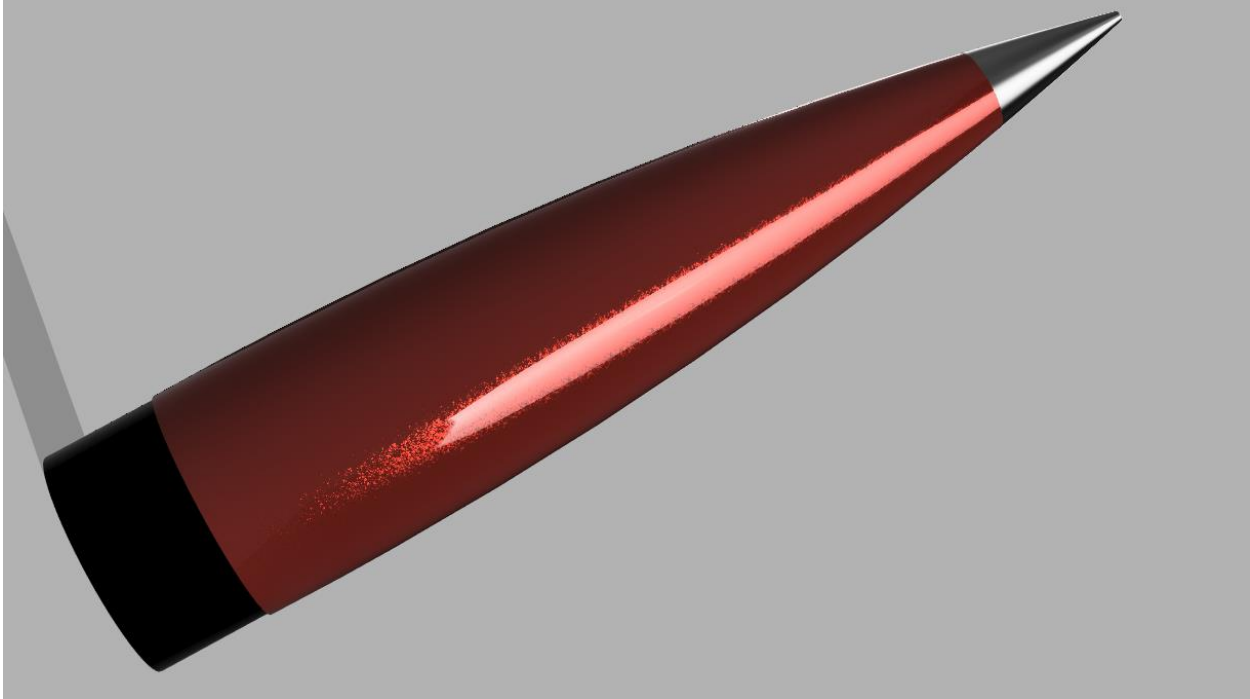


Figure 5: Updated Nosecone Profile

#### 3.1.3.2. Airframe

The airframe of the vehicle consists of three main components:

- Payload Bay
- Avionics Bay
- Booster Bay

The airframe has an inside diameter of 6" and an outside diameter of 6.16". Initially the plan was to use a standard fiberglass airframe. Even though carbon fiber is stronger, the main reason as to why most teams deviate away from carbon fiber is due to the cost. Usually carbon fiber costs twice as much as fiberglass. However, our analysis indicated that it is possible to use a different form of carbon fiber (braided) which would increase the rigidity of the structure while also keeping the cost low.

Most of the carbon fiber tubing sold by vendors that also sell high power rocket components have a price tag that is marked up by a significant margin due to the hobbyist industry. Our team purchased it directly from the manufacturer, which decreased our cost by roughly \$400. Two 48" sections were purchased from which all three sections of the launch vehicle will be cut.

The payload bay section is the shortest bay as designed to meet the requirements of the payload team. The specifications of the payload bay is as follows:

**Table 3: Payload Airframe Specs**

Specification	Value
Material:	Braided Carbon Fiber
Manufacturer	Dragon Plate
Outside Diameter	6.17 inches
Inside Diameter	6.0 inches
Length	17 inches



**Figure 6: Payload Airframe Model**

The avionics bay is the longest section of the rocket. The length was determined by the requirements of the avionics team which include the packing length of the main and drogue chutes and the avionics section. A safety factor was applied to the required length since it might be more difficult to deploy the parachutes if they are very tightly packed inside the rocket. The specifications of the avionics bay is as follows:

**Table 4: Avionics Airframe Specs**

Specification	Value
Material:	Braided Carbon Fiber
Manufacturer	Dragon Plate
Outside Diameter	6.17 inches
Inside Diameter	6.0 inches
Length	32.9 inches



Figure 7: Avionics Airframe Model

The avionics bay will also be utilized as a ballast bay. The center of gravity of the rocket was altered so that it is directly in the center of the avionics assembly which has 2 plates that are equidistant from the center. The purpose of doing this is to allow the team to alter the weight of the rocket depending on the wind conditions and launch day variables without affecting the stability margin which is crucial to the success of the project.

The booster bay is the second shortest section of the rocket since our team had complete control over its specifications. The length was chosen based on the length of the VDS Canister and the motor setup. The motor was chosen such that it minimizes the length of the bay and thus cut down on weight. While standard motors have a length of roughly 27" to 28", the motor chosen by our team has a length of roughly 16" since it packs the same amount of black powder in a smaller volume. Therefore, this allowed the team to make the booster bay very short and cut down on weight and cost. The bay is slotted for the VDS blades and the fin system of the rocket. The specifications of the booster bay are listed below:

Table 5: Booster Bay Airframe Specs

Specification	Value
Material:	Braided Carbon Fiber
Manufacturer	Dragon Plate
Outside Diameter	6.17 inches
Inside Diameter	6.0 inches
Length	31 inches

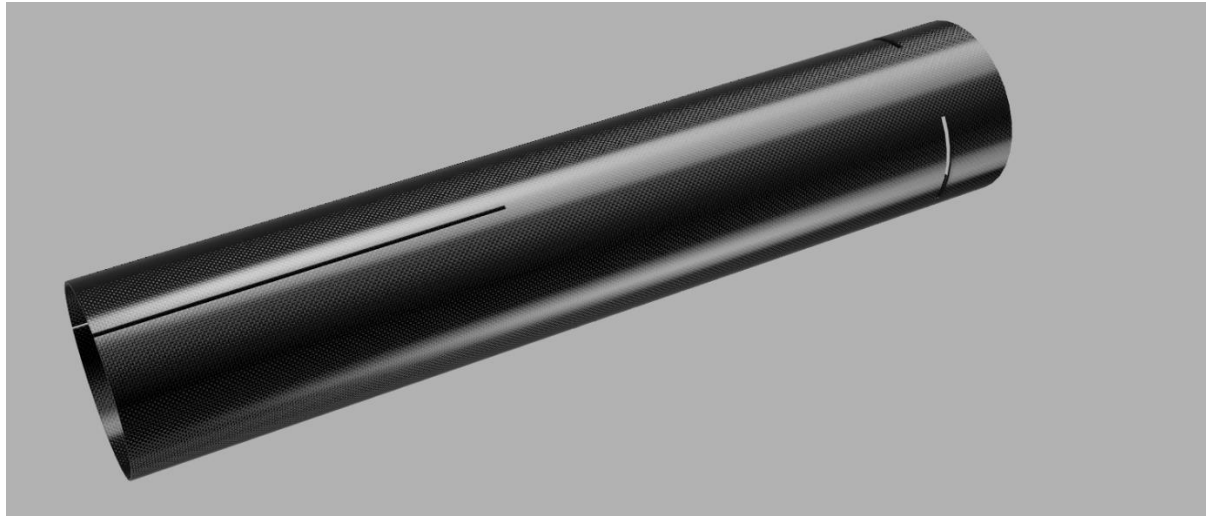


Figure 8: Booster Bay Airframe Model

# DragonPlate™

Material Specifications

**Braided Carbon Fiber Round Tube**

Comprised of carbon fiber braid and Unidirectional Fabrics our round tube is ideal for building light weight frames and structures such as trusses. Engineered to be much stronger under torsional and side loading than pultruded tubing and significantly lighter. Designed so that the unidirectional layers are captured, eliminating longitudinal cracking and splitting.

STANDARD SIZES		
SMALL SIZES	ID	WEIGHT (lbs/ft)
0.415" ± 0.015 OD	0.29" (± 0.010)	0.04
0.53" ± 0.015 OD	0.40" (± 0.010)	0.05
0.79" ± 0.015 OD	0.54" (± 0.010)	0.16

LARGE SIZES	WALL THICKNESS	WEIGHT (lbs/ft)
0.75" [0.75 ± 0.010] ID	0.040" (± 0.010)	0.06
1" [1.000 ± 0.010] ID	0.040" (± 0.010)	0.08
1.5" [1.500 ± 0.010] ID	0.040" (± 0.010)	0.11
2" [2.015 ± 0.010] ID	0.045" (± 0.015)	0.15
3" [3.012 ± 0.010] ID	0.085" (± 0.015)	0.47
4" [4.013 ± 0.010] ID*	0.080" (± 0.015)	0.56
6" [6.010 ± 0.010] ID*	0.080" (± 0.015)	0.90

**Lengths:** 96", 72", 48", 24" [-0, +0.5]  
\* Only available up to 48"

**Finishes:** Natural, Gloss

## Additional Options

- Custom Sizes
- Custom Lengths
- Custom Wall Thickness
- CNC Machining
- Design and Engineering Services

## TECHNICAL SPECIFICATIONS

**Properties of Braid Fiber**  
Tensile Strength: 640 ksi  
Modulus of Elasticity: 34 GPa

**Properties of UNI Fiber (Large Sizes)**  
Tensile Strength: 640 ksi  
Modulus of Elasticity: 34 GPa

**Properties of UNI Fiber (Small Sizes)**  
Tensile Strength: 600 ksi  
Modulus of Elasticity: 34 GPa

**Resin**  
Epoxy resin that accounts for approximately 50% of the composition  
 $W_f \approx 50\%$

**Lay Up Schedule (Large Sizes)**  
 $\pm 45^\circ$  bi-axial CF braid  
 $0^\circ$  uni-directional CF  
 $\pm 45^\circ$  bi-axial CF braid  
 $[\pm 45/0]_f$

**Lay Up Schedule (Small Sizes)**  
 $0^\circ$  uni-directional CF  
 $\pm 45^\circ$  bi-axial CF braid  
 $[0/\pm 45]_f$

DragonPlate.com · 321 Route 5 West · Elbridge, New York 13060 · ph. 315-252-2559 · fax 315-252-0502 · service@dragonplate.com

Figure 9: Braided Carbon Fiber Specifications

### 3.1.3.1. Bulkheads

All bulkheads for connecting bays will be made of G10 Fiberglass. The material was chosen due to its availability, cost and strength. U-Bolts will be connected to the bulkheads for an anchoring point for the shock cords during the deployment of the parachutes. In this manner, after parachute deployment all the bays of the rocket will still be connected, and the rocket will descend in pieces.



Figure 10: G10 Fiberglass Bulkhead Model

Table 6: Bulkhead Details

Specification	Value
Material:	G10 Fiberglass
Vendor:	Madcow Rocketry
Coupler Bulkhead OD	5.773 inches
Airframe Bulkhead OD	5.998 inches
Thickness	0.125 inches

The bulkhead connecting to the booster bay will be more unconventional due to its design requirements. The bulkhead will be mechanically retained instead of epoxied since the VDS system is housed inside the coupler and must be removable. In order to account for inflight vibration and pulling forces during the deployment of the main chute, a simple flat bulkhead will be very easily offset. Therefore, the team will epoxy a section of small coupler section to the bulkhead to provide a resting surface inside of the VDS canister.

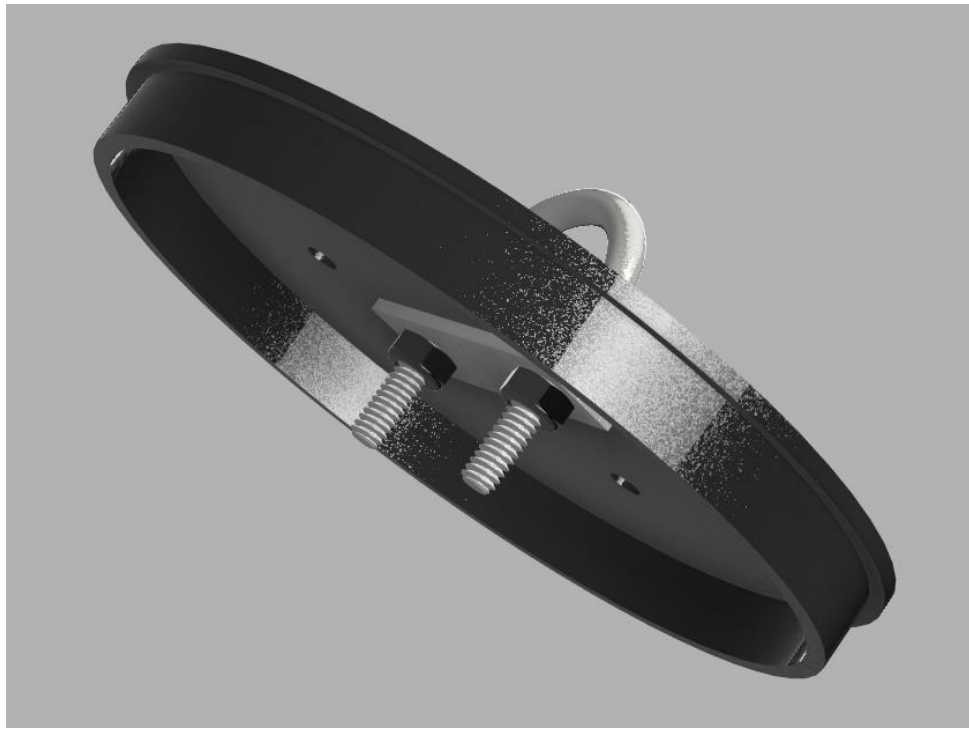


Figure 11: VDS Canister Bulkhead Model

#### 3.1.3.1. Fins

The finalized design for the fins is the trapezoidal design. Models such as cropped delta were initially considered since they are easier to manufacture than the trapezoidal fins. However, cropped delta fins are more prone to breaking during the landing phase due to the sharp 90-degree angle at the base. The cropped delta design for the rocket has a trailing edge which helped in minimizing surface area and lowered the center of pressure of the rocket to give a more viable stability margin which dictates the off-rail flight characteristics of the rocket.

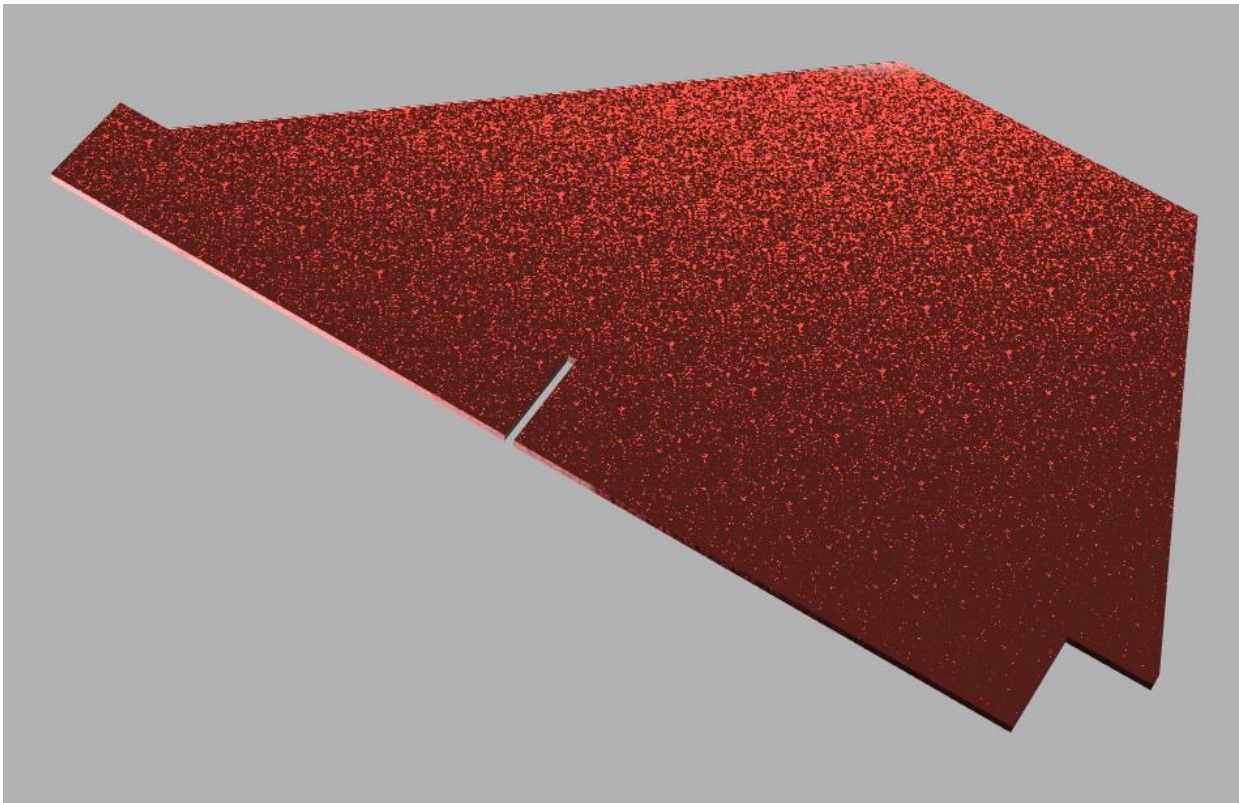


Figure 12: Finalized Fin Model

Table 7: Finalized Fin Shape Parameters

Dimension	Value
Root Chord	14 inches
Tip Chord	4.5 inches
Height	6.5 inches
Sweep Length	7 inches
Sweep Angle	47.1 degrees

### 3.1.3.1. Motor Retainer

A flanged AeroPack motor retainer was chosen for the motor retention mechanism. The retainer comes with an externally threaded piece and a cap which locks the motor in place afterwards. The flanged retainer has holes which will be used to connect it to a center ring holding the motor mount.

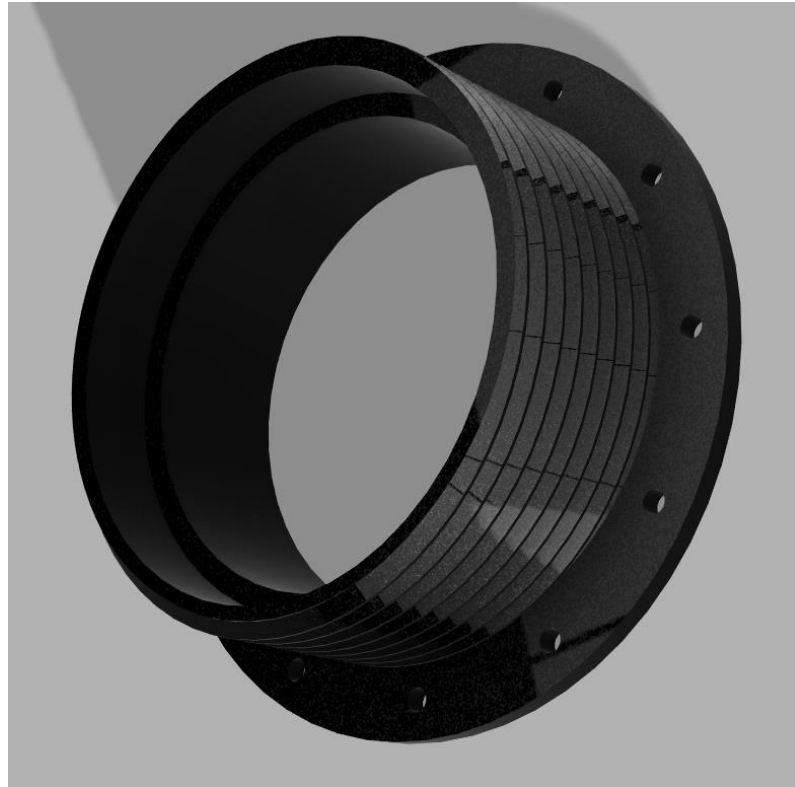


Figure 13: Motor Retainer Model

#### 3.1.3.1. Centering Rings

Standard centering rings with the same inside diameter as the outside diameter of the motor mount and the same outside diameter as the inside diameter of the airframe will be used. The 3 centering rings will be epoxied to the motor mount and to the inside of the air frame. These will then be used to mount the fins as well and align them respect to each other and with respect to the rocket.

Table 8: Centering Ring Specifications

Dimension	Value
Material:	G10 Fiberglass
OD	5.998 inches
ID	3 inches
Vendor:	Madcow Rocketry
Thickness:	0.125 inches

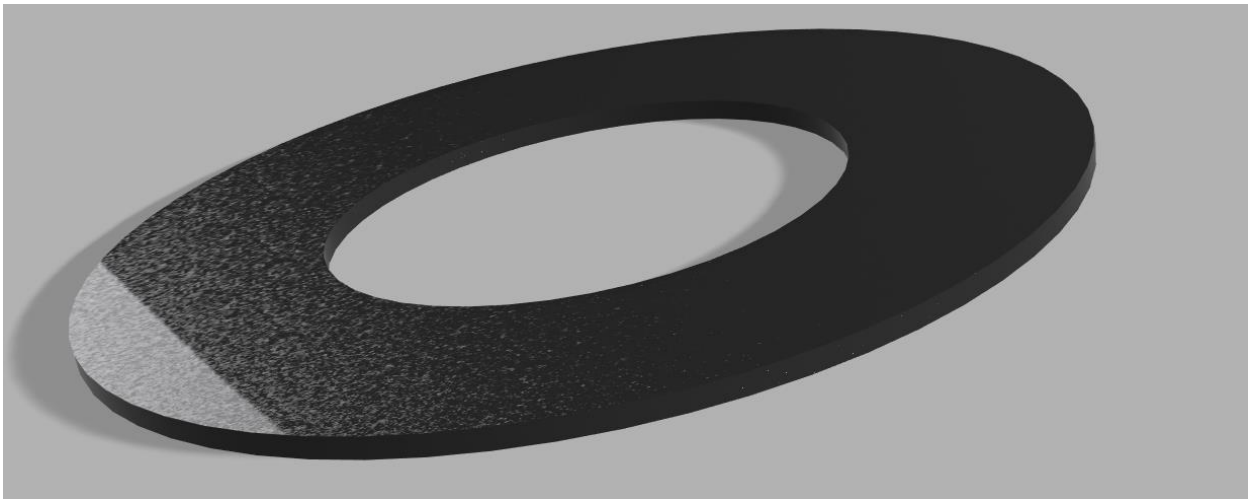


Figure 14: Centering Ring Model

#### 3.1.3.1. Motor Mount

The motor chosen for the rocket fits into a sleeve with an outer diameter of 75mm. Therefore, a motor mount was purchased with an inner diameter of roughly 75mm. The motor mount will hold the motor which will then be retained at the tail end using the motor retainer.

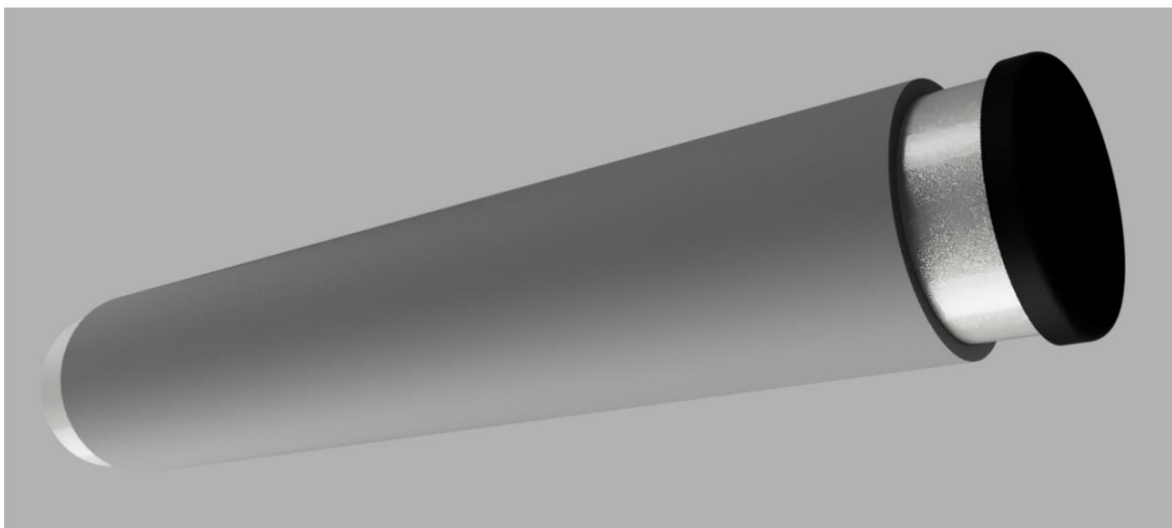


Figure 15: Motor Mount Model

Table 9: Motor Mount Specifications

Dimension	Value
Material:	G12 Fiberglass
OD	3 inches
ID	2.95 inches
Vendor:	Madcow Rocketry
Length:	16 inches

### 3.1.3.1. Fin Assembly

The fins will be assembled with the centering rings using G5000 rocketepoxy utilizing the TTW method. The motor mount will be epoxied first to the middle centering ring. The assembly will then be slid into the booster bay airframe. The fins will be slid into the slots one by one and then epoxied to the airframe. The top and bottom centering rings will be epoxied last from either side afterwards. Methods of making the system modular were explored however this requires a mechanical retention method instead of using epoxy. It was also discovered that all methods of retaining the fins mechanically to the surface were weaker than the TTW method.

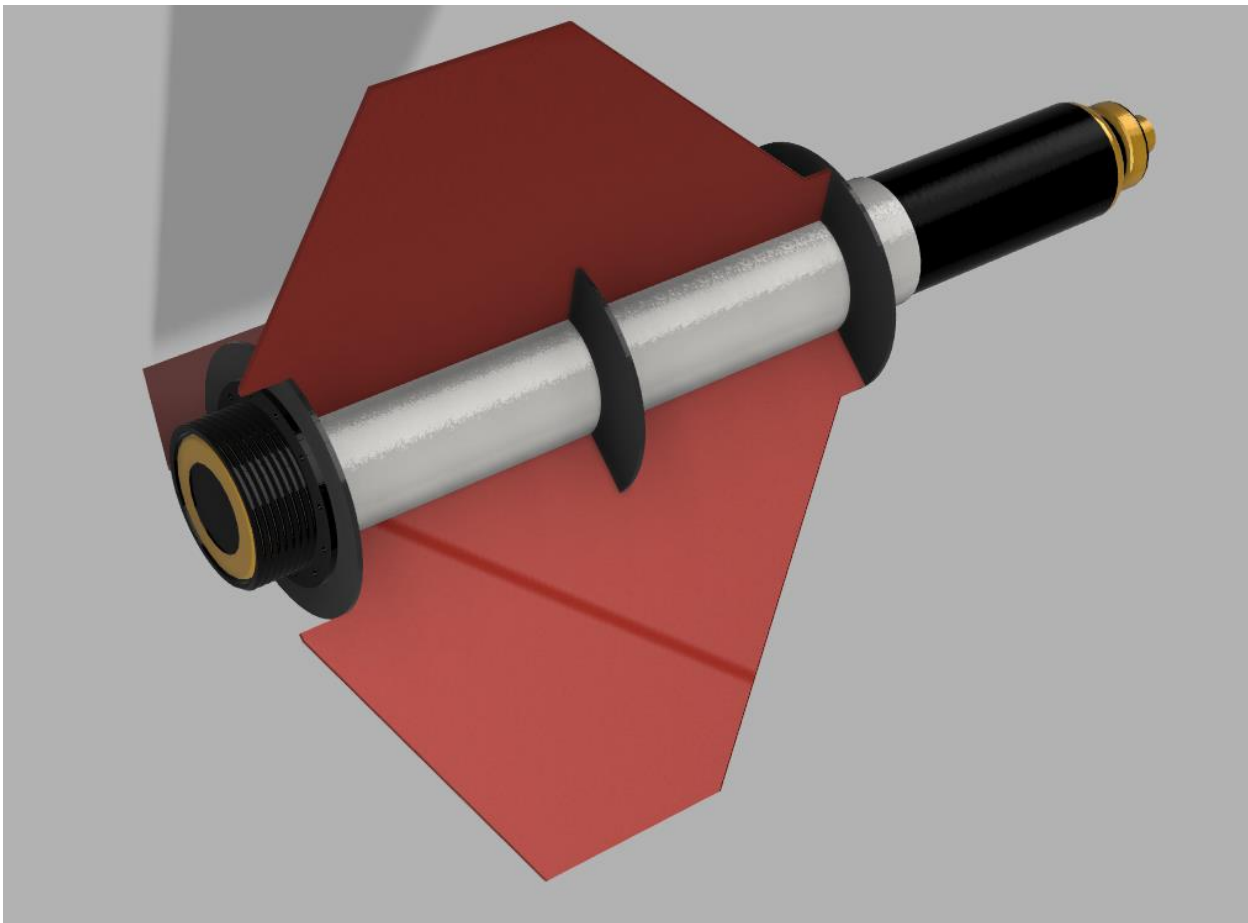


Figure 16: Fin Assembly Model

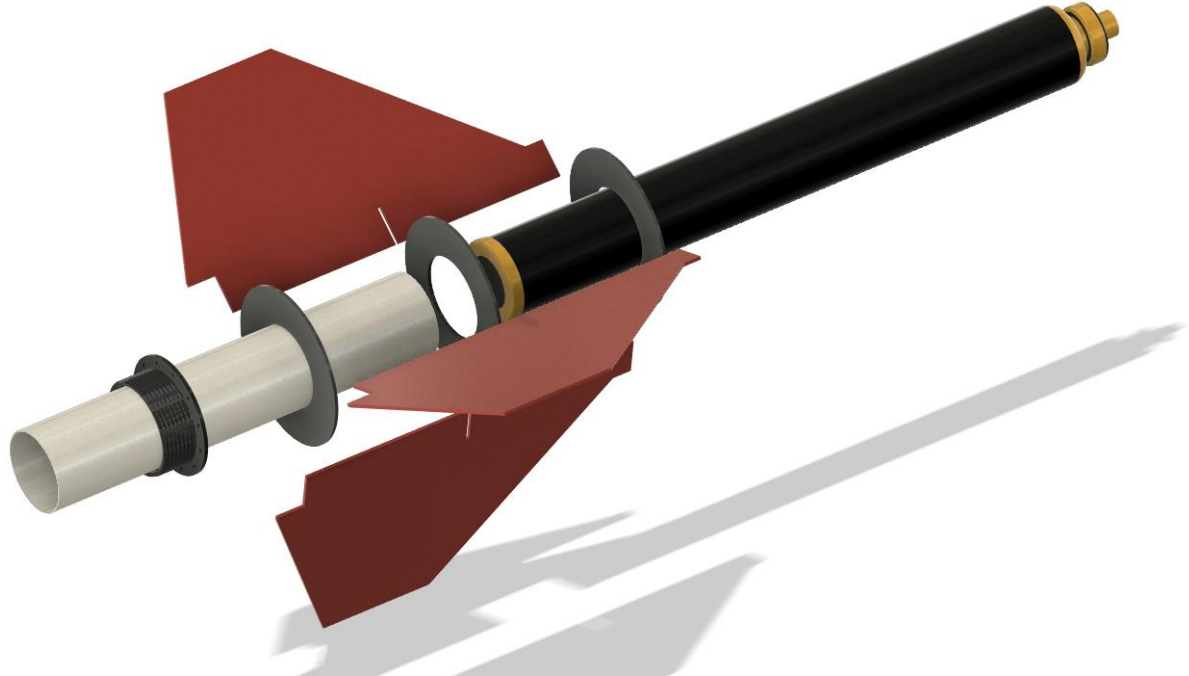


Figure 17: Fin Assembly Exploded View

#### 3.1.3.1. Motor

The L1420 R-P motor, as discussed in the PDR, was chosen as the final candidate motor. Three motors and a hardware kit were ordered from Wildman rocketry which should be received by the team within a week. The thrust provided by the L1420R-P resulted in a very desirable apogee which was the guiding factor for the design

Table 10: Motor Comparison Matrix

Motor	Manufacturer	Apogee (ft)	Max Velocity (ft/s)	Max Acceleration (ft/s <sup>2</sup> )
L850W	Aerotech	3460	436	162
L1500T-P	Aerotech	3715	513	368
L1520T-P	Aerotech	3824	520	235
<b>L1420R-P</b>	<b>Aerotech</b>	<b>4860</b>	<b>615</b>	<b>230</b>
L1365M-P	Aerotech	4985	586	205
L2375-WT	CTI	5478	682	373
L2200G	Aerotech	5673	677	437

Table 11: L1420R-P Motor Specs

Aerotech L1420R-P Specs	
Total Impulse:	1035 lbf-sec

Burn Time:	3.2 sec
Peak Thrust:	407.8 lb
Average Thrust	319.9 lb
Mass Before & After Burn	10.05/4.47 lb
Motor Retention Method	Screw on Retainer
Hardware Kit	RMS 75/5120

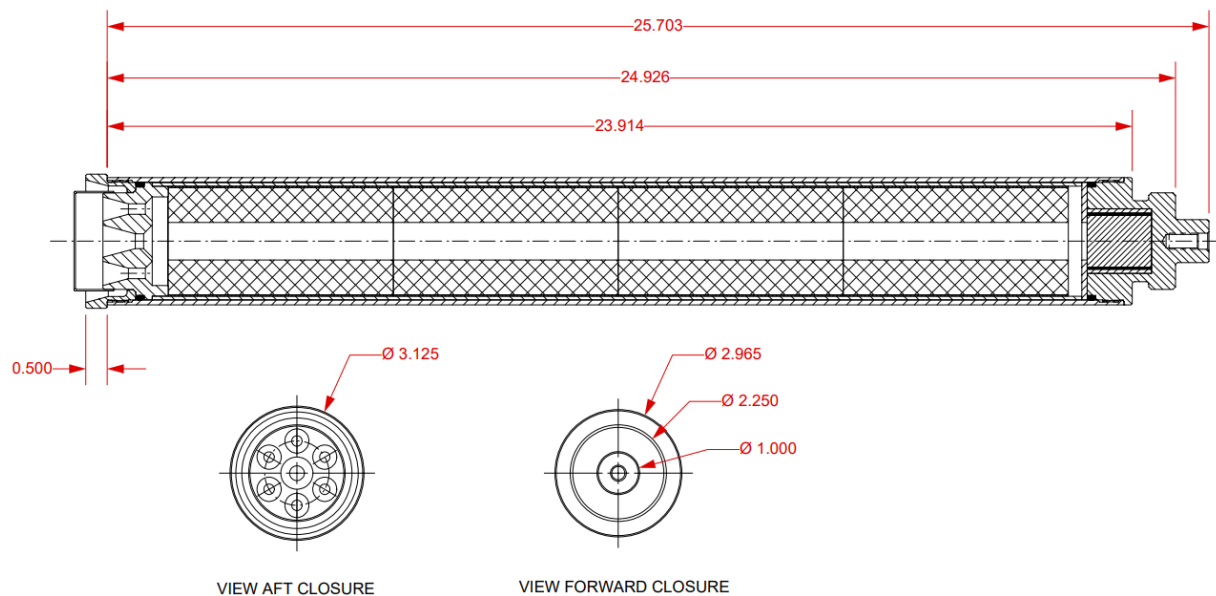


Figure 18: Motor Casing Drawing

Table 12: Motor Assembly Mass Breakdown

Component	Weight (lb.)
Forward Seal Disc	0.25
Forward Closure	2.5
Aft Closure	0.75
Case	1.9943
Propellant Weight	5.643834
Total Weight	10.05749

### 3.1.3.1. Camera Bay

The camera chosen is the 808 #16 Keychain camera which can record footage in 60 fps. It can take still pictures in HD quality as well as record video. Three of these cameras will be housed in the

booster bay of the rocket. While the GoPro camera previously chosen was very heavy, these cameras have a negligible weight when compared to the rest of the rocket.

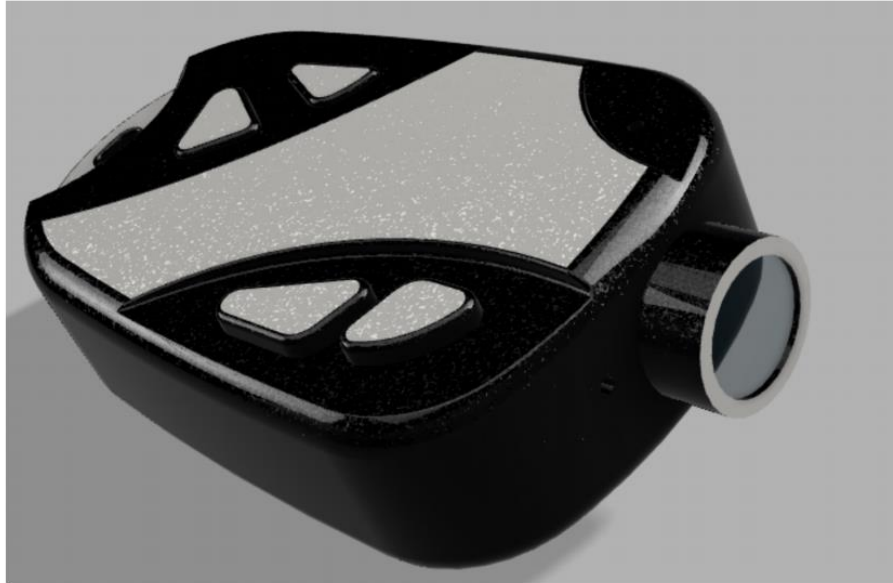


Figure 19: 808 Keychain Camera Model

The camera will be housed in a 3D printed unit which will be made of ABS plastic. The housing will have the negative profile of the cameras for a nice fit and for 3 3.7 V 700mAh external batteries which boost the possible recording time of the cameras from 45 min to 3+ hours. Therefore, in theory no footage will be lost if the vehicle sits on the pad for a prolonged amount of time.

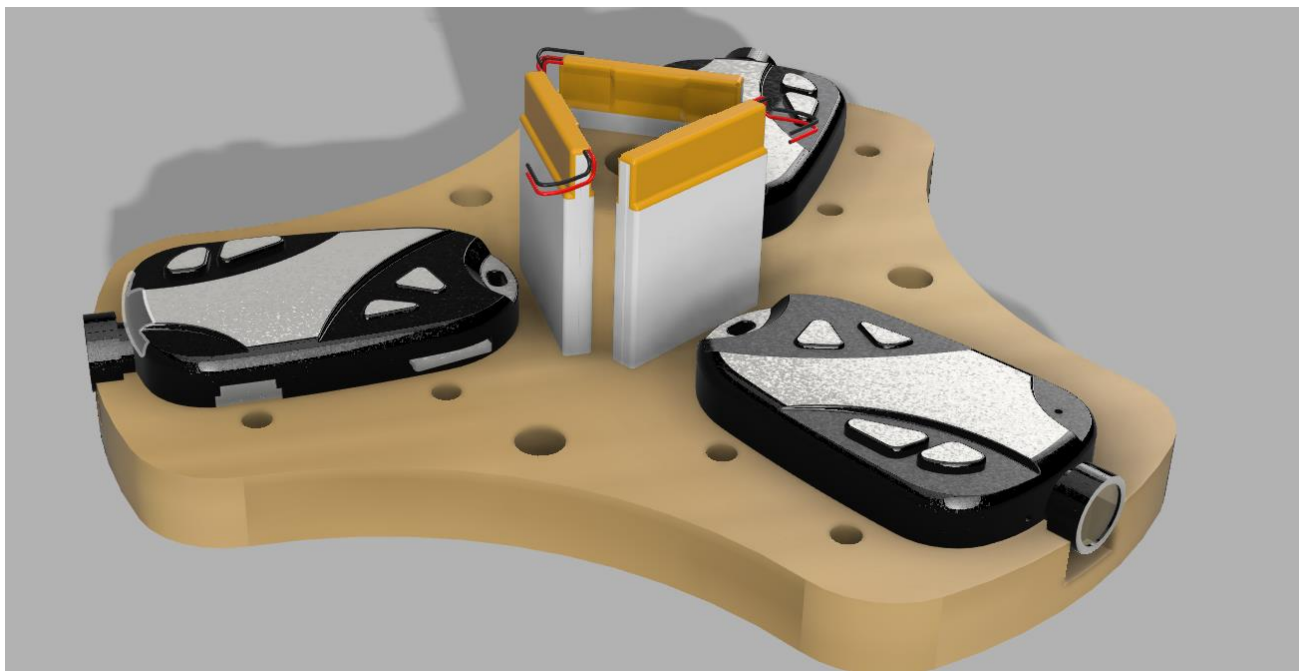


Figure 20: Camera Bay Model

### 3.1.3.1. VDS

The variable drag system consists of a three-blade system which will be actuated by a rail and carriage using a 3-bar linkage. The profile of the blades has been optimized to get the largest surface area value perpendicular to the direction of thrust. The profile has parallel sides instead of a “fan” like shape in order to keep the effective induced drag linear in terms of deploying the blades out of the body. A “fan” like shape would also require larger slots through the airframe which would compromise the structural integrity of the design.

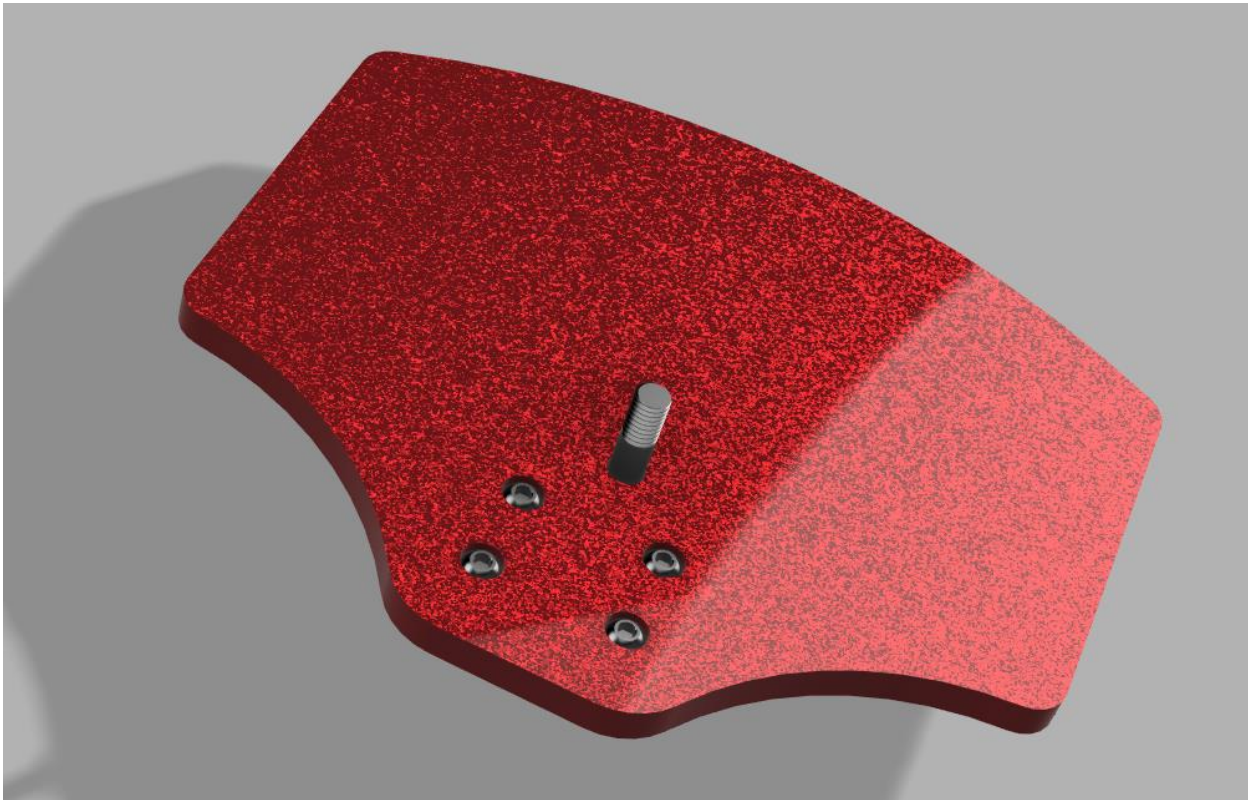


Figure 21: VDS Blade Model

The central actuating component sits on a flanged radial bearing which will be force fitted into a fiberglass bulkhead containing an accurately drilled hole. The outside track of the radial bearing will then be epoxied to ensure no lateral motion.

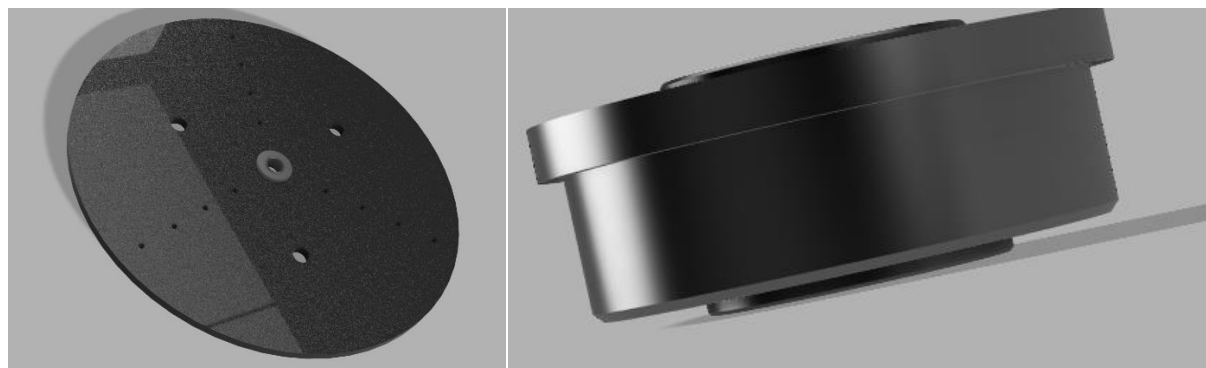


Figure 22: VDS Baseplate Model & Flanged Radial Bearing

## **Stainless Steel Ball Bearing**

Flanged, Shielded with Extended Inner Ring, Number R188-2Z



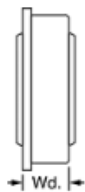
Each

In stock

\$7.20 Each

57155K337

**ADD TO ORDER**



Bearing Type	Ball
For Load Direction	Radial
Construction	Single Row
Seal Type	Shielded
Inner Ring Type	Extended
Ball Bearing Type	Flanged
Trade No.	R188-2Z
For Shaft Type	Round
For Shaft Diameter	1/4"
ID	0.25"
ID Tolerance	-0.0002" to 0"
For Housing ID	1/2"
OD	0.5"
OD Tolerance	-0.0002" to 0"
Width	3/16"
Width Tolerance	-0.001" to 0"
Flange	
OD	0.547"
Thickness	0.05"
Inner Ring	
OD	0.291"
Width	0.219"
Ring Material	440C Stainless Steel
Ball Material	440C Stainless Steel
Cage Material	400 Series Stainless Steel
Shield Material	300 Series Stainless Steel
Radial Load Capacity, lbs.	
Dynamic	240
Static	90
Maximum Speed	50,000 rpm
Lubrication	Lubricated
Lubricant	Oil
Shaft Mount Type	Press Fit
Temperature Range	-20° to 250° F
ABEC Rating	ABEC-5
Radial Clearance Trade No.	MC3
Radial Clearance	0.0002" to 0.0004"
RoHS	RoHS 3 (2015/863/EU) compliant

**Figure 23: Flanged Radial Bearing Specs**

A rail and carriage system will be utilized for the sliding mechanism as shown below. The pitch moment, yaw moment and maximum roll of the blades were considered in order to finalize the design.

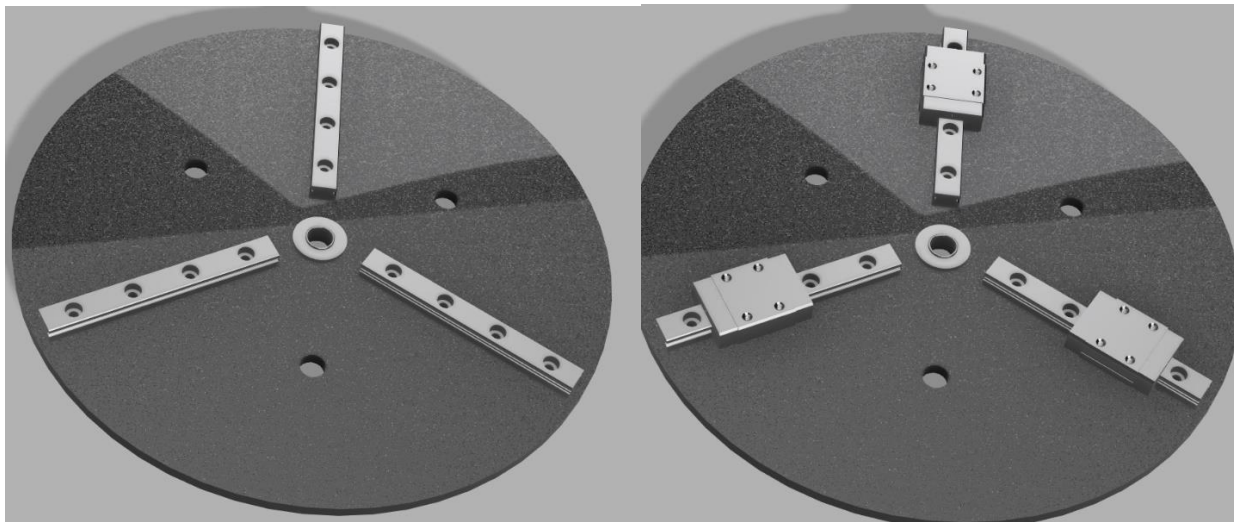


Figure 24: VDS Carriage and Rail Model

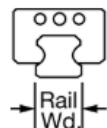
### 7 mm Wide Guide Rail for Ball Bearing Carriage



Rail Length, mm  
✓ 60

Each

**ADD TO ORDER**



In stock  
\$25.20 Each  
6725K33

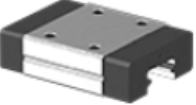
Rail Width	7 mm
Rail Length	60 mm
Rail Height	5 mm
Rail Material	440 Stainless Steel
Number of Mounting Holes	4
For Mounting Fastener Thread Size	M2
Mounting Hole Center-to-Center	15 mm
Mounting Hole Center-to-End	7.5 mm
Mounting Hole Depth	2.7 mm
Mounting Fasteners Included	Yes
RoHS	RoHS 3 (2015/863/EU) compliant

Suitable for clean room use, these carriages and guide rails are made entirely of stainless steel. Ball bearings provide accurate movement and positioning at high speeds under heavy loads. Mount in any orientation without affecting load capacity. End seals keep lubricant in and dirt out.

Figure 25: VDS Rail Specs

## Corrosion-Resistant Ball Bearing Carriage

for 7 mm Wide Rail

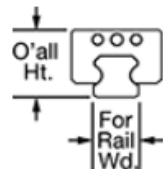
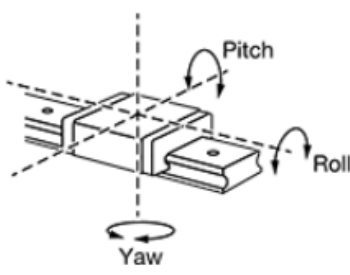
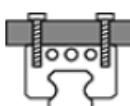


Each

In stock

\$67.27 Each  
8438K2

ADD TO ORDER

Load Fastening from Top

Carriage and Guide Rail Type	Ball Bearing
Carriage Profile	Standard
Bearing Type	Ball
Load Fastening	From Top
For Rail Width	7 mm
Dynamic Load Capacity	290 lbs.
Static Load Capacity	420 lbs.
Static Pitch Moment Load Capacity	3.4 ft.-lbs.
Static Roll Moment Load Capacity	5 ft.-lbs.
Static Yaw Moment Load Capacity	2.8 ft.-lbs.
Overall Height	8 mm
Carriage Width	17 mm
Carriage Length	23.5 mm
Carriage Material	440 Stainless Steel
Bearing Material	440 Stainless Steel
End Seal Material	Rubber
Maximum Temperature	210° F
Mounting	
Number of Holes	4
Hole Thread Size	M2
Hole Thread Pitch	0.4 mm
Hole Depth	2.5 mm
Fasteners Included	No

Figure 26: VDS Carriage Specs

The blades will be attached to the carriages therefore being rigidly affixed to the baseplate. The designed travel distance on each rail is 1.75 inches. The rail system chosen is able to withstand very high loads and it also weighs very little. The chosen carriage also has a very small profile which means that the blades can extend outwards more without the carriage going off track.

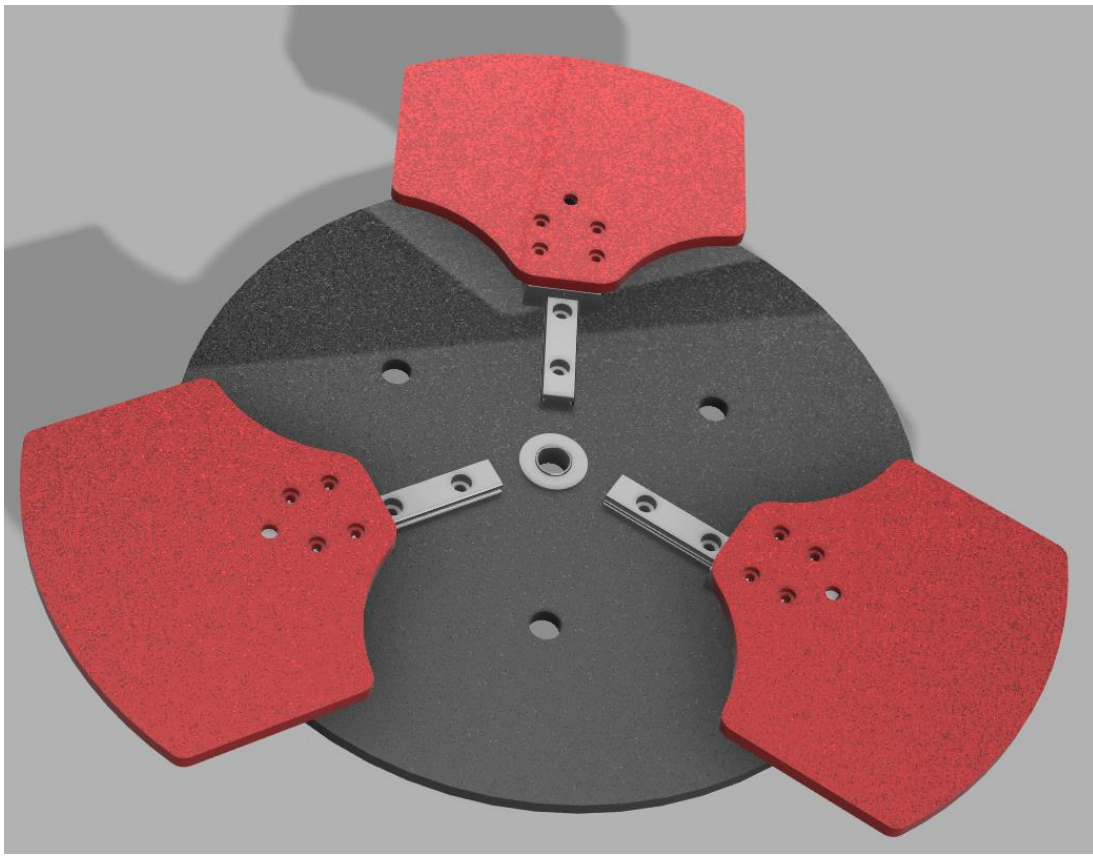


Figure 27: VDS Fully Extended Model

Since there needs to be a method which rigidly affixes the actuation on the same plane, a tri-bearing system was designed which is capable of handling extremely high radial and thrust loads. Two thrust bearings essentially “sandwich” the outer raceway of the flanged radial bearing, thus allowing the shaft to spin freely while also ensuring that its rotation will not be disturbed due to both axial and radial loads during the flight.

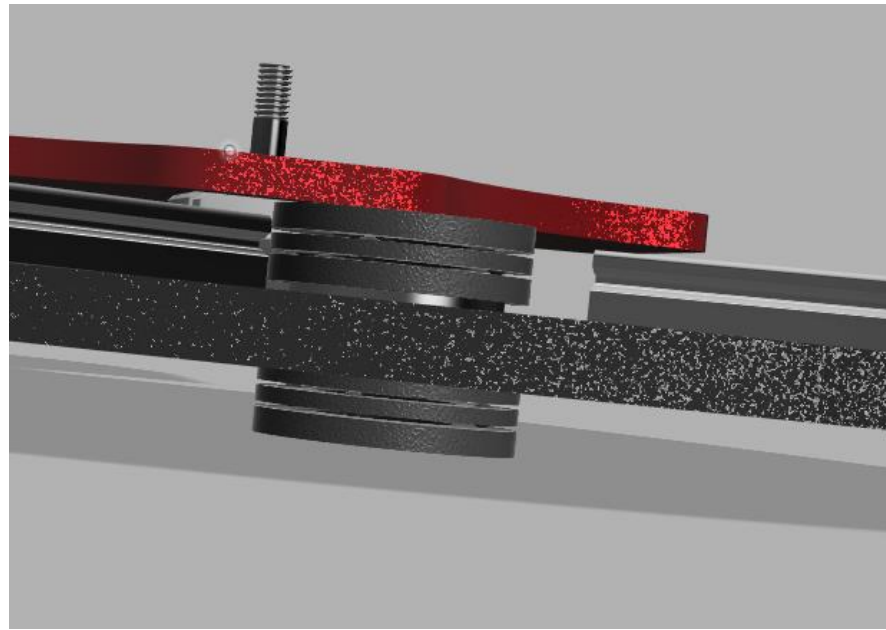


Figure 28: VDS Bearing Assembly

A shaft will be machined-in house which has the same outer diameter as the inner diameter of inner track of the radial bearing. This will essentially be a force fit which will minimize the rotational friction during the actuation of the blades due to the full use of the ball bearings.

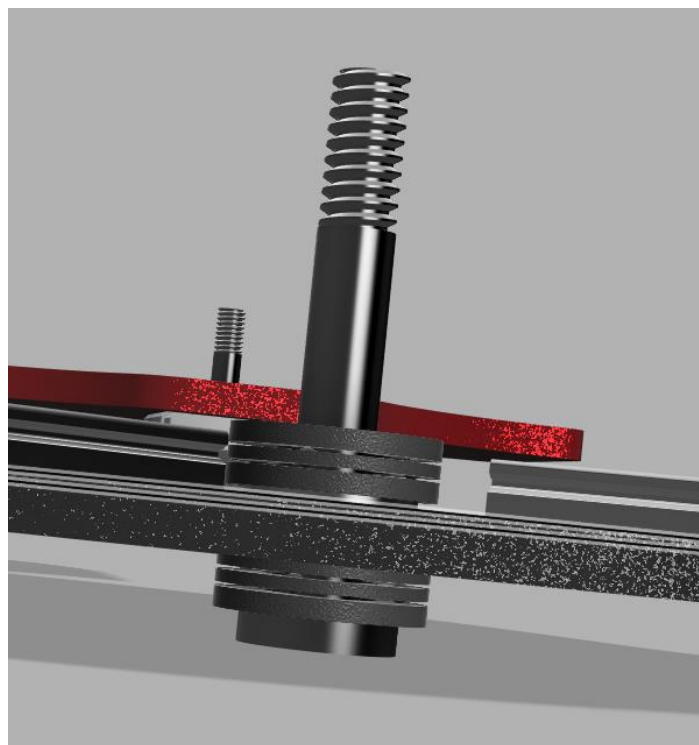


Figure 29: VDS Shaft Assembly

An aluminum actuating plate will be machined in-house which will rest on top of the thrust bearing. The connection to the top washer of the thrust bearing and the actuating bearing will also

be a force fit. This plate will be free to rotate which will be responsible for moving the blades radially outwards from the center of the baseplate.

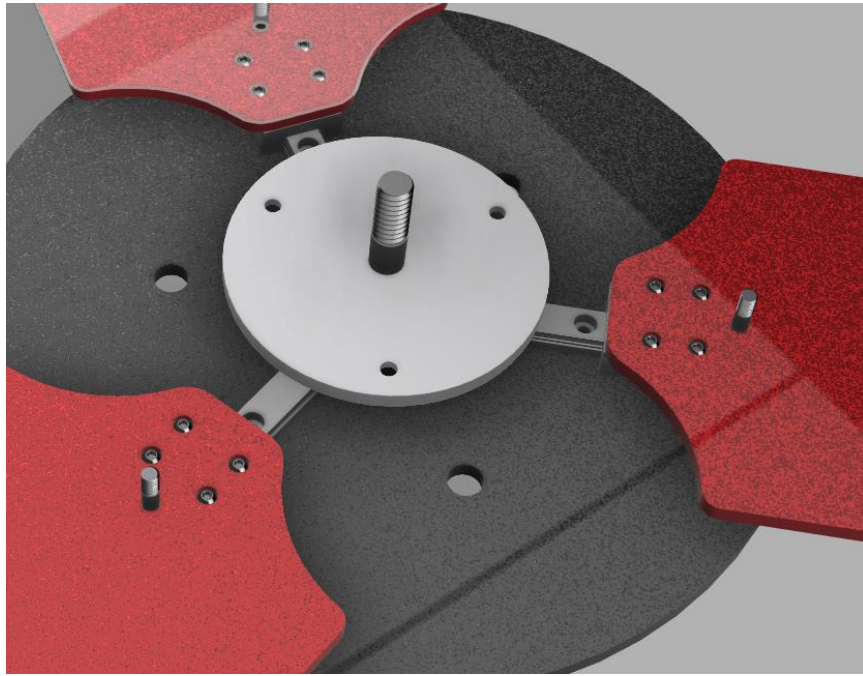


Figure 30: VDS Actuating Plate

The three-bar linkage system was designed such that the forces acting perpendicularly to the rail direction is minimized and the force acting parallel to the rail direction is maximized. The lengths of the links were also calculated to actuate the blade out to 1.75 inches and retract them fully in during liftoff and motor burnout

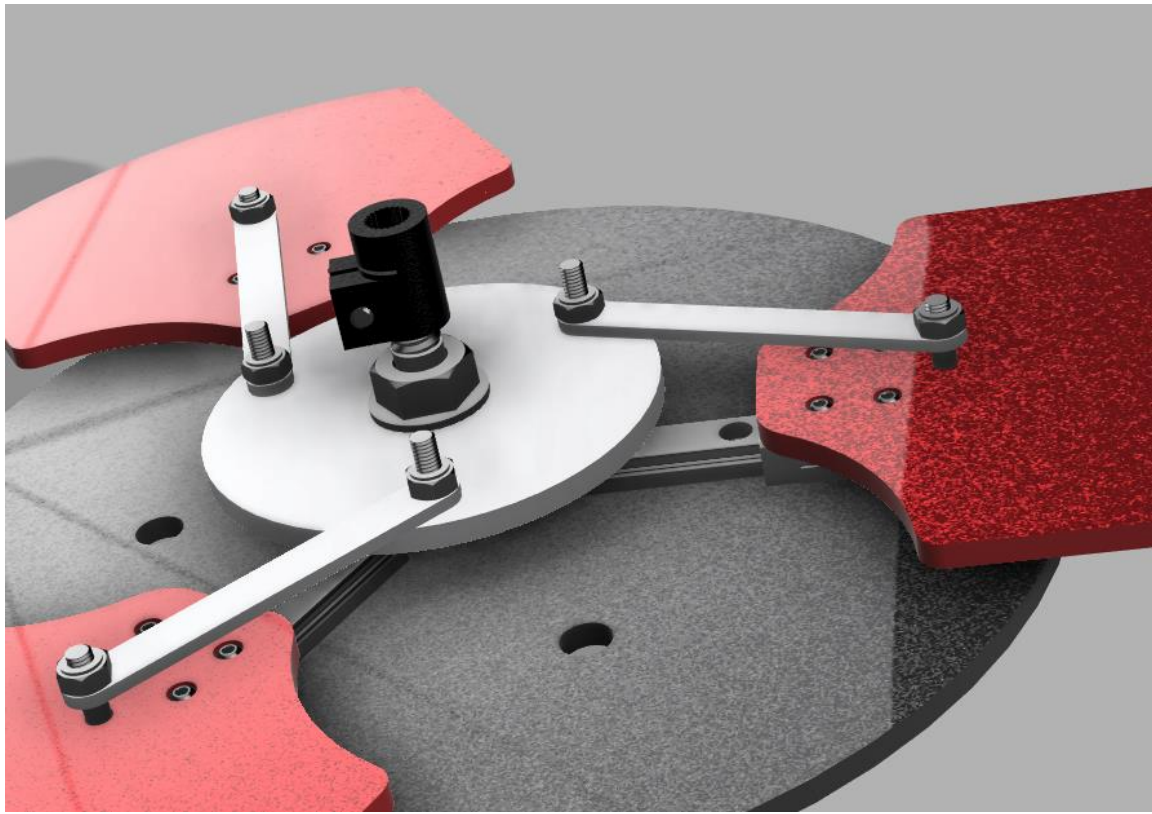


Figure 31: VDS Linkage System

The servomotor was picked out based on the torque requirements of the VDS system. Using safety factors, a design stall torque value of roughly 216 oz-in was calculated. The servomotor will be attached to the shaft via a coupler purchased from ServoCity. The motor will be mounted on a separate 3D printed plate made of ABS plastic which will be held in place using threaded rods inside of the VDS canister.

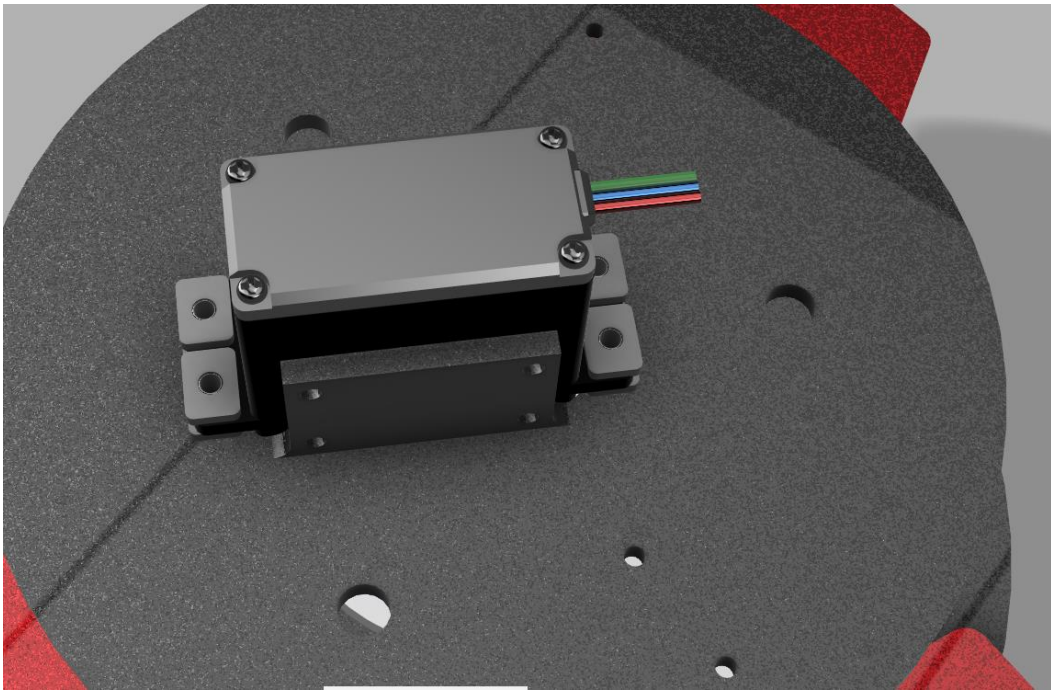


Figure 32: VDS Motor Model

The current draw values of the VDS motor were utilized in order to calculate the required battery size for the flight duration between motor burnout and apogee. A 200mAh 2S 7.4V 30C Li-Po batter will be utilized to actuate the VDS servomotor.

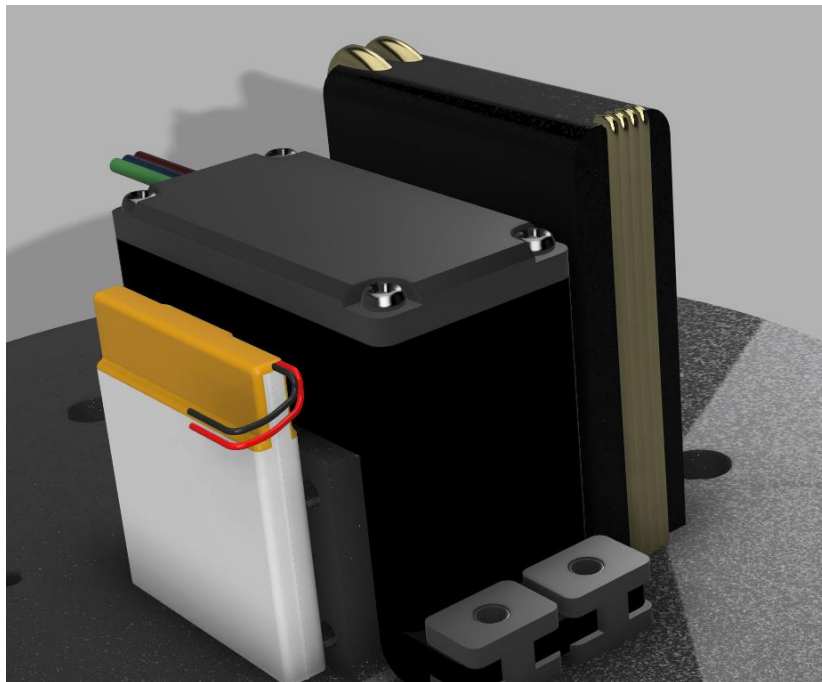


Figure 33: VDS Motor & Battery Model

A nine degree of freedom sensor stick containing a 3-axos accelerometer, a 3-axos gyroscope and a 3-axis magnetometer will be utilized as the main VDS feedback control scheme. The BMP280 I2C barometric pressure sensor will be used as a redundant altitude readout unit.

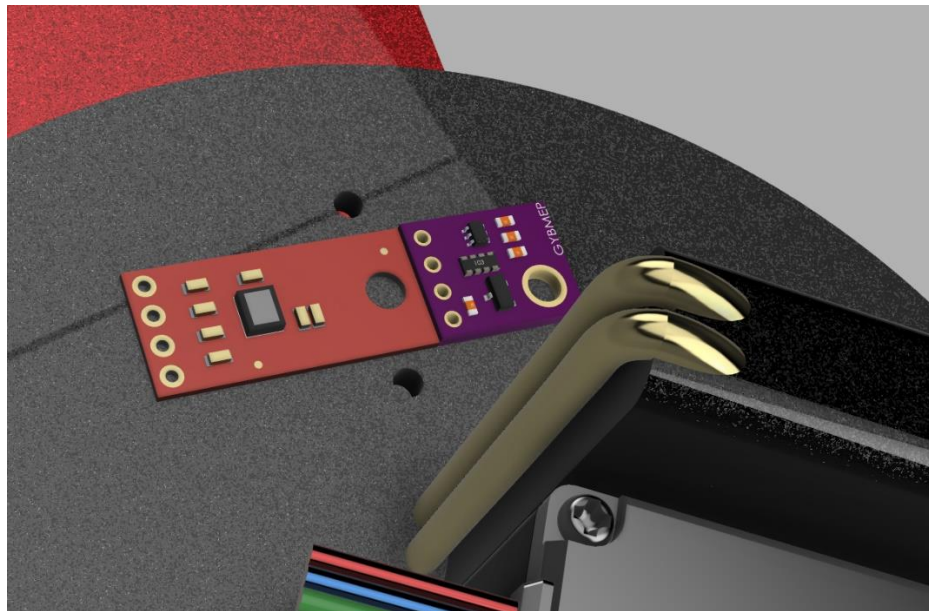


Figure 34: VDS Barometer & Sensor Stick

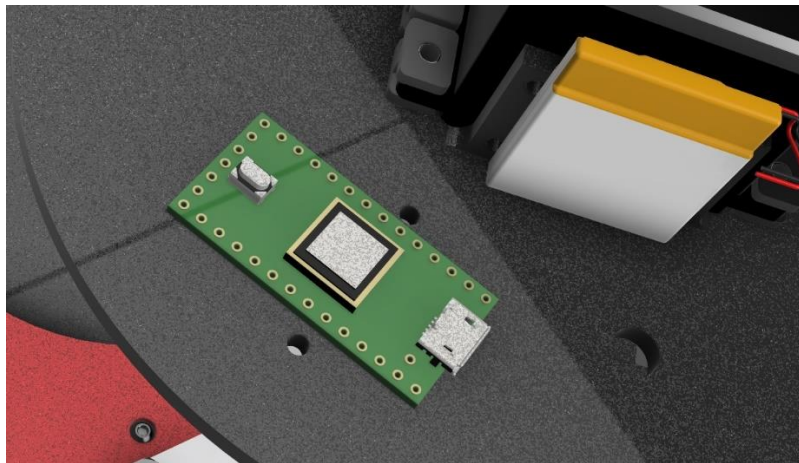


Figure 35: VDS Teensy Microcontroller

A Teensy 4.0 microcontroller will be used in conjunction with the sensors to write embedded software which controls the VDS using a feedback loop. A 3.7V 450 mAh Lipo battery will be shared among the microcontroller, barometric pressure sensor and 9DoF sensor stick.

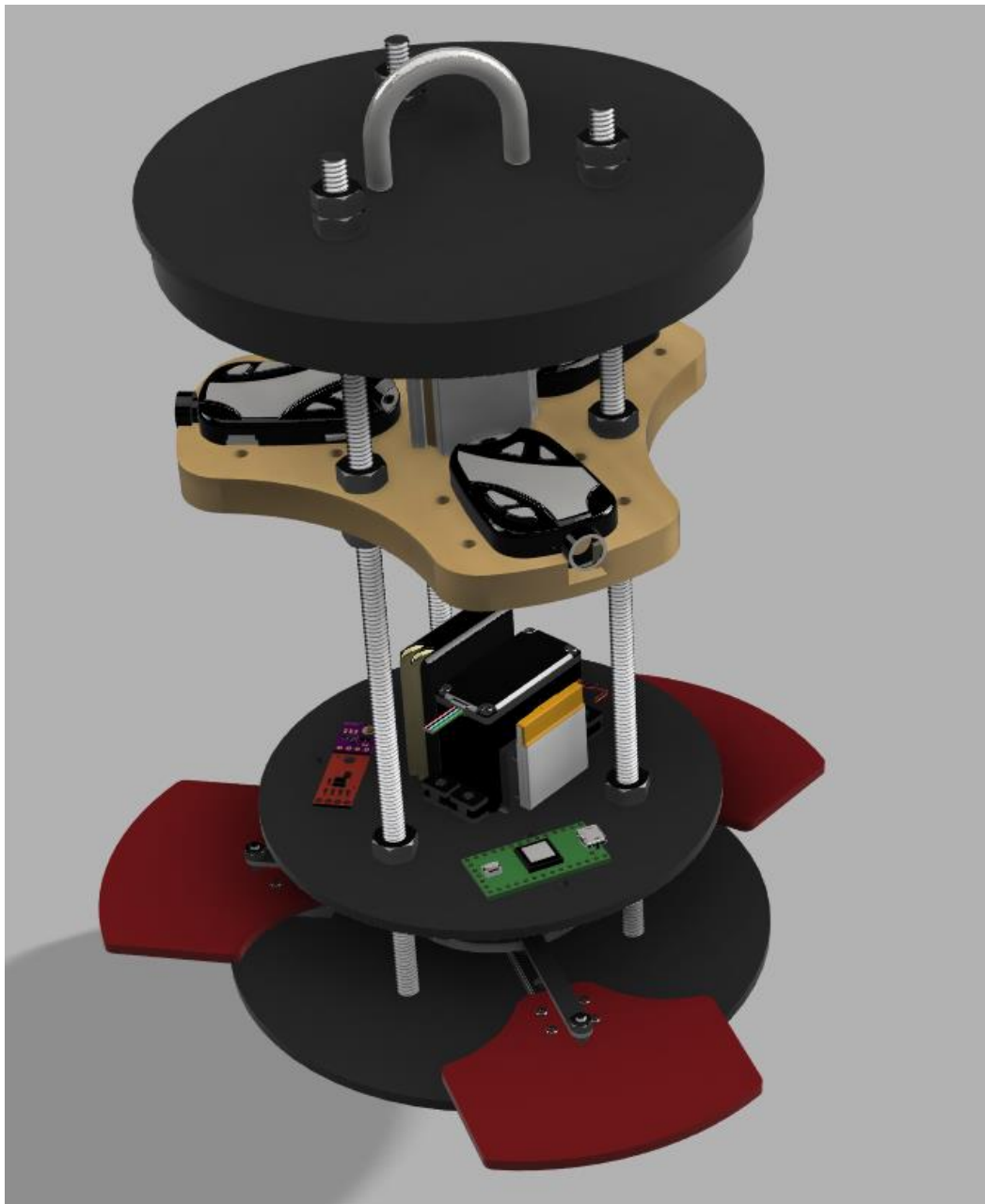


Figure 36: VDS Canister Assembly

Three aluminum threaded rods will secure the camera bay and VDS unit together inside of the coupler of the booster bay. Although unconventional, this design choice allows the team to shave off roughly 6 inches of required length from the rocket, therefore cutting the weight as well.

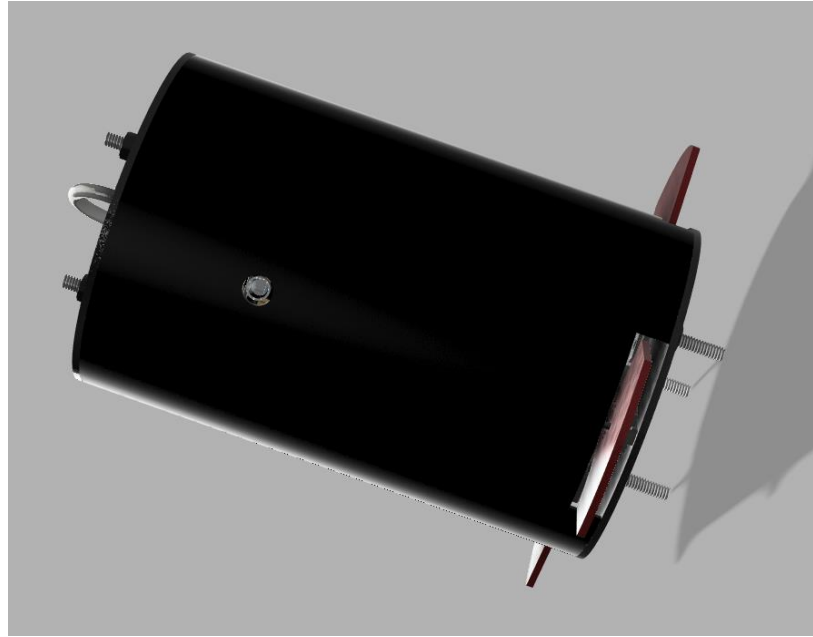


Figure 37: VDS Canister Assembly

A 9-inch G12 fiberglass coupler will serve as the housing unit for the VDS & camera bay therefore turning the system into a canister. The baseplate of the VDS unit will be epoxied to the coupler. A 3-inch section coupler will then be epoxied into the booster bay. For extra support, the coupler inside the booster bay will also be bolted through the airframe. This allows the in-flight separation point of the booster bay to have a coupler short of 6 inches.

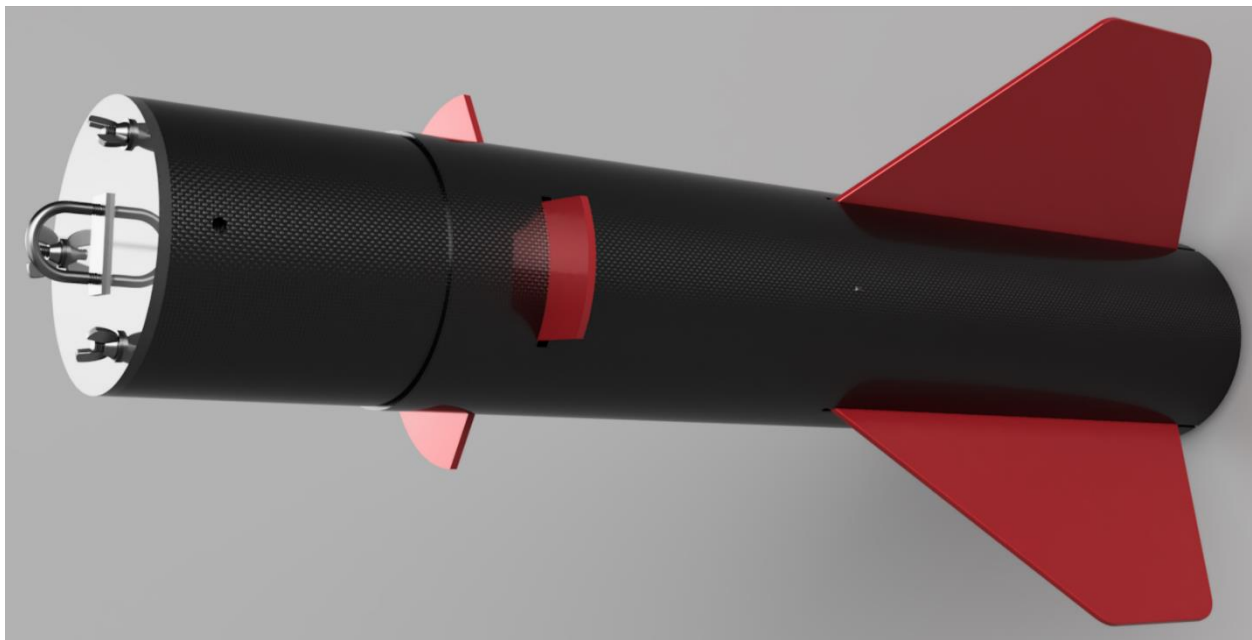


Figure 38: Booster Bay and VDS Canister Integration

Slots for the blades will be cut through the airframe and through the coupler. FEA was performed to ensure that the airframe and coupler will not fail and will be discussed in more detailed in the quantitative section of the report.

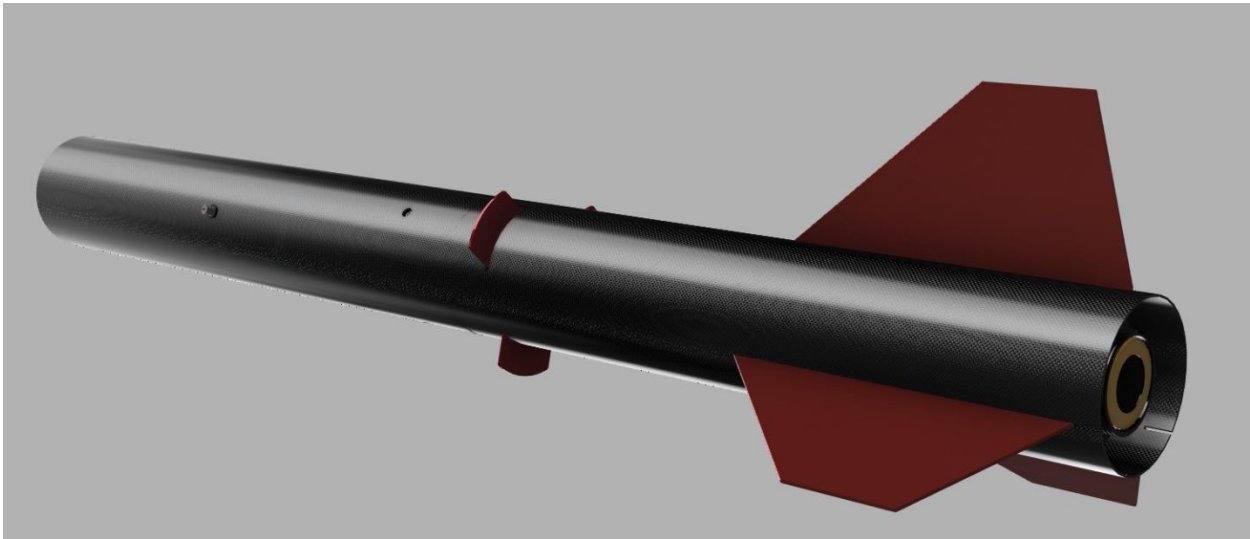


Figure 39: Booster Bay & Avionics Bay Assembly

The booster bay will then be connected to the avionics bay using shear pins. The avionics airframe has the respective holes for the camera subsystem.



Figure 40: Exploded Booster & Avionics View

### 3.1.3.1. VDS Electronics

The following circuit has been designed to ensure the VDS system attains the apogee goal. During flight, useful flight data will be continuously gathered by two sensors: an Adafruit BMP280 and a

SparkFun 9DoF Sensor Stick. This data is relayed into a Teensy 4.0 microcontroller and used to calculate the necessary flight profile alterations. With each successive calculation, the microcontroller will adjust the VDS mechanism through control of a HS-5585MH Servo. As such, this is a closed loop system.

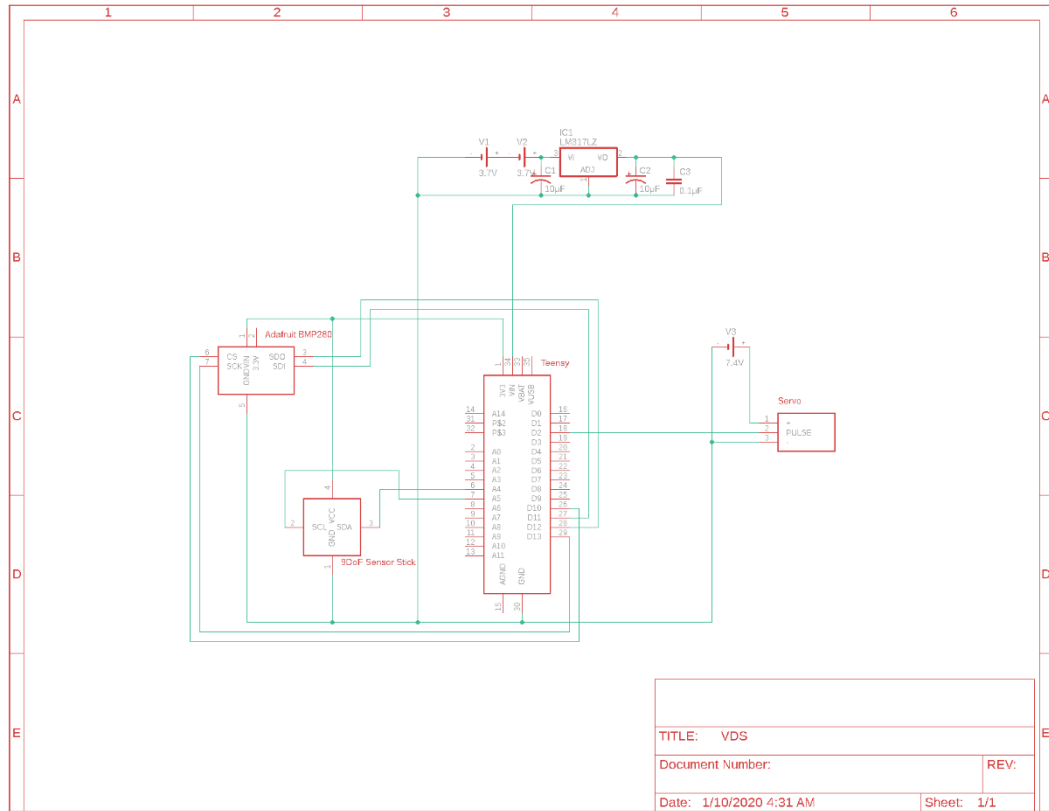


Figure 41: VDS circuit diagram

The Adafruit BMP280 can make both pressure and temperature measurements. Through measurements of pressure and temperature, their relationship with atmospheric height may be exploited to provide a device that functions as an altimeter. With this specific device, altitude may be calculated with  $\pm 1$  meter accuracy.

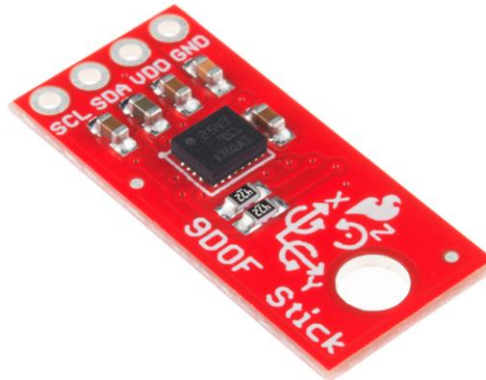


Figure 42: Adafruit BMP280

**Table 13: Adafruit BMP280 technical specs**

Pressure range	300 ... 1100 hPa (equiv. to +9000...-500 m above/below sea level)
Package	8-pin LGA metal-lid Footprint : 2.0 × 2.5 mm <sup>2</sup> , height: 0.95 mm
Relative accuracy (950 ... 1050hPa @25°C)	±0.12 hPa, equiv. to ±1 m
Absolute accuracy (950 ...1050 hPa, 0 ...+40 °C)	typ. ±1 hPa
Temperature coefficient offset (25 ... 40°C @900hPa)	1.5 Pa/K, equiv. to 12.6 cm/K
Digital interfaces	I <sup>2</sup> C (up to 3.4 MHz) SPI (3 and 4 wire, up to 10 MHz)
Current consumption	2.7µA @ 1 Hz sampling rate
Temperature range	-40 ... +85 °C

The SparkFun 9DoF Sensor Stick houses a 3-axis accelerometer, 3-axis gyroscope, and 3-axis magnetometer. Thus, this device produces data for acceleration, angular rotation, and magnetic force in three-dimensional space. Combined with altitude data, these sensor devices provide a very descriptive view of the flight profile.



**Figure 43: SparkFun 9DoF Sensor Stick**

**Table 14: SparkFun 9DoF Sensor Stick technical specs**

3 acceleration channels, 3 angular rate channels, 3 magnetic field channels
±2/±4/±8/±16g linear acceleration full scale
±4/±8/±12/±16 gauss magnetic full scale
±245/±500/±2000dps angular rate full scale
I <sup>2</sup> C serial interface
Operating Voltage: 3.3V

With data from both sensors, the Teensy 4.0 microcontroller may be used to predict flight profile. Using PID calculations, the Teensy will update the servo motor with new position data. It is important to note that the Teensy 4.0 is an exceptionally powerful microprocessor. As such, flight predictions will be limited only by the rate of sensor data collection.



Figure 44: Teensy 4.0

Table 15: Teensy 4.0 technical specs

ARM Cortex-M7 at 600 MHz	32 general purpose DMA channels
1024K RAM (512K is tightly coupled)	31 PWM pins
2048K Flash (64K reserved for recovery & EEPROM emulation)	40 digital pins, all interrupt capable
2 USB ports, both 480 MBit/sec	14 analog pins, 2 ADCs on chip
3 CAN Bus (1 with CAN FD)	Cryptographic Acceleration
2 I2S Digital Audio	Random Number Generator
1 S/PDIF Digital Audio	RTC for date/time
1 SDIO (4 bit) native SD	Programmable FlexIO
3 SPI, all with 16 word FIFO	Pixel Processing Pipeline
3 I2C, all with 4 byte FIFO	Peripheral cross triggering
7 Serial, all with 4 byte FIFO	Power On/Off management

By connecting two 3.7V rechargeable lithium polymer ion battery packs in series and using a voltage regulator as shown in the circuit, the microcontroller may be supplied with a steady 5V. This approach ensures that the microcontroller's sensitive electronics are protected while operating at its maximum clock speed. Capacitors were added to the circuit to ensure a smooth voltage output.

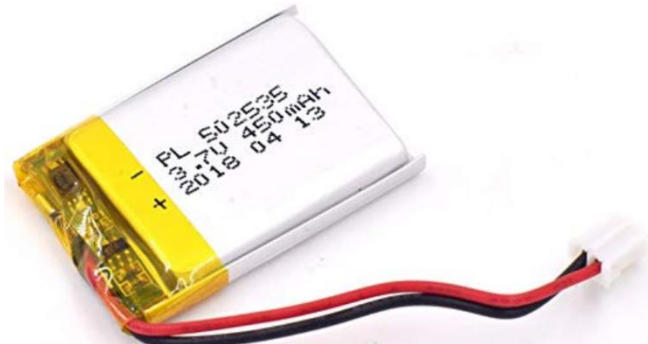


Figure 45: 3.7V rechargeable lithium polymer ion battery

Table 16: 3.7V rechargeable li-po battery technical specs

Voltage: DC 3.7V; Capacity: 450mAh
Material: Lithium Polymer; Net Weight: 9g
Size: 37 x 25 x 5mm / 1.46" x 0.98" x 0.2" (L*W*T)
Connector Type: 2P PH2.0mm Pitch; Cable Length: 5cm / 2"
Package Content: 1 x Lithium Polymer Battery

Once the microcontroller sends position data to the servo motor, the HS-5585MH servo motor will actuate the VDS mechanism. This specific servo was selected for its economic value. While being

inexpensive, it easily meets the maximum torque requirements. Maximum torque calculations will be discussed later in more detail.



Figure 46: HS-5585MH servo motor

Table 17: HS-5585MH servo motor technical specs

Dimensions	1.57" x 0.78" x 1.49" (39.8 x 19.8 x 37.8mm)	Pulse Amplitude	3-5V
Product Weight	2.10oz (60g)	Operating Temperature	-20°C to +60°C
Output Shaft Style	24 tooth (C1) spline	Continuous Rotation Modifiable	Yes
Voltage Range	6.0V - 7.4V	Direction w/ Increasing PWM Signal	Clockwise
No-Load Speed (6.0V)	0.17sec/60°	Deadband Width	2µs
No-Load Speed (7.4V)	0.14sec/60°	Motor Type	Coreless
Stall Torque (6.0V)	194 oz/in. (14 kg.cm)	Internal Feedback Style	5KΩ Potentiometer
Stall Torque (7.4V)	236 oz/in. (17 kg.cm)	Output Shaft Support	Dual Ball Bearings
Max PWM Signal Range (Standard)	750-2250µsec	Gear Type	Straight Cut Spur
Travel per µs (out of box)	.079°/µsec	Gear Material	Metal
Travel per µs (reprogrammed normal res)	.134°/µsec	Wire Length	11.81" (300mm)
Travel per µs (reprogrammed high res)	118.5°	Wire Gauge	22AWG
Max Travel (out of box)	200.5°		

To avoid damaging lower current components, the servo will be powered using a separate battery. An E-flite lithium polymer battery pack will provide sufficient battery life for the short duration of flight in which the servo motor is active. Furthermore, it is capable of supplying 7.4V; this is enough to generate maximum torque from the servo. Both lithium polymer battery packs are rechargeable.



Figure 47: E-flite lithium polymer battery pack

Table 18: E-flite li-po technical specs

Battery Voltage:	7.4V
Capacity:	200mAh
Cell Configuration:	2S1P
Charge Protection Circuitry:	No
Connector Type:	PH

### 3.1.3.2. Subsystem Integration Overview

## 3.1.4 Design Integrity: Quantitative Analysis

### 3.1.4.1. General Deflection Estimates

The maximum flight force can be derived from the maximum acceleration of the rocket due to the thrust from the L1420R-P motor chosen. The mass of the rocket is 47.1 lbs with a maximum acceleration of 230 feet per second squared so therefore:

$$F = \frac{ma}{g_c} = 47.1 * \frac{230}{32.2} = 336.43 [lbf]$$

Knowing that the inside diameter of the airframe is 6" and the outside diameter is 6.16", the cross-sectional area of the body tube can be calculated as follows:

$$A = \pi * \frac{(D_o^2 - D_i^2)}{2} = \pi * \frac{(6.16^2 - 6.0^2)}{4} = 1.53 [in^2]$$

Therefore, the maximum compressive stress due to the L1420R-P motor is:

$$\sigma = \frac{F}{A} = \frac{336.43}{1.53} = 219.9 [psi]$$

The area moment of inertia was calculated as follows:

$$I_x = \pi * \frac{D_o^4 - D_i^4}{64}$$

where  $I_x$  is the moment of inertia,  $D_o$  is the outer diameter and  $D_i$  is the inner diameter. This calculation can be seen below:

$$I_x = \frac{\pi(6.16^4 - 6.0^4)}{64} = 7.06 [in^4]$$

The Young's modulus of the chosen carbon fiber airframe 0 degrees to loading axis is estimated to be:

$$E = 1.96E7 [psi]$$

The deflection of the airframe due to the maximum flight force can be calculated as follows:

$$\delta = \frac{FL^3}{3EI_x}$$

Starting with the payload bay which has a length of 17", the maximum deflection is:

$$\delta = 336.43 * \frac{17.0^3}{3 * 1.96E7 * 7.06} = 0.003 [in]$$

Similarly, for the avionics bay which has a length of 32.9", the maximum deflection is:

$$\delta = 336.43 * \frac{32.9^3}{3 * 1.96E7 * 7.06} = 0.028 [in]$$

Lastly for the booster bay which has a length of 31", the maximum deflection is:

$$\delta = 336.43 * \frac{31.0^3}{3 * 1.96E7 * 7.06} = 0.024 [in]$$

### 3.1.4.1. Nosecone Shape Calculations

The profile of the spherically blunted tangent ogive nose cone can be calculated in the following manner. Firstly, the length of the nose cone must be known. Since we are using a 4:1 ogive tangent nose cone, and our body tube diameter is 6.16", the length of the nose cone must be:

$$L = 4 * 6.16 = 24.64"$$

Now the ogive radius can be calculated knowing the radius of the nose cone base and its length:

$$\rho = \frac{R^2 + L^2}{2R} = \frac{3.08^2 + 24.64^2}{2 * 3.08} = 104.72"$$

The radius of the spherical nose cap:  $r_n$  will be calculated based on the ideal bluffness ratio of 0.15 which minimized pressure drag and friction drag:

$$r_n = 0.15 * R = 0.15 * 3.08 = 0.462"$$

Moving on, we can now calculate the location of the center of the spherical nose cap as follows:

$$x_0 = L - [(\rho - r_n)^2 - (\rho - R)^2]^{0.5} = 1.42"$$

Lastly, the x and y coordinates of the point of tangency can be calculated:

$$y_t = \frac{r_n * (\rho - R)}{\rho - r_n} = \frac{0.462 * (104.72 - 3.08)}{104.72 - 0.462} = 0.45"$$

$$x_t = x_0 - [r_n^2 - y_t^2]^{0.5} = 1.32"$$

Therefore, the complete profile of the nose cone is now achieved.

#### 3.1.4.1. Bearing calculations

The design life of the bearing can be calculated as follows:

$$L_d = (h)(\omega)(60 \text{ min/hr})$$

Where  $h$  is the number of hours of operation and  $\omega$  is the angular velocity in RPM. Although the exact values for the design life and angular velocity are not known, we can estimate reasonable values such as  $h = 50$  [hrs.] and  $\omega = 600$  [RPM] which means that:

$$L_d = 50 * 600 * 60 = 1.8E6 \text{ [rev]}$$

Knowing the design revolutions, the basic dynamic load rating was calculated as follows:

$$C = P_d \left( \frac{L_d}{10E6} \right)^{\frac{1}{k}}$$

Where  $k = 3$  for ball bearings.

Using a design load value of:

$$P_d = 336.43 * 2 = 672.86 \text{ [lbf]}$$

which is essentially the maximum flight force with a safety factor of 2.0. This leads to the calculation of:

$$C = 379 \text{ lbf}$$

Using this value, the proper thrust bearing was chosen with a dynamic load rating value of 410 [lbf].

Using a similar process, the proper radial bearing was chosen with a dynamic load rating value of 290 [lbf].

#### 3.1.4.2. VDS FEA

##### Sim 1: Area Perpendicular to Flow

The purpose of this simulation is to estimate the drag coefficient and the drag force on the blades at the maximum velocity region of roughly 600 ft/s. Even though the VDS will be deployed after burnout when the velocity drops to roughly 300 ft/s, running the simulations at 600 ft/s automatically incorporates a safety factor of 2 into the design which is essential due to the unpredictable nature of the turbulence.

The guiding equations behind the simulations are as follows:

$$F_d = (C_d * A * \rho * V^2) / 2$$

The simulations neglect friction drag and focuses on the pressure drag in order to give an estimate which should be accurate to within 10 percent.

Table 19: VDS CFD Parameters (Sim 1)

Orientation	Airflow parallel to rocket's motion
Global Goals	$C_d$ and $F_d$

<b>Temperature</b>	293.2 K
<b>Static Pressure</b>	101325 Pa
<b>Velocity (x)</b>	0 m/s
<b>Velocity (y)</b>	183 m/s
<b>Velocity (z)</b>	0 m/s
<b>Area exposed to flow</b>	5.5 inches squared
<b>Density of air</b>	1.225 kg per cubic meters

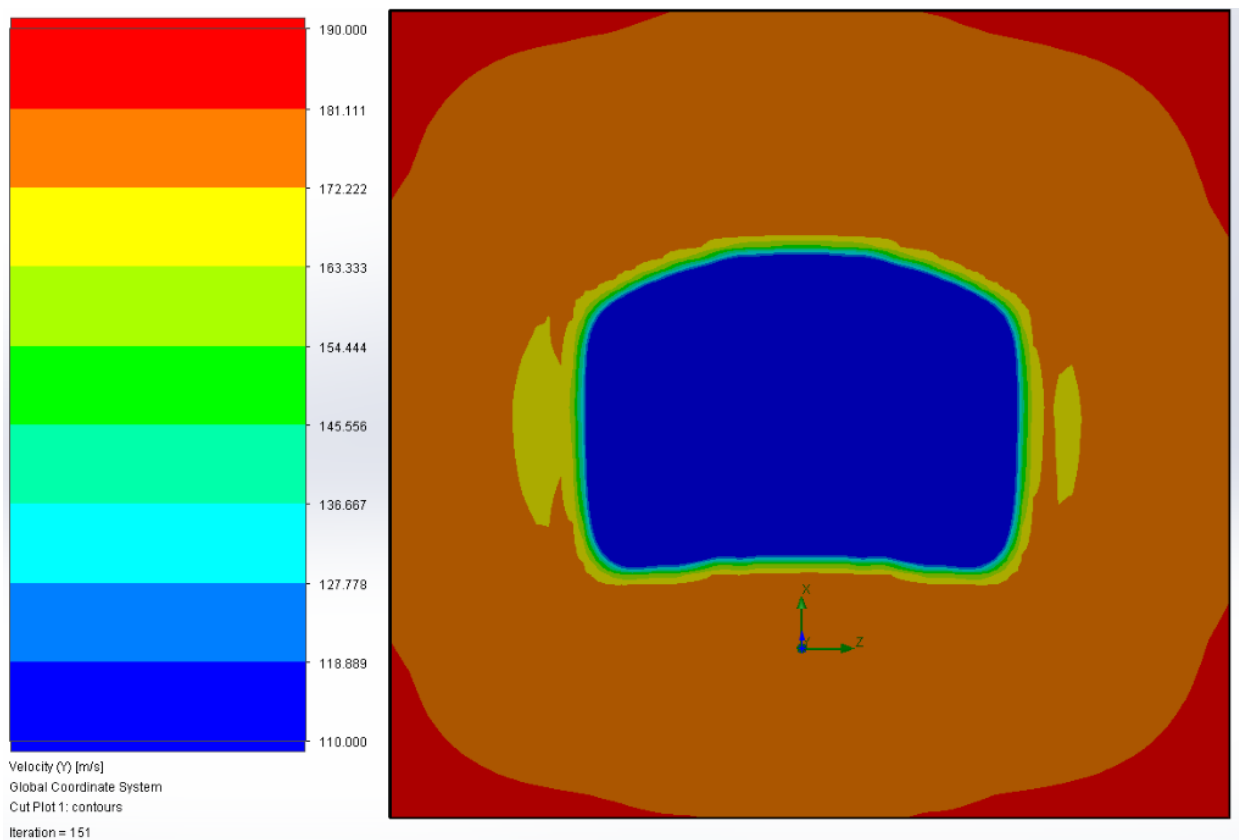


Figure 48: VDS Velocity Gradient (Sim 1)

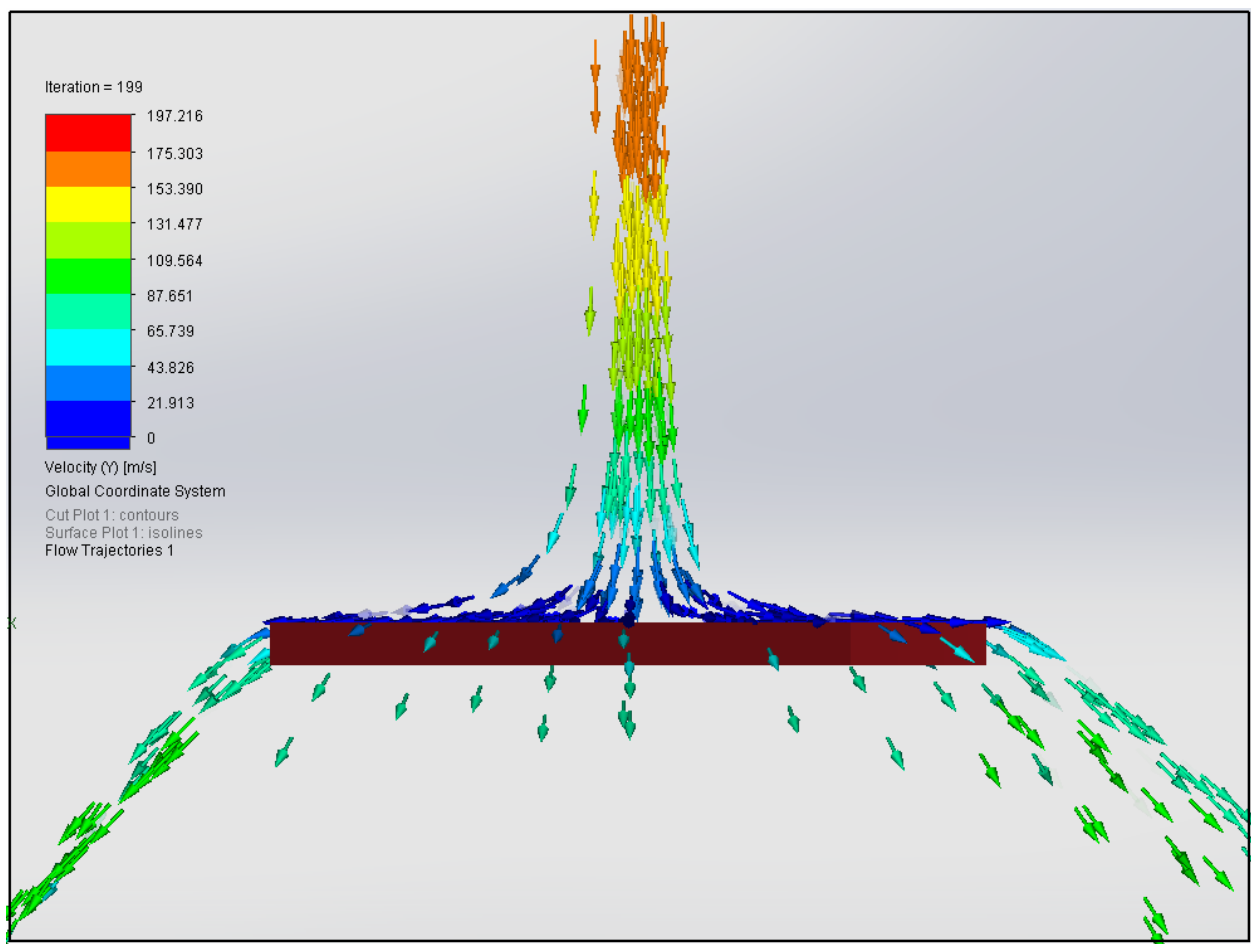


Figure 49: VDS Flow Visualization A (Sim 1)

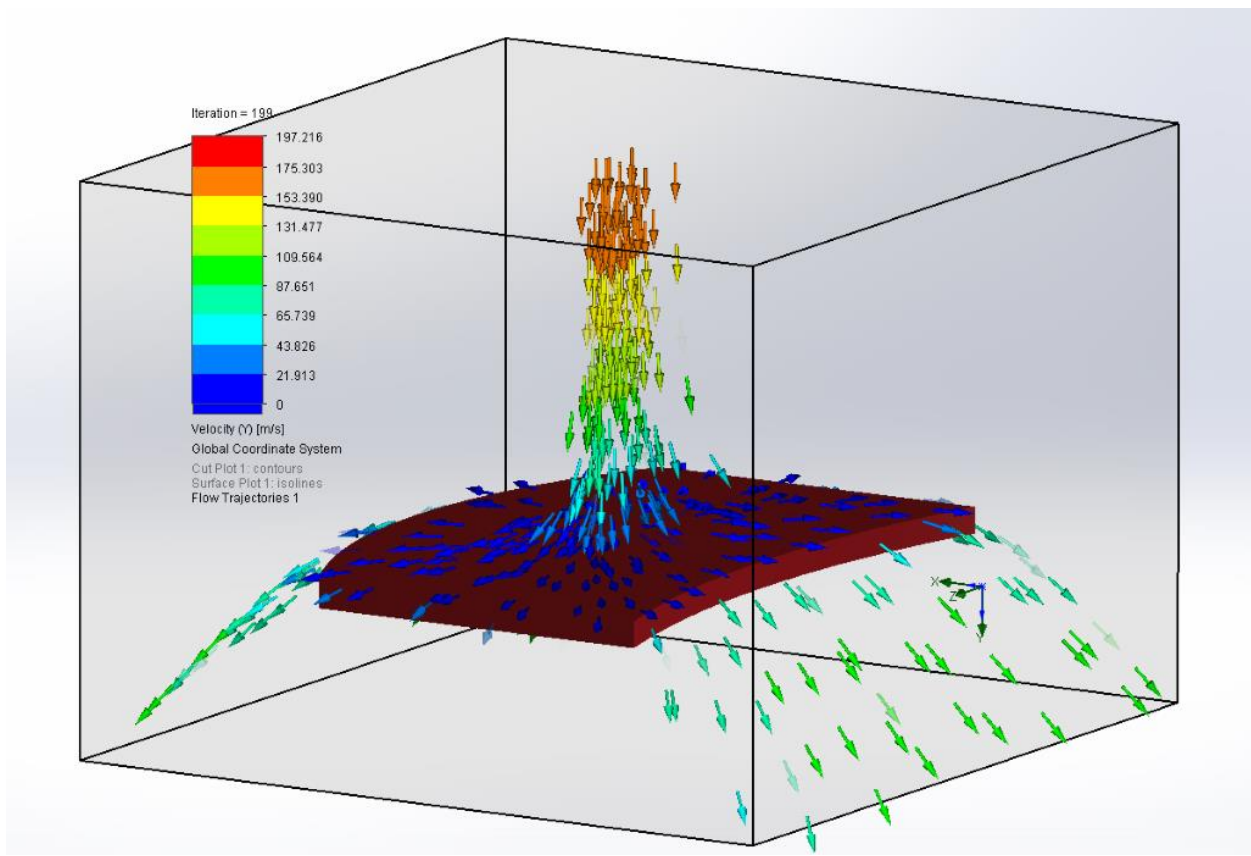


Figure 50: VDS Velocity Flow Visualization B (Sim 1)

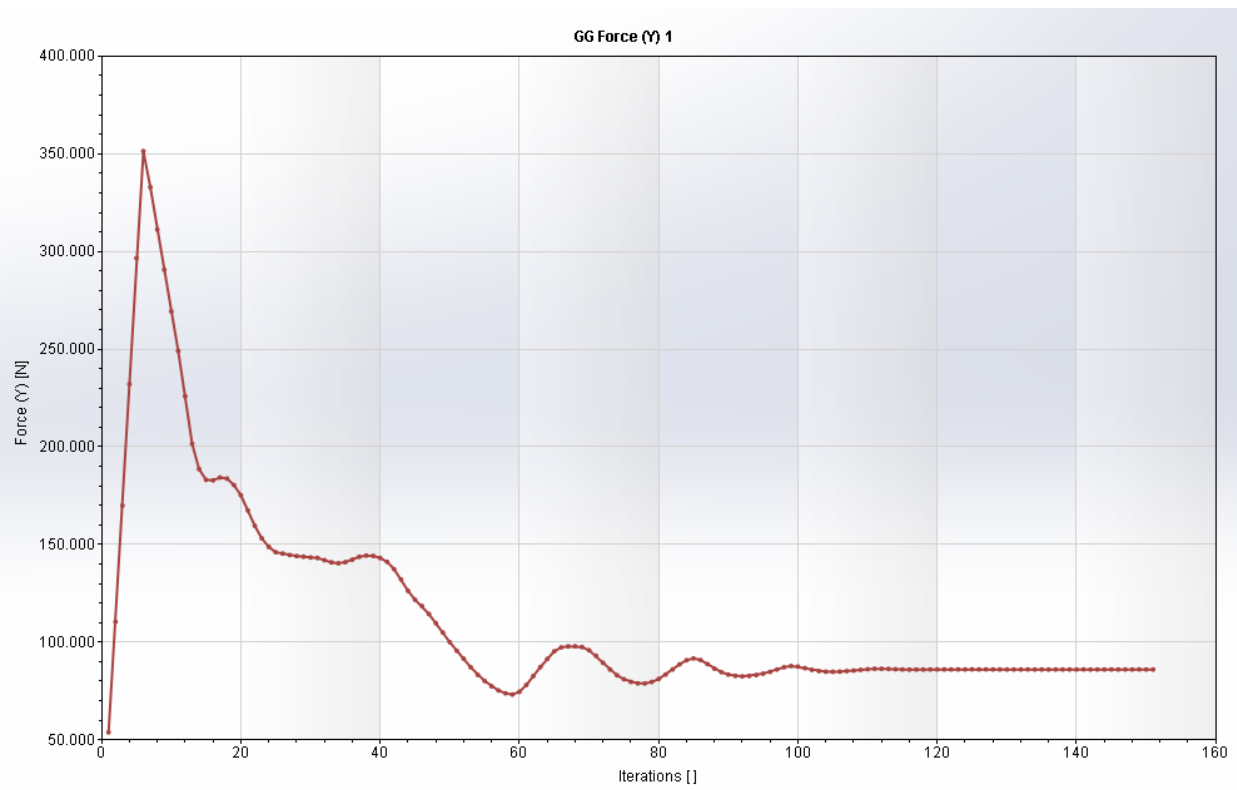


Figure 51: VDS Drag Force vs. Iteration

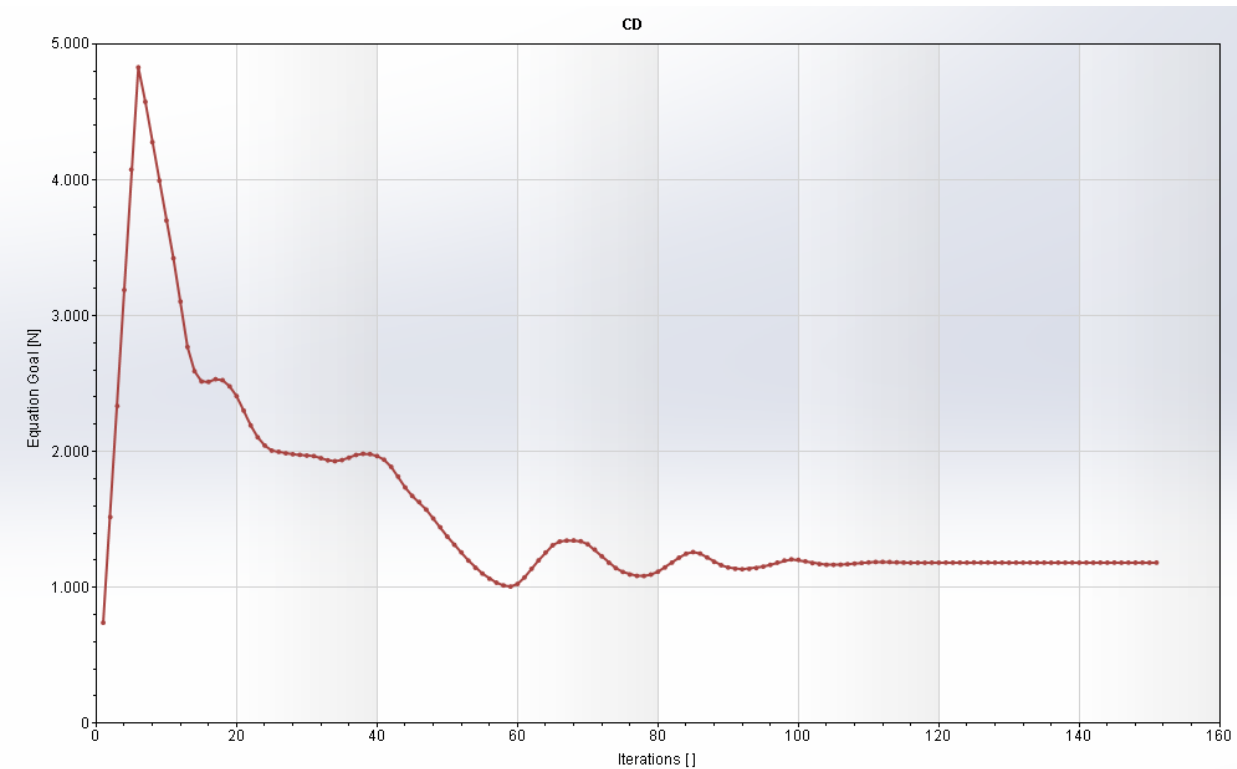


Figure 52: VDS Drag Coeffiecient vs. Iteration

Table 20: VDS CFD Sim 1 Results

<b>Final Drag Force (lbf)</b>	19.35
<b>Final Drag Coefficient</b>	1.18
<b>Minimum Drag Force (lbf)</b>	18.55
<b>Minimum Drag Coefficient</b>	1.13
<b>Max Drag Force (lbf)</b>	19.97
<b>Max Drag Coefficient</b>	1.22
<b>Iterations</b>	150

Therefore, the drag force on each blade is roughly 19.35 lbf and the simulated drag coefficient is 1.18. Comparing to the known drag coefficient of 1.17 of flat plates in perpendicular flow, the simulated results closely match expectations with a percent difference of 0.76%. Assuming the drag force will act at the centroid of the blades, the calculated lever arm is 1.07". Therefore, the maximum pitch moment on the carriage is as follows:

$$\text{Lever Arm} = 1.07"$$

The maximum moment can be calculated:

$$\text{Max Moment} = 19.35 * \frac{1.07}{12} = 1.73 \text{ lbf} * \text{ft}$$

### Sim 2: Airflow Along the z-direction

The purpose of this simulation is to estimate the drag coefficient and the drag force on the sides of blades at the maximum velocity region of roughly 600 ft/s. This is a massive over approximation since the airflow along the z-direction is not going to have the same velocity as the airflow parallel to the rocket's motion.

Table 21: VDS Parameters (Sim 2)

<b>Orientation</b>	Area oriented along the z-direction
<b>Global Goals</b>	$C_d$ and $F_d$
<b>Temperature</b>	293.2 K
<b>Static Pressure</b>	101325 Pa
<b>Velocity (x)</b>	0 m/s
<b>Velocity (y)</b>	0 m/s
<b>Velocity (z)</b>	183 m/s
<b>Area exposed to flow</b>	0.31821 inches squared
<b>Density of air</b>	1.225 kg per cubic meters

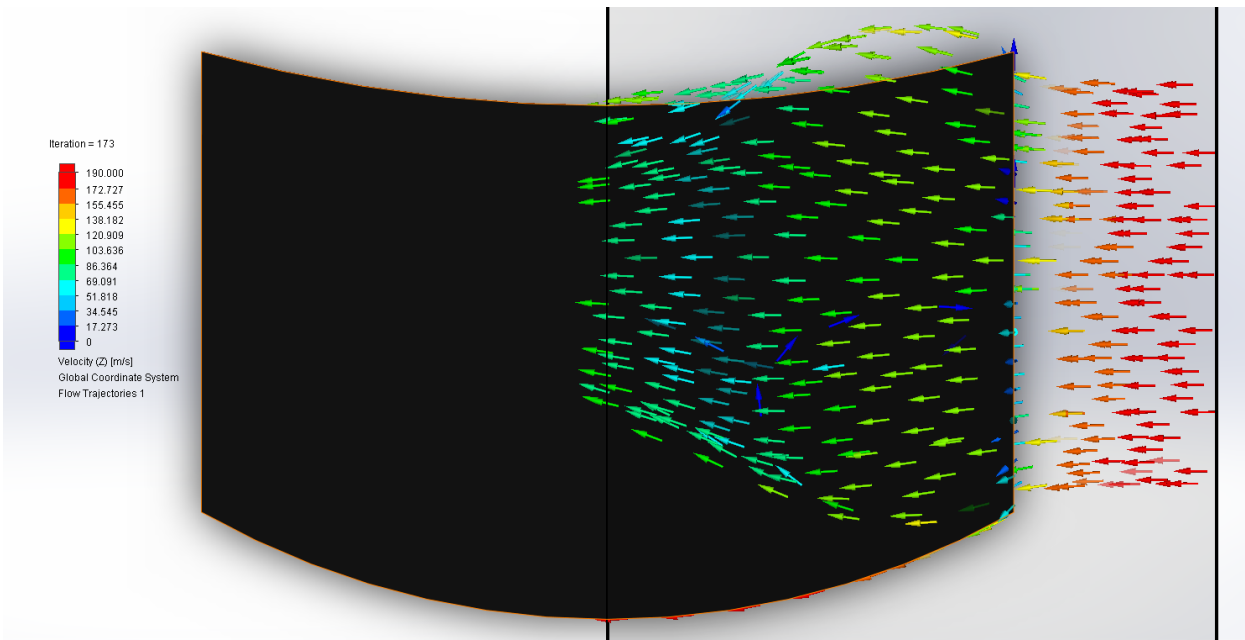


Figure 53: VDS Flow Visualization (Sim 2)

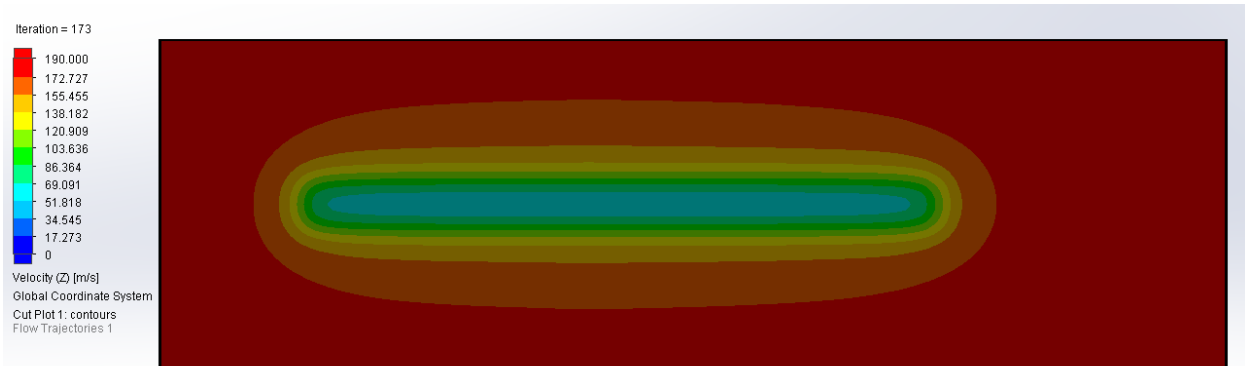


Figure 54: VDS Velocity Gradient A (Sim 2)

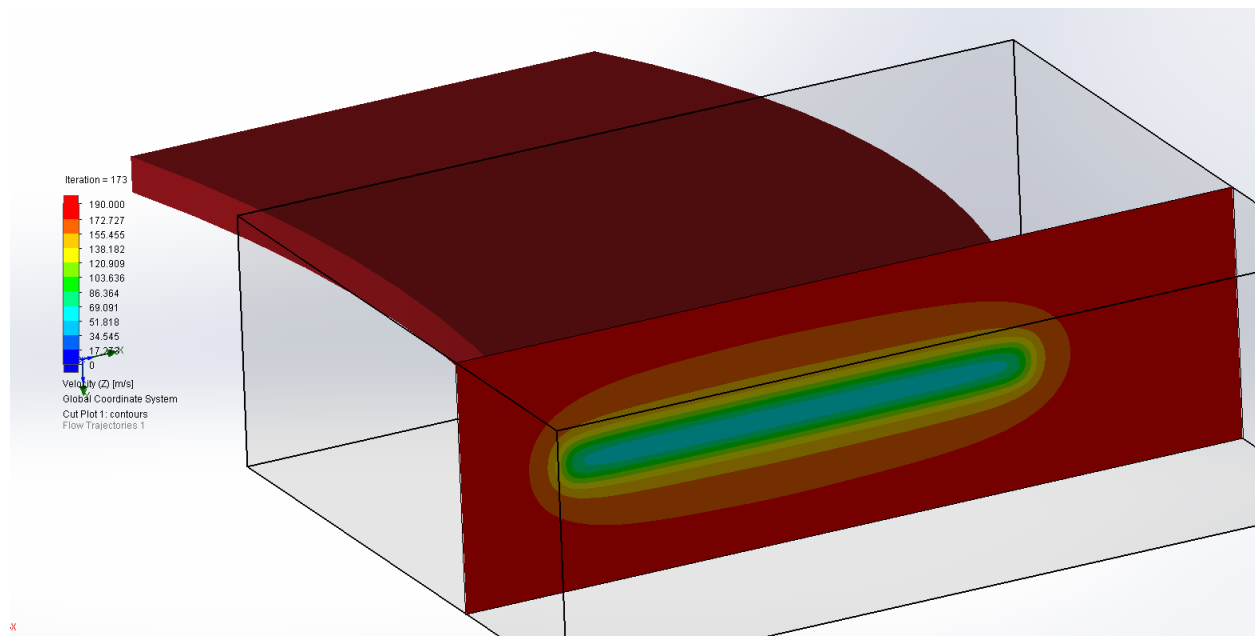


Figure 55: VDS Velocity Gradient B (Sim 2)

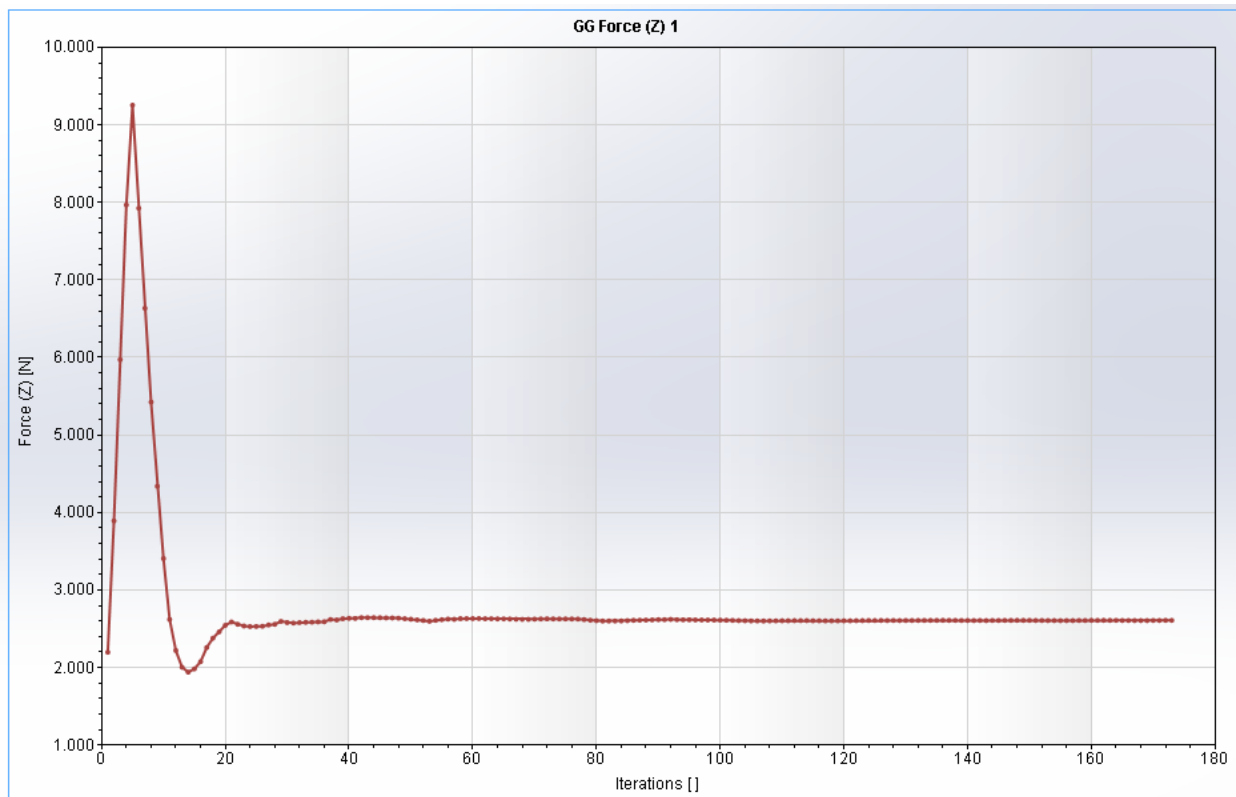


Figure 56: VDS Drag Force vs. Iterations (Sim 2)

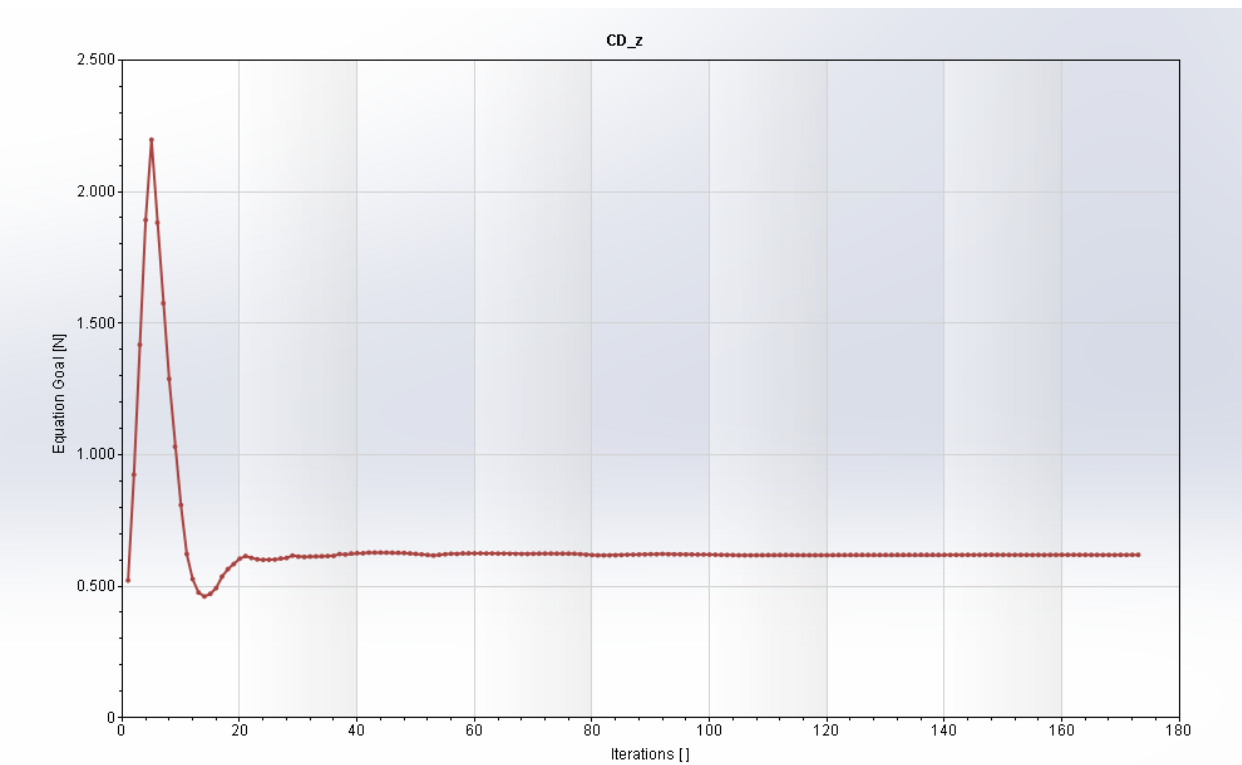


Figure 57: VDS Drag Coefficient vs. Iterations (Sim 2)

Table 22

<b>Final Drag Force (lbf)</b>	0.59
<b>Final Drag Coefficient</b>	0.62
<b>Minimum Drag Force (lbf)</b>	0.58
<b>Minimum Drag Coefficient</b>	0.61
<b>Max Drag Force (lbf)</b>	0.59
<b>Max Drag Coefficient</b>	0.62
<b>Iterations</b>	175

Therefore, the drag force on each blade is roughly 0.59 lbf and the simulated drag coefficient is 0.62. Assuming the drag force will act at the centroid of the blades, the calculated lever arm is 0.25.”

Therefore, the maximum roll moment can be calculated:

$$\text{Max Roll Moment} = 0.58 * \frac{0.25}{12} = 0.0121 \text{ lbf} * \text{ft}$$

### Sim 3: Airflow in the Axial Direction

The purpose of this simulation is to estimate the drag coefficient and the drag force on the sides of blades at the maximum velocity region of roughly 600 ft/s. This is a massive over approximation since the airflow along the x-direction is not going to have the same velocity as the airflow axial to the rocket's motion.

Table 23: VDS CFD Parameters (Sim 3)

<b>Orientation</b>	Area oriented along the x-direction
<b>Global Goals</b>	$C_d$ and $F_d$
<b>Temperature</b>	293.2 K
<b>Static Pressure</b>	101325 Pa
<b>Velocity (x)</b>	183 m/s
<b>Velocity (y)</b>	0 m/s
<b>Velocity (z)</b>	0 m/s
<b>Area exposed to flow</b>	0.5881 inches squared
<b>Density of air</b>	1.225 kg per cubic meters

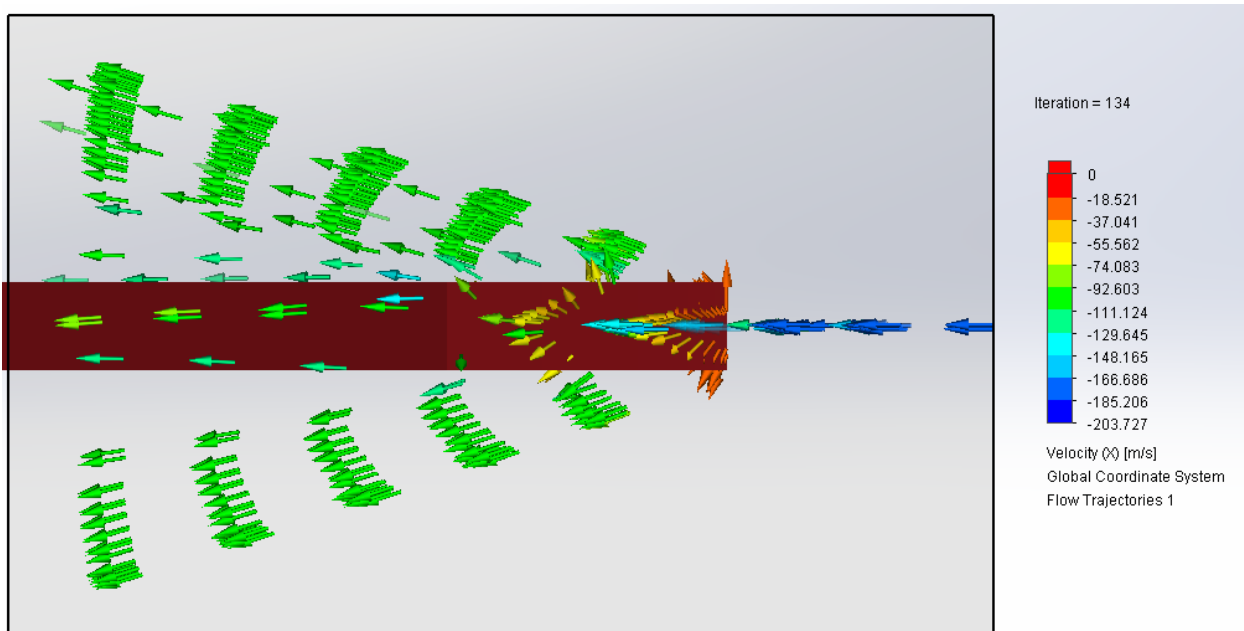


Figure 58: VDS Flow Visualization (Sim 3)

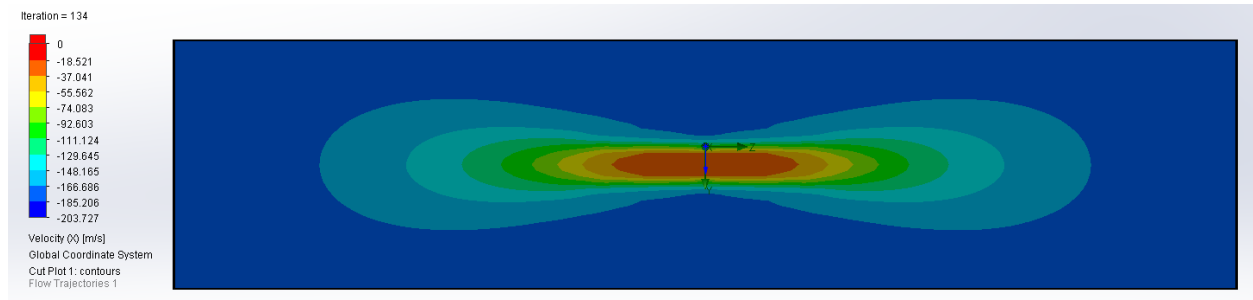


Figure 59: VDS Velocity Gradient A (Sim 3)

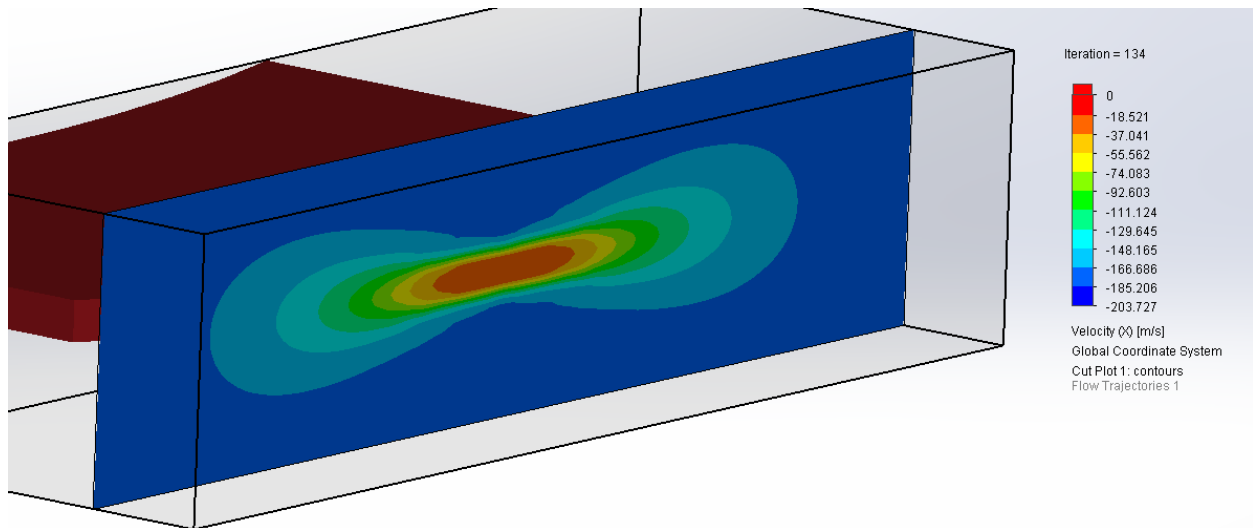


Figure 60: VDS Velocity Gradient B (Sim 3)

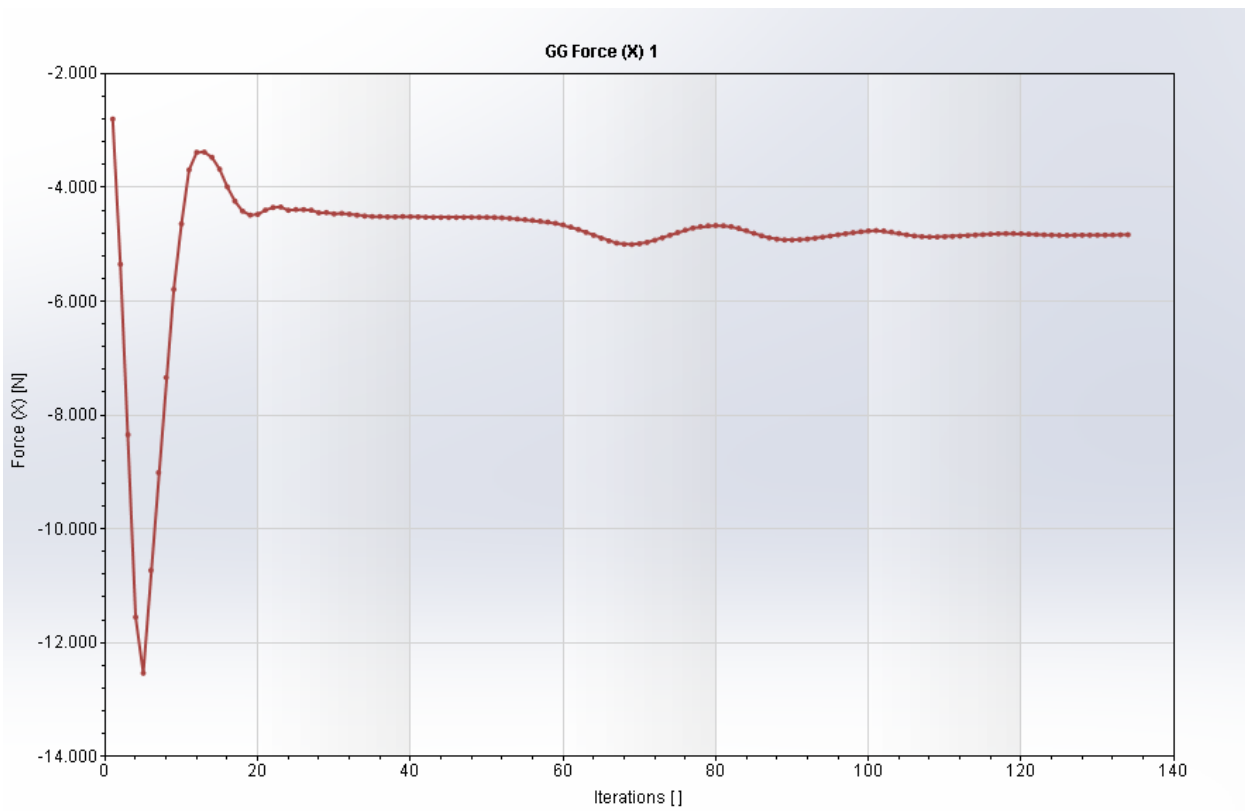


Figure 61: VDS Drag Force vs. Iterations (Sim 3)

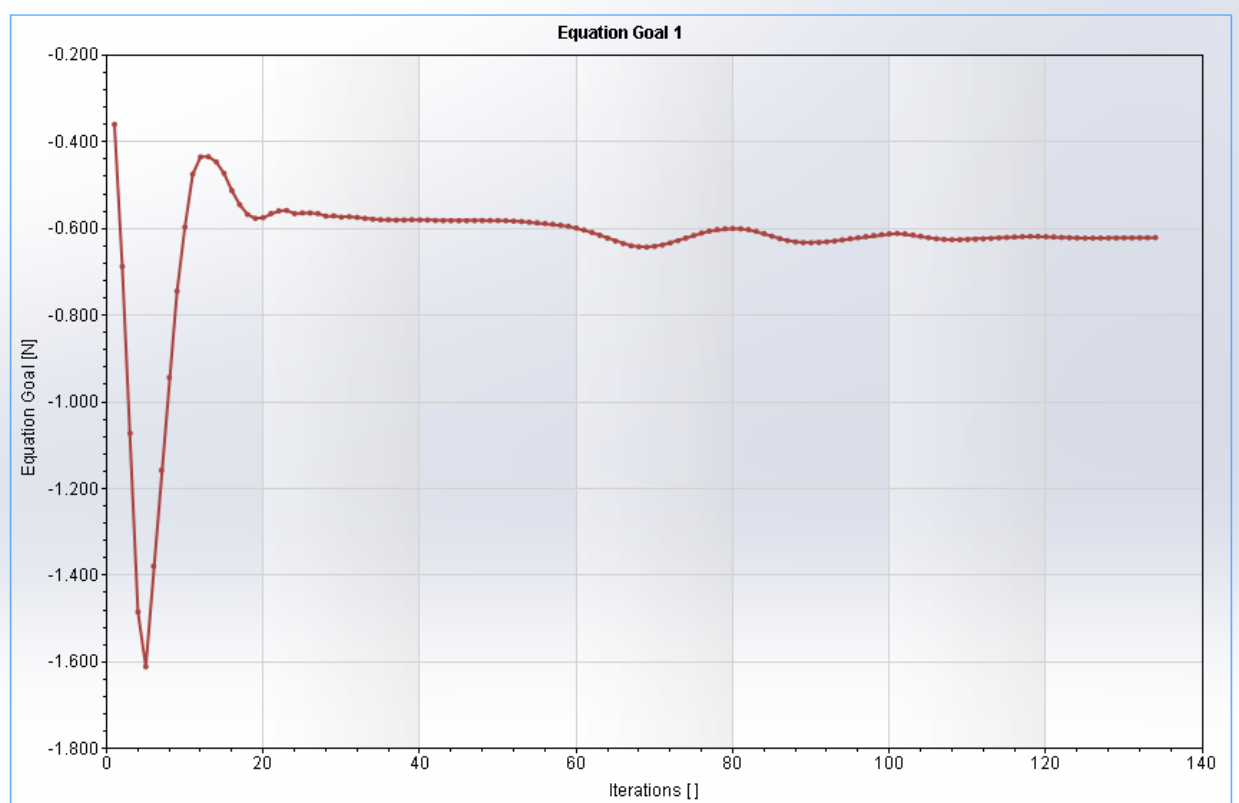


Figure 62: Figure 63: VDS Drag Coefficient vs. Iterations (Sim 3)

Table 24: VDS CFD Results (Sim 3)

<b>Final Drag Force (lbf)</b>	1.086
<b>Final Drag Coefficient</b>	0.621
<b>Minimum Drag Force (lbf)</b>	1.05
<b>Minimum Drag Coefficient</b>	0.60
<b>Max Drag Force (lbf)</b>	1.11
<b>Max Drag Coefficient</b>	0.633
<b>Iterations</b>	135

Therefore, the drag force on each blade is roughly 1.086 lbf and the simulated drag coefficient is 0.621. Assuming the drag force will act at the centroid of the blades, the calculated lever arm is 0.25". Therefore, the maximum yaw moment on the carriage is as follows:

$$\text{Max Yaw Moment} = 1.086 * \frac{0.25}{12} = 0.023 \text{ lbf} * \text{ft}$$

Knowing the moments, the rail and carriage system was picked out with the following specs:

Table 25: Carriage Moment Load Capacities

<b>Static Pitch Moment Load Capacity (ft.-lbs)</b>	3.4
<b>Static Roll Moment Load Capacity (ft.-lbs)</b>	5.0
<b>Static Yaw Moment Load Capacity (ft.-lbs)</b>	2.8

Therefore, the safety factors for the calculated moments are as follows:

Table 26: Carriage Moment Safety Factors

<b>Static Pitch Moment SF</b>	1.97
<b>Static Roll Moment SF</b>	41.3
<b>Static Yaw Moment SF</b>	121.7

Even though the system is overdesigned with respect to the roll moment and yaw moment, the high pitch moment faced by the system resulted in the final design with a minimum safety factor of roughly 2.0.

Now the motor for the VDS unit can be sized by approximating the ball bearing friction coefficient in the carriage to be 0.003. For the calculation purposes we will assume it is 0.01 with a safety factor of 3.33 since it is very difficult to accurately estimate the coefficient of friction. Assuming that each blade experiences 200 lbf of force with a safety factor of 10, the friction force can be calculated as follows:

$$F_f = \mu F_N = 0.01 * 200 = 2 \text{ lbf}$$

The force due to airflow along the rail direction was previously calculated to be 1.086 lbf via the CFD analysis. Therefore, the total force towards the rail direction is:

$$F_R = 2 + 1.086 = 3.086 \text{ lbf}$$

With the designed length of each actuating link being 0.91 inches, the maximum force towards the link can be calculated at an angle of 28.6 degrees when the linkage is fully retracted inside of the airframe. The force towards the link is therefore:

$$F_L = \cos(28.6) * 3.086 = 2.71 \text{ lbf}$$

The force perpendicular to the lever arm is:

$$F_{perp} = 2.71 * \sin(46.9) = 1.98$$

The torque on each blade is therefore:

$$T_B = FL = 1.98 * 0.91 * 16 = 28.83 [\text{oz} * \text{in}]$$

The total torque due to the three blades is then:

$$T_T = 3 * 28.83 = 86.5 [\text{oz} * \text{in}]$$

Using a safety factor of 2.5, the required stall torque from the motor must be 215.225 oz-in.

### 3.1.4.3. Fin Flutter

Above a certain velocity boundary, rocket fins will amplify the oscillations and rapidly increase the energy in the fin to the point of destruction. This velocity is known as the flutter velocity. To ensure the rocket does not exceed this velocity, the flutter velocity must be higher than the maximum velocity experienced by the fins. The flutter velocity can be calculated using the following formulation:

$$V_f = 1.223 * C_s * \exp\left(\frac{0.4h}{H}\right) * \left(\frac{G}{P_0}\right)^{0.5} \left(\frac{2+B}{1+\alpha}\right)^{0.5} \left(\frac{T}{B}\right)^{\frac{3}{2}}$$

Where:

**Table 27: Fin Flutter Variables**

$V_f$	Flutter Velocity
$c_r$	Root Chord
$c_t$	Tip Chord
$b$	Fin Height
$t$	Fin Thickness
$G$	Shear Modulus
$H$	Scale Height
$h$	Altitude at Max Velocity
$P_0$	Atmospheric Pressure
$C_s$	Speed of Sound

S	Fin Area
$\alpha$	Taper Ratio
B	Aspect Ratio
T	Normalized Thickness

Since the shear modulus of G10 Fiberglass is not readily known, it can be estimated from the Young's modulus. Using a Young's modulus value of 3500000 psi, and a Poisson's ratio value of 0.12, the shear modulus can be calculated as follows:

$$G = \frac{E}{2(1 + \nu)} = \frac{3500000}{2 * (1 + 0.12)} = 1.5625E6 \text{ psi}$$

Using input values as listed below, the flutter velocities can be calculated for a thickness value of 0.125":

Table 28: Fin Flutter Input Values

$V_f$	940 ft/s
$c_r$	14"
$c_t$	4.5"
$b$	6.5"
$t$	0.125"
G	1.5625E6 psi
H	26500 ft
h	3000 ft
$P_0$	14.7 psi
$C_s$	1100 ft/s
S	60.125 in^2
$\alpha$	0.3214
B	0.7027
T	0.0089

Therefore, the flutter velocity of the fins is 940 ft/s which is significantly higher than the maximum velocity of 615 ft/s as experienced by the launch vehicle thus resulting in a safety factor of 1.53.

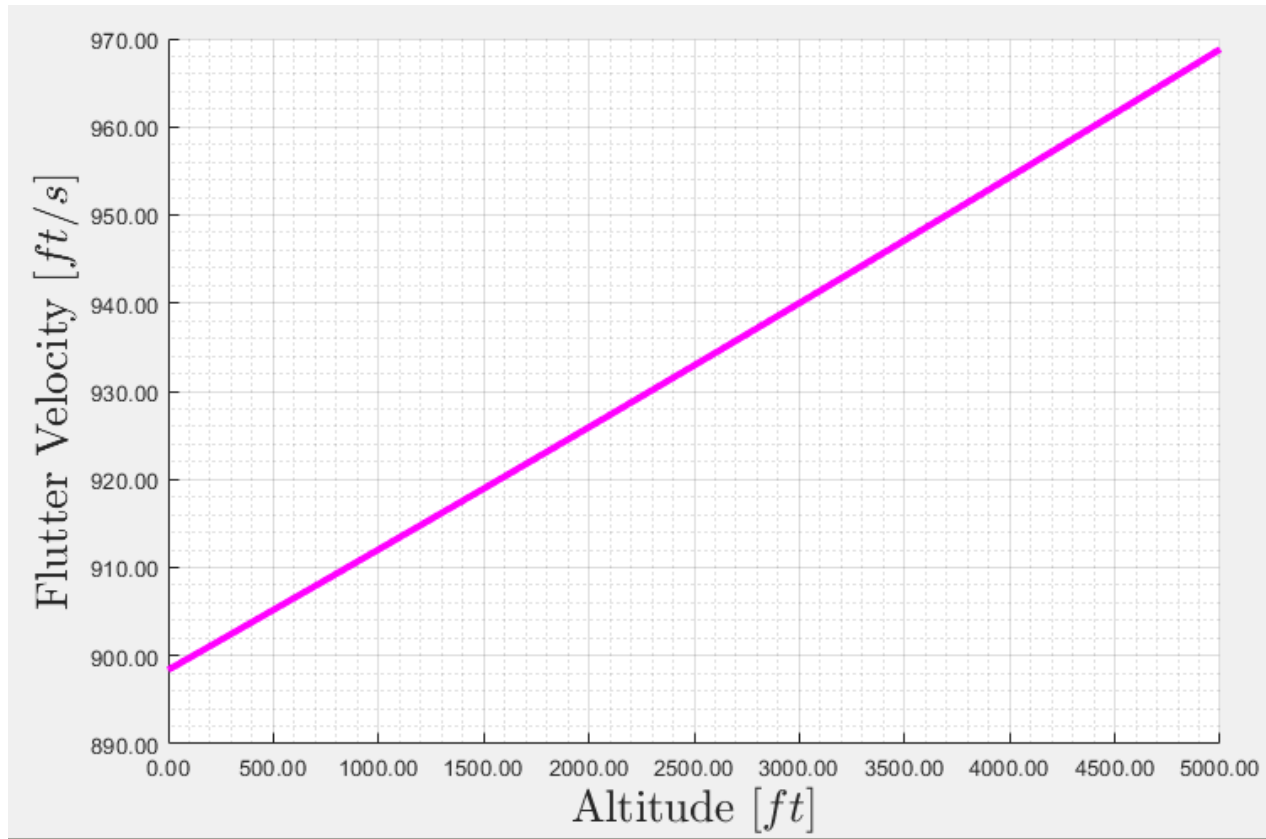


Figure 64: Fin Flutter vs. Altitude for 0.125" Fiberglass Fins.

The flutter velocity of the same set of fins with a thickness of 0.1875" was calculated to be 1726.9 ft/s with a safety factor of 2.81. Since these thick fins would add extra weight and has an unnecessarily large safety factor, the final design incorporates fins with a thickness of 0.125".

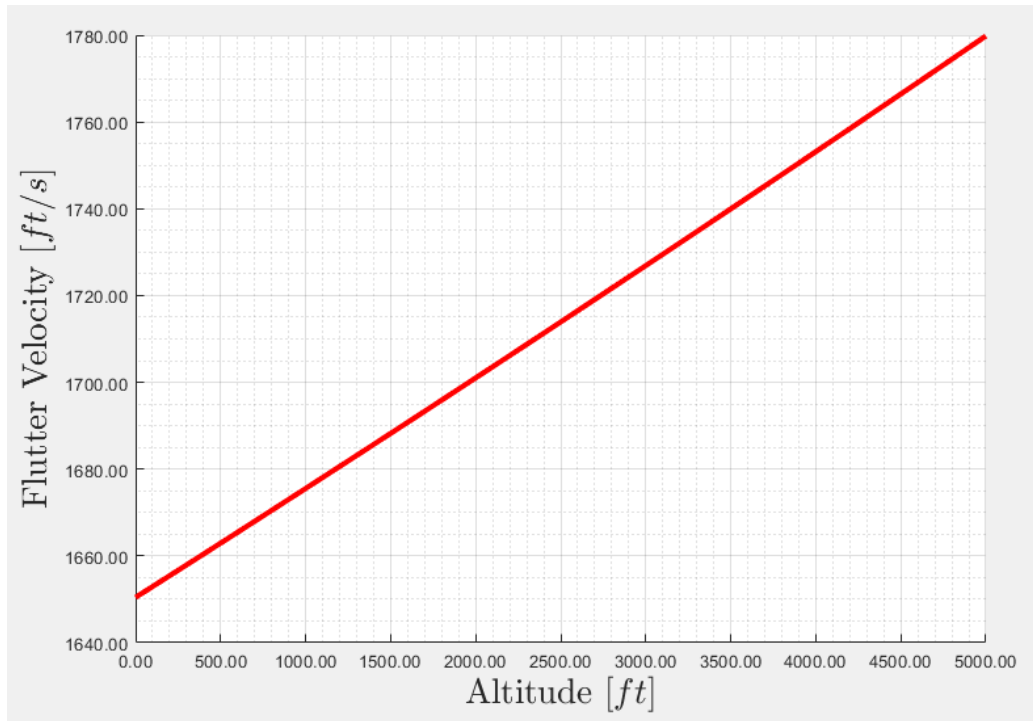


Figure 65: Fin Flutter vs. Altitude for 0.1875" Fiberglass Fins.

#### 3.1.4.1. Fin Torque: CFD & FEA

The purpose of this set of simulations is calculate the torque on the fins which will cause rotation of the rocket. This will be a result of crossflow during the flight. The estimated velocity of air is taken to be 61 m/s or 200 ft/s. Once again, this was simulated at the worst-case scenario to see how the fins will perform when pushed to the limits.

Table 29: Fin Torque CFD Parameters

<b>Orientation</b>	Cross section of fin directly in airflow
<b>Global Goals</b>	$C_d$ and $F_d$
<b>Temperature</b>	293.2 K
<b>Static Pressure</b>	101325 Pa
<b>Velocity (x)</b>	0 m/s
<b>Velocity (y)</b>	0 m/s
<b>Velocity (z)</b>	61 m/s
<b>Area exposed to flow</b>	0.0388 meters squared
<b>Density of air</b>	1.225 kg per cubic meters

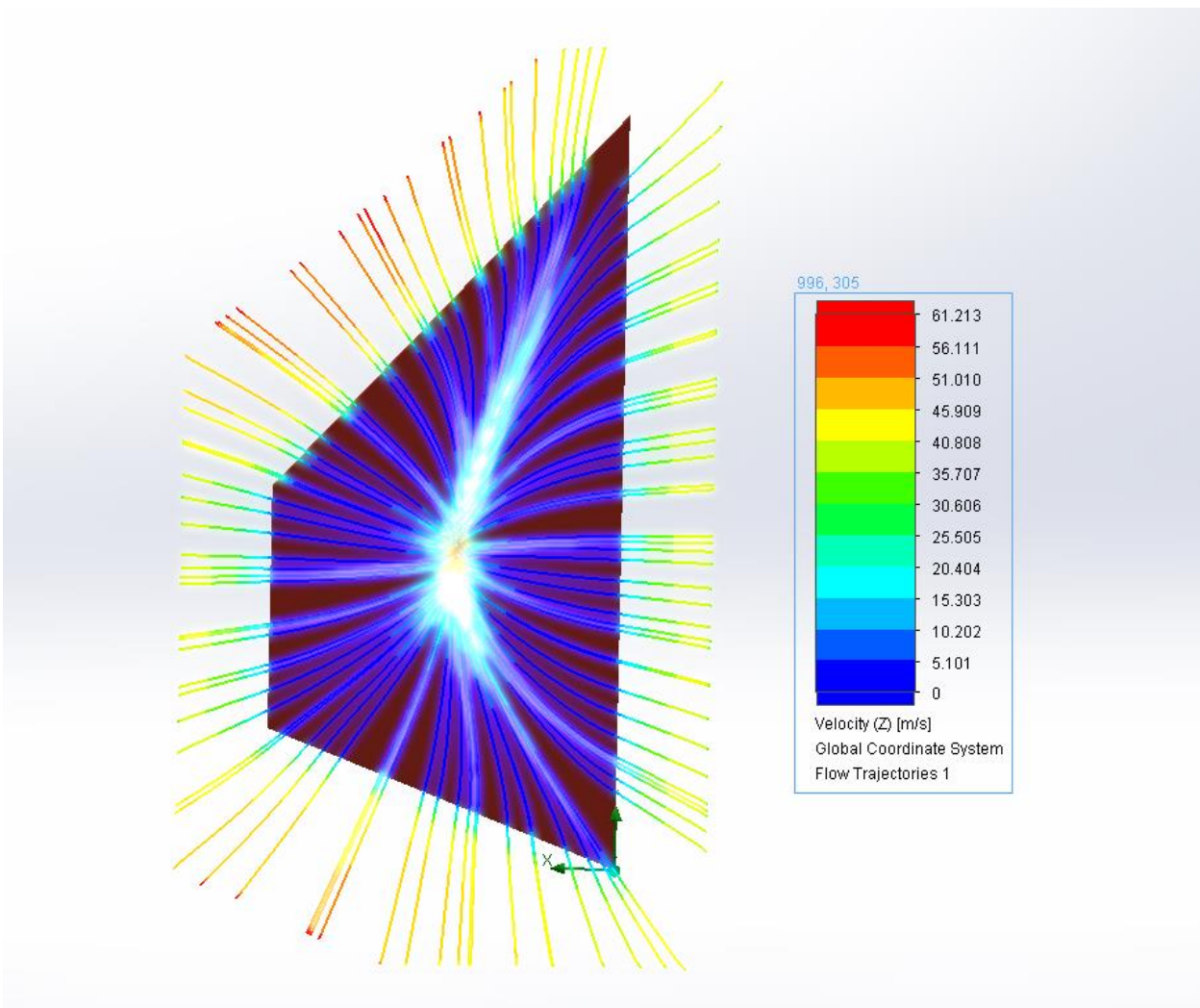


Figure 66: Fin Torque CFD Flow Visualization A.

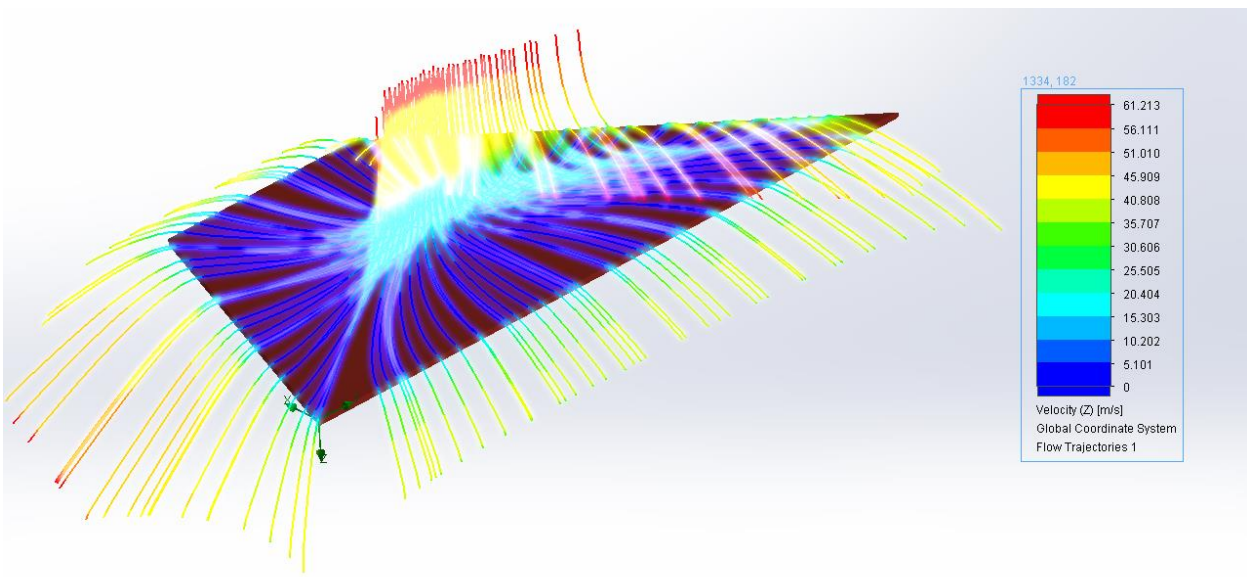


Figure 67: Fin Torque CFD Flow Visualization B.

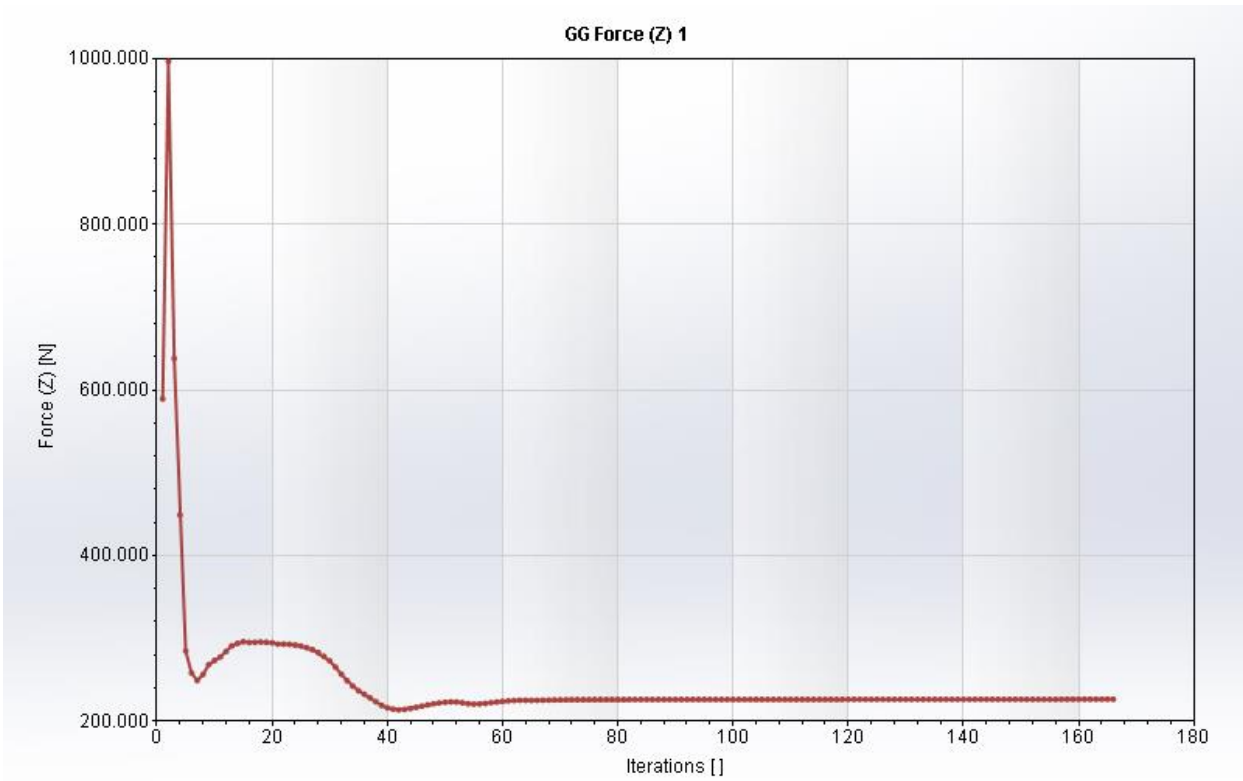


Figure 68: Fin Torque Drag Force vs. Iterations.

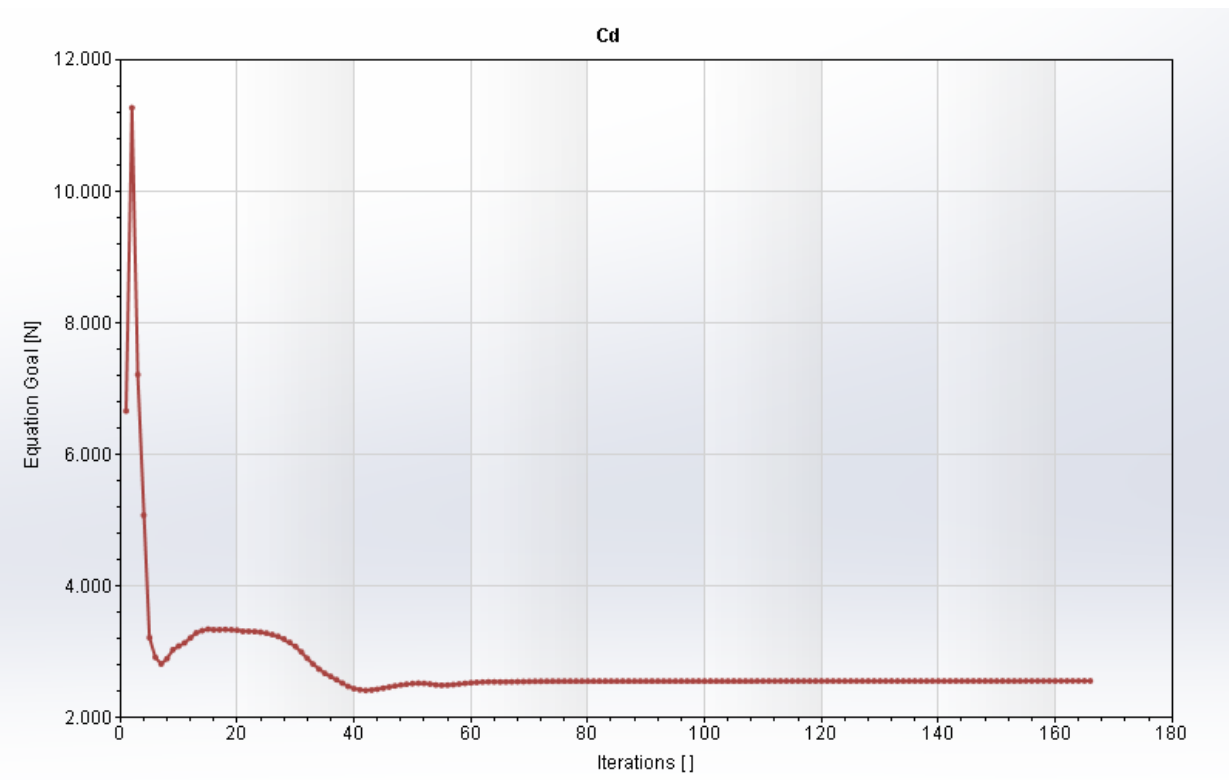


Figure 69: Fin Torque Drag Coefficient vs. Iterations.

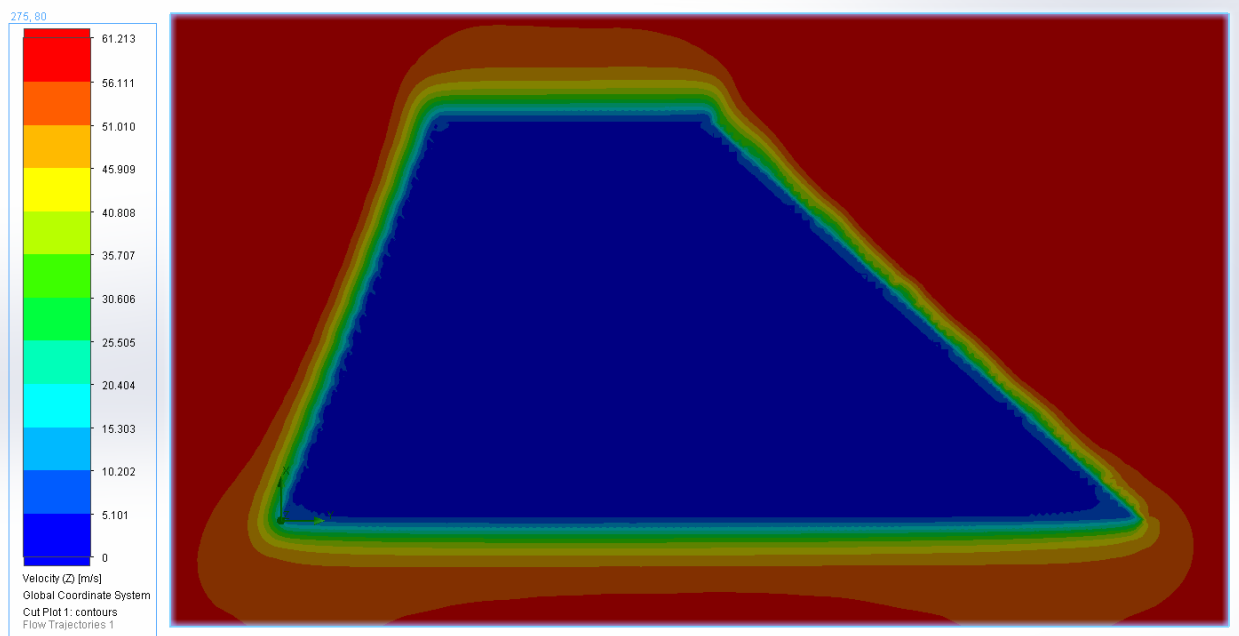


Figure 70: Fin Torque Velocity Gradient.

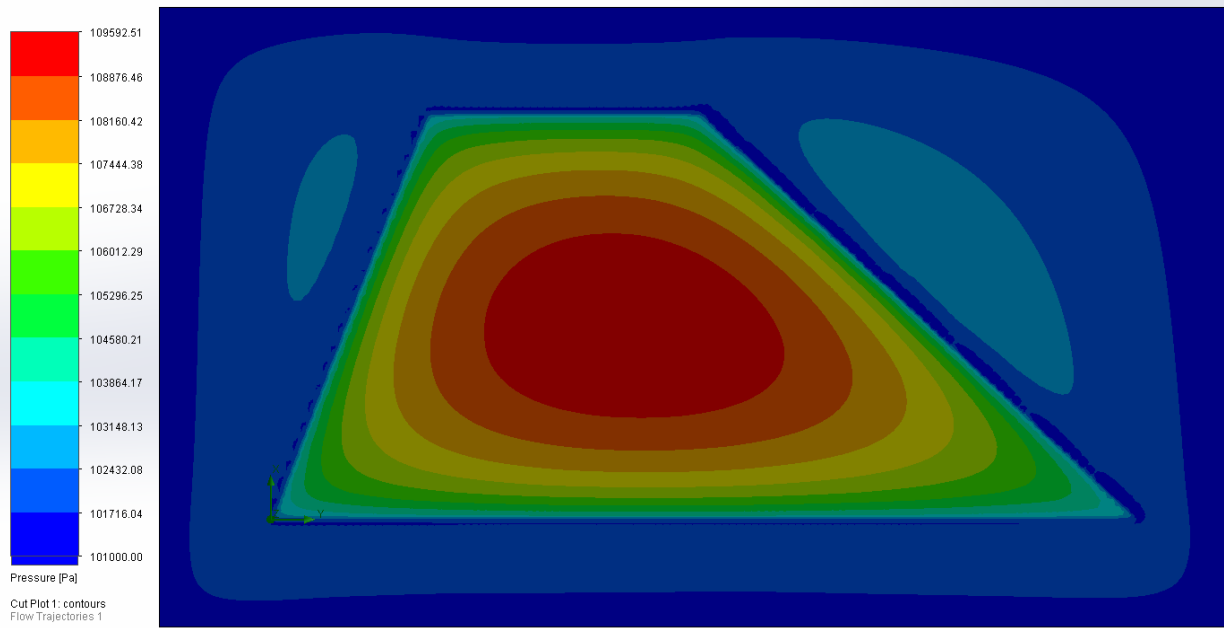


Figure 71: Fin Torque Pressure Gradient.

Table 30: Fin Torque CFD Results

<b>Final Drag Force (lbf)</b>	50.888
<b>Final Drag Coefficient</b>	2.56
<b>Minimum Drag Force (lbf)</b>	50.85
<b>Minimum Drag Coefficient</b>	2.558
<b>Max Drag Force (lbf)</b>	1.11
<b>Max Drag Coefficient</b>	50.89
<b>Iterations</b>	~170

Therefore the force on the fins at the worst possible conditions was simulated to be 50.89 lbs. This value can now be used to perform FEA. Since it is very difficult to simulate G10 fiberglass in modeling, aluminum was used since it is a very predictable metal. Upon research, it was found that the tensile and compressive strengths of G10 fiberglass is essentially a 1/3 of 6061 aluminum

perpendicular to the fiber direction (worst-case).

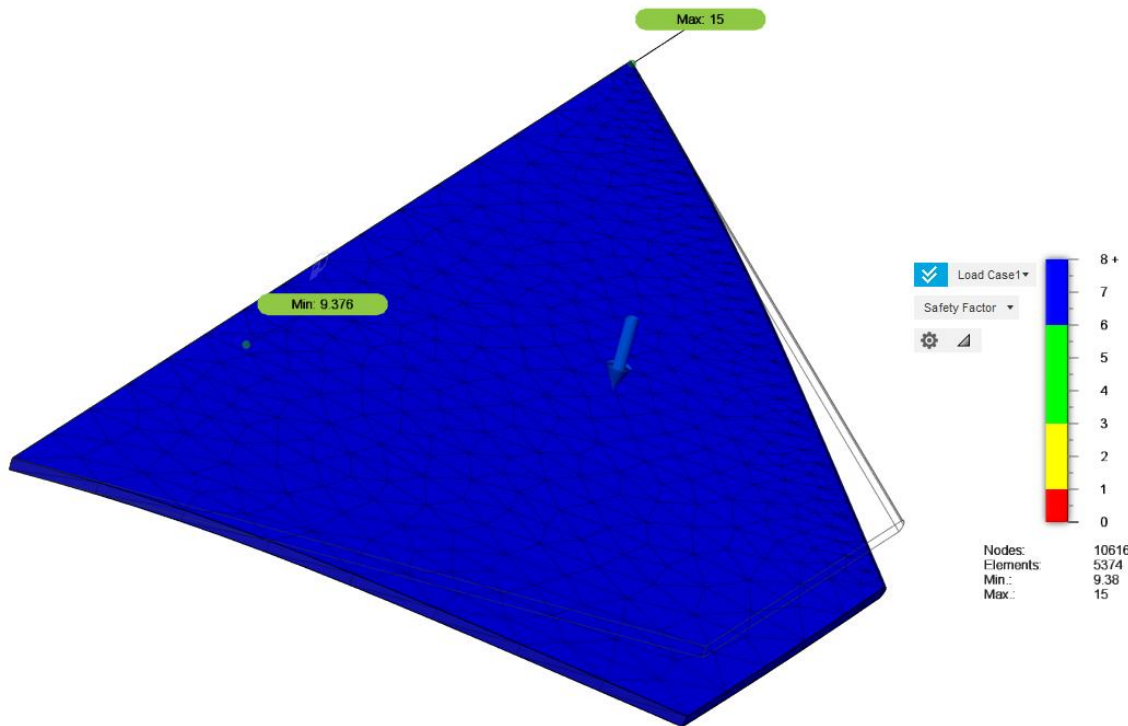


Figure 72: SF FEA (Fins)

FEA results conclude a minimum safety factor of bending 3.1 when adjusted for G10 fiberglass properties.

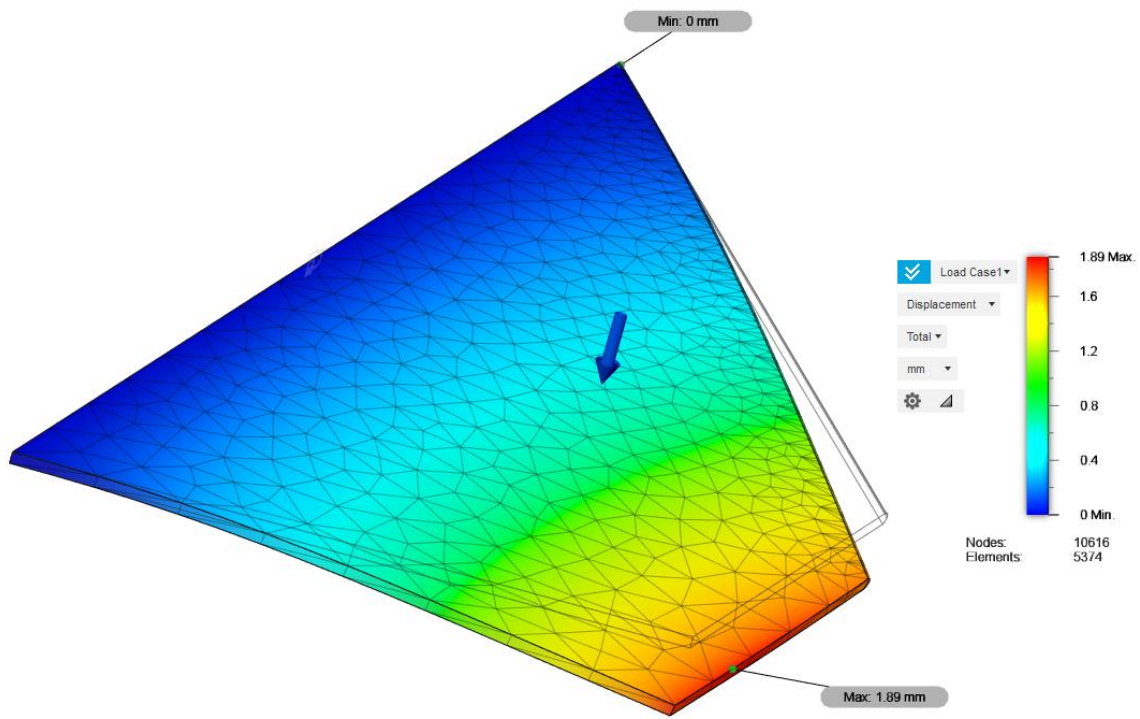
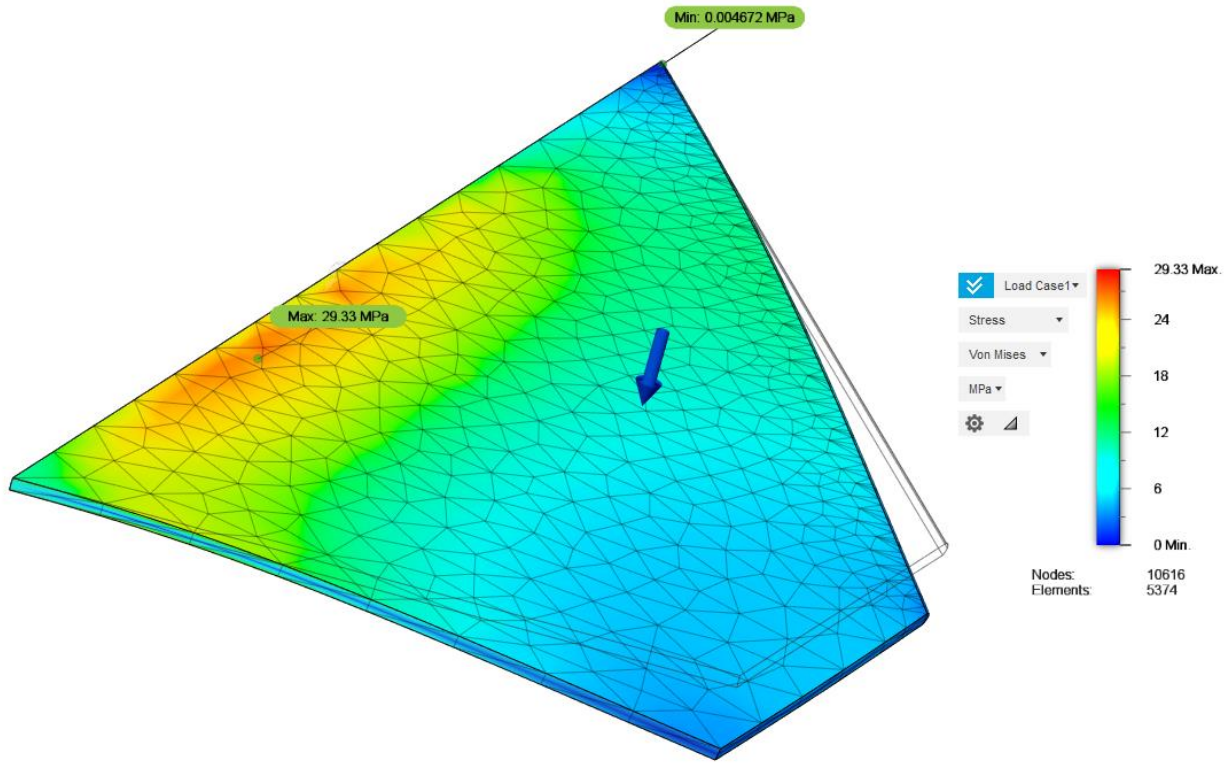


Figure 73: Displacement FEA (Fins)

FEA results conclude a maximum displacement of 5.67 mm when adjusted for G10 fiberglass properties.



**Figure 74: Stress Profile FEA (Fins)**

FEA results conclude a maximum Von Mises stress value of 88 MPa when adjusted for G10 fiberglass properties.

#### 3.1.4.2. Center of Pressure CFD

The purpose of this set of simulations is to calculate the center of pressure of the vehicle based on flow conditions.

**Table 31: CP CFD Parameters**

Global Goals	Perpendicular Torques and Force Values
Temperature	293.2 K
Static Pressure	101325 Pa
Velocity (x)	200 m/s
Velocity (y)	0 m/s
Velocity (z)	200 m/s
Density of air	1.225 kg per cubic meters

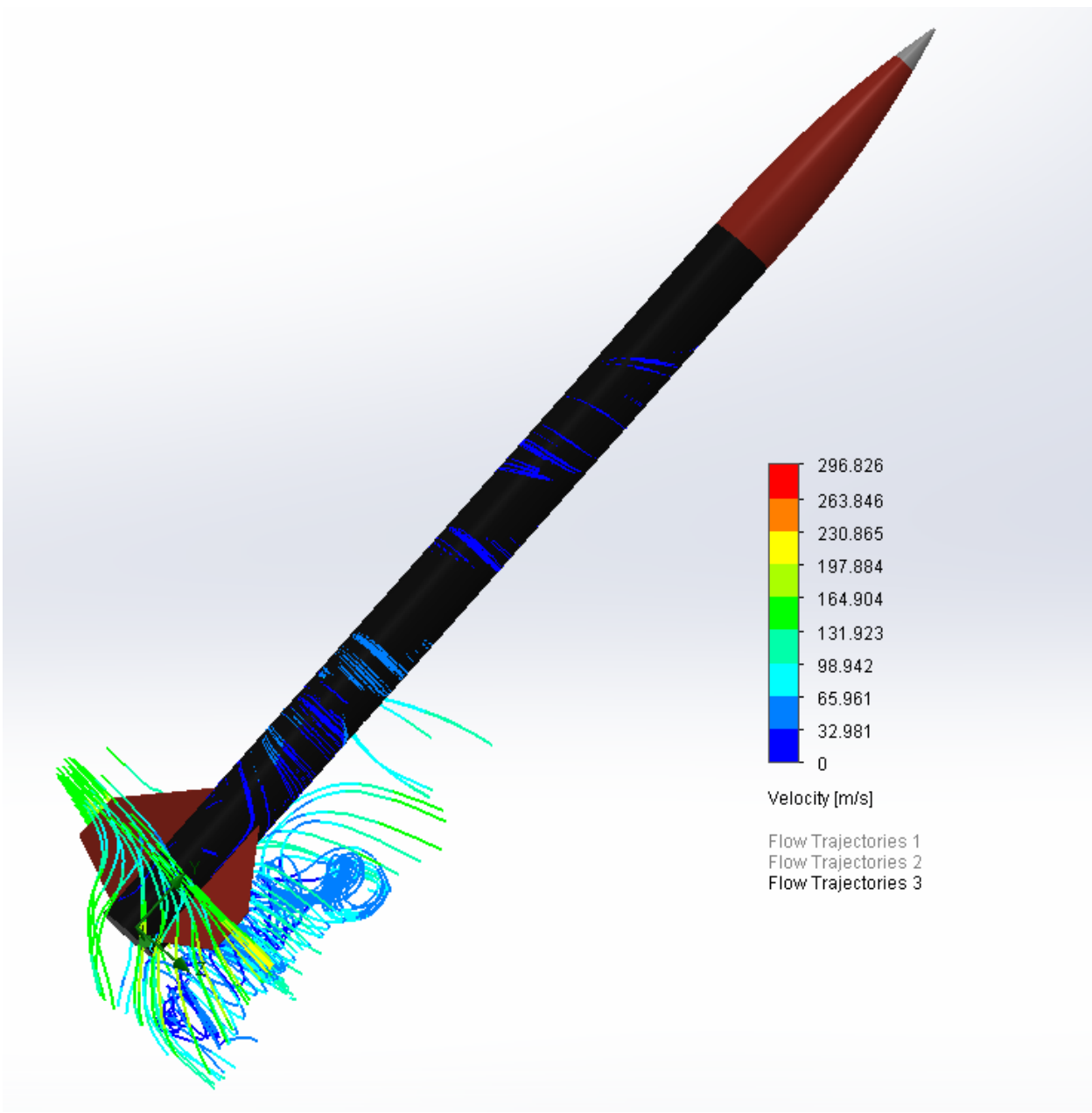


Figure 75: CP CFD Flow Visualization A.

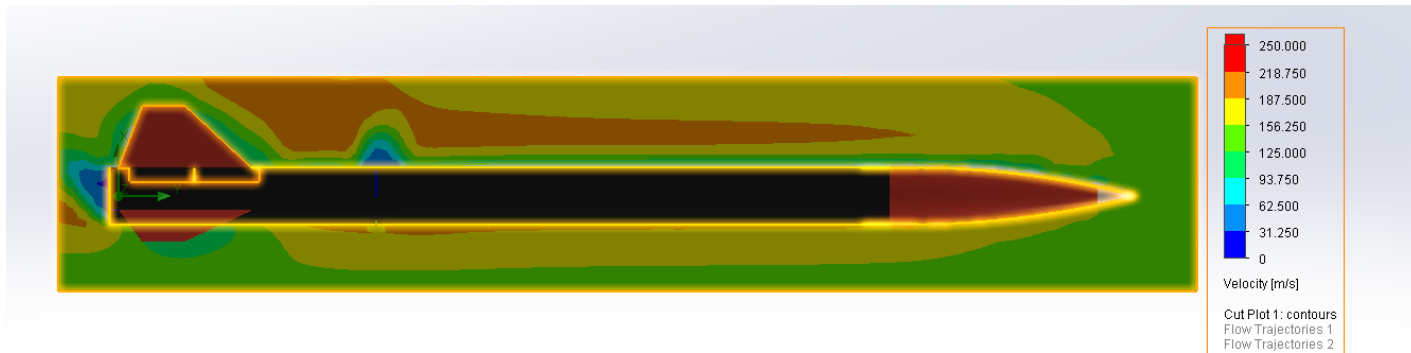


Figure 76: CP CFD Flow Visualization B.

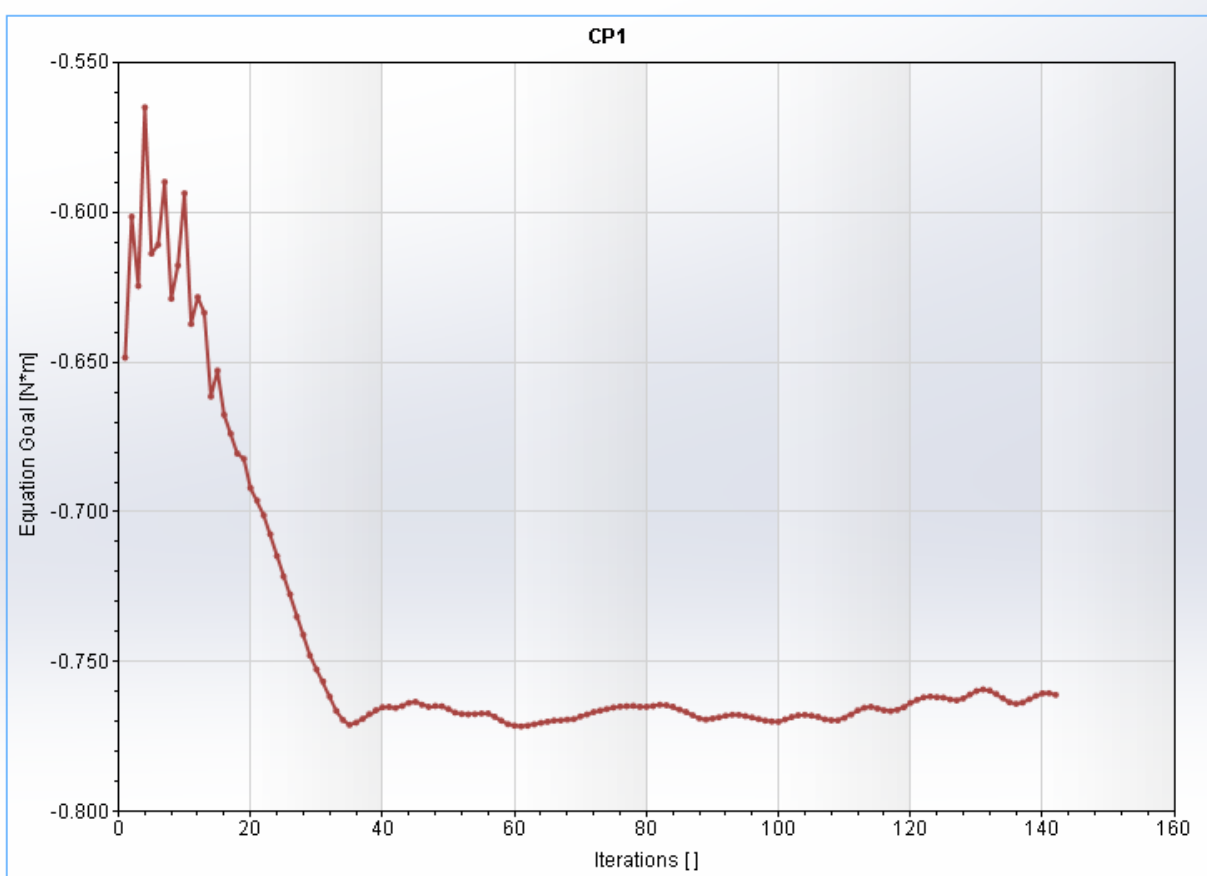


Figure 77: CP vs. Iterations.

Based on this analysis, the CP of the launch vehicle can be estimated to be 0.76m from the base of the rocket or 29.53 inches, meaning that the CP from the nosecone is:

$$CP = 107 - 29.53 = 77.5"$$

Compared to OpenRocket which estimates it to be 80.14", there is a percent difference value of 3.29%. Therefore, it can be concluded that the CP values as retrieved through CFD agrees with the CP values calculated using the barrowman equations in OpenRocket within a reasonable margin.

### 3.1.4.1. Drag Coefficient (no VDS) CFD

The purpose of this set of simulations is to estimate the drag coefficient of the rocket without the deployment of the VDS blades. The diameter of the rocket is used to calculate the reference area of 0.019 meters-squared. The simulation was performed at the maximum velocity region of the flight profile using a value of 600 ft/s.

**Table 32: Drag Coefficient CFD (no VDS)**

<b>Global Goals</b>	$C_d$ and $F_d$
<b>Temperature</b>	293.2 K
<b>Static Pressure</b>	101325 Pa
<b>Velocity (x)</b>	0 m/s
<b>Velocity (y)</b>	183 m/s
<b>Velocity (z)</b>	0 m/s
<b>Density of air</b>	1.225 kg per cubic meters
<b>Cross Sectional Area</b>	0.019 meters-squared



**Figure 78: Drag Coefficient CFD (no VDS) Flow Visualization**

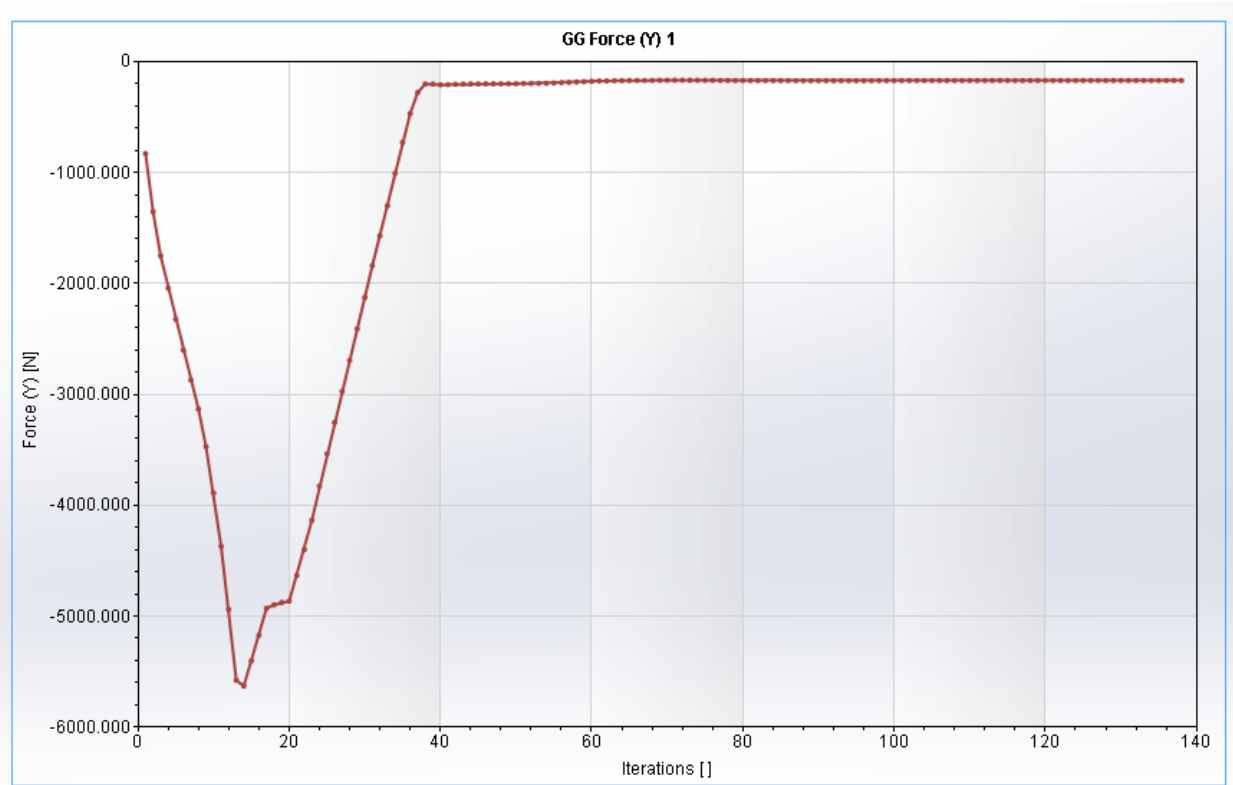


Figure 79: Drag Force vs. Iterations.

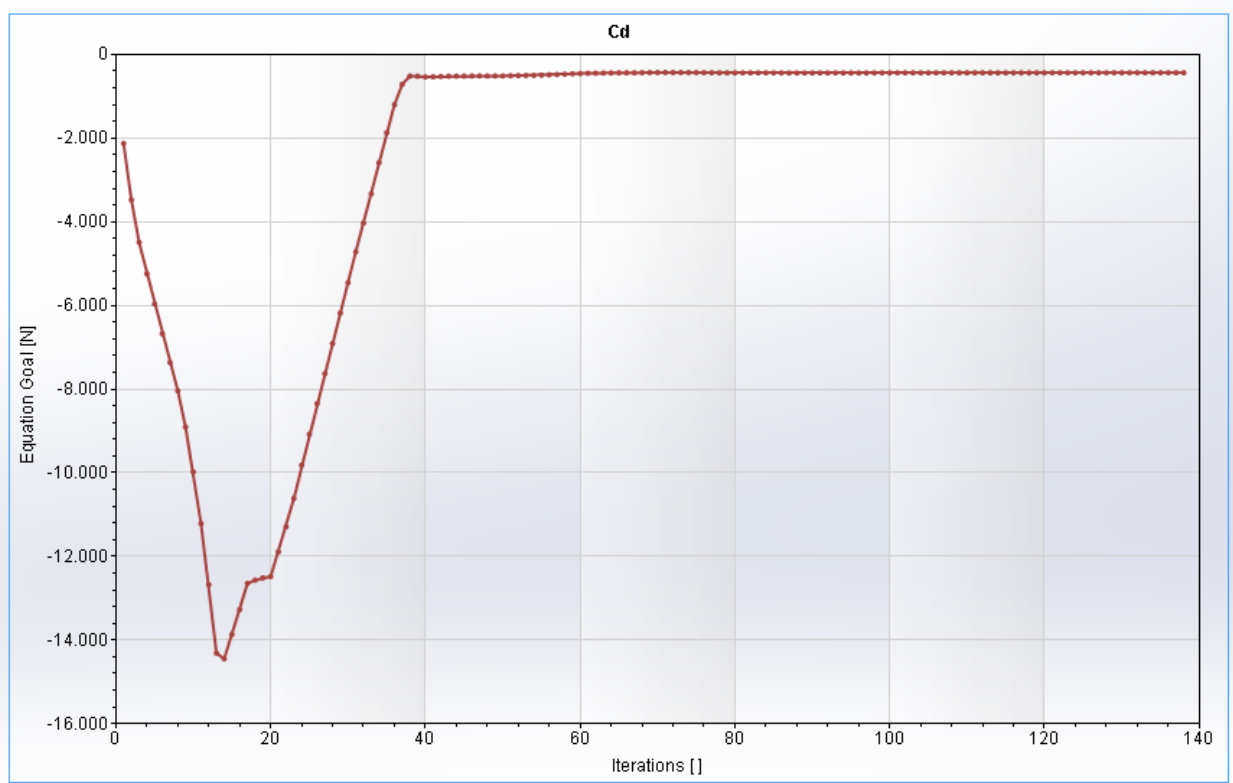


Figure 80: Drag Coefficient vs. Iterations.

The CFD results led finding a value of the drag coefficient to be 0.435 which is reasonable when compared to the drag coefficient of most high-power rockets. The maximum calculated drag force was found to be 38.184 lbf

#### 3.1.4.1. Drag Coefficient (VDS) CFD

The purpose of this set of simulations is to estimate the drag coefficient of the rocket with the deployment of the VDS blades. The diameter of the rocket is used to calculate the reference area of 0.019 meters-squared. The simulation was performed at the maximum velocity region of the flight profile using a value of 600 ft/s.

Table 33: Drag Coefficient CFD (VDS) Parameters.

<b>Global Goals</b>	$C_d$ and $F_d$
<b>Temperature</b>	293.2 K
<b>Static Pressure</b>	101325 Pa
<b>Velocity (x)</b>	0 m/s
<b>Velocity (y)</b>	183 m/s
<b>Velocity (z)</b>	0 m/s
<b>Density of air</b>	1.225 kg per cubic meters
<b>Cross Sectional Area</b>	0.019 meters-squared

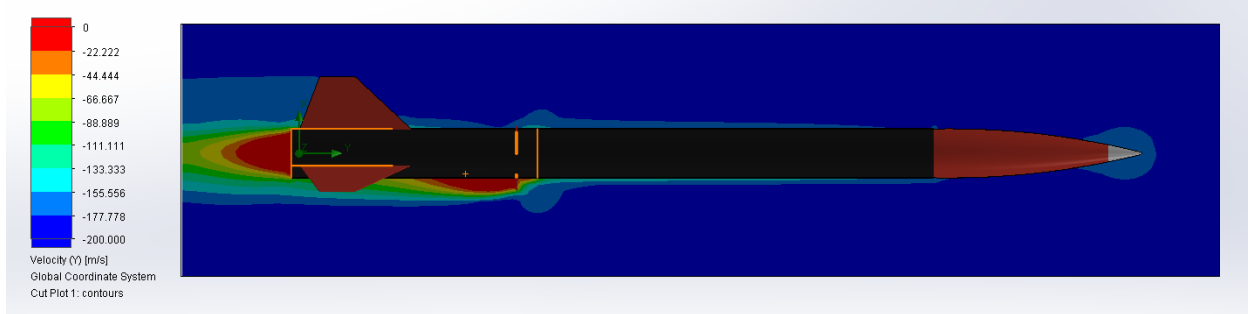


Figure 81: Drag Coefficient CFD (VDS) Velocity Gradient.

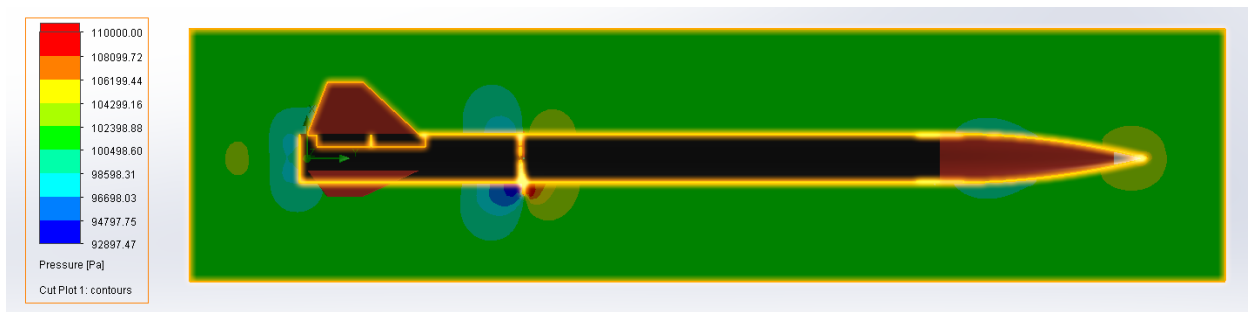


Figure 82: Drag Coefficient CFD (VDS) Pressure Gradient.

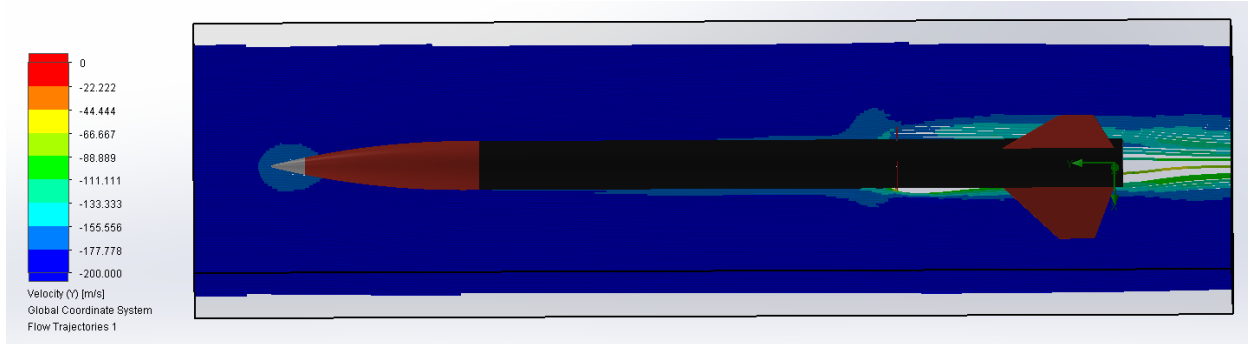


Figure 83: Drag Coefficient CFD (VDS) Velocity Gradient B.

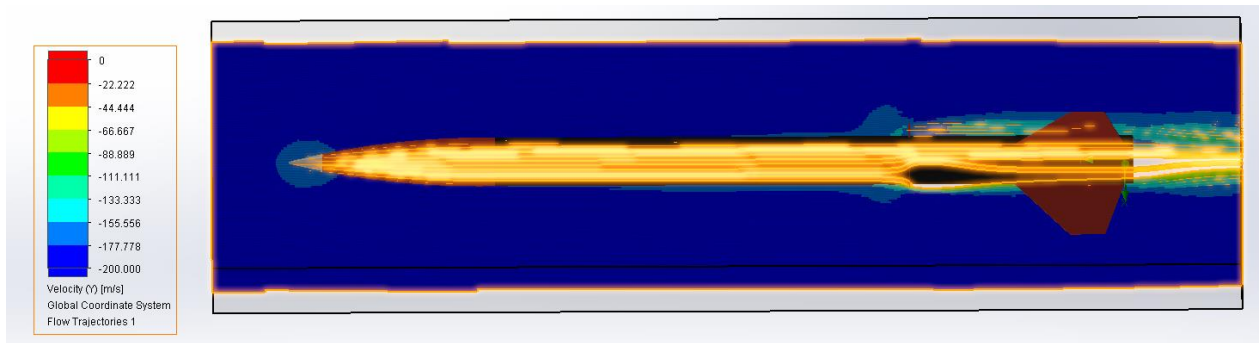


Figure 84: Drag Coefficient CFD (VDS) Velocity Gradient C.

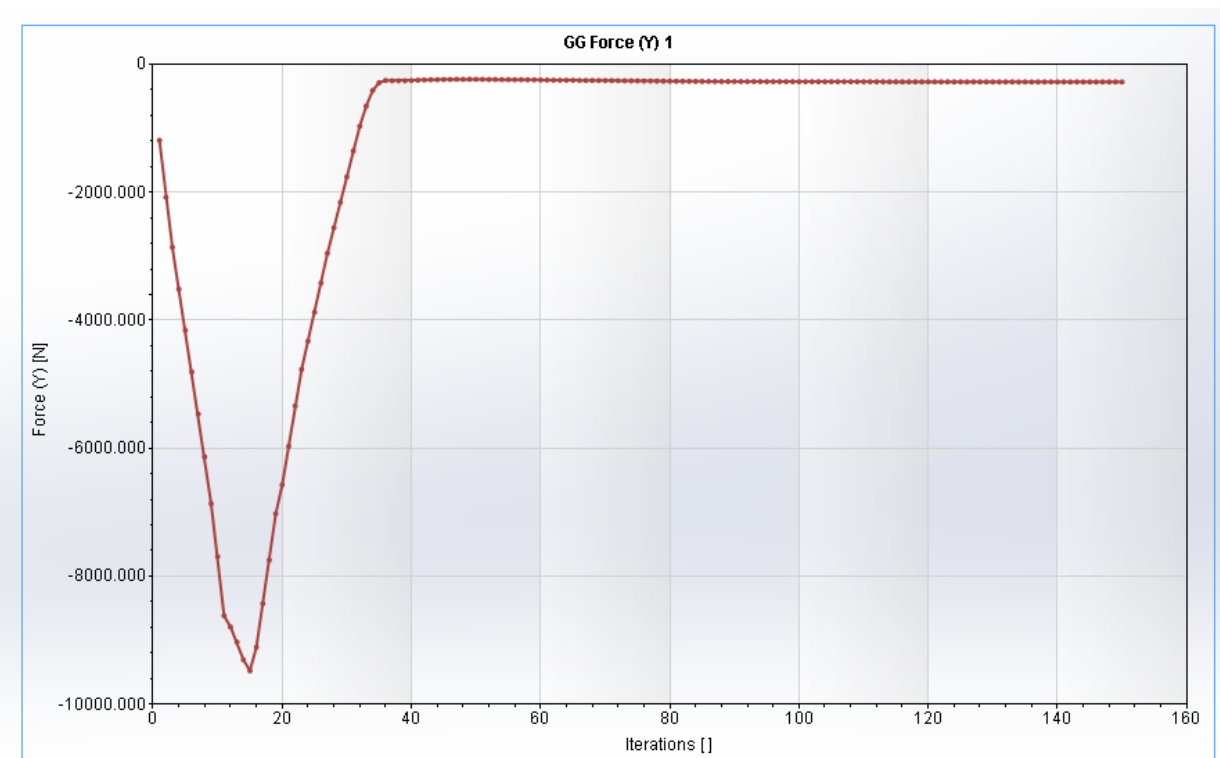


Figure 85: Drag Force vs. Iterations.

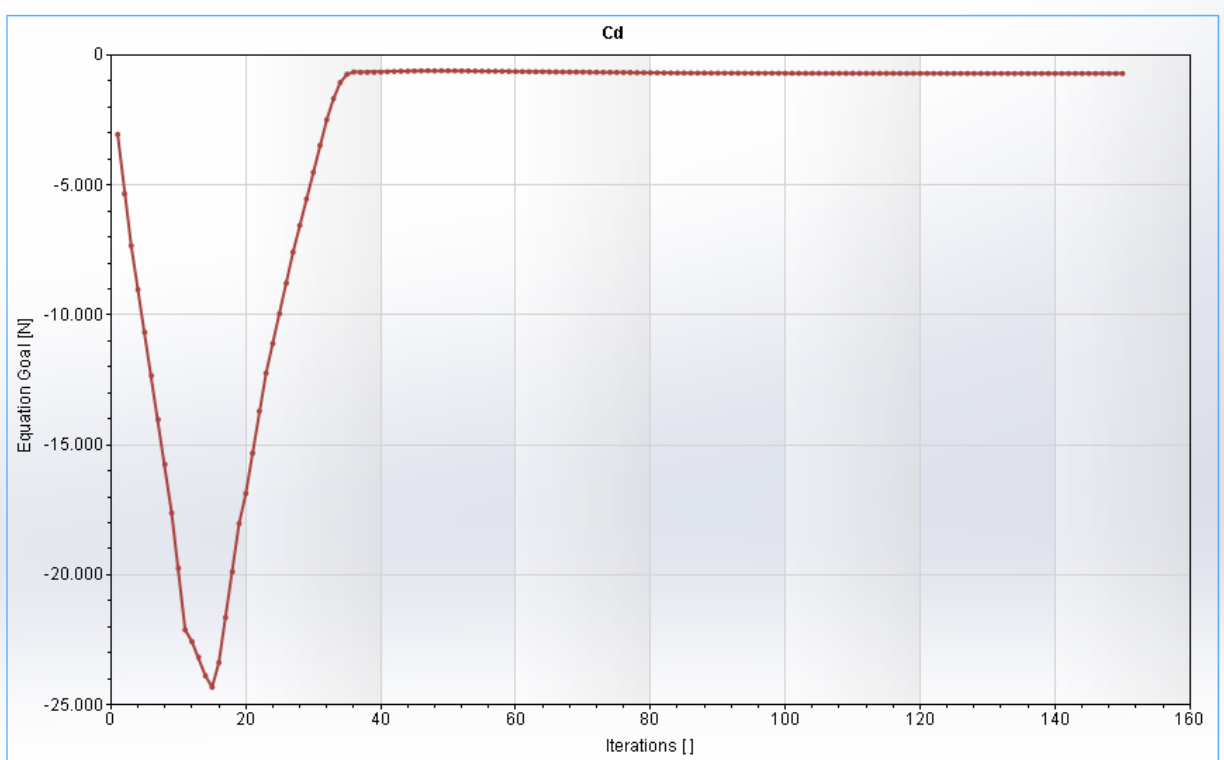


Figure 86: Drag Coefficient vs. Iterations

The CFD model utilized 150 iterations to zone in a drag coefficient value of 0.71 with a maximum drag force value of 62.05 lbf. Since the simulations with and without the deployment of the VDS were ran under the same exact conditions, it can be concluded that the VDS blades increased the drag coefficient and the drag force by a factor of 1.63. Therefore, the deployment of the VDS will result in considerable apogee reduction if controlled properly.

#### 3.1.4.1. Bulkhead FEA

The purpose of this section is to conduct FEA on the booster bay bulkhead to understand failure regimes. The FEA was conducted on 6061 aluminum and will be extrapolated to get an understanding of how G10 Fiberglass will perform since it was found that G10 fiberglass has usually 1/3 the compressive and tensile strength properties as aluminum perpendicular to the fiber direction.

Table 34: Bulkhead FEA Parameters

<b>Density</b>	1.06E-06 kg/mm <sup>3</sup>
<b>Young's Modulus</b>	2.24 GPa
<b>Poisson's Ratio</b>	0.38
<b>Yield Strength</b>	20 MPa
<b>Ultimate Tensile Strength</b>	29.6 MPa
<b>Thermal Conductivity</b>	1.6E-4 W/(mm C)

<b>Thermal Expansion Coefficient</b>	8.57E-5/C
<b>Specific Heat</b>	1500 J/(kg C)
<b>Constraints</b>	Fixed Outer Edge & Holes for Threaded Rods
<b>Loading Conditions</b>	450 lbf from Maximum Flight Acceleration (w/ SF)

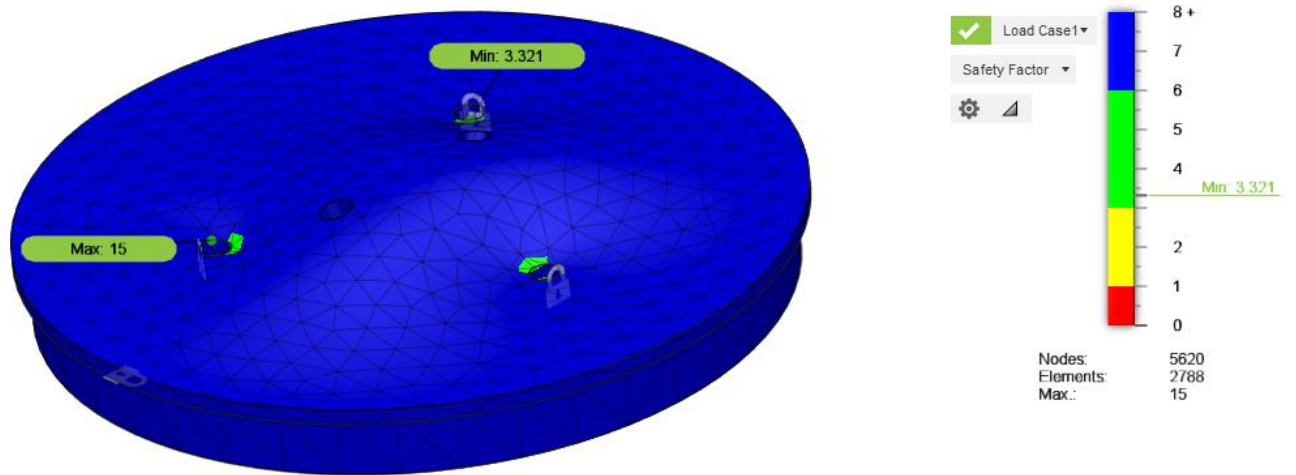


Figure 87: Bulkhead SF FEA Profile.

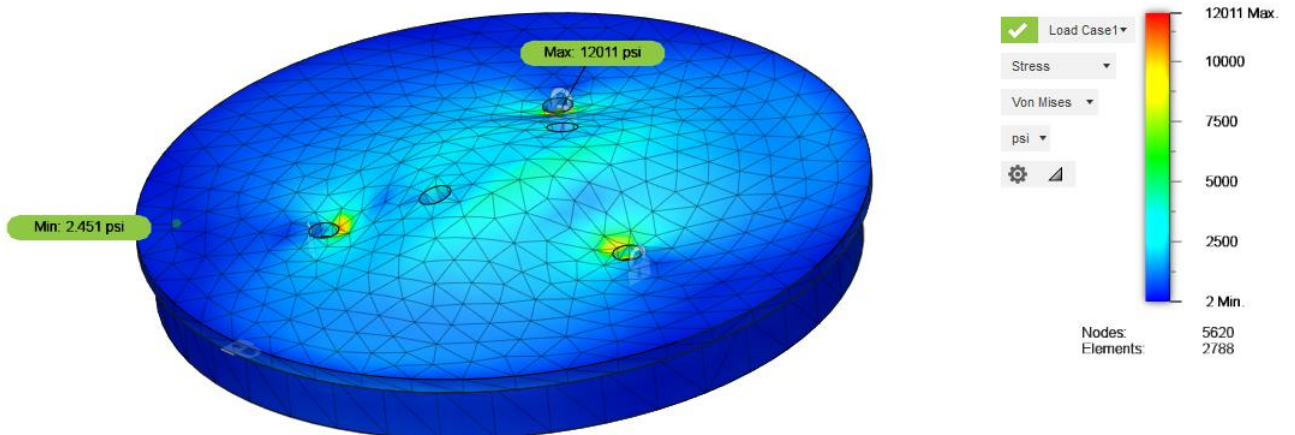


Figure 88: Bulkhead Von Mises Stress FEA Profile.

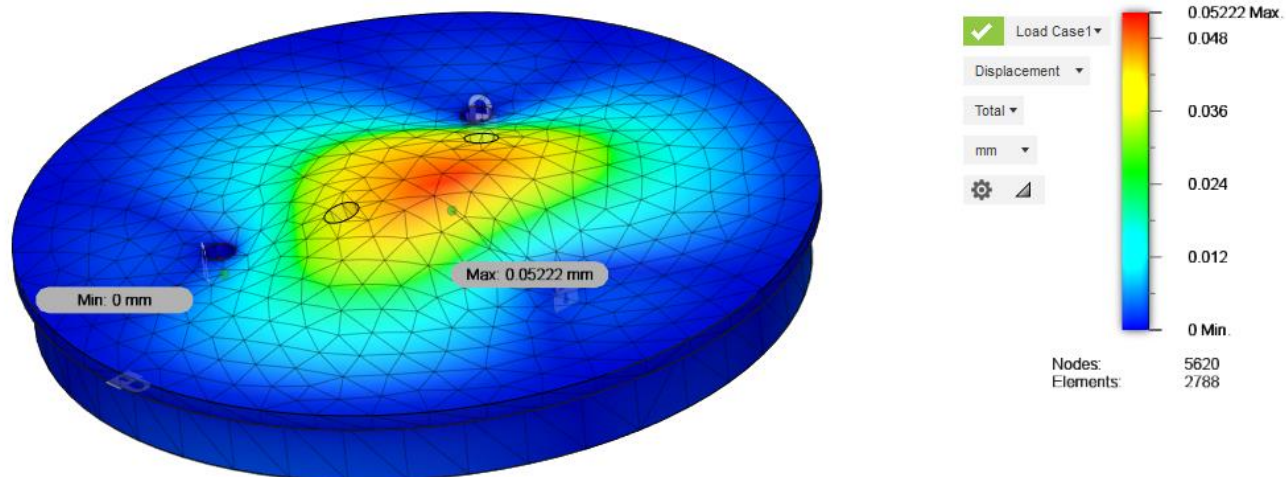


Figure 89: Bulkhead Displacement FEA Profile.

Table 35: Bulkhead FEA Results

<b>Max Displacement (G10 Fiberglass)</b>	0.156 mm
<b>Max Von Mises Stress (G10 Fiberglass)</b>	30.025 ksi
<b>Minimum Safety Factor (G10 Fiberglass)</b>	2.32

### 3.1.4.2. Centering Ring FEA

The purpose of this section is to conduct FEA on the centering rings to understand failure regimes. The FEA was conducted on 6061 aluminum and will be extrapolated to get an understanding of how G10 Fiberglass will perform since it was found that G10 fiberglass has usually 1/3 the compressive and tensile strength properties as aluminum perpendicular to the fiber direction.

Table 36: Centering Ring FEA Parameters

<b>Density</b>	1.06E-06 kg/mm <sup>3</sup>
<b>Young's Modulus</b>	2.24 GPa
<b>Poisson's Ratio</b>	0.38
<b>Yield Strength</b>	20 MPa
<b>Ultimate Tensile Strength</b>	29.6 MPa
<b>Thermal Conductivity</b>	1.6E-4 W/(mm C)
<b>Thermal Expansion Coefficient</b>	8.57E-5/C
<b>Specific Heat</b>	1500 J/(kg C)
<b>Constraints</b>	Fixed outer edge w/ airframe
<b>Loading Conditions</b>	450 lbf on inner edge due to motor thrust (w/ SF)

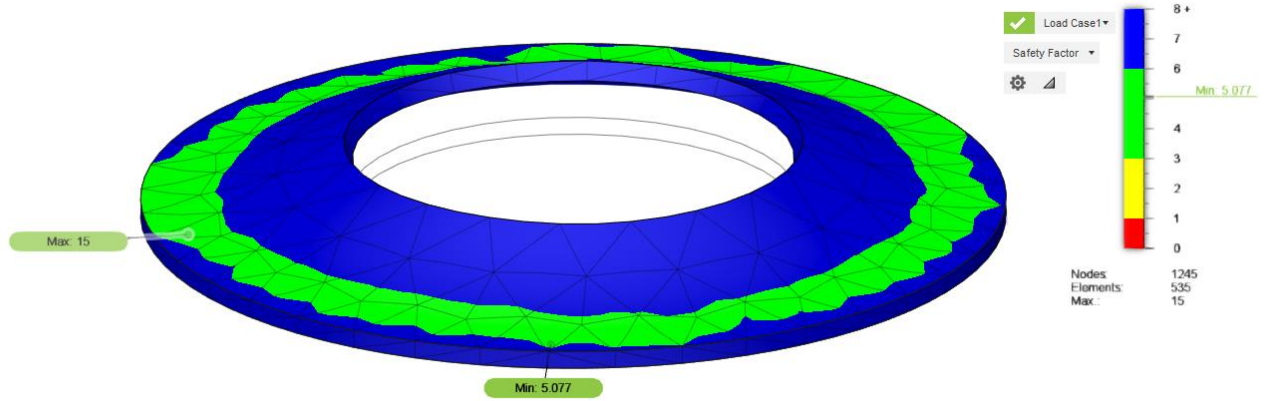


Figure 90: Centering Ring FEA SF Profile.

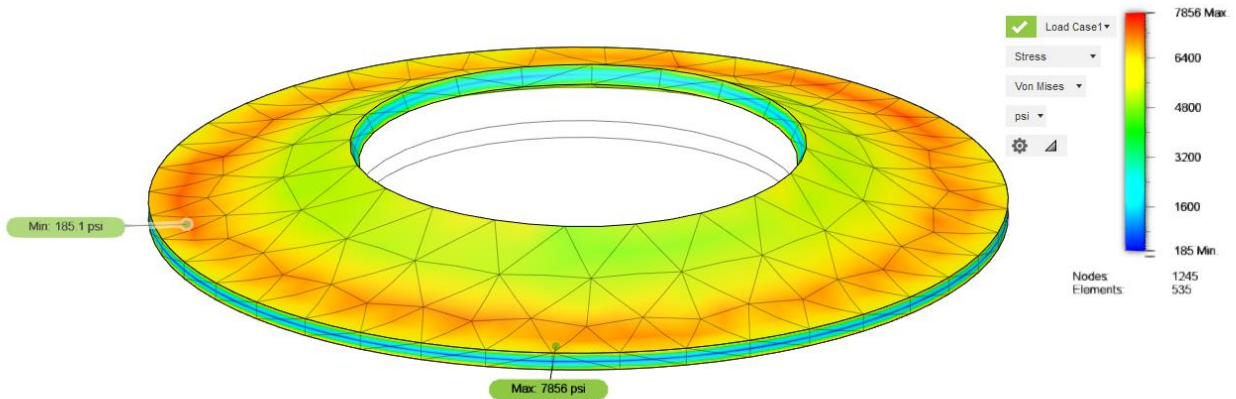


Figure 91: Centering Ring FEA Von Mises Stress Profile.

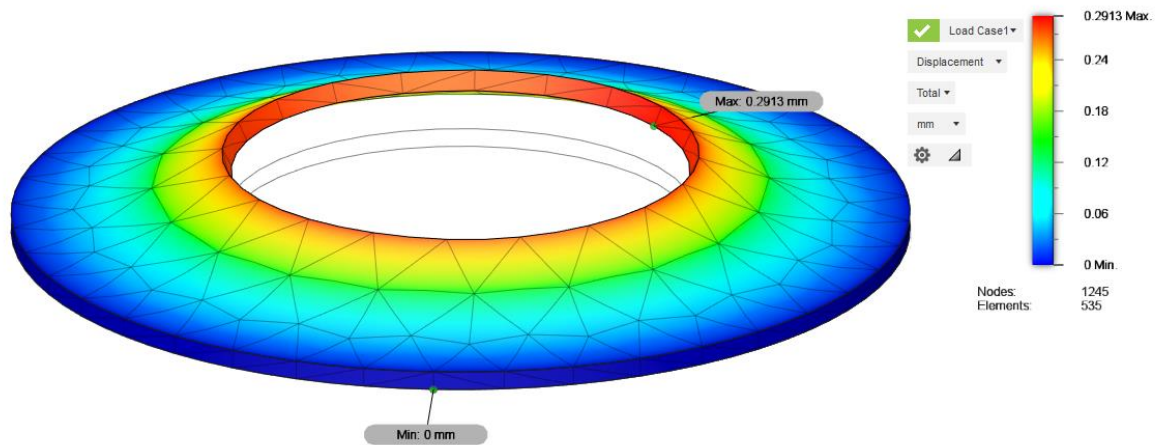


Figure 92: Centering Ring FEA Displacement Profile.

Table 37: Centering Rings FEA Results

<b>Max Displacement (G10 Fiberglass)</b>	0.87 mm
<b>Max Von Mises Stress (G10 Fiberglass)</b>	23.6 ksi
<b>Minimum Safety Factor (G10 Fiberglass)</b>	3.38

### 3.1.4.3. Airframe FEA

The purpose of this section is to conduct FEA on the booster bay airframe to understand failure regimes. The FEA was conducted on 6061 aluminum and will be extrapolated to get an understanding of how braided carbon fiber will perform since it was found that it has usually 0.75 the compressive and tensile strength properties as aluminum perpendicular to the fiber direction.

Table 38: Airframe FEA Parameters.

<b>Density</b>	1.06E-06 kg/mm <sup>3</sup>
<b>Young's Modulus</b>	2.24 GPa
<b>Poisson's Ratio</b>	0.38
<b>Yield Strength</b>	20 MPa
<b>Ultimate Tensile Strength</b>	29.6 MPa
<b>Thermal Conductivity</b>	1.6E-4 W/(mm C)
<b>Thermal Expansion Coefficient</b>	8.57E-5/C
<b>Specific Heat</b>	1500 J/(kg C)
<b>Constraints</b>	Fixed top end (farther from motor)
<b>Loading Conditions</b>	450 lbf on bottom surface due to compression

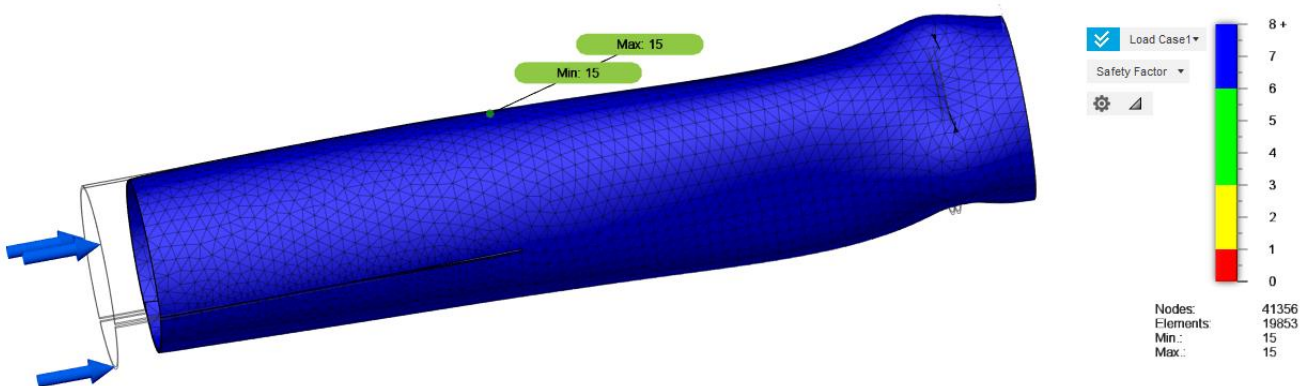


Figure 93: Airframe FEA SF Profile.

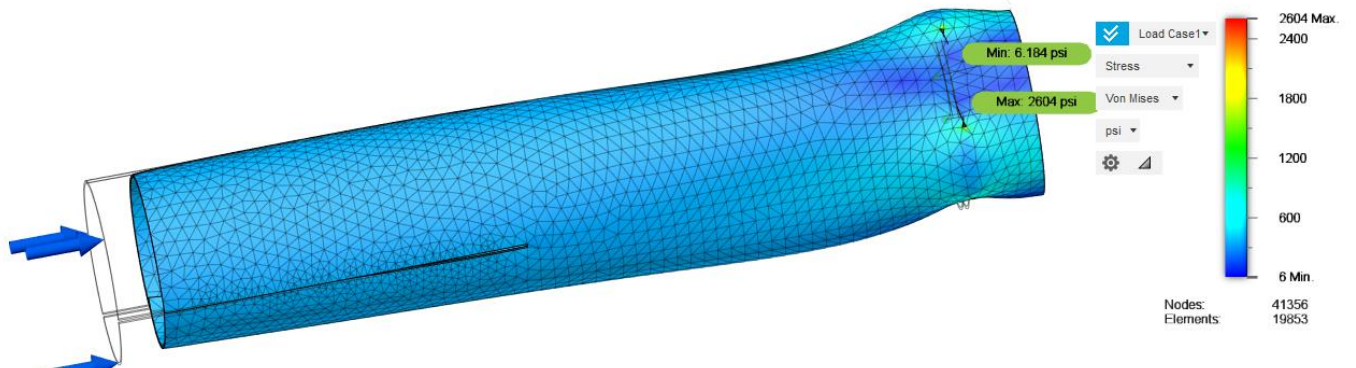


Figure 94: Airframe FEA Von Mises Stress Profile.

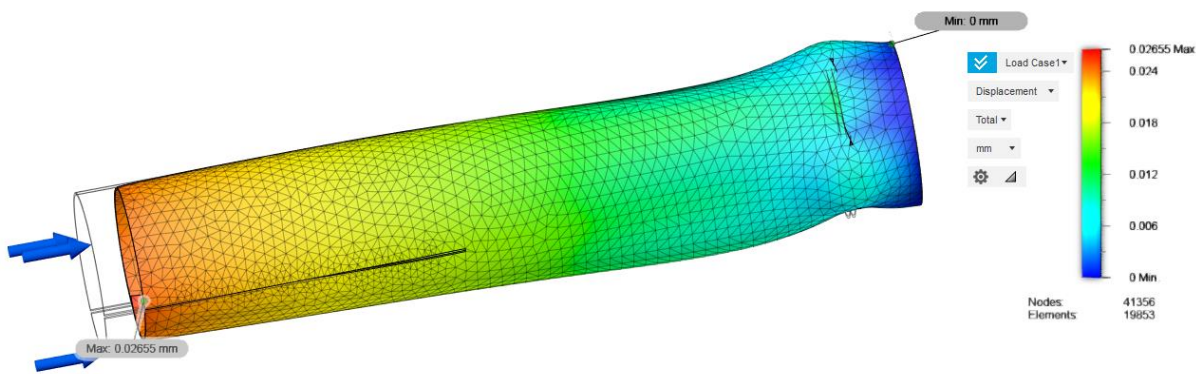


Figure 95: Airframe FEA Displacement Profile.

Table 39: Airframe FEA Results

<b>Max Displacement (Braided Carbon Fiber)</b>	0.04 mm
<b>Max Von Mises Stress (Braided Carbon Fiber)</b>	3.96 ksi
<b>Minimum Safety Factor (Braided Carbon Fiber)</b>	10

Table 40: Airframe FEA Parameters.

<b>Density</b>	1.06E-06 kg/mm <sup>3</sup>
<b>Young's Modulus</b>	2.24 GPa
<b>Poisson's Ratio</b>	0.38
<b>Yield Strength</b>	20 MPa
<b>Ultimate Tensile Strength</b>	29.6 MPa
<b>Thermal Conductivity</b>	1.6E-4 W/(mm C)
<b>Thermal Expansion Coefficient</b>	8.57E-5/C
<b>Specific Heat</b>	1500 J/(kg C)

<b>Constraints</b>	Fixed bottom end (closer to motor)
<b>Loading Conditions</b>	450 lbf on top surface due to tension

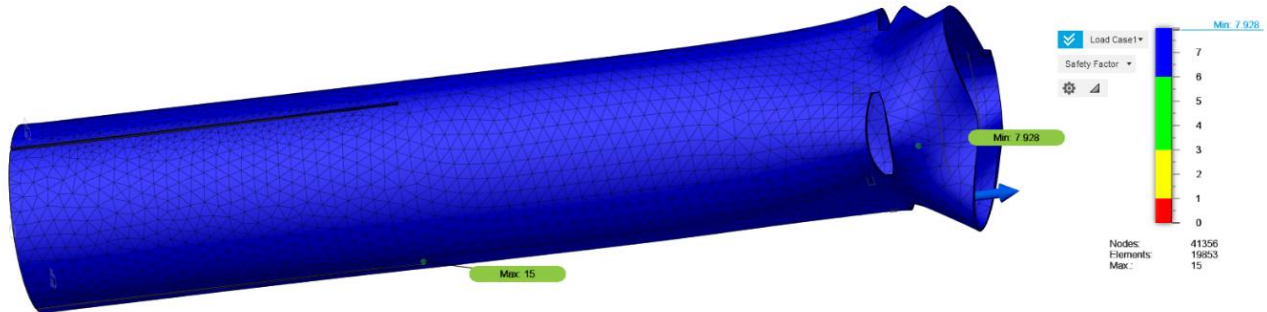


Figure 96: Airframe FEA SF Profile.

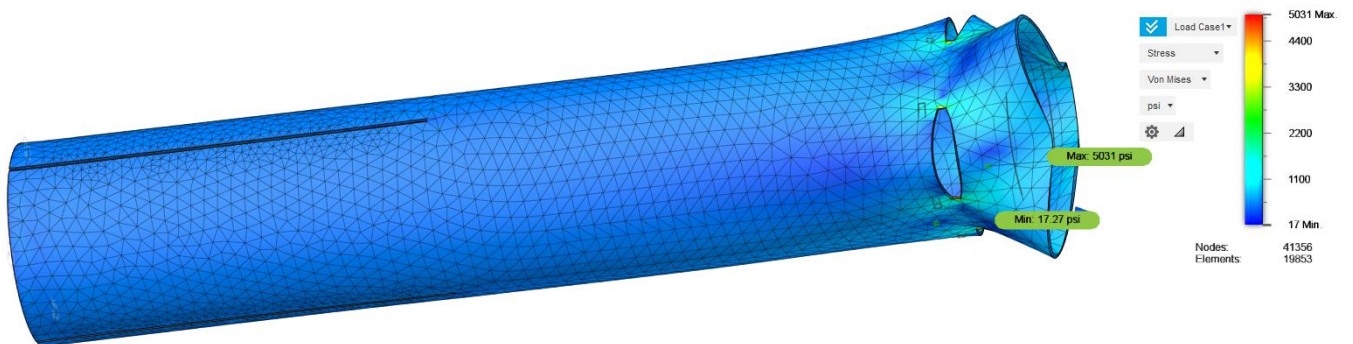


Figure 97: Airframe FEA Von Mises Stress Profile.

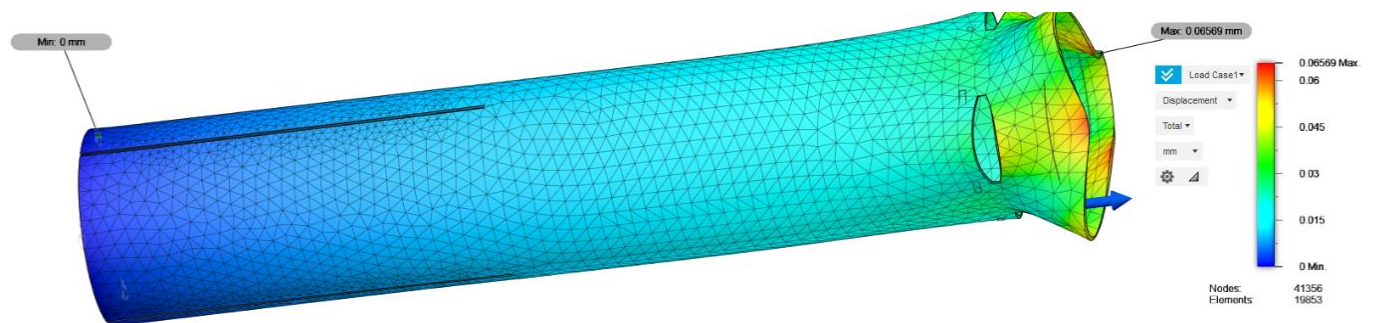


Figure 98: Airframe FEA Displacement Profile.

Table 41: Airframe FEA Results

<b>Max Displacement (Braided Carbon Fiber)</b>	0.105 mm
<b>Max Von Mises Stress (Braided Carbon Fiber)</b>	7.55 ksi
<b>Minimum Safety Factor (Braided Carbon Fiber)</b>	5.29

### 3.1.4.4. Coupler FEA

The purpose of this section is to conduct FEA on the booster bay coupler to understand failure regimes. The FEA was conducted on 6061 aluminum and will be extrapolated to get an understanding of how G10 fiberglass will perform since it was found that G10 fiberglass has usually 1/3 the compressive and tensile strength properties as aluminum perpendicular to the fiber direction.

Table 42: Coupler FEA Parameters.

<b>Density</b>	1.06E-06 kg/mm <sup>3</sup>
<b>Young's Modulus</b>	2.24 GPa
<b>Poisson's Ratio</b>	0.38
<b>Yield Strength</b>	20 MPa
<b>Ultimate Tensile Strength</b>	29.6 MPa
<b>Thermal Conductivity</b>	1.6E-4 W/(mm C)
<b>Thermal Expansion Coefficient</b>	8.57E-5/C
<b>Specific Heat</b>	1500 J/(kg C)
<b>Constraints</b>	Fixed bottom end (close to motor)
<b>Loading Conditions</b>	450 lbf on top surface due to tension



Figure 99: Coupler FEA SF Profile.

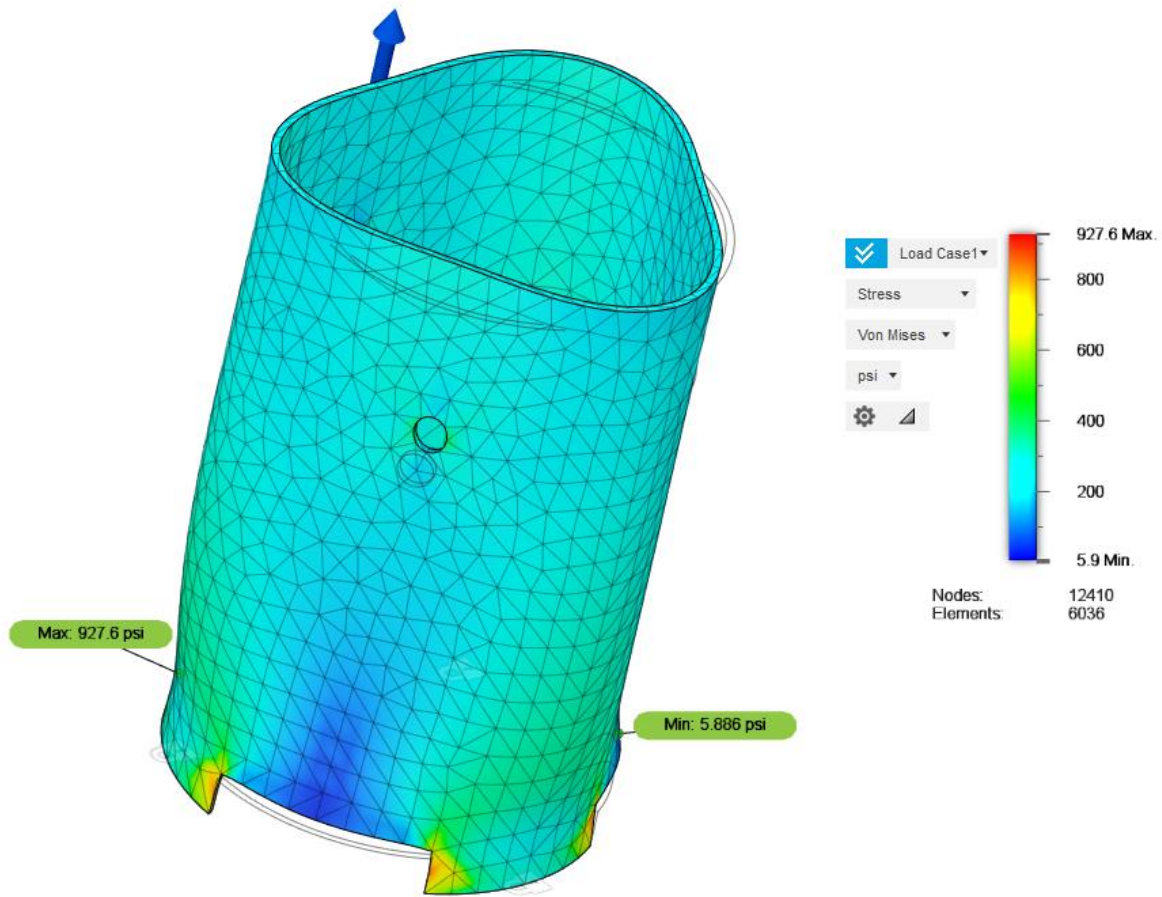


Figure 100: Coupler Von Mises Stress Profile.

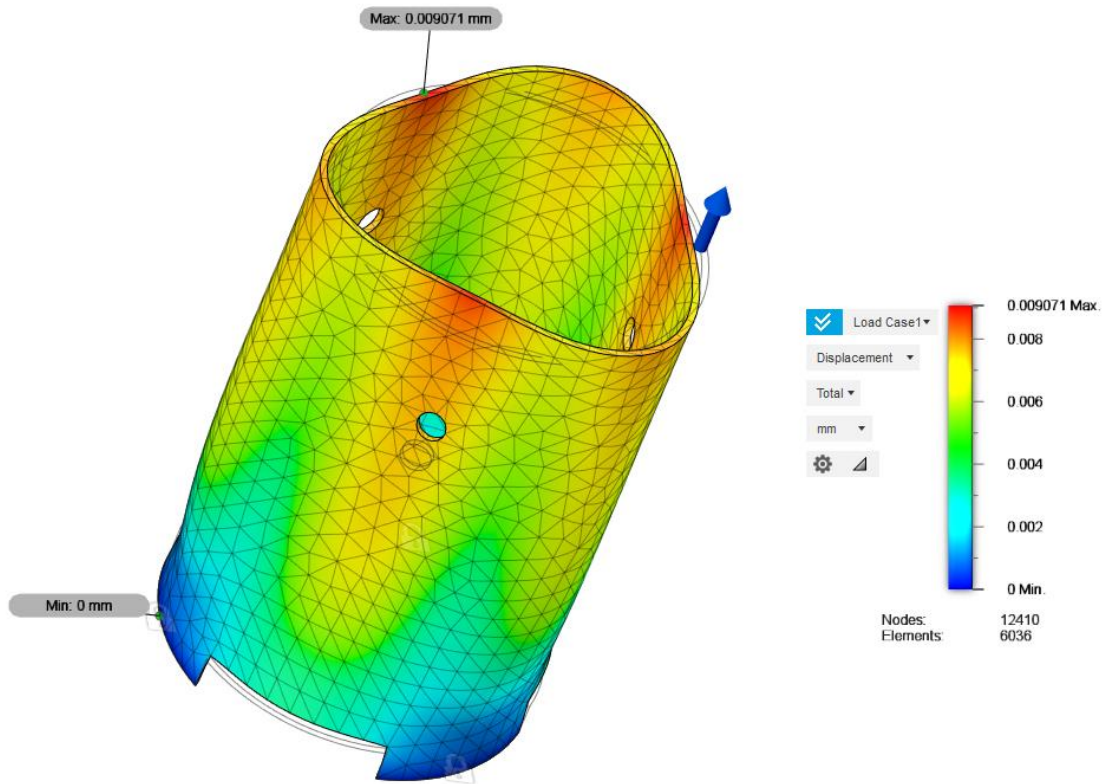


Figure 101: Coupler FEA Displacement Profile.

Table 43: Coupler FEA Results.

<b>Max Displacement (Braided Carbon Fiber)</b>	0.027 mm
<b>Max Von Mises Stress (Braided Carbon Fiber)</b>	2.784 ksi
<b>Minimum Safety Factor (Braided Carbon Fiber)</b>	5

Table 44: Coupler FEA Parameters.

<b>Density</b>	1.06E-06 kg/mm <sup>3</sup>
<b>Young's Modulus</b>	2.24 GPa
<b>Poisson's Ratio</b>	0.38
<b>Yield Strength</b>	20 MPa
<b>Ultimate Tensile Strength</b>	29.6 MPa
<b>Thermal Conductivity</b>	1.6E-4 W/(mm C)
<b>Thermal Expansion Coefficient</b>	8.57E-5/C
<b>Specific Heat</b>	1500 J/(kg C)

Constraints	Fixed top end (far from motor)
Loading Conditions	450 lbf on bottom surface due to compression

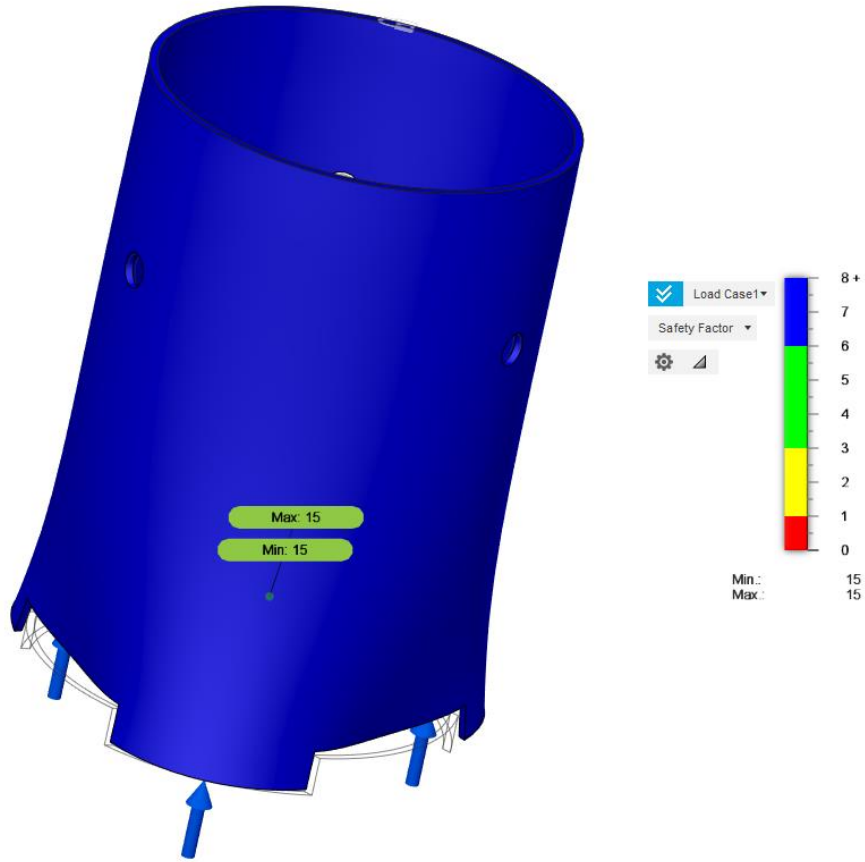


Figure 102: Coupler FEA SF Profile.

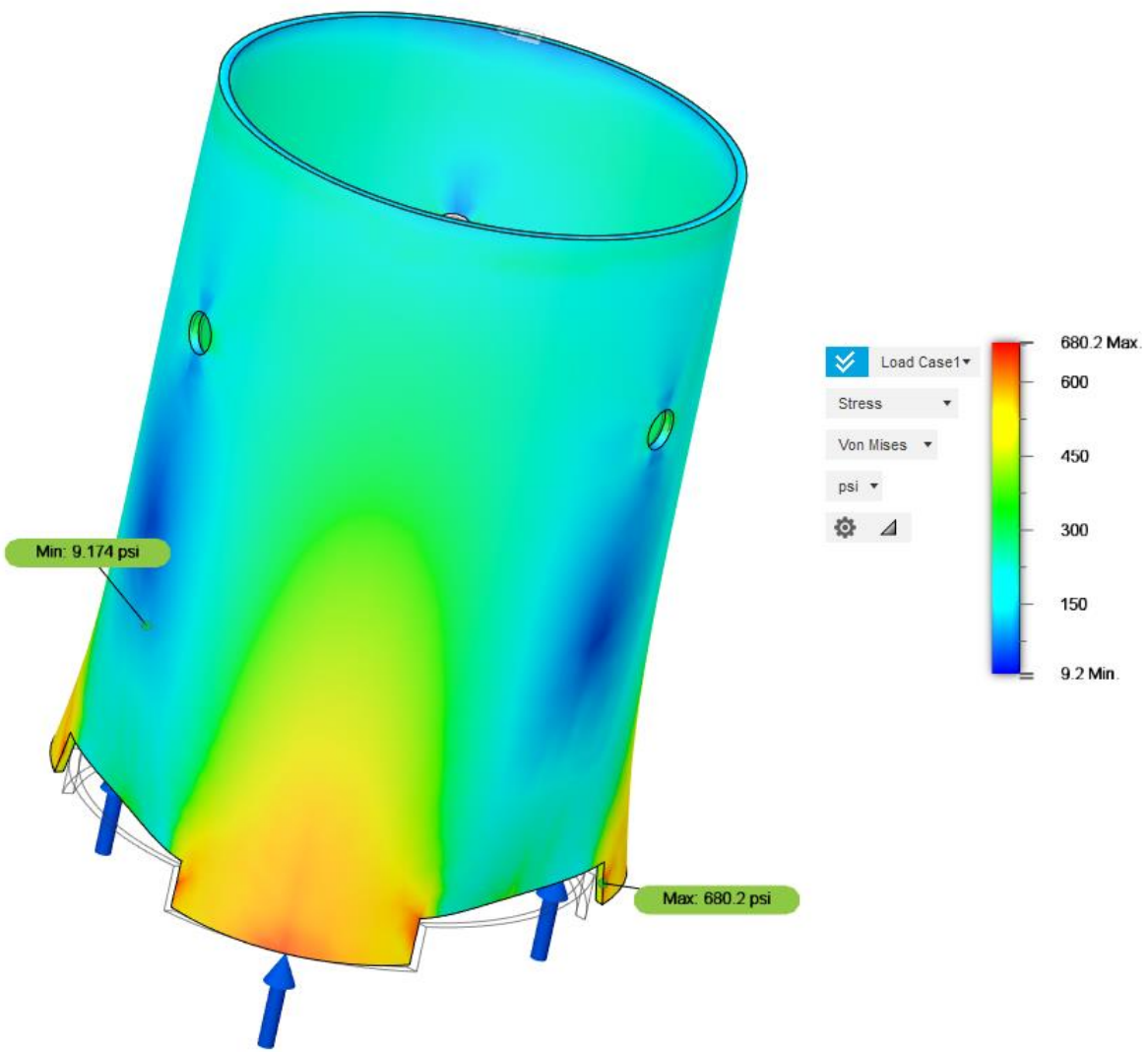


Figure 103: Coupler Von Mises Stress Profile.

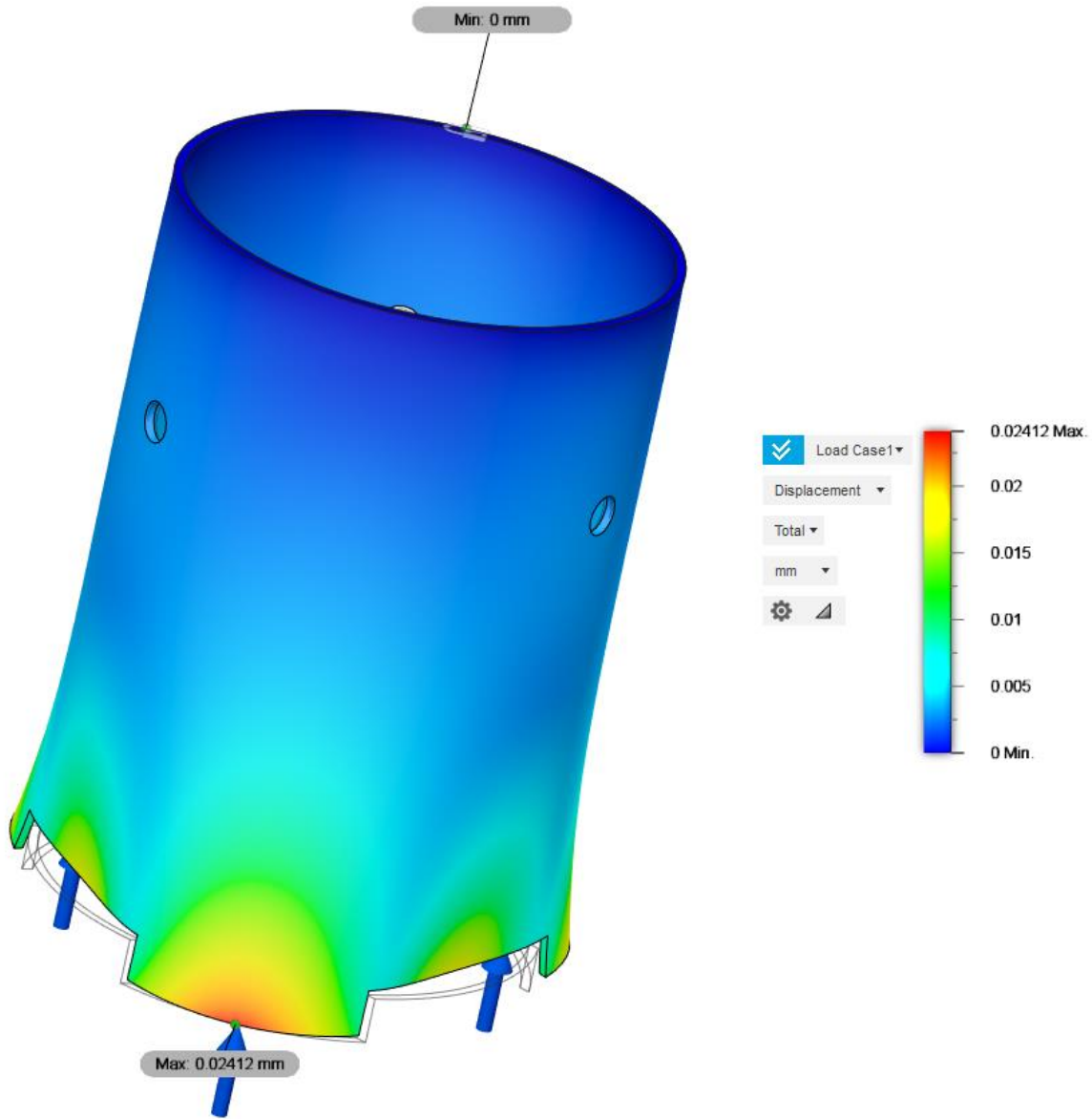


Figure 104: Coupler FEA Displacement Profile.

Table 45: Coupler FEA Results

<b>Max Displacement (Braided Carbon Fiber)</b>	0.0724 mm
<b>Max Von Mises Stress (Braided Carbon Fiber)</b>	2.041 ksi
<b>Minimum Safety Factor (Braided Carbon Fiber)</b>	5

### 3.1.4.5. VDS Blades FEA

The purpose of this section is to conduct FEA on the VDS blades to understand failure regimes. The FEA was conducted on 6061 aluminum which properly reflects the material chosen.

Table 46: VDS Blades FEA Parameters.

<b>Density</b>	1.06E-06 kg/mm <sup>3</sup>
<b>Young's Modulus</b>	2.24 GPa
<b>Poisson's Ratio</b>	0.38
<b>Yield Strength</b>	20 MPa
<b>Ultimate Tensile Strength</b>	29.6 MPa
<b>Thermal Conductivity</b>	1.6E-4 W/(mm C)
<b>Thermal Expansion Coefficient</b>	8.57E-5/C
<b>Specific Heat</b>	1500 J/(kg C)
<b>Constraints</b>	Fixed mounting holes
<b>Loading Conditions</b>	20 lbf on top surface due to drag force

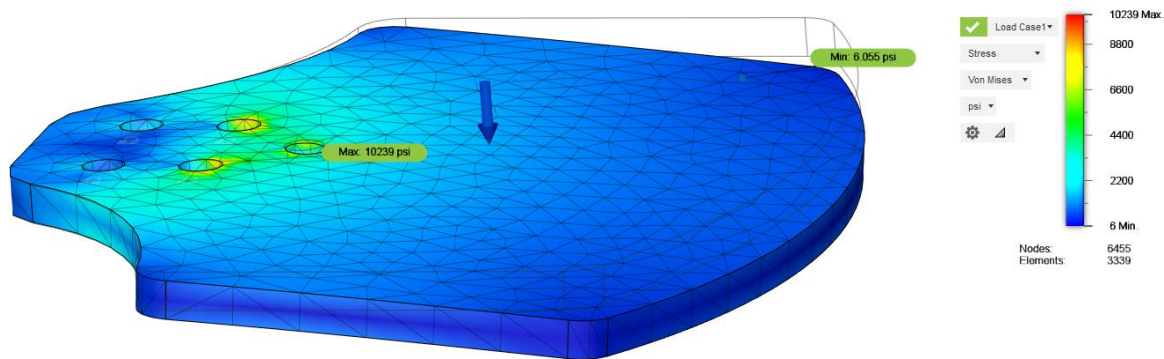


Figure 105: VDS Blades FEA Von Mises Stress Profile.

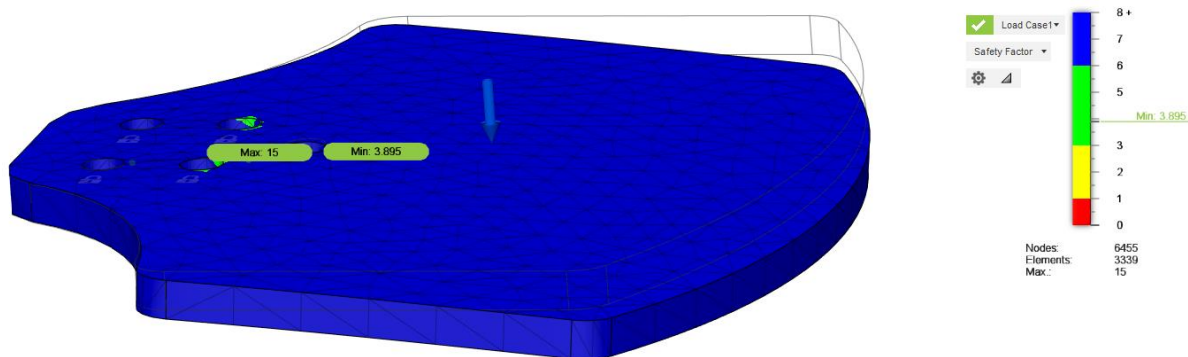


Figure 106: VDS Blades FEA SF Profile.

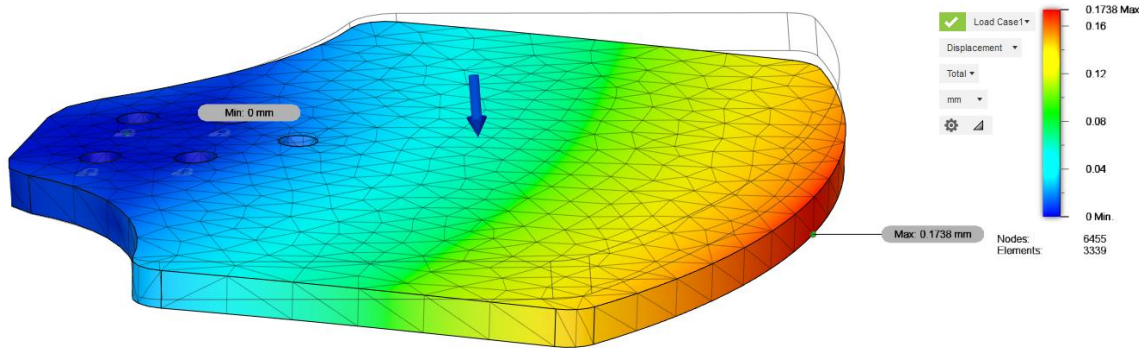


Figure 107: VDS Blades FEA Displacement Profile.

Table 47: VDS Blades FEA Results

<b>Max Displacement (Braided Carbon Fiber)</b>	0.174 mm
<b>Max Von Mises Stress (Braided Carbon Fiber)</b>	10.2 ksi
<b>Minimum Safety Factor (Braided Carbon Fiber)</b>	3.895

## 3.2 Subscale Flight Results

Two subscale launches were conducted by the team in order to get a better understanding of the performance of the full-scale launch vehicle. The first launch utilized a BT-20 size tubing and the second launch utilized a BT-60 size tubing. Although the BT-20 rocket had a small altimeter inside, it malfunctioned and did not record flight data. However, the apogee could be estimated to be roughly 300 feet. Nevertheless, the BT-60 sized subscale did record flight data and will be discussed in detail below. Before proceeding, an important thing to note is that since the subscale was launched a few weeks before the CDR deadline, the general launch vehicle characteristics now are different than they were before the subscale launch. These changes mainly include a weight reduction of roughly 2 lbs and length increase of roughly 2 inches. When scaled down, these minor changes do not take away from the validity of the subscale launches by a significant amount.

### 3.2.1 Subscale Design

The design of the subscale vehicle revolved around minimizing cost and being able to utilize the resources that were readily available to us. This included 3D Printing, chemical welding, and essentially designing around tubing and components that our mentor already had. Although it would have been possible to fully fabricate the subscale while maintain all the details of the full scale, such an endeavor would have cut into the time that could be spent working on the full scale and into the manufacturing budget allocated for the full scale.

#### 3.2.1.1 Scaling Factors

The BT-20 size rocket had a scale down factor of roughly 0.12 since the BT-20 Tubing has an outer diameter of 0.74 inches and the full-scale airframe has an outer diameter of 6.17 inches. The

dimensions of the full-scale launch vehicle at the time of the subscale launch and the dimensions of the scaled down subscale design for the BT-20 Size rocket are listed below:

**Table 48: BT-20 Subscale Scaling Factors**

	<b>Full Scale</b>	<b>BT-20 Size Subscale</b>
<b>Nosecone Length (in)</b>	24.0	2.88
<b>Payload Bay Length (in)</b>	21.0	2.52
<b>Avionics Bay Length (in)</b>	32.9	3.95
<b>Booster Bay Length (in)</b>	27.0	3.24
<b>Fin Root Chord (in)</b>	14.0	1.68
<b>Fin Tip Chord (in)</b>	4.5	0.54
<b>Fin Height (in)</b>	6.25	0.75
<b>Fin Sweep Length (in)</b>	7.0	0.84

The BT-20 size rocket had a scale down factor of roughly 0.265 since the BT-60 Tubing has an outer diameter of 1.64 inches and the full-scale airframe has an outer diameter of 6.17 inches. The dimensions of the full-scale launch vehicle at the time of the subscale launch and the dimensions of the scaled down subscale design for the BT-20 Size rocket are listed below:

**Table 49: BT-60 Subscale Scaling Factors**

	<b>Full Scale</b>	<b>BT-60 Size Subscale</b>
<b>Nosecone Length (in)</b>	24.0	6.38
<b>Payload Bay Length (in)</b>	21.0	5.58
<b>Avionics Bay Length (in)</b>	32.9	8.74
<b>Booster Bay Length (in)</b>	27.0	7.18
<b>Fin Root Chord (in)</b>	14.0	3.72
<b>Fin Tip Chord (in)</b>	4.5	1.196
<b>Fin Height (in)</b>	6.25	1.66
<b>Fin Sweep Length (in)</b>	7.0	1.86

### 3.2.1.2. Material Justification

For the construction of both subscale launch vehicles, the materials chosen minimized cost and maximized the time that could be spent on the launch analysis. Since our full-scale vehicle is made of carbon fiber, ideally it would have been the best to construct the subscale from the same material. However, this would have significantly reduced the budget of the team which is already low when compared to other teams in USLI. Therefore, for the construction of the subscale launch vehicles, Kraft Paper tubing manufactured by Apogee Rockets was utilized. In a similar manner,

the cost for the fin designs were also minimized by using balsawood for the BT-60 size and Kraft Paper for the BT-20 size rockets. A plastic nosecone was used for the BT-20 size subscale due to weight and size constraints. However, an exact scaled down 4:1 ogive nosecone was 3D printed with ABS Plastic for the BT-60 size rocket. T

#### **3.2.1.3. Variables Held Constant**

Since the purpose of the subscale was to get a better understanding of the flight characteristics of the full-scale launch vehicle, it was made sure that the center of gravity and center of pressure were both accordingly scaled down and held constant. This meant that the subscale launch vehicles would have the same stability margin as the full-scale rocket.

#### **3.2.1.4. Variables Not Held Constant**

Although it would have been nice to scale down the mass of the subscale vehicles with respect to the full scale to get a very perfect fidelity design, it was not necessary since the motors could be picked in order to achieve a proper scaled down apogee value. The individual lengths of each bay were also not held constant even though the overall length of the launch vehicle was scaled down accordingly. The deviation from the full scale with respect to the lengths of each bay did not affect the flight characteristics of the subscale launch since the overall length of the rocket was adjusted for accordingly.

### **3.2.2 Subscale Manufacturing**

Along with launching the BT-20 size and BT-60 size rockets, a BT-80 scaled down model was also manufactured but not launched due to time constraints and weather in the east coast. Multiple BT-20 size rockets were built with the purpose of testing the effects of using different number of fins with varying fin profiles. The PerfectFlite Stratologger CF was flown during the launch of the BT60 size rocket. This was done since the full-scale launch vehicle will utilize the same altimeter. The subscales were manufactured with the resources and guidance of our mentor George. The construction process is shown below:

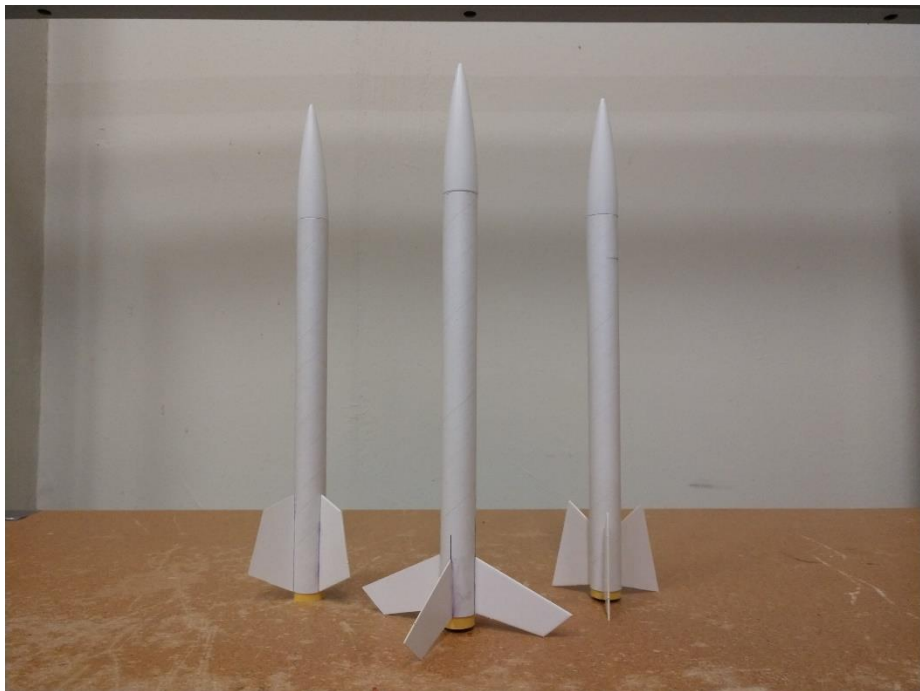


Figure 108: BT-20 Size Rockets Built for Launch



Figure 109: BT-20 Size Rockets Built for Launch



Figure 110: Construction Process for Building the BT20 size, BT60 size and BT80 size rockets.



Figure 111: Avionics Bay Containing the Altimeter for the BT60 Rocket.



Figure 112: 3D Printed Nosecone for BT60 Rocket.



Figure 113: Booster Bay Assembly for BT60 Sized Subscale.

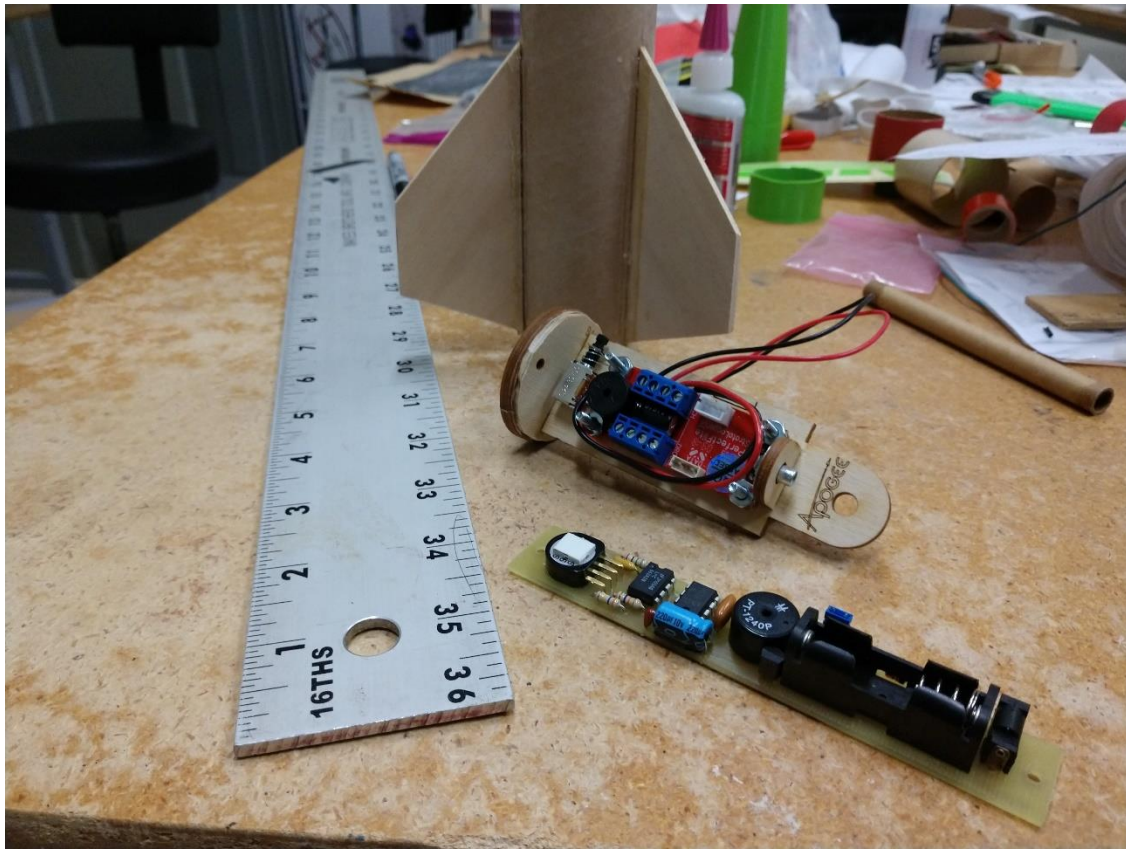


Figure 114: Avionics Bays for the BT20 Subscale and BT60 Subscale.

### 3.2.3 Launch Day Conditions

<b>Launch Time</b>	3:56 PM EST
<b>Temperature (deg Fahrenheit)</b>	41
<b>Wind Speed (mph)</b>	5.0
<b>Weather</b>	Cloudy
<b>Location</b>	Stony Brook, NY



Figure 115: BT20 Sized Subscale on Launch Rod.



Figure 116: Fully Assembled BT60 sized Subscale

### 3.2.4 Subscale Flight Predictions

Subscale flight predictions were performed for the BT60 size subscale vehicle. The OpenRocket Schematic is as follows:

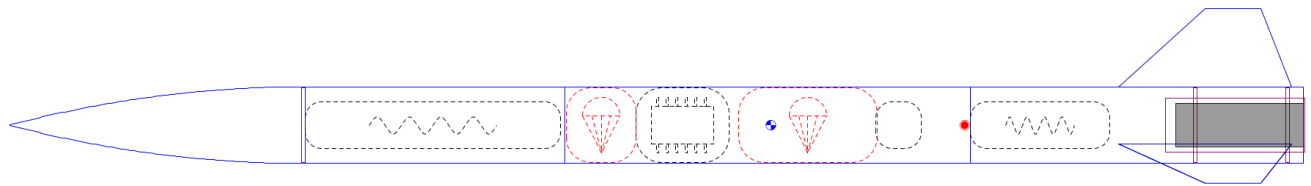


Figure 117: OpenRocket Schematic for BT60 Subscale

The BT-60 rocket was launched using an Estes E30-4 motor. The launch vehicle was also weighed to be 0.581 lbs before launch along with measuring the CP and CG with respect to the nosecone. The measured launch characteristics can be summarized below:

<b>Mass (lb)</b>	0.581
<b>Length (in)</b>	27.902
<b>CP (in)</b>	20.577
<b>CG (in)</b>	16.402
<b>Stability (cal)</b>	2.55

	<b>Apogee (ft)</b>	<b>Velocity off Rod (ft/s)</b>	<b>Time to Apogee (s)</b>	<b>Flight Time (s)</b>
<b>0 mph</b>	1262	61.6	8.3	39.1
<b>5 mph</b>	1247	61.6	8.22	38.9
<b>10 mph</b>	1266	61.6	8.13	38.6
<b>15 mph</b>	1200	61.6	8.04	38.4
<b>20 mph</b>	1172	61.6	7.91	37.6

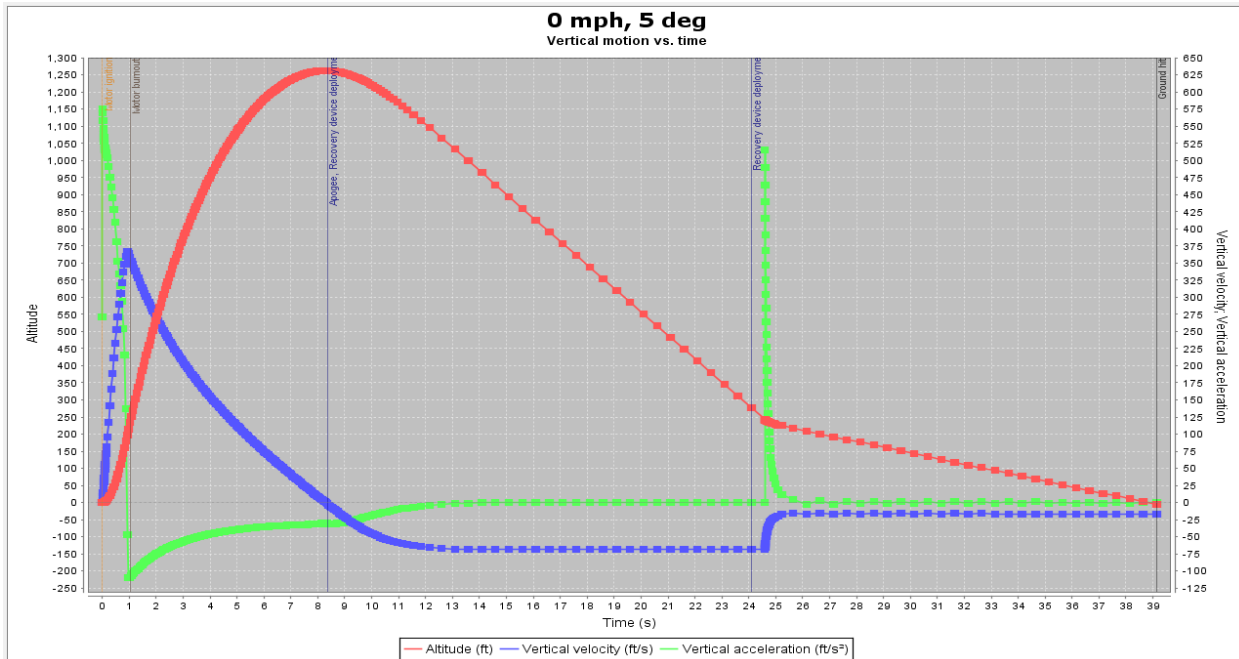


Figure 118: Subscale Flight Simulation (0 mph, 5 deg)

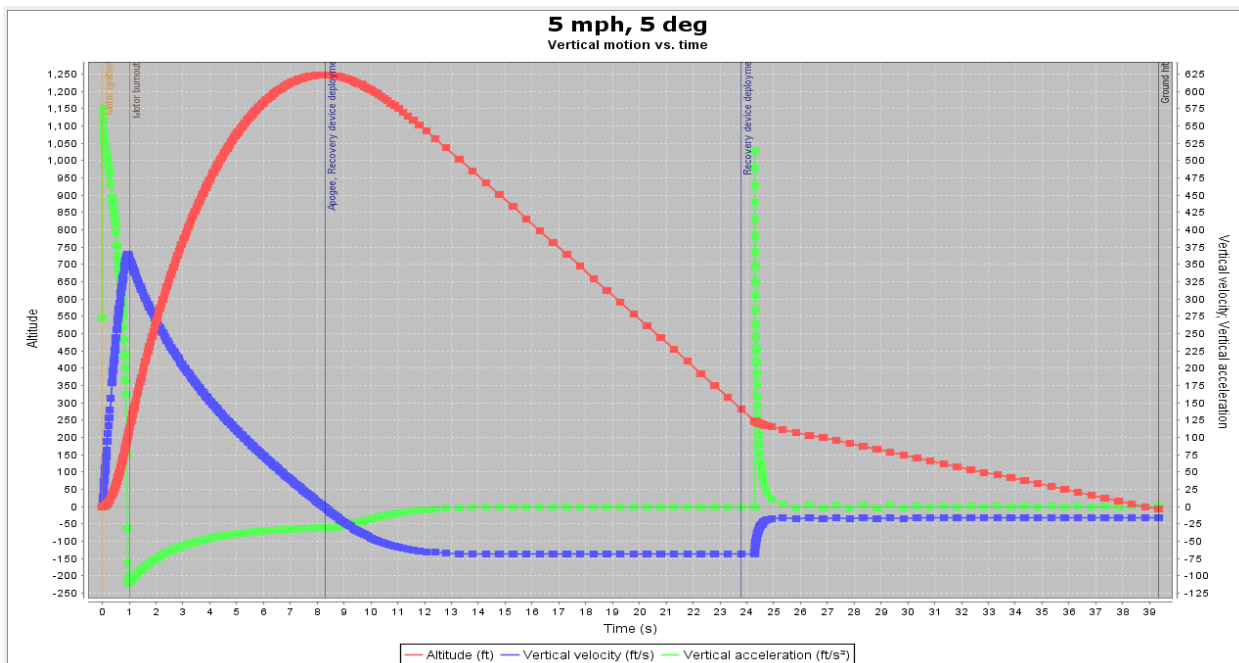


Figure 119: Subscale Flight Simulation (5 mph, 5 deg)

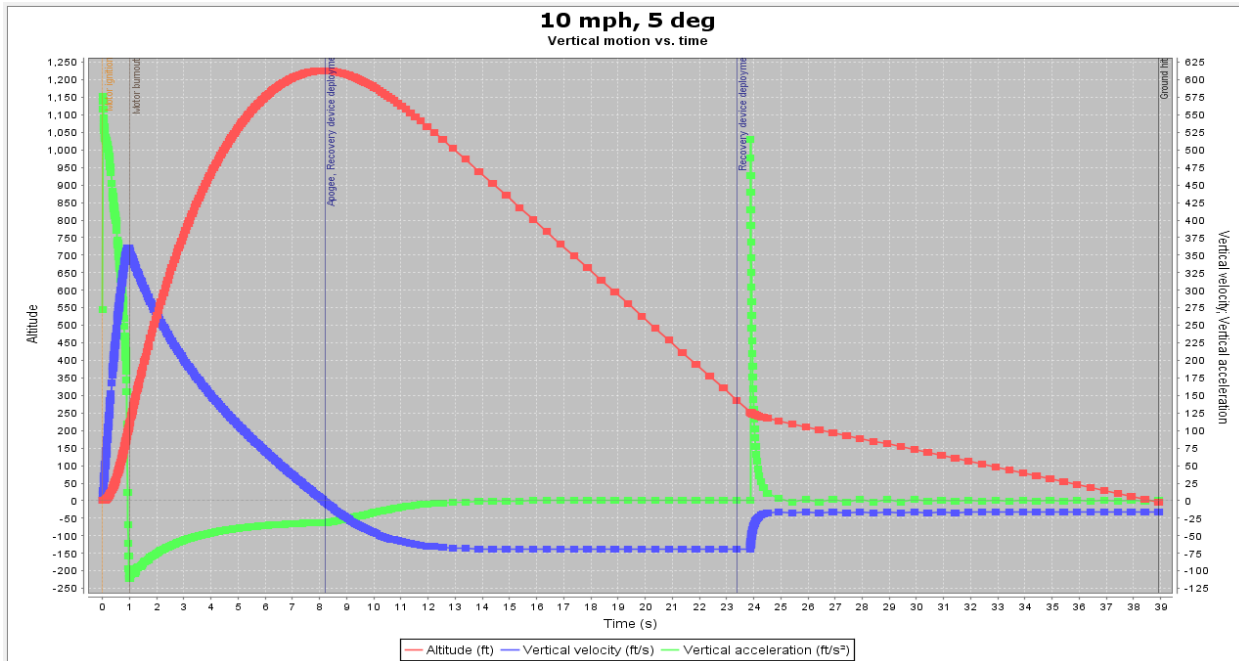


Figure 120: Subscale Flight Simulation (10 mph, 5 deg)

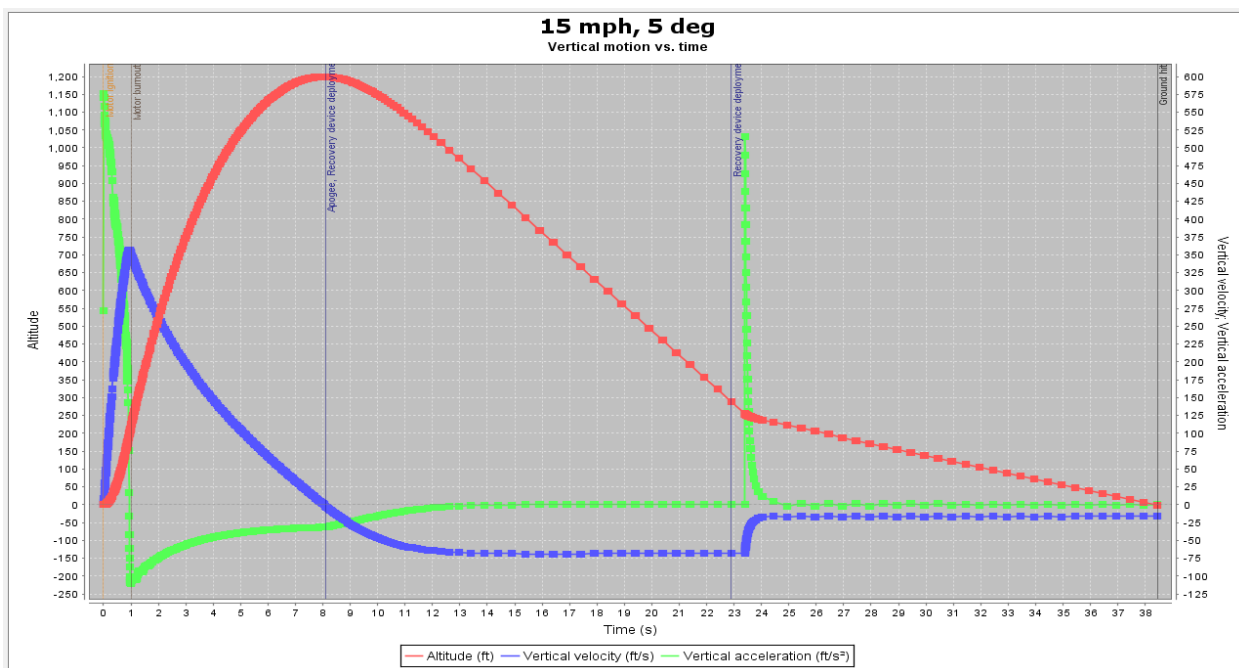


Figure 121: Subscale Flight Simulation (15 mph, 5 deg)

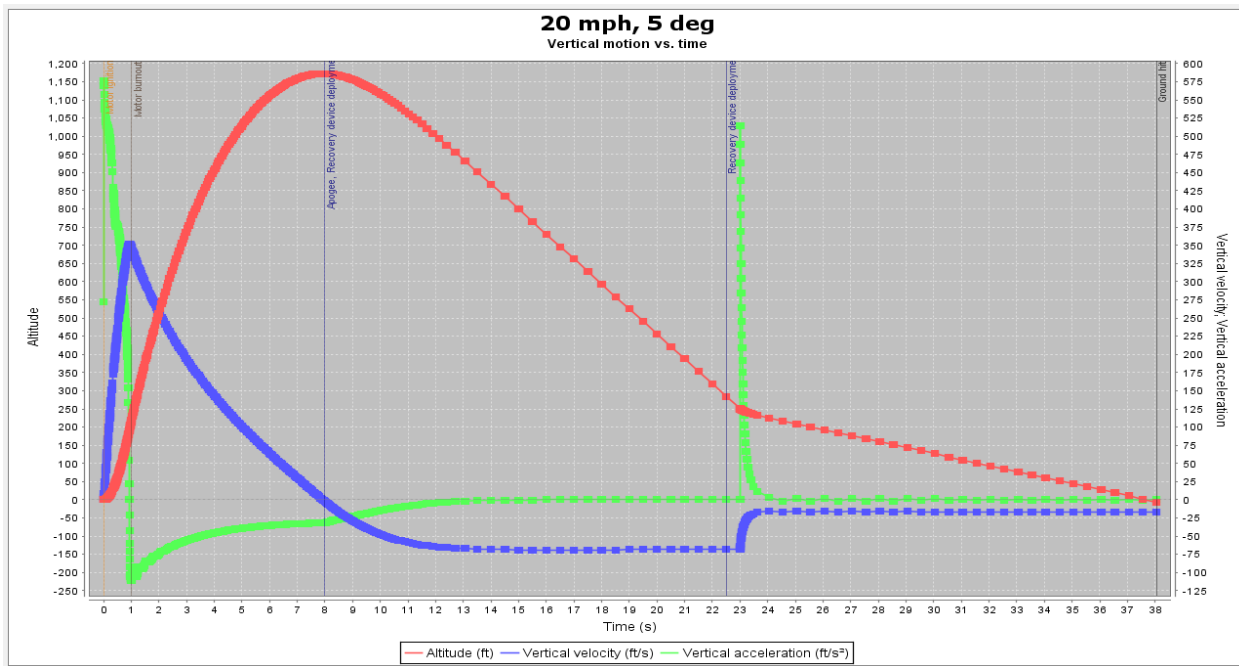


Figure 122: Subscale Flight Simulation (20 mph, 5 deg)

### 3.2.5 Subscale Flight Analysis

Using the PerfectFlite Stratologger the altitude data was able to be recorded properly. Since it is a pressure-based sensor, it records the altitude and then derives the velocity and acceleration values.

### 3.2.5.1. Raw Flight Data

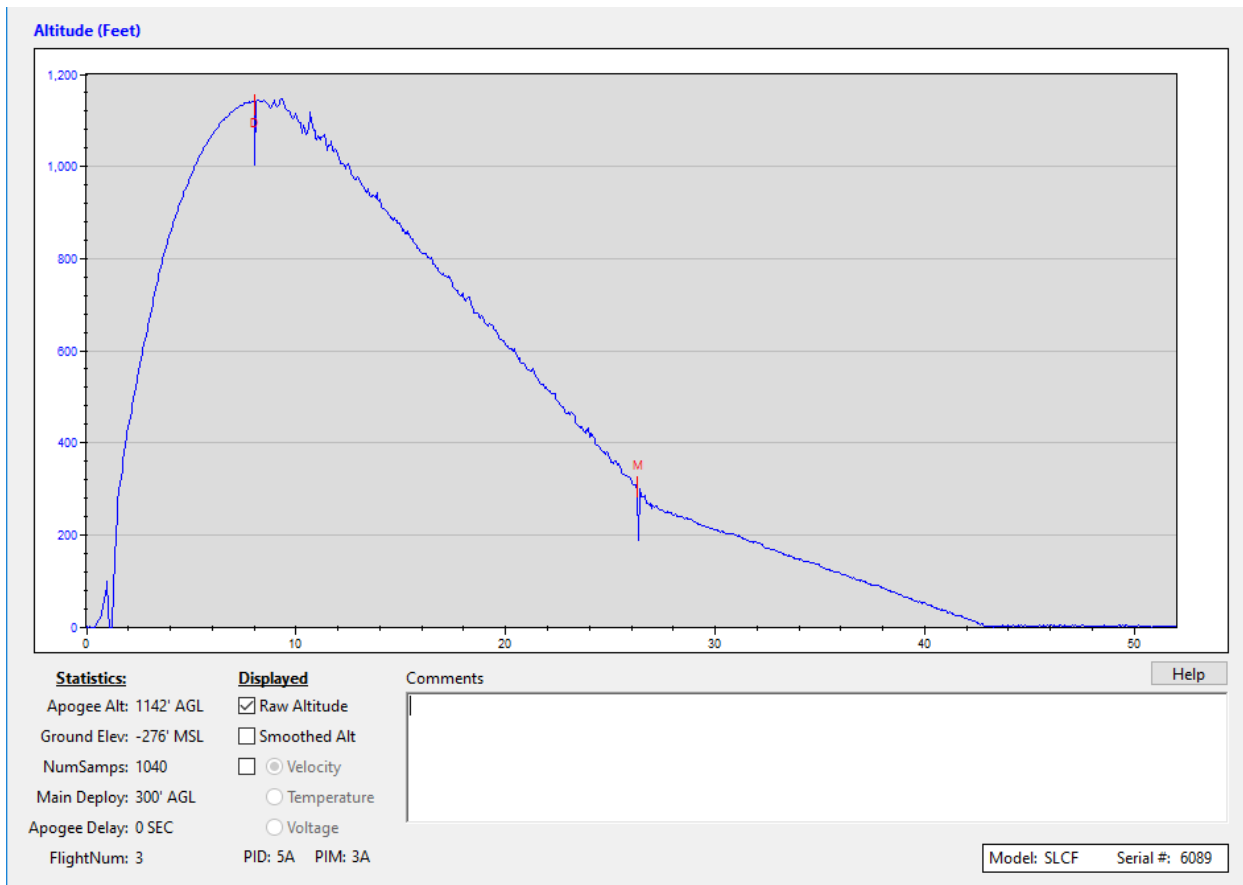


Figure 123: BT60 Subscale Raw Altitude Flight Data.

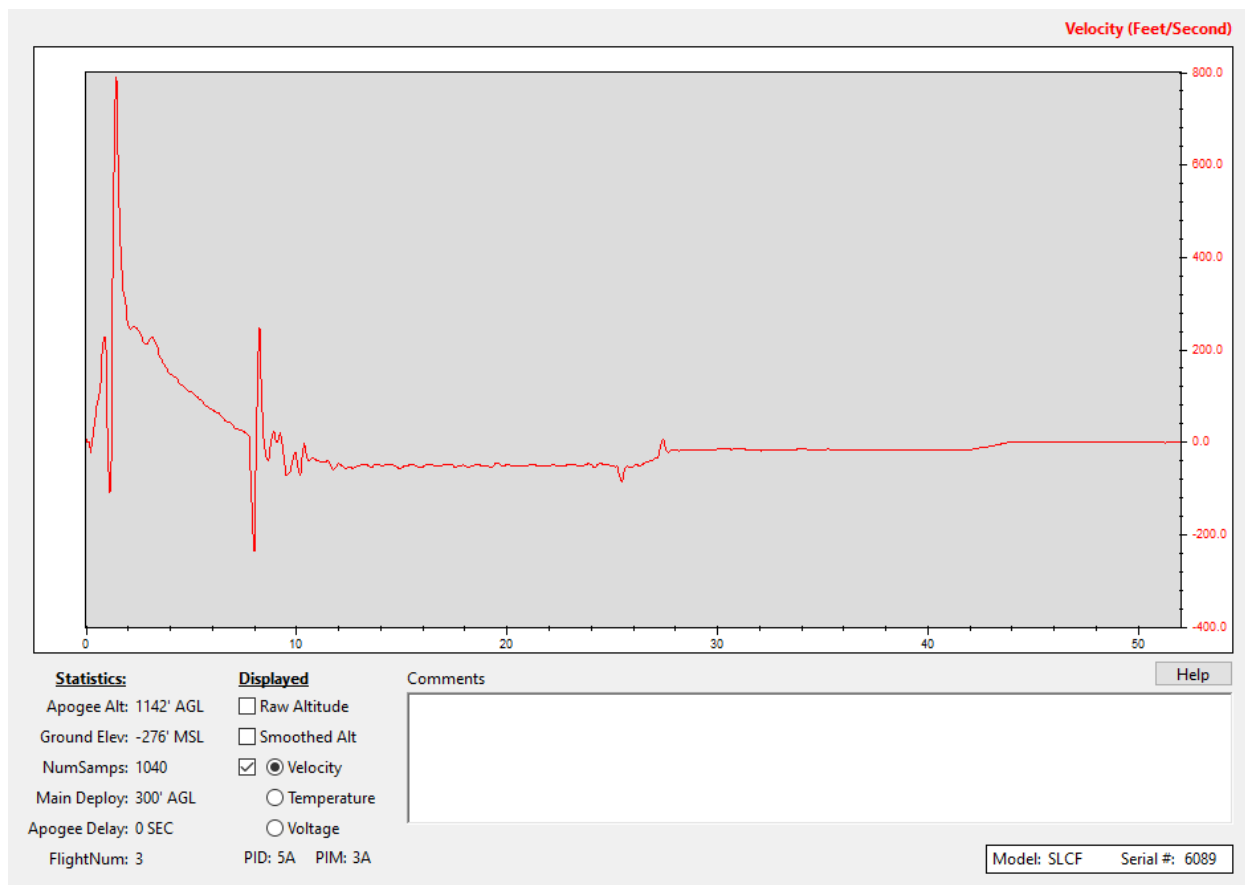


Figure 124: BT60 Subscale Raw Velocity Flight Data.

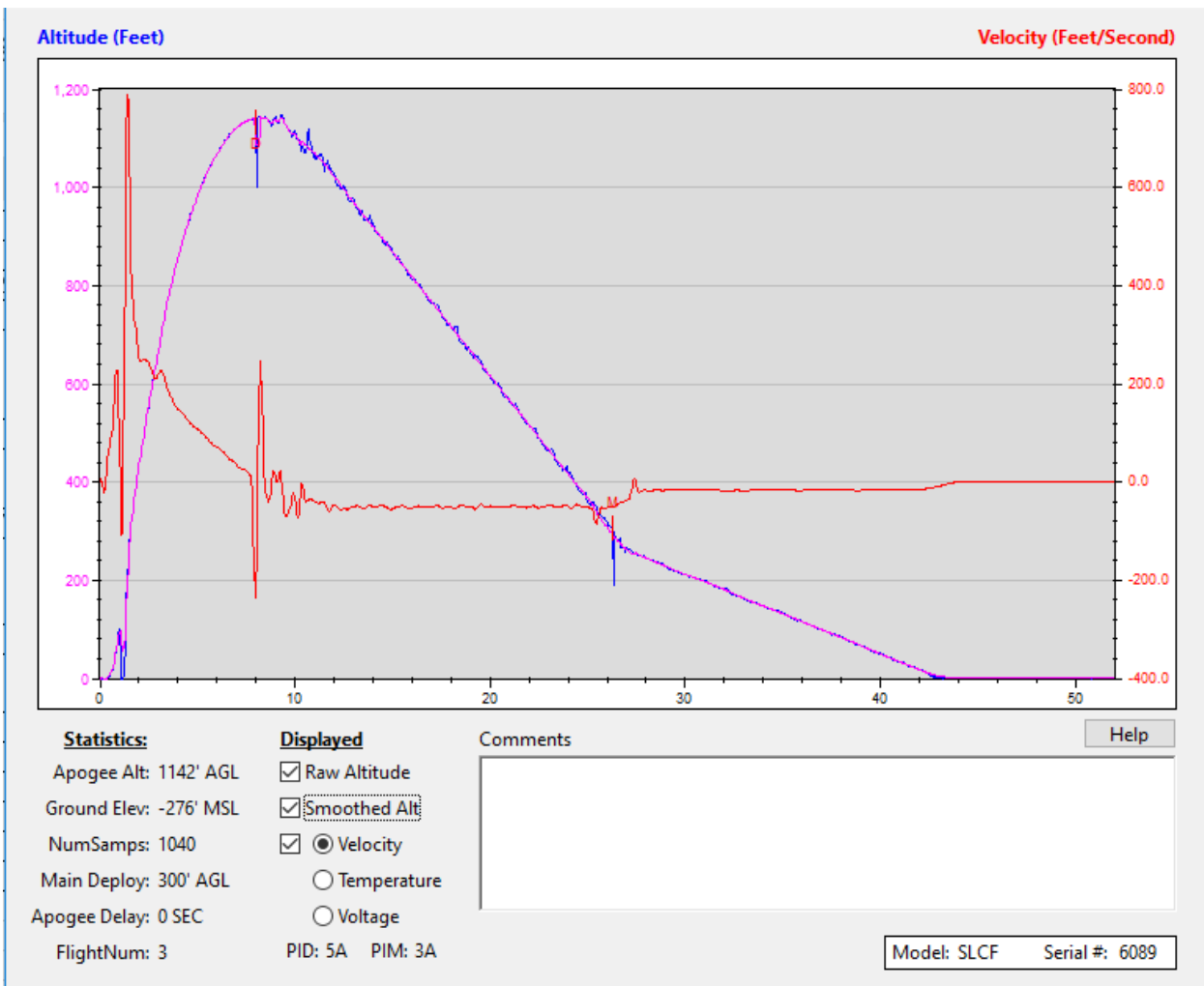


Figure 125: BT60 Subscale Raw Altitude & Velocity Flight Data.

Using Matlab, the altitude data was retrieved from the altimeter and further analysis was done in order to get the respective velocity and acceleration plots. From the raw altitude data, the pronounced downward spikes at altitude and main deployment can be seen. This was perhaps due to the avionics bay pointing downward when the charges fired which propelled it downward. Since the spikes are so pronounced, it could even be an issue with an acceleration sensitivity.

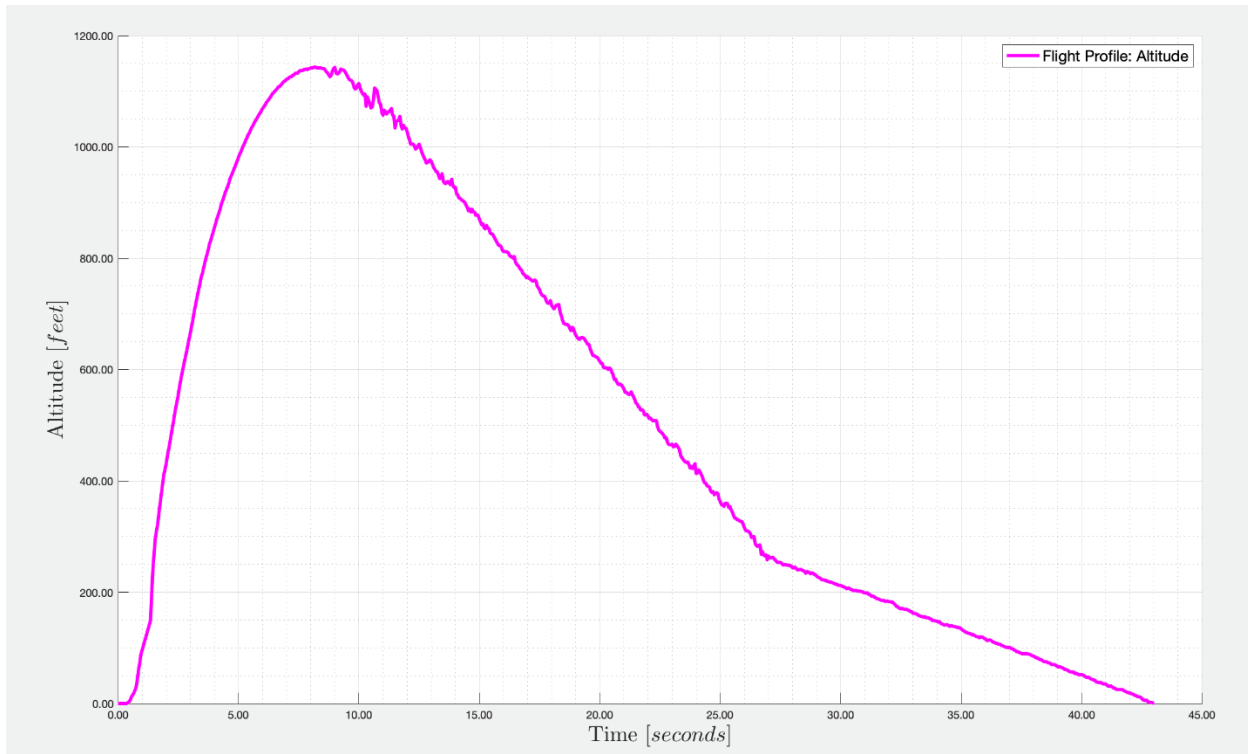


Figure 126: BT60 Subscale Matlab Altitude Data.

In order to get a more reliable velocity profile, the downward altitude profile was smoothed out but nevertheless the velocity plot was not perfect. Right before the coasting region the velocity can be seen decreasing at a constant rate due to the drogue chute. At this region the acceleration was essentially recorded to be zero.

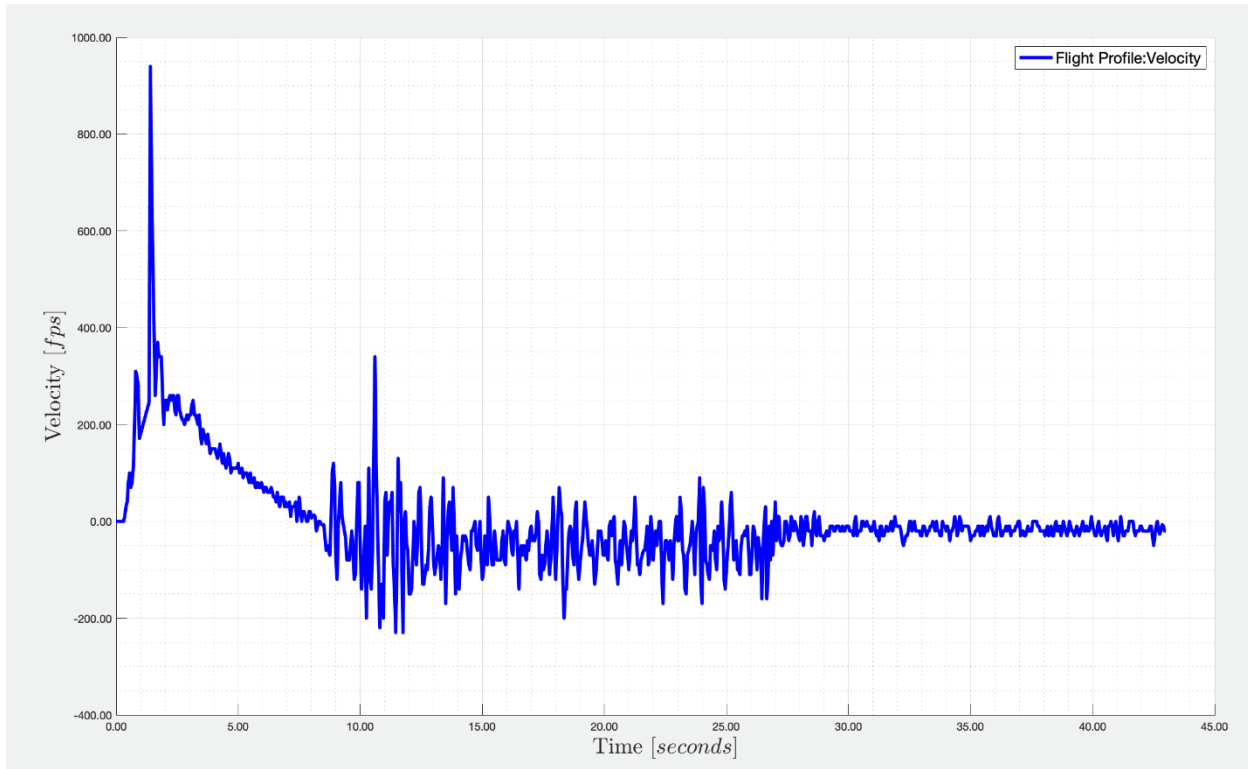


Figure 127: BT60 Subscale Matlab Velocity Data.

Due to the massive amounts of vibrations due to the main and drogue deployment, large spikes in the acceleration can be observed.

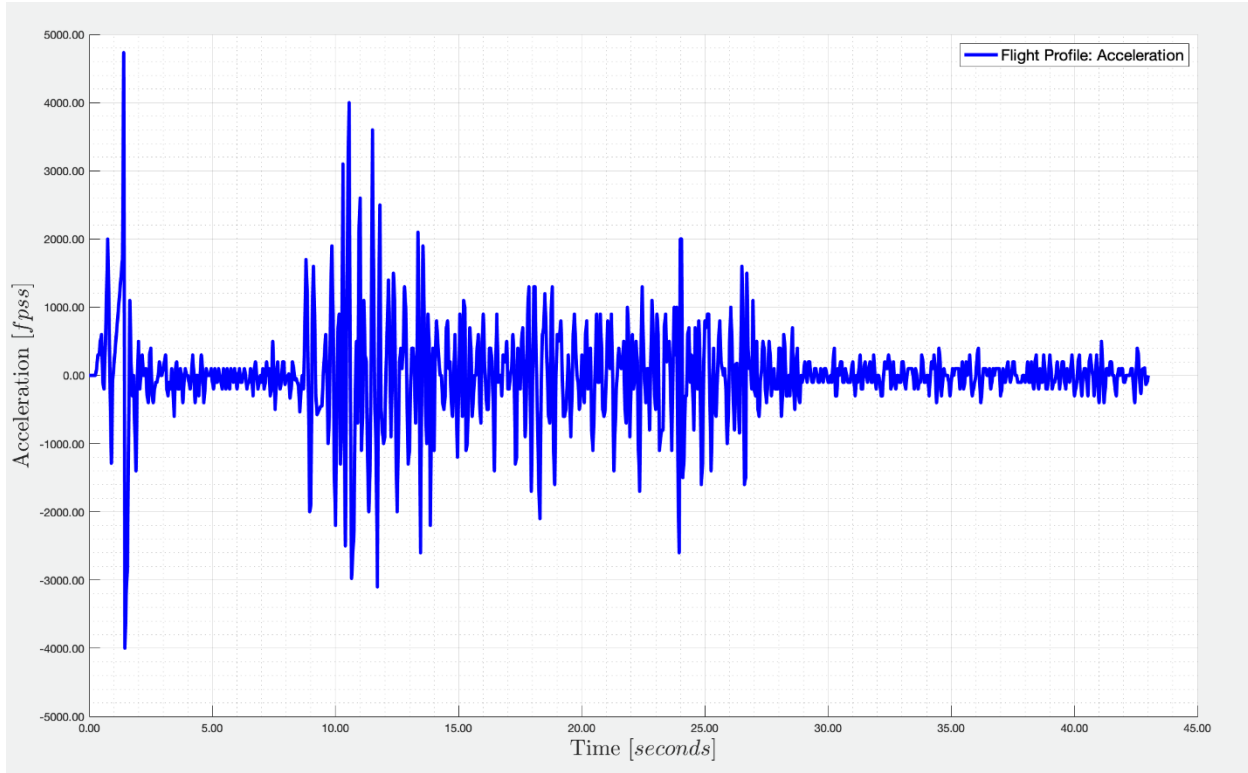


Figure 128: BT60 Subscale Matlab Acceleration Data.

Due to the large variation in the acceleration and velocity data, a reliable value for the drag force could not be calculated in order to estimate the drag coefficient. If the acceleration profile was smoother, the drag force would be able to be calculated as follows:

$$F_d = ma + mg$$

Using the drag force and velocity data, the drag coefficient could be calculated as follows:

$$C_d = 2 * \frac{F_d}{\rho V^2 A}$$

The apogee recorded by the altimeter on board was 1142 ft. The windspeed during the launch day is estimated to be 5 mph and the launch rod at an angle of 5 degrees. The predicted apogee at these conditions was simulated to be 1247 ft. Therefore, the percent difference between the predicted apogee and the observed apogee could be calculated to be 9.19% which falls within a reasonable margin. The projected apogee of the full-scale launch vehicle is 4500 ft. When scaled down using the same BT-60 subscale scaling factor, the apogee should be roughly 1170 ft. Since the BT-60 subscale rocket maintained the same stability, scaled down CG, CP and apogee, it can be concluded that it was a very high-fidelity model.

### 3.2.6 Impact of subscale launch on full scale

The subscale launch had a very large impact on the team in terms of cutting weight on the full-scale rocket. It is known that OpenRocket mostly likely always overestimates the apogee due to ideal conditions. However, this was amplified when the percent overshoot was roughly 10 percent at an apogee of one fourth of that of the full scale. Therefore after the subscale launch, the SBU

team started to design based on the worst case scenario instead of the mostly likely scenario. In the PDR the weight of the launch vehicle was 49.3 lbs with a projected apogee of roughly 4800 ft. After the subscale launch, the unreliable nature of OpenRocket in estimating the apogee was highlighted therefore resulting in the weight being dropped down to 47.1 lb with a projected apogee of over 5000 ft.

The downward spikes observed in the subscale launch also impacted the full-scale launch vehicle. The team is now planning on flying 2 different types of altimeters (one standard pressure based, and another accelerometer based). Flying two different altitude recording devices will allow to the team to compare recorded apogees during each flight and determine the validity of the devices and account for worst discrepancies.

Lastly, the inability to accurately calculate the drag coefficient of the launch vehicle for the subscale led to team to start delving deeper in CFD. These efforts resulted in calculating the drag coefficient of full scale launch vehicle to be: 0.435 without the deployment of the VDS and 0.71 with the VDS blades fully actuated.

### 3.3 Recovery Subsystem

### 3.4 Mission Performance Predictions

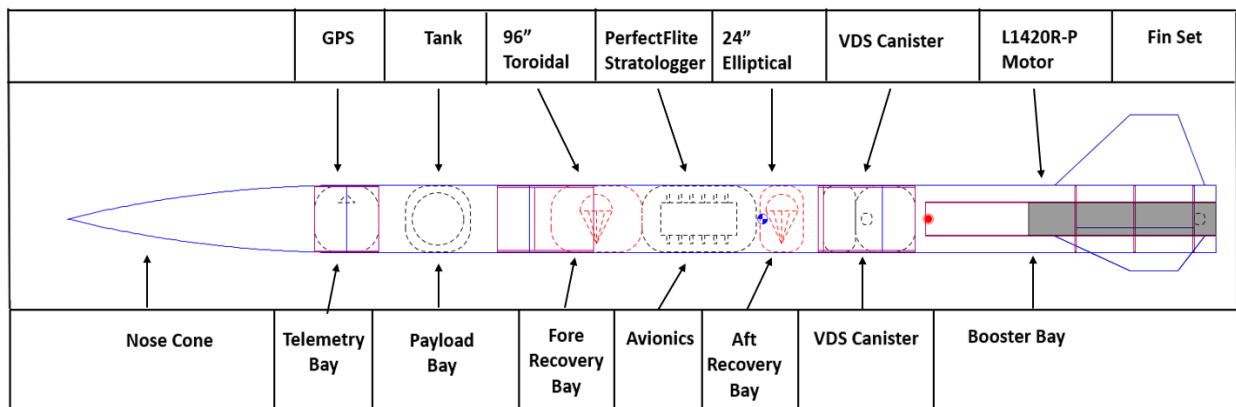


Figure 129: General Vehicle Overview.

The primary software utilized to predict mission performance characteristics was OpenRocket. However, both hand calculations and other simulation software such as RockSim was utilized to verify the OpenRocket findings. The mass breakdown and detailed flight characteristics are listed in the section below.

### 3.4.1 Component Mass Breakdown

#### 3.4.1.1. Component Mass Breakdown

Table 50: Nosecone & Telemetry Bay Mass Breakdown

Components	Mass (lbs)
Nosecone	3.0
6" Coupler	0.829
Telemetry & Payload Interface	0.8
<b>Subtotal</b>	<b>4.629</b>

Table 51: Payload Bay Mass Breakdown

Components	Mass (lbs)
19" Payload Airframe	1.47
Rover & Payload Assemblies	8.7
Bulkhead & U-Bolt	0.37
9" Coupler	1.27
<b>Subtotal</b>	<b>11.81</b>

Table 52: Avionics Bay Mass Breakdown

Components	Mass (lbs)
32.9" Avionics Airframe	2.54
Avionics Equipment	2.98
Main Bay	1.78
Drogue Bay	0.286
<b>Subtotal</b>	<b>7.586</b>

Table 53: Booster Bay Mass Breakdown

Components	Mass (lbs)
33" Propulsion Airframe	2.4
Centering Rings	0.57

16" Motor Tube	0.786
VDS	2.2
Camera Bay	0.5
Fins	2.4
Epoxy	2.5
9" Coupler	1.27
Motor & Hardware	10.1
Motor Retainer	0.31
<b>Total</b>	<b>23.036</b>

Table 54: Overall Vehicle Mass Summary

Subsystems	Mass (lbs)
Nosecone & Telemetry Bay	4.629
Payload Bay	11.81
Avionics Bay	7.586
Propulsion Bay	23.036
<b>Total Loaded Weight</b>	<b>47.1</b>
<b>Total Unloaded Weight</b>	<b>41.5</b>

### 3.4.2 Simulated Motor Thrust Curve

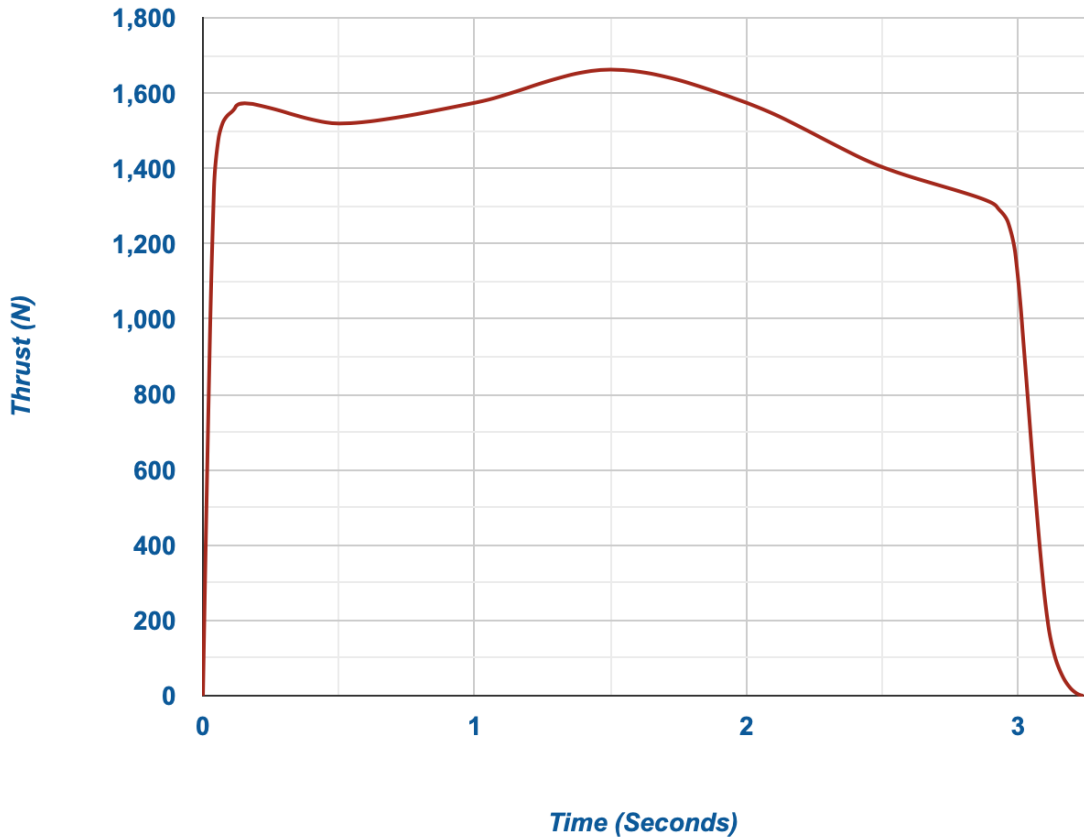


Figure 130: Simulated Motor Thrust Curve.

### 3.4.3 Altitude Predictions (launch rail at 7.5 deg)

Table 55: Altitude Prediction Summary for Rail at 7.5 Deg.

	Apogee (ft)	Velocity off Rod (ft/s)	Time to Apogee (s)	Flight Time (s)	Descent Time (s)
<b>0 mph</b>	4986	59.9	18.0	103	85
<b>5 mph</b>	4908	59.9	17.9	102	84.1
<b>10 mph</b>	4800	59.9	17.7	101	83.3
<b>15 mph</b>	4720	59.9	17.5	99.8	82.3
<b>20 mph</b>	4611	59.9	17.3	99.7	82.4

### 3.4.4 Simulated Flight Profiles (launch rail at 7.5 deg)

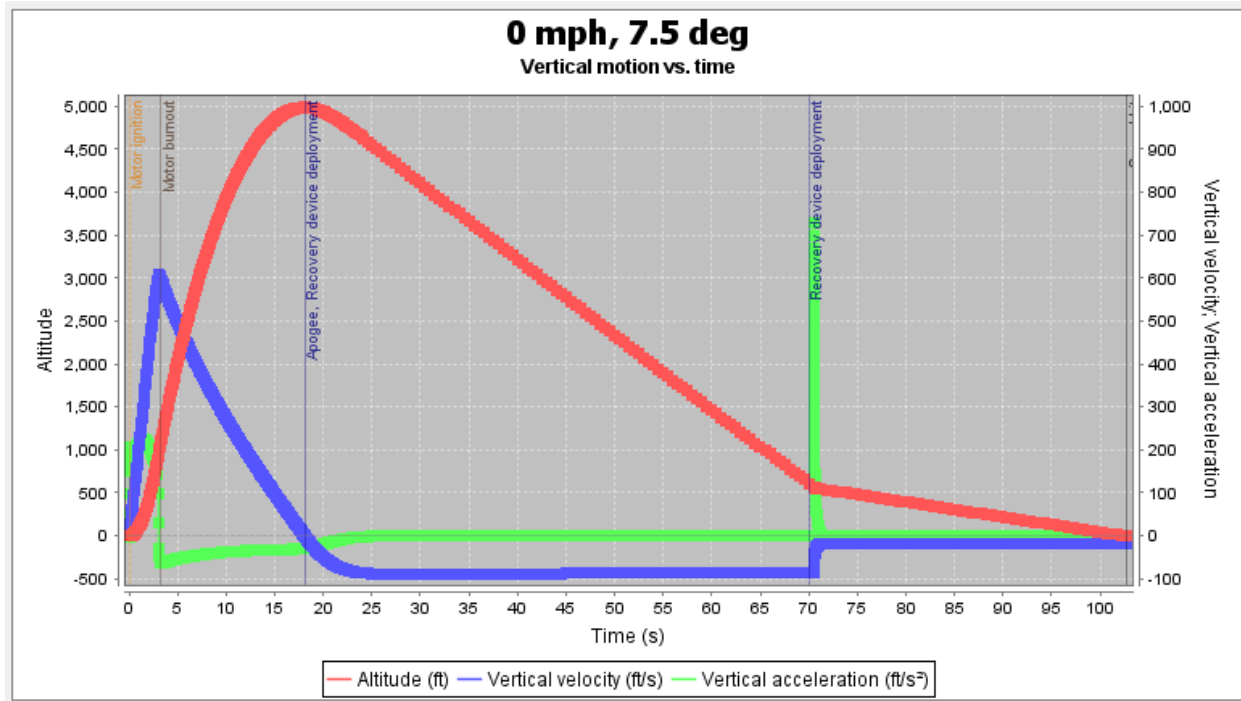


Figure 131: Simulated Flight Profile (0 mph, 7.5 deg).

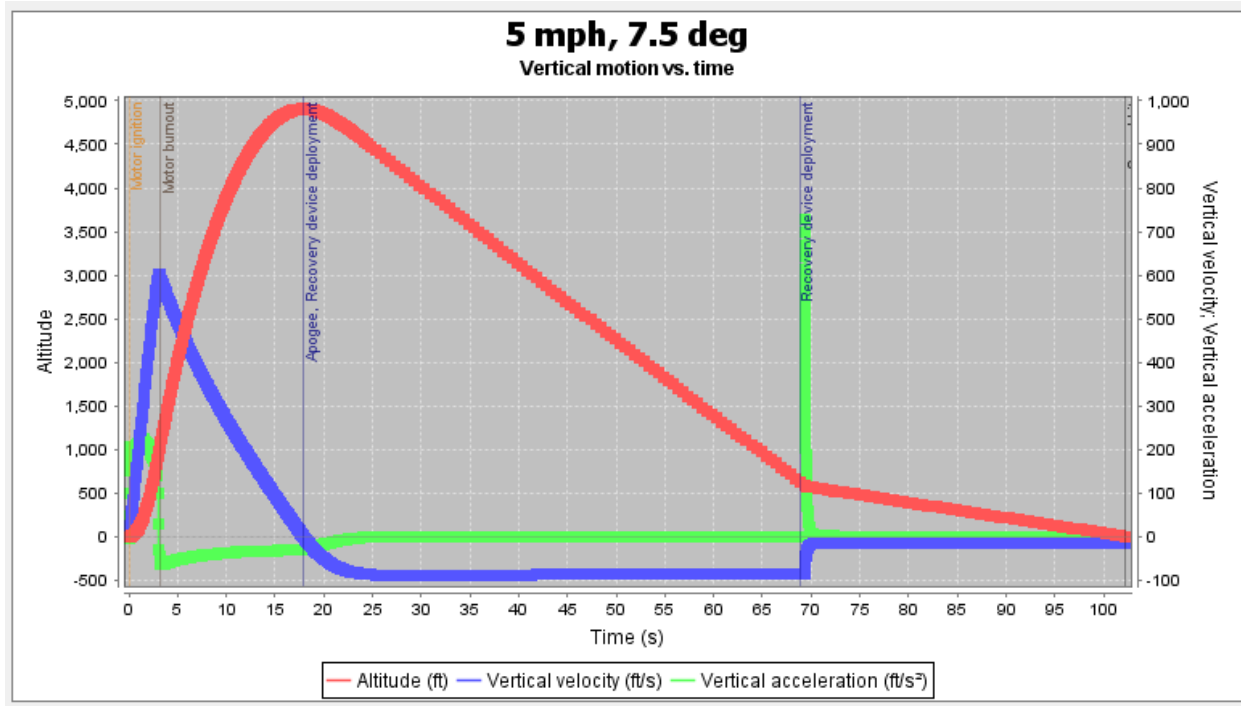


Figure 132: Simulated Flight Profile (5 mph, 7.5 deg).

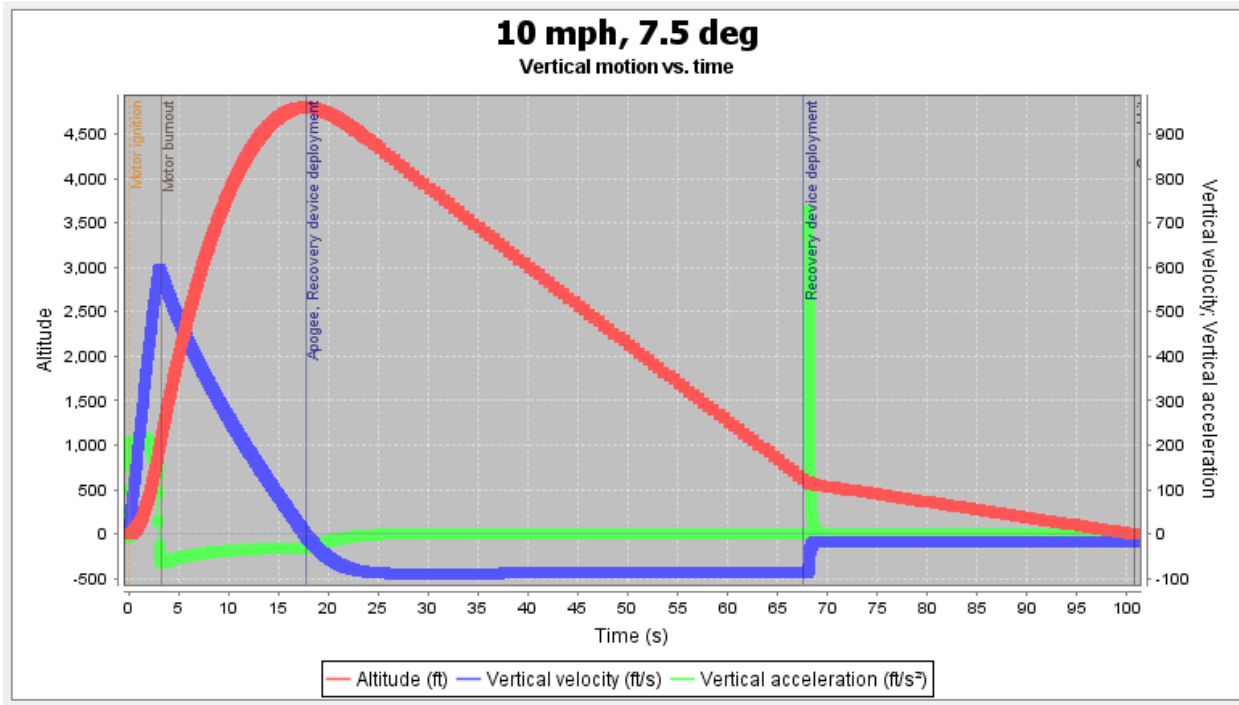


Figure 133: Simulated Flight Profile (10 mph, 7.5 deg).

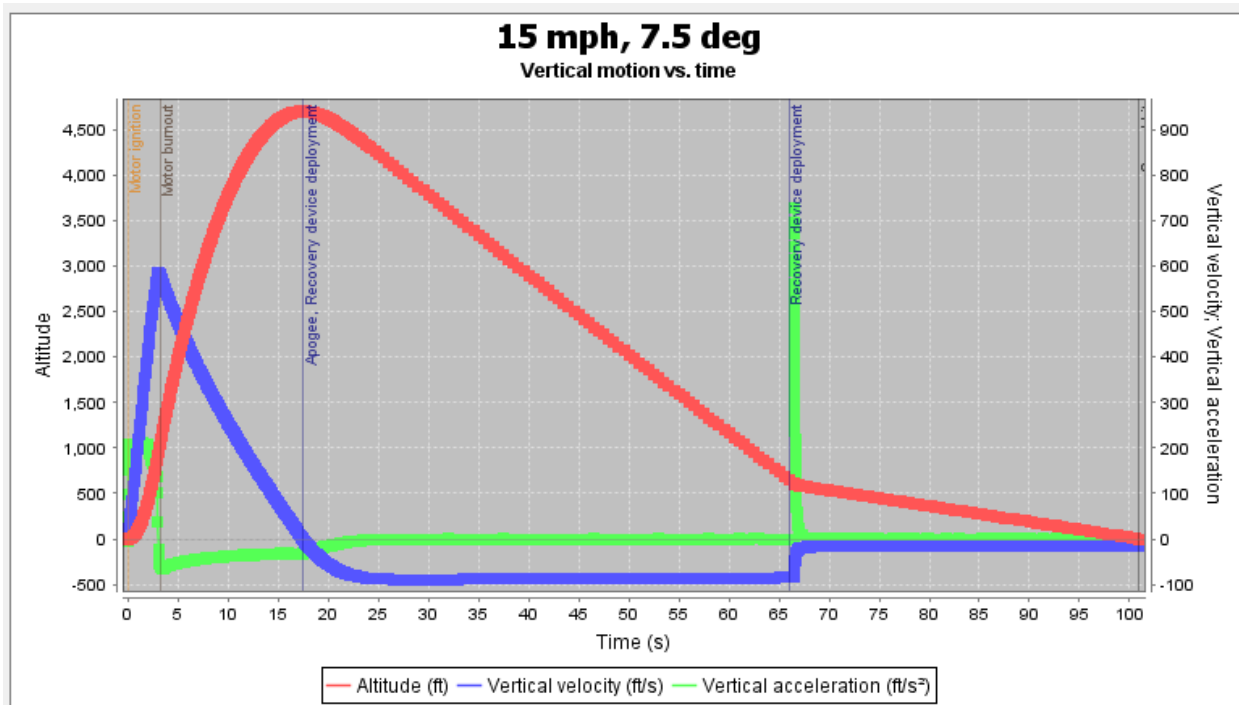


Figure 134: Simulated Flight Profile (15 mph, 7.5 deg).

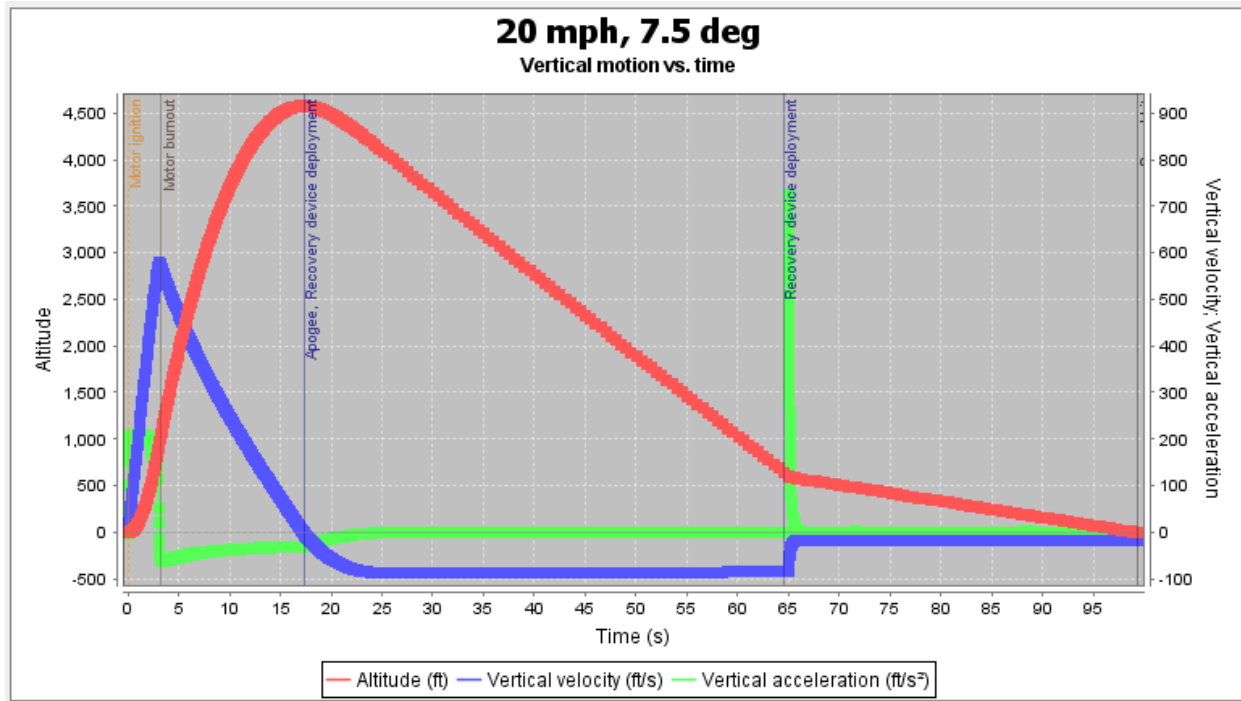


Figure 135: Simulated Flight Profile (20 mph, 7.5 deg).

### 3.4.5 Altitude Predictions (launch rail at 10 deg)

Table 56: Altitude Prediction Summary for Rail at 10.0 Deg.

	Apogee (ft)	Velocity off Rod (ft/s)	Time to Apogee (s)	Flight Time (s)	Descent Time (s)
<b>0 mph</b>	4895	60	17.9	103	85.1
<b>5 mph</b>	4800	60	17.7	101	83.3
<b>10 mph</b>	4712	60	17.5	99.9	82.4
<b>15 mph</b>	4571	59.9	17.2	98	80.8
<b>20 mph</b>	4484	59.9	17.1	96.8	79.7

### 3.4.6 Simulated Flight Profiles (launch rail at 10 deg)

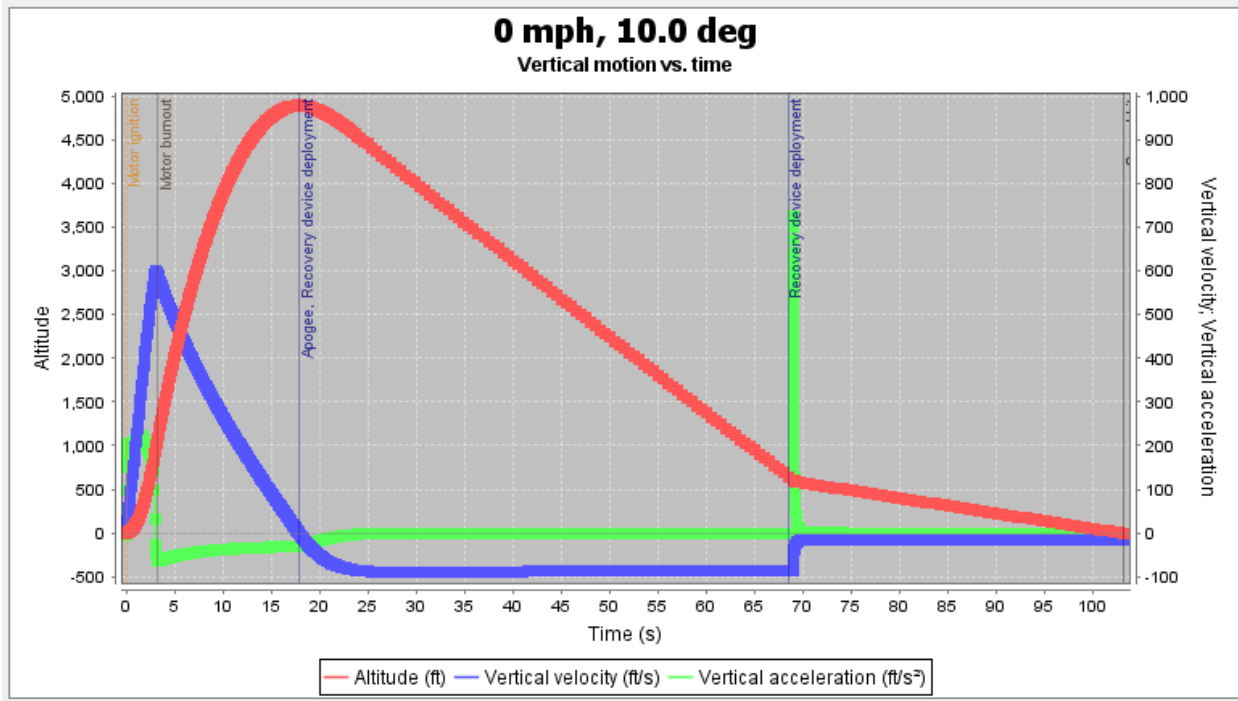


Figure 136: Simulated Flight Profile (0 mph, 10.0 deg).

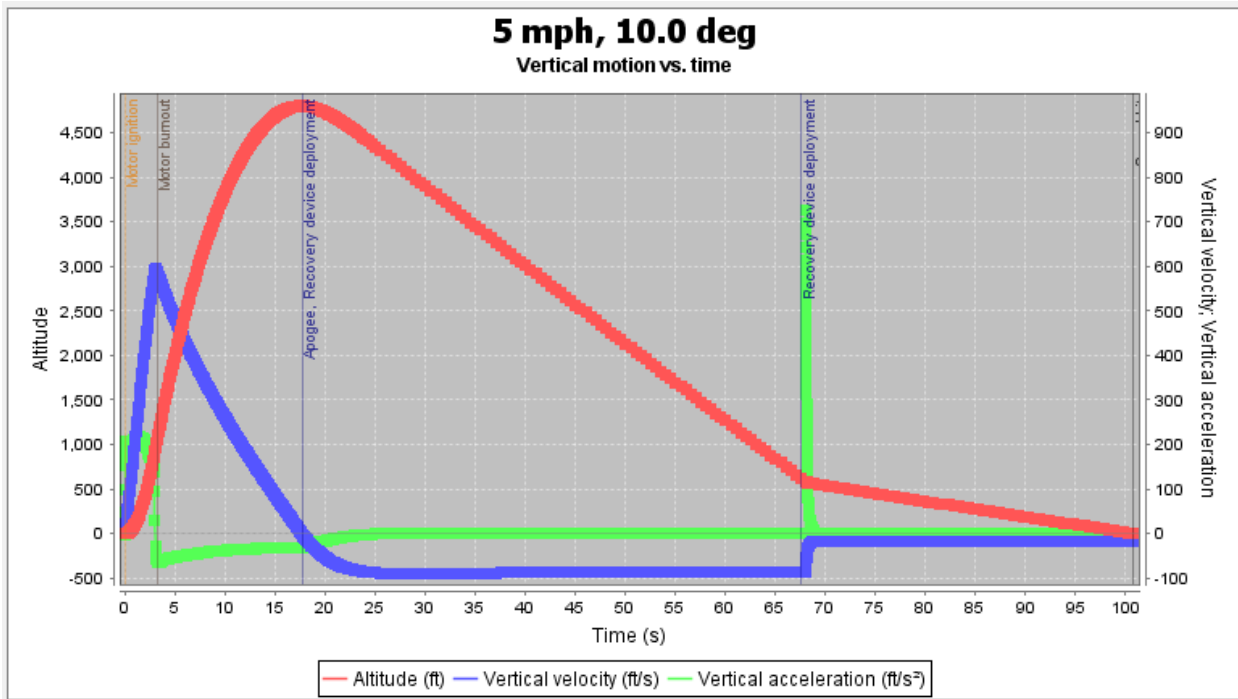


Figure 137: Simulated Flight Profile (5 mph, 10.0 deg).

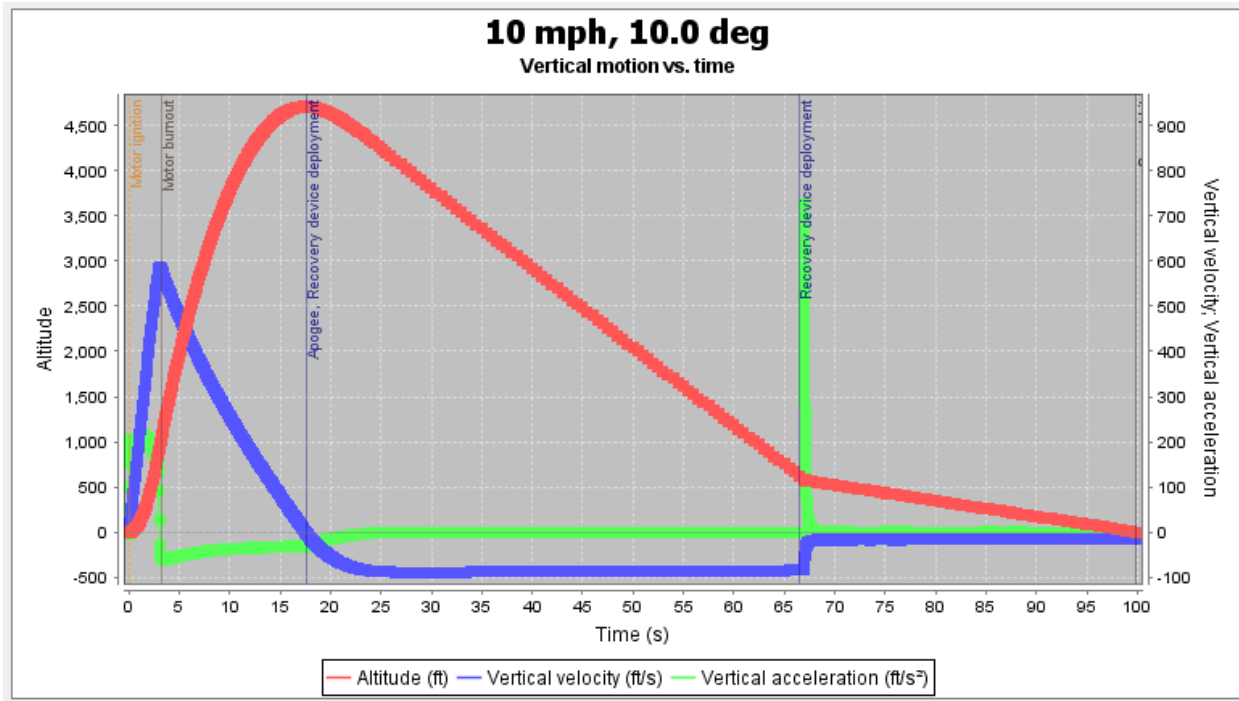


Figure 138: Simulated Flight Profile (10 mph, 10.0 deg).

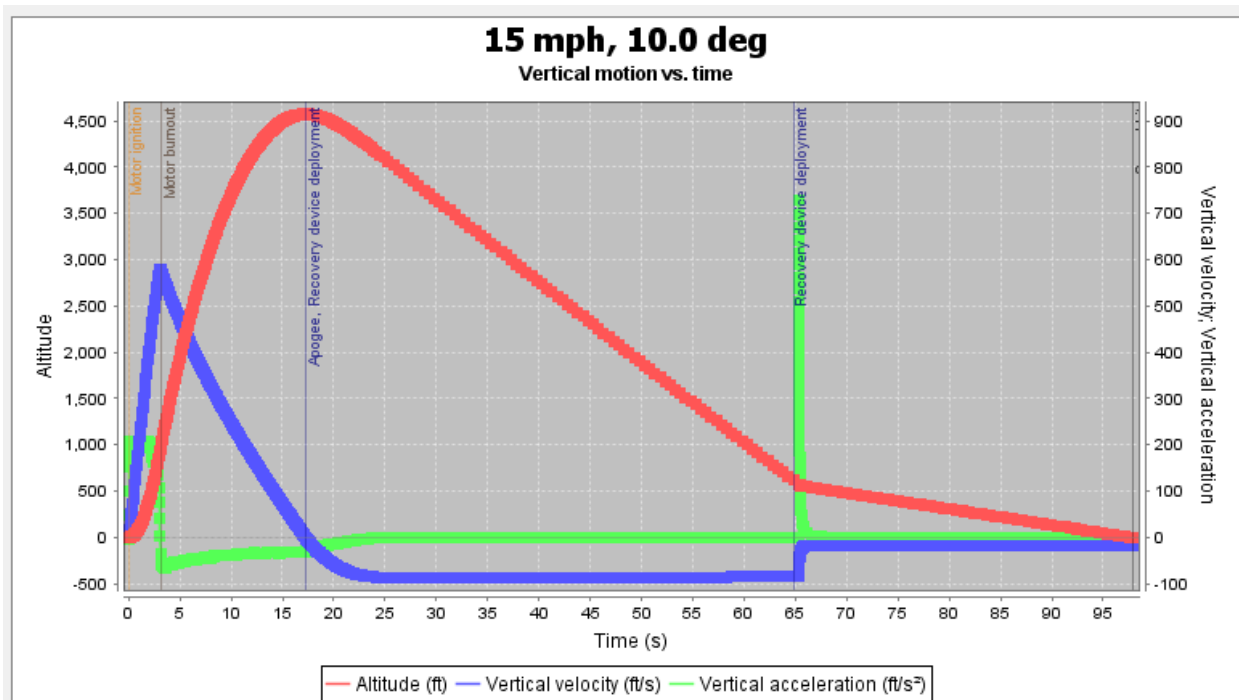


Figure 139: Simulated Flight Profile (15 mph, 10.0 deg).

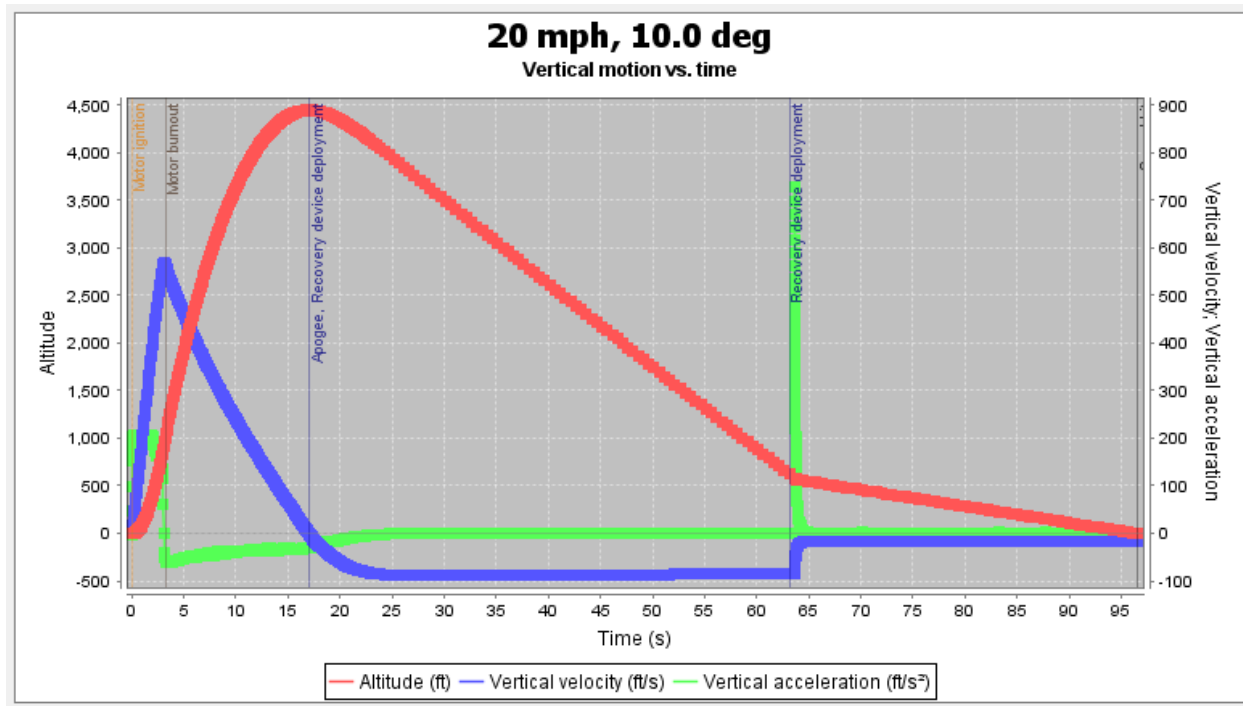


Figure 140: Simulated Flight Profile (20 mph, 10.0 deg).

### 3.4.7 Stability Margin, CP & CG

Table 57: Flight Characteristics.

Maximum Velocity (ft/s)	615.0
Max Mach Number	0.55
Max Acceleration (ft/s <sup>2</sup> )	231
Target Apogee (ft)	4500
Best Case Projected Apogee (ft)	5104
Worst Case Projected Apogee (ft)	4484

Table 58: Stability Marin, CP and CG.

Stability Margin (on pad)	2.50 cal
Static Stability Margin (at rail exit)	2.5625 cal
Location of CP from Nose Cone Tip	80.139 inches
Location of CG from Nose Cone Tip	64.721 inches
Rail Exit Velocity	59.9 ft/s

<b>Thrust to Weight Ratio</b>	8.66
-------------------------------	------

### 3.4.8 RockSim vs. OpenRocket

The apogee estimates from OpenRocket were cross checked with those from RockSim. The results indicated that both simulation software resulted in extremely similar values with a maximum percent difference of 2.25%. This makes both qualitative and quantitative sense since the software both use the standard barrowman equations and the Runge-Kutta method to make the approximations for the flight characteristics. The results are listed below:

Table 59: OpenRocket vs. Rocksim Apogee Comparison at 0 Deg Launch Rail.

	<b>OpenRocket Apogee (ft)</b>	<b>RockSim Apogee (ft)</b>
<b>0 mph</b>	5104	5092
<b>5 mph</b>	5091	5078
<b>10 mph</b>	5064	5033
<b>15 mph</b>	5009	4956
<b>20 mph</b>	4957	4848

Table 60: OpenRocket vs. Rocksim Apogee Comparison at 5 Deg Launch Rail.

	<b>OpenRocket Apogee (ft)</b>	<b>RockSim Apogee (ft)</b>
<b>0 mph</b>	5052	5038
<b>5 mph</b>	4992	4983
<b>10 mph</b>	4923	4889
<b>15 mph</b>	4835	4763
<b>20 mph</b>	4749	4642

Table 61: OpenRocket vs. Rocksim Stability Comparison

	<b>OpenRocket</b>	<b>RockSim</b>
<b>CG (in from NC)</b>	64.721	64.48
<b>CP (in from NC)</b>	80.139	80.0284
<b>Stability (cal)</b>	2.50	2.52
<b>Max Velocity (ft/s)</b>	615.0	615.7
<b>Max Acceleration (ft/s<sup>2</sup>)</b>	230.0	232.35

### 3.5 Recovery Subsystem

A main parachute deployment height of 600ft was chosen to ensure the deployment is above the minimum deployment bound of 500ft, while being low enough to where the drift would be minimized as much as possible. The drogue chute will be deployed at the apogee point of 4500ft in order to control the descent of the rocket enough to minimize the drift of the rocket.

The main parachute will be deployed several thousand feet after the drogue chute to minimize descent time and drift, while still being as controlled as possible. The main parachute is primarily used to allow safe descent of the rocket as it returns to the ground.

Properties and parameters of the main parachute were found through using mathematical models utilizing both dynamics and fluid mechanics. This allows estimations for parachutes parameters and nominal diameter. One important equation used for this process is the equation for terminal velocity, which is written as:

$$v_{term} = \sqrt{2KE/m}$$

In which,

$v_{term}$ : Terminal Velocity

KE: Kinetic Energy

m: Mass

It is required that each independent section of the rocket have a maximum kinetic energy of no more than 75 ft-lbf.

With the terminal velocity now being known, it is simple to calculate the drag force using the following equation.

$$F_d = .5\rho v_{term}^2 C_d A_{on}$$

For which:

$F_d$ : Drag Force

$\rho$ : Fluid Density (of air is 0.0023769 slug/ft<sup>3</sup>)

$C_d$ : Drag Coefficient

n: Number of Parachutes

$A_o$ : Canopy Surface Area

Since the shape of the parachute can be modeled as a circle, the canopy surface area can be replaced by the equation for area of a circle seen below.

$$A_o = \pi d_o^2 / 4$$

Where:

$d_o$ : Nominal Diameter

This diameter is unknown and needs to be found in order to meet the minimum kinetic energy requirement. To find this value, we can equate the drag force and the force due to gravity and solve for the diameter if several assumptions are made. These include constant air density and that only drag on main parachute is accounted for. The equation is as follows:

$$d_o = \sqrt{8mg/(\rho v_{term}^2 C_d n)}$$

In this case:

$g$ : Acceleration Due to Gravity (32.2 ft/s<sup>2</sup>)

Through use of these formulas, it was possible to get a good idea of what was needed for the recovery system to function properly. In the end, the annular parachute known as [Iris Ultra 96'' Standard Parachute](#) was selected as the main parachute for the rocket. This is because while being more expensive than its elliptical counterpart by a significant margin, it has a notably higher drag coefficient and is also more stable. Therefore, it appears to be a more reliable parachute.

### 3.5.1 Drogue Parachute

The drogue parachute will be deployed at an apogee of 4,700 ft. By extension, it is vital to have a reliable parachute to function as the drogue. The chosen parachute is the [24'' Elliptical Parachute](#) because it is cost efficient while allowing for stability. In addition, the drag coefficient will be lower than that of an annular drogue, and thus it will allow for the descent to be faster while still controlled.

### 3.5.2 Descent Velocity and Drift

The kinetic energy of any independent rocket section can be found via the classical formula for kinetic energy.

$$KE = .5mv^2$$

In addition, the terminal velocity of each section can be found by combining previously derived formulas, as seen below.

$$v_{ter} = \sqrt{2mg/(\rho C_d n (\frac{\pi}{4}) d_c^2)}$$

From this equation and noting that the maximum kinetic energy of any independent section of the rocket can be found by using the kinetic energy formula with terminal velocity, it is possible to compare these values for each section.

Table 3.62: Rocket Section Mass, Velocity, and Kinetic Energy Data

Section	Mass (slug)	Maximum Kinetic Energy (ft*lb)
Payload	0.5205	69.4956
Avionics	0.2356	32.0697
Booster Bay	0.5421	73.7950

It is also required to calculate the rocket's rate of decent. This will be done by using both an open rocket simulation as well as a numerical calculation via Fourth Order Runge-Kutta (RK4). The RK4 calculation for descent rate will be set up by solving for the net acceleration in the following way.

$$y''(t) = -32.2 + (\rho y'(t)^2 C_d \left(\frac{\pi}{4}\right) d_{parachute}^2)/(2m_{total})$$

Where the diameter of the parachute is equal to that of the drogue chute above and at an altitude of 600ft, and equal to that of the main parachute below its deployment altitude of 600 ft. In addition, the boundary conditions for the descent are set at  $y(0)$  is equal to the apogee height and  $y'(0)$  equals zero due to simple kinematics. From here, it is possible to calculate the descent time using RK4. The total descent time was numerically calculated to be 77.1 seconds.

#### Drift Calculations

To calculate the drift experienced by the rocket, the following formula was used.

$$\text{Drift}(t) = tV$$

$t$  = time

$V$  = wind speed

Using the previously discussed = descent time of 77.1s it is possible to attain the following values.

Table 3.63: Descent Drift

Wind Speed (mph)	Wind Speed (ft/s)	Drift (ft)
20	29.33	2261.3
15	22	1696.2
10	14.67	1121.1
5	7.33	565.1
0	0	0

### 3.5.3 Shear Pins and Ejection Charges

### 3.5.4 Shear Pins

Shear pin selection is closely tied to the process of selecting the appropriate ejection charges. First, the force that is imparted onto the rocket during flight must be calculated. The shear pins must be thin enough to break when the black powder charges ignite, and they should be thick enough to not cause the rocket to separate due to the pressure difference between the inside and outside of the rocket. This pressure difference comes into play while the rocket is launched as the altitude causes a decrease in the external pressure while the internal pressure remains constant. Our design will use 4-40 X 5/16" long Fillister Nylon Slotted Machine Screws as they can withstand the initial launch forces but can easily shear off during ejection charge ignition. These pins were also selected as they are relatively cheap and multiple ground tests will be performed to determine a more accurate amount of ejection charge mass in addition to our theoretical calculations. [Studies have been performed, noting how these shear pins have a maximum shear strength of about 38lbf each when three or more are used.](#)



Figure 3.141: 4-40 Shear Pins

The primary concerns are that the charges cause irreversible damage to a component outside the shear pins or that not enough is used to properly deploy the parachutes, ejection tests will be conducted to confirm the amount of black powder selected separates the parachutes while not damaging any of the rocket sections. This test will also confirm the electronics are configured correctly.

### 3.5.5 Black Powder

The quantity of shear pins used as well as the volume of the parachute bays allow for calculations of the ejection charges mass. First, the required pressure to break apart the shear pins needs to be calculated, which by using basic physics can be done with the equation below.

$$P = (4F)/(\pi D^2)$$

For which

F: Required shear force in pound-force

D: diameter of parachute bay in inches

P: Pressure required to break pins

The volume of the parachute bay can be seen below.

$$V = \left(\frac{\pi}{4}\right)D^2L$$

Where

L: length of the parachute bay in inches

V: volume of parachute bay

The formula for cross-sectional area of the parachute bay can be found using the circular area formula.

$$A = \left(\frac{\pi}{4}\right)D^2$$

A: cross-sectional area of parachute bay

As for calculating the actual mass of the black powder required in the ejection charge, it can be found with the ideal gas law, which is presented below.

$$m = (PV)/(RT)$$

m: mass of black powder (lbm)

R: gas constant [in\*lbf/lbm]

T: temperature in degrees Rankine

It is important to note that the standard mass unit used for ejection chargers is in grams, so it is necessary to use a conversion factor of 454 g/lbf in order to convert into grams. By plugging this and the previous formula for pressure into the ideal gas law, the new formula is as follows.

$$m = (454FL)/(RT)$$

To make the formula even more simple to use, the ideal gas constant can be assumed to be 266 in lbf/lbm

and temperature to be at 3307 degrees Rankine. Using these values results in the simplified formula below.

$$m = 0.000516FL$$

If four shear pins are used, then it takes at least 152.38 lbf to break them.

The length of the parachute bays are about 11.5" and 7" for the main and drogue respectively. It is recommended that the pressures the bulkheads of the parachute bays experience ranges from 8-15 psi. From here, the required black powder mass can be [calculated](#). For a pressure of 7psi on the drogue bay bulkhead to break the drogue bay shear pins, 0.71g of black powder is required, which generates 197.92lbf. For a pressure of 10.43psi on the main parachute bay bulkhead that interfaces

with the payload bay, the mass of black powder required is about 1.75g, which generates 294lbf. Considering the choice of shear pins, we selected 3 shear pins for the drogue side coupler and 5 shear pins for the main parachute side coupler.

These calculations are just a simple estimation of the mass of black powder that will need to be purchased for the rocket to function as desired. Using ground ejection tests, these numbers will be verified and updated.

## 3.6 Parachute Deployment

### 3.6.1 Pistons

Pistons are included in order to help push the parachutes out of the parachute bay after the ejection charges are ignited and also protect the recovery system by physically separating them from the hot gases. They must be made of a sturdy material which will be able to push out the parachutes after the ejection charges have been ignited. They must also have a hole in them to allow for the passage of the shock cord.

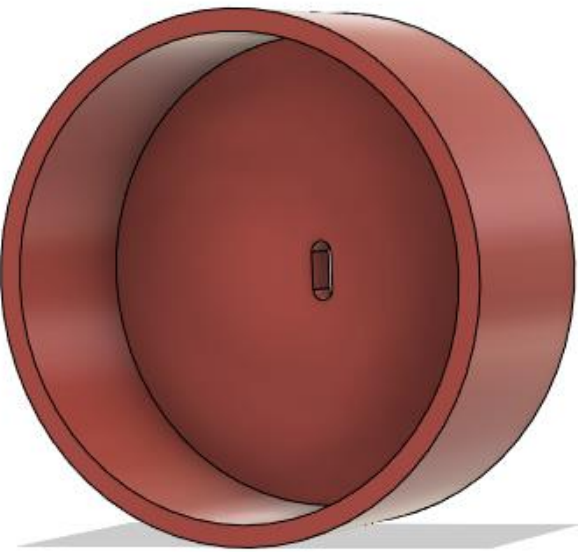


Figure 3.142: Piston Design

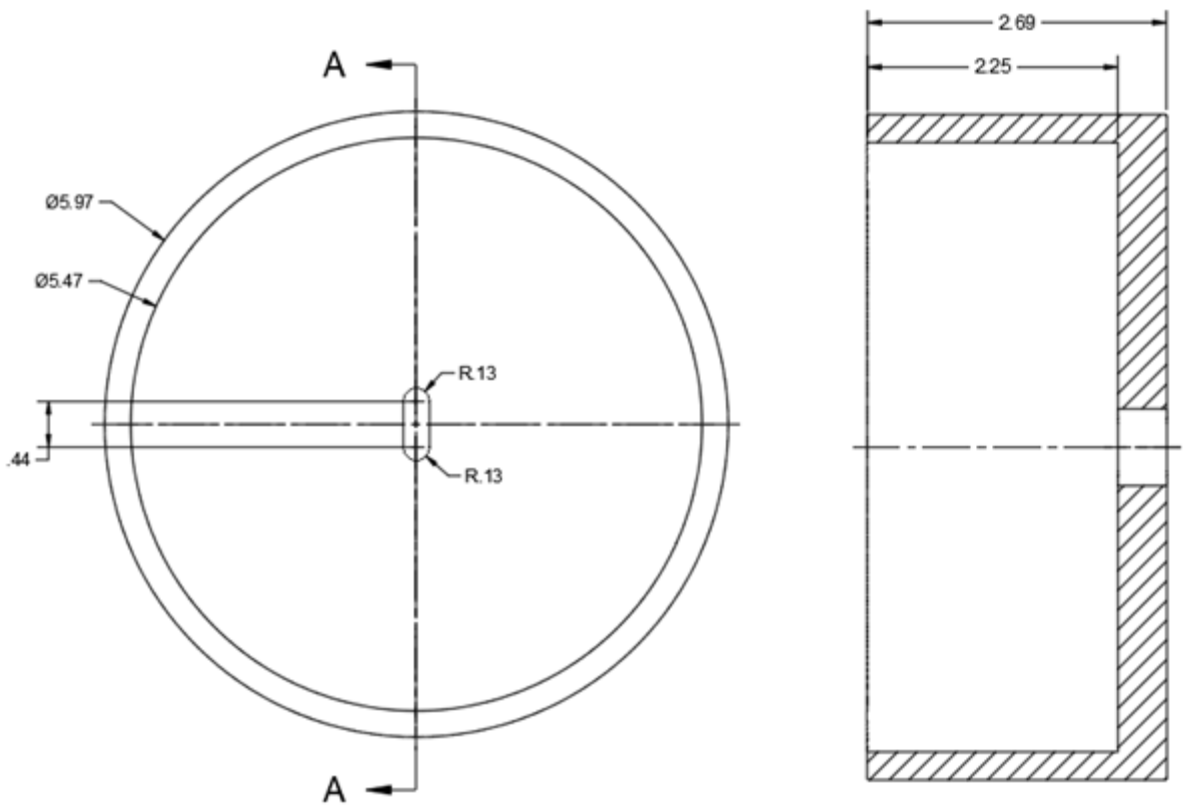


Figure 3.143: Piston Dimensioned Drawing

The piston design is a cylinder of balsa wood with a hole for a shock cord in the middle. The piston is 2.6875" long to maintain stability in the airframe with a hollowed outside that also has a smaller diameter such that the piston can be rested against the avionics bay tube and to mitigate the weight of the piston. The material is balsa wood, which is light, but not very strong. However, these pistons do not need to be strong or have as they are not part of the rocket structure. They are also replaceable, such that if they are damaged, more can be made. In order to make them, blocks of the wood would be bought, then cut with a CNC machine, including the shock cord hole, and then put on a lathe to hollow out the inside. The larger diameter side of the piston should have a close running fit so it can slide quickly within the airframe to push out the parachutes.

### 3.6.2 Recovery Harness

The recovery harness is a cord that connects to the parachutes and allows for their deployment. It also keeps the sections of the rocket together upon parachute deployment so that parts of the rocket will all land together. As such, it must be strong enough to withstand flight forces and resist corrosion due to high heat.

For this reason, a two 7/16" wide Kevlar cords were chosen over nylon ones as the former is both very strong and resistant to high temperatures, whereas nylon is known to be flammable and would require additional protection that Kevlar Harnesses do not require. The drogue harness is 20 feet long while the main harness is 30 feet long for a total length of 50 feet of cord.



Figure 3.144: Kevlar Recovery Harness

### 3.6.3 Avionics Bay Requirements for Deployment

The avionics bay houses and protects the electronics required for altitude determination and parachute ejection during flight. The electronics required for the avionics bay of a Dual Event Recovery System include altimeters, batteries, electric matches, and a switch. The physical objects required for the avionics bay to function correctly are an avionics sled, ejection charge wells, an avionics tube/coupler, end plates, pistons, and fittings to hold the avionics bay together.

The avionics sled retains the altimeters, as well as their power supplies. Since two parachutes have to be deployed, and the recovery system must be fully redundant, there must be two altimeters, each with their own battery, connected to the ejection charges. Thus, the avionics sled must be capable of containing both of the altimeters and their power supplies.

The avionics tube must fit inside of the airframe and sequester as well as protect the electronics from ejection gases and electromagnetic interference from other rocket sections. This tube must be strong enough to withstand impact of the rocket upon the ground as per the 75 lb·ft kinetic energy limit of landing.

### 3.6.4 End Plates

The end plates of the avionics bay house the ejection charge wells and shock cord mounts. They are also responsible for sealing the electronics away from the hot ejection gases required for parachute deployment. The end plates themselves must be able to withstand these gases and resist corrosion.

### 3.6.5 Fittings

The fittings holding the avionics bay together must be strong enough to resist ejection charge forces and be able to handle vibration during flight, staying locked in place. Fittings on the outside of the end plates should also be corrosion resistant. The recovery harnesses must attach to the end plates with the help of recovery harness mounts. They must be able to withstand the hot ejection gases, be strong enough to withstand the force of parachute deployment, and resist corrosion.

$\frac{1}{4}$ " U-Bolts were selected to spread out the force of ejection over a larger area than eyebolts are capable of. We also included a mounting plate in the design to do this even more efficiently.  $\frac{1}{4}$ " Zinc-plated steel quicklinks are then attached to the U-bolts and shock cord end loops for ease of assembly and disassembly of the recovery system.

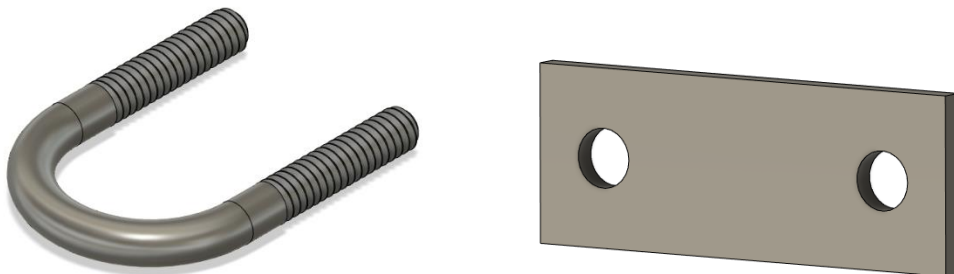


Figure 3.145: U-Bolt with Mounting Plate

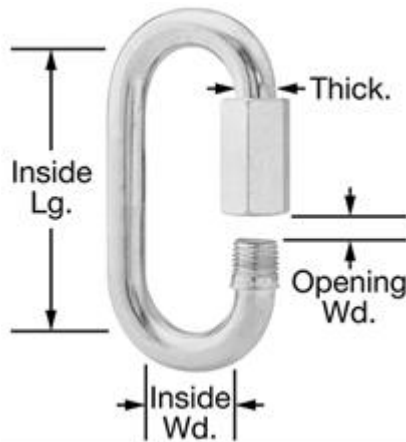


Figure 3.146:  $\frac{1}{4}$ " Zinc-Plated Steel Quicklink

### 3.6.6 Ejection

The ejection itself requires charge wells that will contain black powder which will be ignited with electric matches, as per Requirement 3.1.3. The amount of black powder required to eject the parachutes depends on the lengths of the parachute bays as well as cross-sectional area of the airframe. The charge wells are sized based on those calculations. As the charges are all below 2g in mass, the charge well need only hold a maximum of 2g.

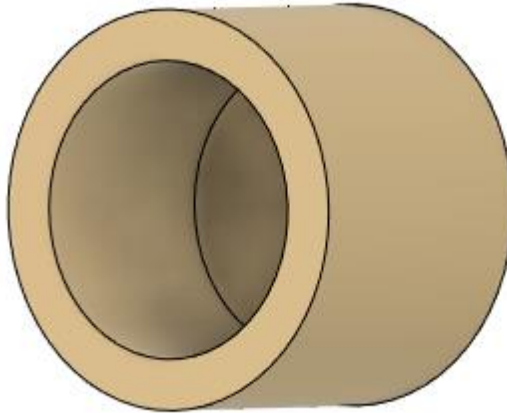


Figure 3.147: 2g Capacity PVC Charge Well CAD Model

The design of the charge wells are identical to that of the previous report, they are made of PVC and can support 2 grams of black power. Since the amount of required powder is less than their capacity, these charge wells can be used. These are chosen over aluminum pieces due to their light weight.

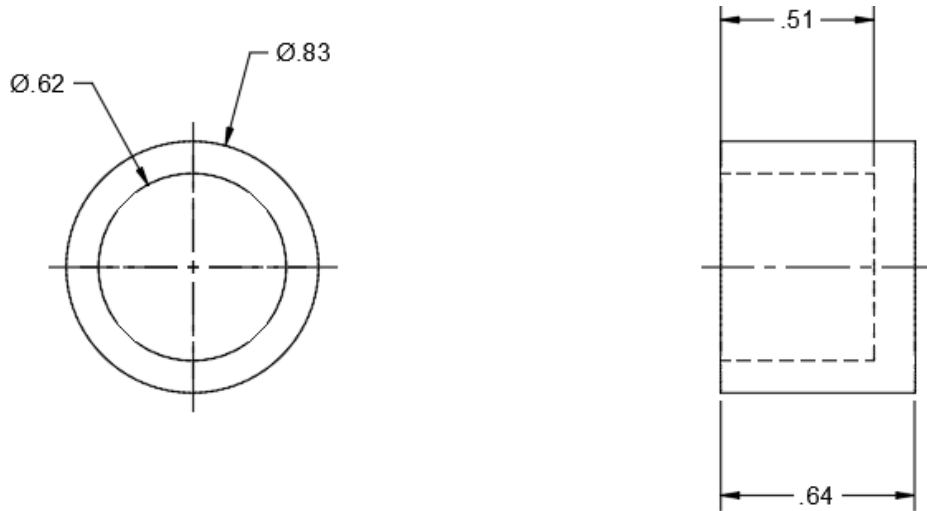


Figure 3.148: Charge Wells Dimensioned Drawing

### 3.6.7

### Altimeters

Altimeters must be able to send electronic signals such that parachutes may be launched at altitudes of 5500 feet or less, to connect to two black powder charge canisters, and to operate using commercially available batteries. The altimeters also need to be set up in a redundant system so if one charge or one altimeter fails, another can be triggered to complete parachute deployment procedures.

The altimeter that was chosen was the PerfectFlite StratologgerCF. This altimeter: may deploy parachutes from 100-9999 feet AGL, record maximum velocity, store data for 16 flights of 18 minutes each, has an accuracy of  $\pm$  (0.1% altitude reading + 1 foot), may be powered by 4-16V batteries, is very easy to use and assemble, weighs 0.38oz, may perform dual deployment, is resistant to false trigger, has brownout protection and will tolerate 2 second power loss in flight, and has selectable apogee delay for dual altimeter setups that prevents overpressure from simultaneous charge firing. As such, it meets all of our requirements for an altimeter.

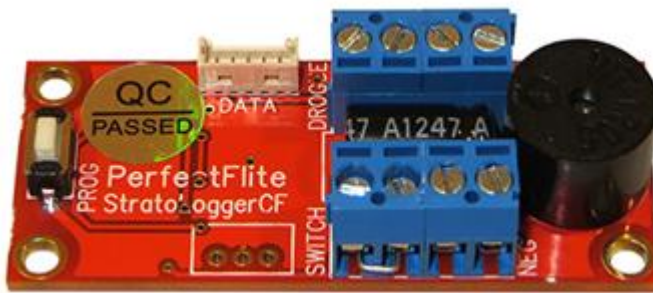


Figure 3.149: PerfectFlite StratoLoggerCF Altimeter

## 3.7 Avionics Electronics

### 3.7.1

### Altimeter Circuit Configuration

The altimeter electrical circuit must be fully redundant as per Requirement 3.4, must have their own commercially available batteries according to Requirement 3.5, and must not be connected to electrical circuits of other sections as per Requirement 3.8. Therefore, each altimeter is connected to its own battery and two charge canisters, one main and one drogue canister. The electrical circuit will be arranged as shown below:

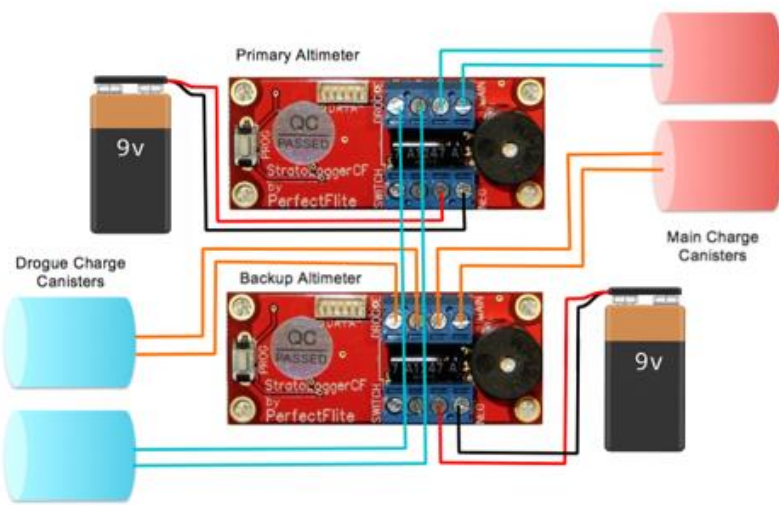


Figure 3.150: Avionics Circuit Configuration

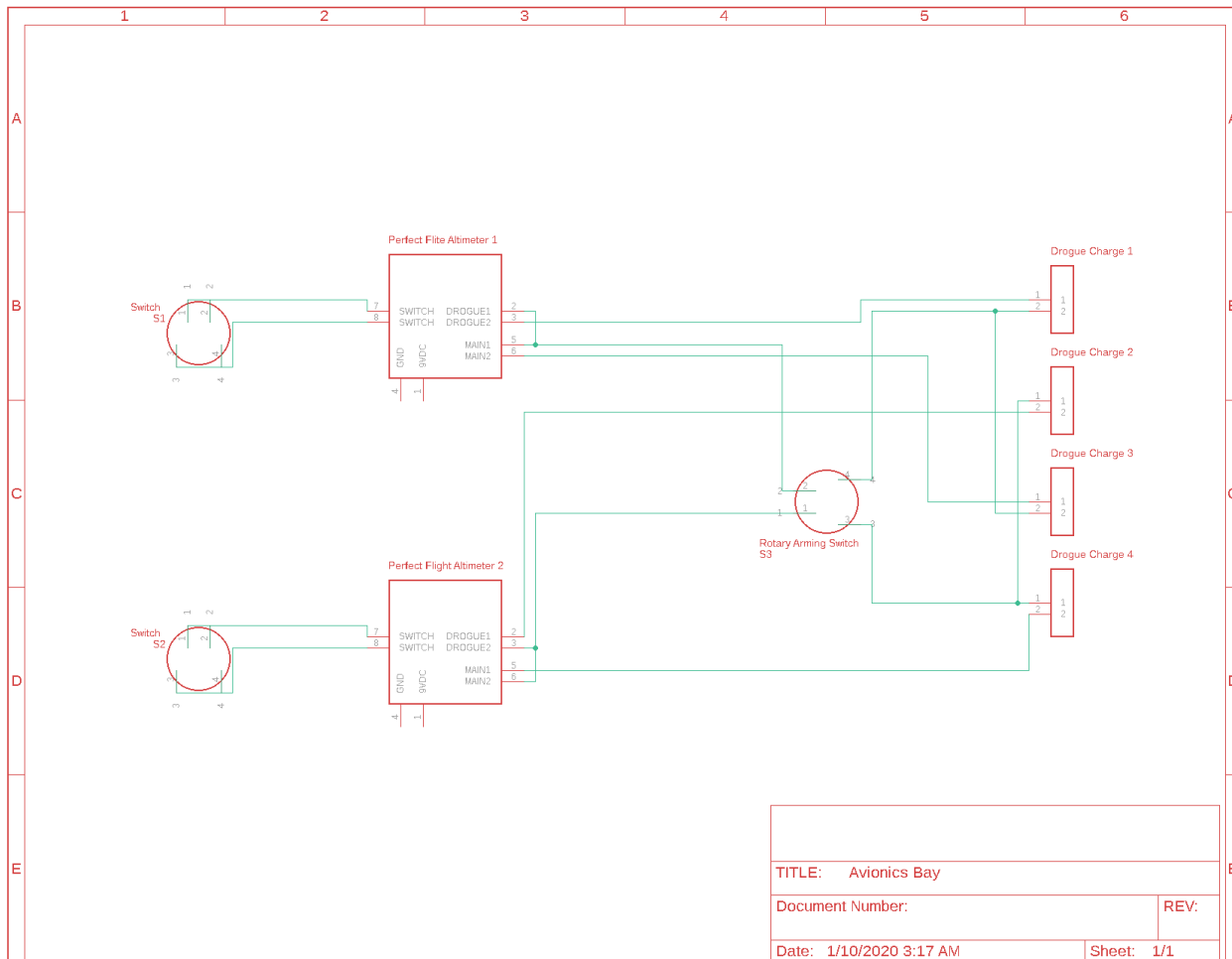


Figure 3.151: Electrical Schematic for Avionics Bay

The batteries required must be commercially available, so 9V batteries and LiPo batteries were considered. While LiPo batteries are often lighter, take up less space, and are rechargeable, 9V batteries were selected for the avionics bay power supplies since they require less maintenance, are far less expensive and hence easily replaceable, less dangerous (as LiPo batteries can melt or otherwise be damaged if overcharged), and are recommended for use with many commonly used altimeters.

### 3.7.2 Arming Switch

The avionics bay must be able to be turned on from the outside of the airframe and must be able to stay on despite flight forces as per Requirements 3.6 and 3.7. There were two types of arming switches considered: a keylock switch and a rotary switch. A keylock switch requires a key to turn and activate while a rotary switch does not require one, only needed pressure applied in a circular motion by something hard, sharp, and or thin. The rotary switch was selected as keys can be misplaced, and the rotary switch can be turned on easily by a person with a coin, Allen key, or a screwdriver, but not by flight forces.



Figure 3.152: Rotary Switch

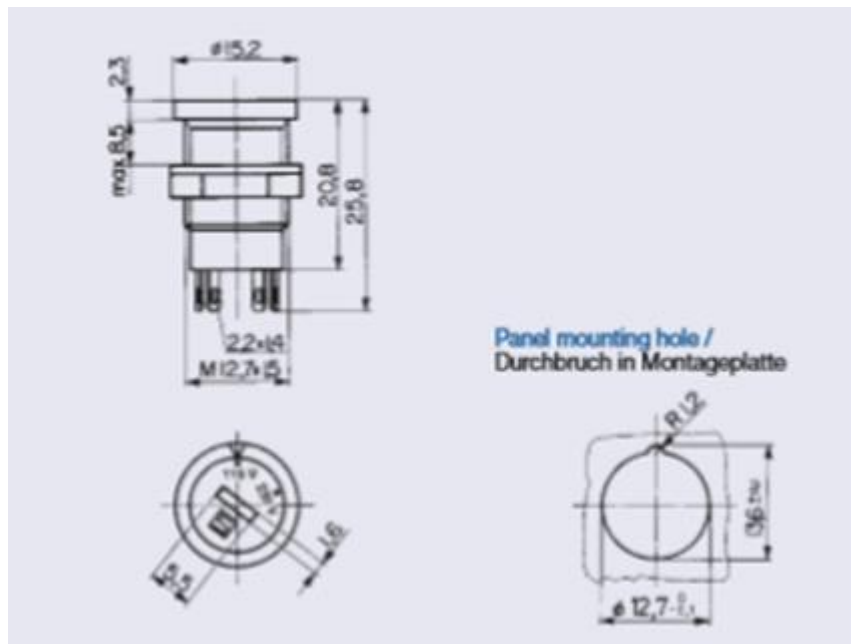


Figure 3.153: Rotary Switch Dimensioned Drawing

### 3.7.3

### E-Matches

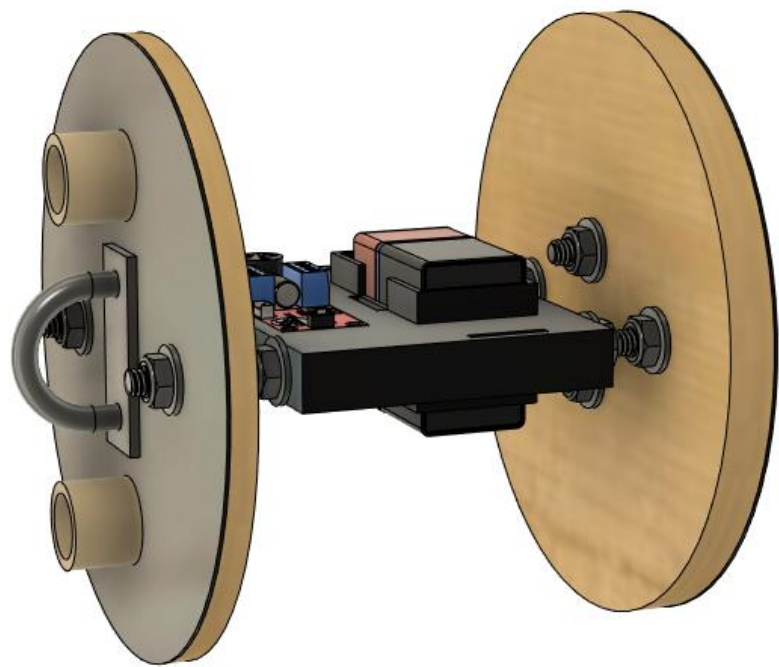
Electric matches ignite the black powder charges for the purpose of parachute deployment. For this purpose, Firewire Mini-Initiators were selected to ignite the charges as they are pre-dipped in an explosive chemical called pyrogen, which is not only safer for the team, but also cheaper than buying more charges than needed. Also, these can be used without licenses, are small and easy to handle, are quite light, and do not require hazmat shipping. It is necessary, however, to review the datasheet for these matches in preparation for use.



Figure 3.154: Firewire Mini Initiator Electric Match

## 3.8 Avionics Bay

Below are images of our Avionics Bay design which consists of a few main parts: avionic sled, avionic tube, and end plates. The avionic sled is fastened to the end plates using two threaded rods, 16 zinc-plated steel locknuts, and 16 stainless steel washers.



*Figure 3.155: Avionics Bay Isometric View*

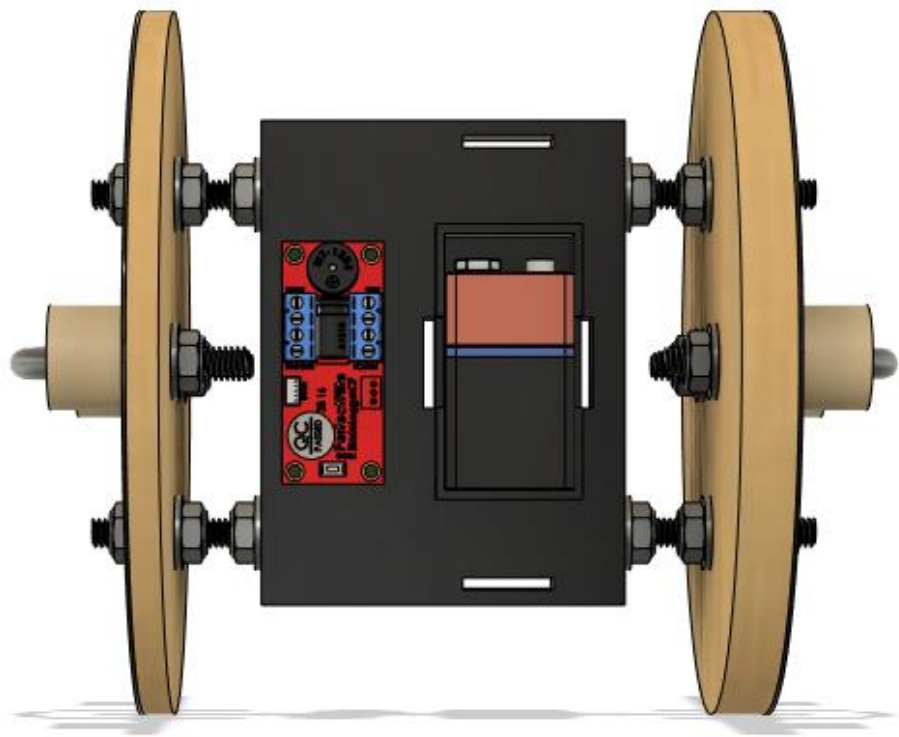


*Figure 3.156: Avionics Bay Top View*

This is a top-view of the avionics sled with endplates. It allows for a simpler visualization of the layout of the altimeter and its respective battery. Since the avionic systems are fully redundant, the bottom-view of the sled would look the same as the top.

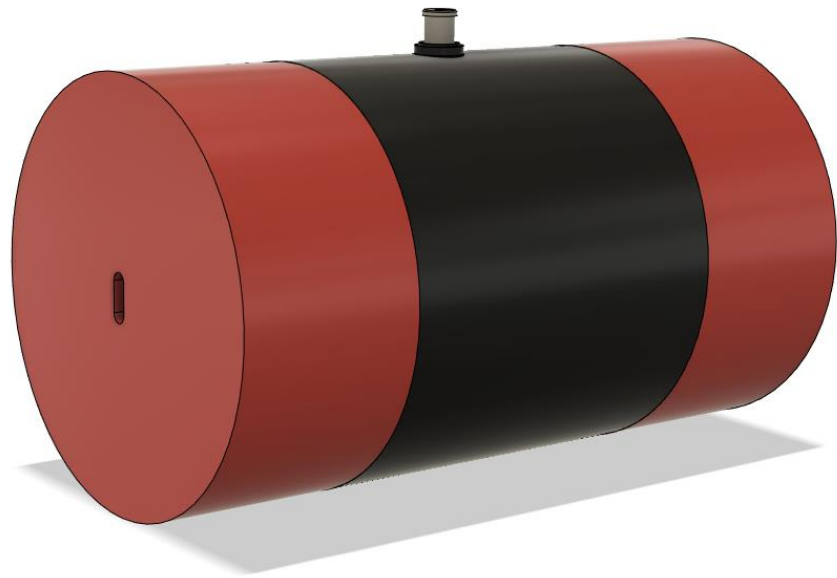


*Figure 3.157: Avionics Bay Packaging*

Image of the updated avionics bay packaging, which shows the coupler, pistons, as well as the arming switch. The pistons are depicted to be in contact with the avionics bay packaging, covering the U-bolts and ejection charge wells. On the inside of the tubing, there lies the avionics bay proper. The inside will be lined with aluminum foil in order to block RF signals from the GPS system in order to prevent false altimeter triggering.



Figure 3.158: Avionic Tube

The above is the model of the tube that will be used in the avionics bay packaging. The hole in the tube allows for the passage of the rotary switch that will arm the altimeters. This switch requires torque to turn which prevents in-flight forces from turning on the altimeters. This switch may be operated by a screwdriver or Allen key. It will also be visible from the outside airframe of the rocket, and as such, a hole in the airframe will have to be correctly sized for this device based upon its dimensions as shown in following sketches.

According to the PerfectFlite StratoLoggerCF User Manual, there need to be static pressure holes drilled into the avionic tube and airframe. Using four holes spaced at 90 degree intervals is best to minimize pressure disturbances. The holes must also be sanded, not overly large, and placed as far away from the nosecone as possible. We have chosen the four hole configuration, and the holes are sized like so:

$$\text{Hole Diameter} = (\text{Diameter of AV Bay})^2 * \text{Length of AV Bay} * 0.0008.$$

As such, our static pressure ports should be four 1/8" holes drilled 1/2" from drogue side of tube to abide by these recommendations and ensure these holes are far enough away from the edge of the tube and preserve structural integrity.

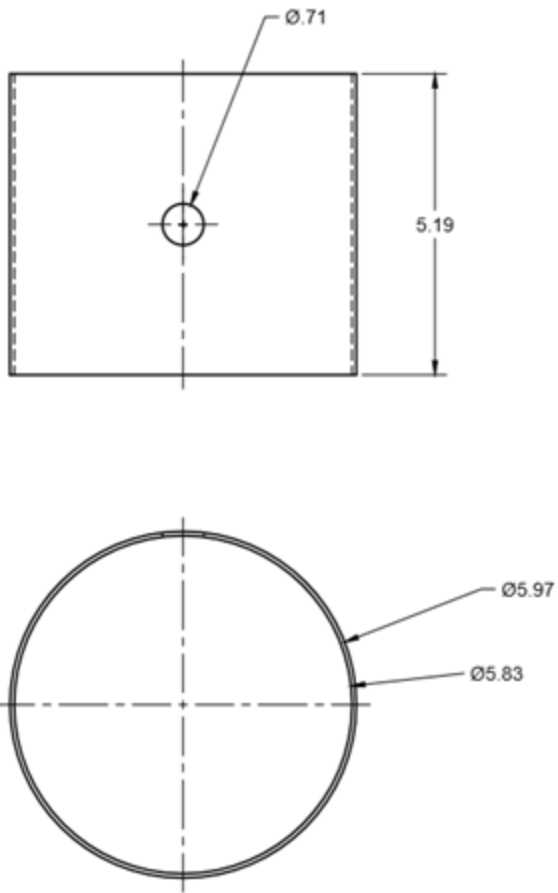


*Figure 3.159: Avionics Tube Dimensioned Drawings*

These sketches demonstrate the dimensions of the designed coupler, as well as the hole of which the arming switch will be fitting into. Logically, the diameter is slightly larger than that of the avionics bay interior such that the coupler will be able to hold the system together.

The 3D-printed ABS plastic avionic sled houses the battery with properly sized indentations, vertical walls, and zip ties that will pass through the four rectangular slots in the sled. The altimeters will similarly be placed inside their own indentations in the sled and further secured by nylon screws and nuts. The avionics bay will be attached to the rest of the assembly using  $\frac{1}{4}$ " steel threaded rods. So there are two holes that will be drilled through the sled after 3D printing in order to allow for this.

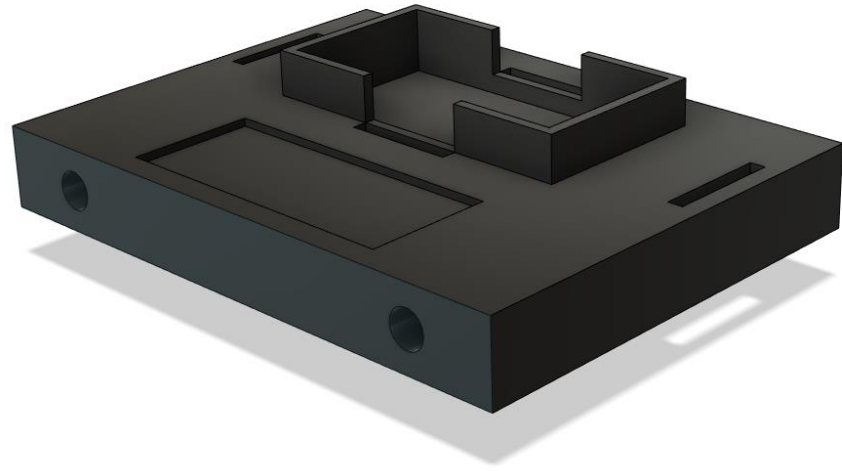


Figure 3.160: Avionics Sled

Dimensions for the avionic sled can be seen below.

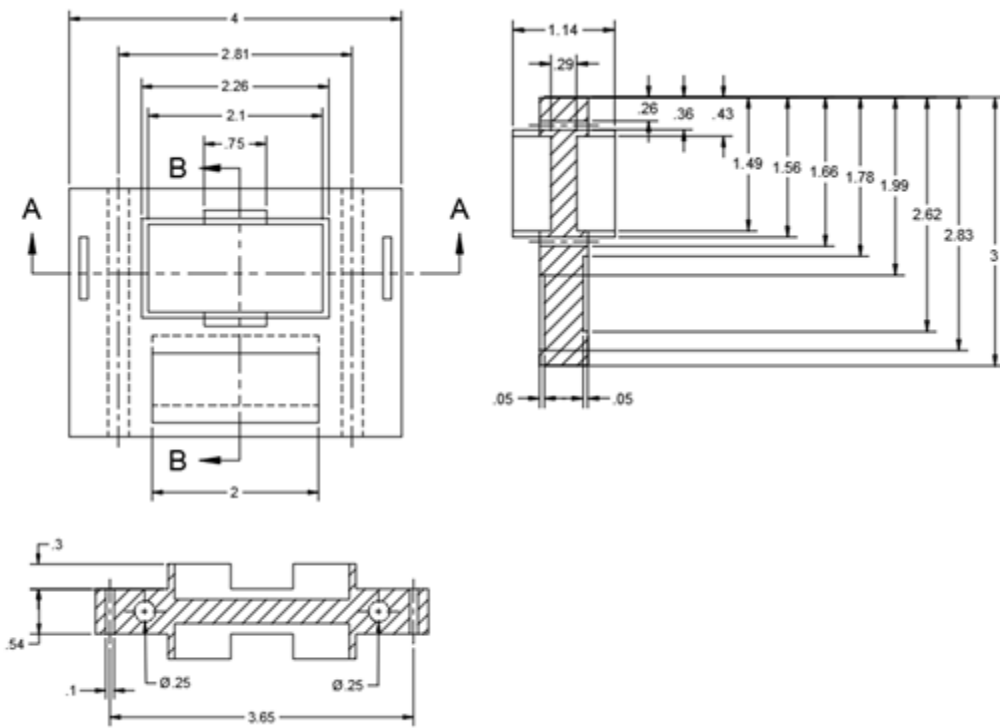
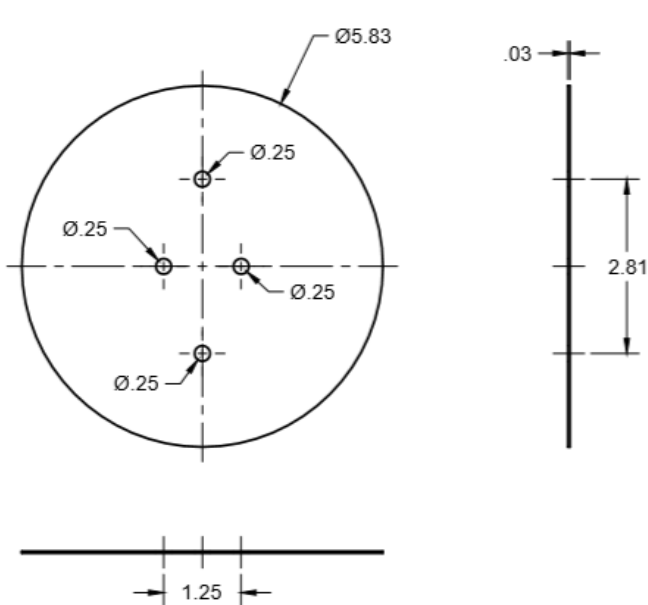


Figure 3.161: Avionic Sled Dimensioned Drawing



*Figure 3.162: End Plates*

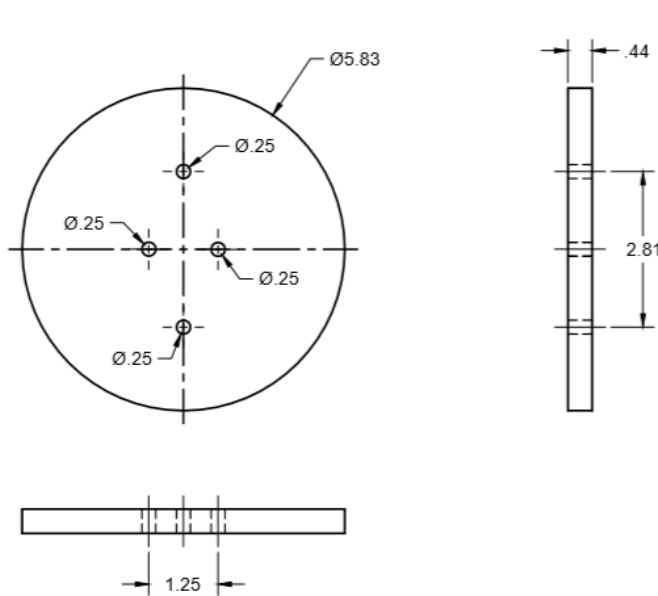
These threaded rods then pass through the end plates, which consist of a plywood inside and a fiberglass outer covering which may be secured with epoxy or through purely mechanical means (i.e. nuts, washers, etc). While the fiberglass will protect the wood due to its higher corrosion resistance, the wood will supply its greater strength to the end plate assembly.



	PROJECT NASA 2019-2020 USLI Master Project		
	TITLE End Plates-Fiberglass Outside		
APPROVED	SIZE	CODE	DWG NO
CHECKED	B		REV

Figure 3.163: Dimensioned Fiberglass Outer Endplates

Both plates are secured in place on the threaded rods using washers and locknuts as before. In addition, one of the wooden plates is thicker than the other and will be epoxied into the avionics tube as a permanent addition. This will be installed on the side of the avionics bay that interfaces with the main parachute, as the powder charge required to fire it is greater than that of the drogue chute, and in order to epoxy the plate effectively, it has to have a moderately large surface area. This method of a permanent plate is also recommended by the altimeter user manual.



	PROJECT		
	NASA 2019-2020 USLI Master Project		
	TITLE		
	Epoxied Bulkplate		
APPROVED	SIZE	CODE	DWG NO
CHECKED	B		REV

Figure 3.164: Avionic Retention Bulkplate Dimensioned Drawing

The end plates also ensure the recovery harness mounts,  $\frac{1}{4}$ " zinc-plated steel U-bolts, are secure. Mounting plates are used on the outside of the endplates in order to spread out the force of ejection over a larger area of the end plate for the sake of greater structural integrity.

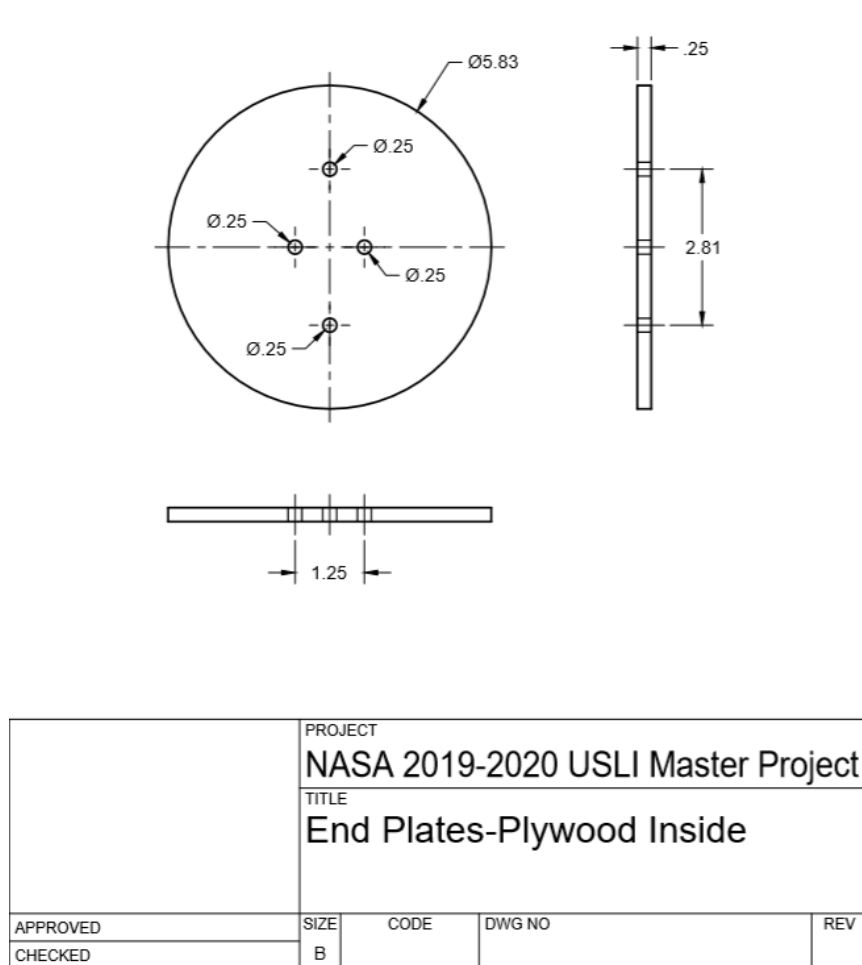


Figure 3.165: Dimensioned Plywood Outer Endplate

### 3.9 Telemetry Bay

The telemetry bay houses and protects the GPS tracking electronics. This bay must be located near the front of the rocket either in or near the nosecone and must not interfere with other sections. The bay cannot be surrounded by metal which will block signals of the GPS transmitter. The tracking device(s) must be able to transmit position from a far distance that at least covers the recovery area of 2500 ft radius. There must be a tracking device for each rocket section that lands untethered from the rest of the vehicle. They must be powered by commercially available power supplies.

The selected GPS tracking device selected for recovery is the BRB900 GPS Telemetry System. This type of device was chosen because it does not require a HAM license, which provides more convenience. It has a range of 6 miles, which is more than enough as the landing area is only 2,500 feet in diameter. The transmitter can also store 2.5 hours of data before recording stops. It operates in “wrapping mode” which saves the last 2.5 hours of data before it has been turned off, so the rocket may be found even if it must remain on the launch pad for awhile. The BRB900 also

includes a handheld LCD receiver that is paired with the transmitter to ensure data is not received from the wrong device. Additionally, it includes a 3.7V LiPo battery for the transmitter and USB Interface / battery charger, with an added option that prevents overcharge which could result in the melting of the battery. The GPS transmitter can be programmed using a data cable and downloading the appropriate software from the BigRedBee website. It also makes use of a Reverse Polarity SMA antenna which is about 4.25" long and the transmitter itself is quite small with a length of 2.85" and a width of 1.25", a size that may easily fit inside the nosecone.

When in use, the LCD receiver and the transmitter will send data packets and the former will get a lock on the latter after 15 minutes at most. Then, the LCD receiver will be able to display the coordinates of the transmitter as the latter uses satellites to find its position. After the rocket has landed, these coordinates can then be entered into a program or app on a phone, such as MotionX, which can then be used to direct personnel to the rocket for retrieval. Lastly, this transmitter uses a frequency of 900MHz with a power output of 250mw.



Figure 3.166: BRB900 GPS Telemetry System

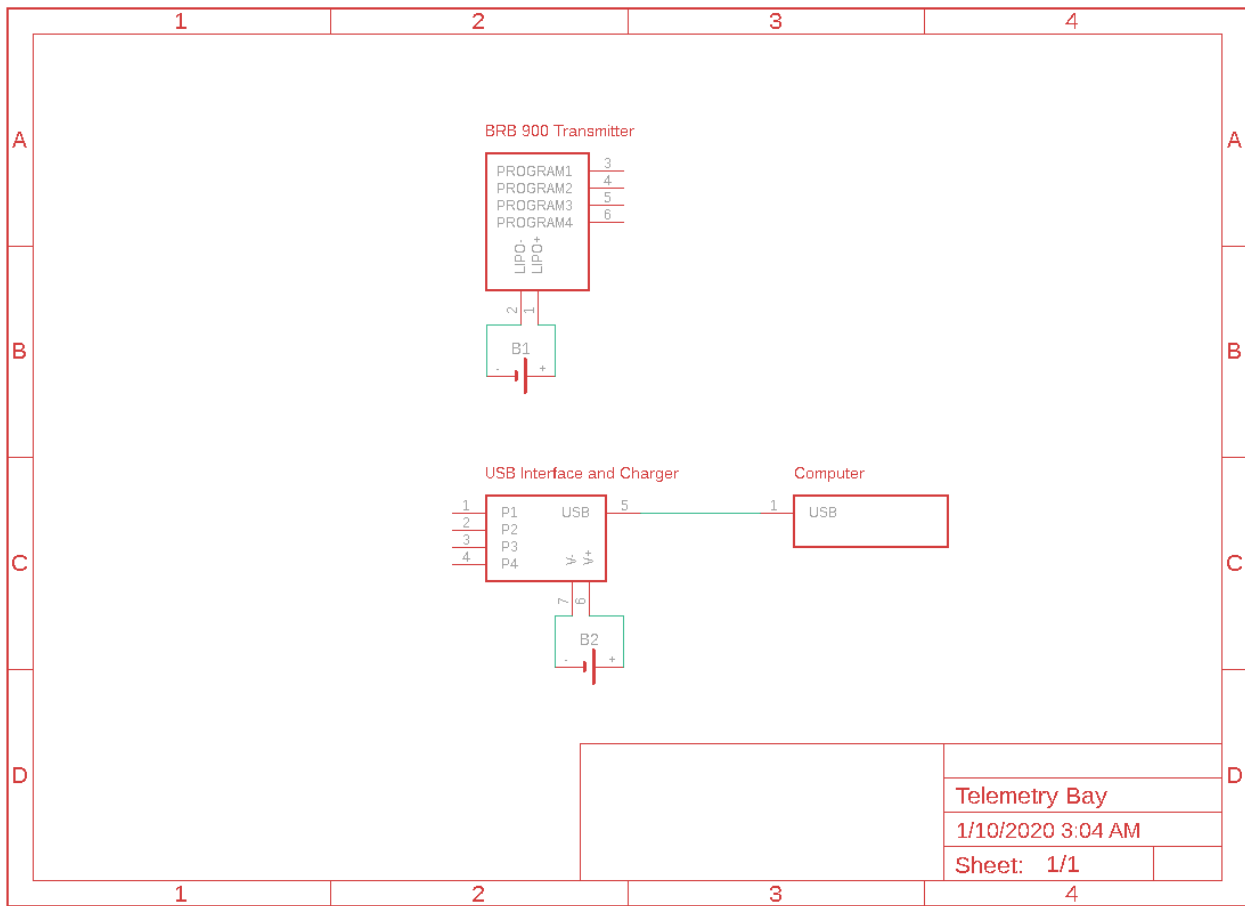


Figure 3.167: Telemetry Bay Electrical Schematic

This is the electrical schematic for the telemetry bay. It demonstrates how the USB connects to the computer, and the layout of the battery and antenna of the system. The GPS transmitter may be configured by connecting the programming pins on both devices and utilizing the device's software.



*Figure 3.168: Telemetry Sled*

The telemetry sled houses the GPS transmitter and it's LiPo battery. Holes in sled allow for threaded rod and fitting attachment to a plate, holes in back allow for passage of zip ties, slots in front sides make sure zip ties are constrained, GPS transmitter and LiPo battery are strapped together and attach in the same compartment, this configuration is updated from the previous one in which the slots for zip ties were cut into the sled, which compromised structural integrity and made single extrusion FDM 3D printing difficult. This design increases structural integrity with vertical struts in the back and fillets on the bottom of the sled. The two holes seen in the main body of the sled allow for nylon standoffs to be used to attach the transmitter and the battery to the sled.

These components will be further constrained by zip ties.

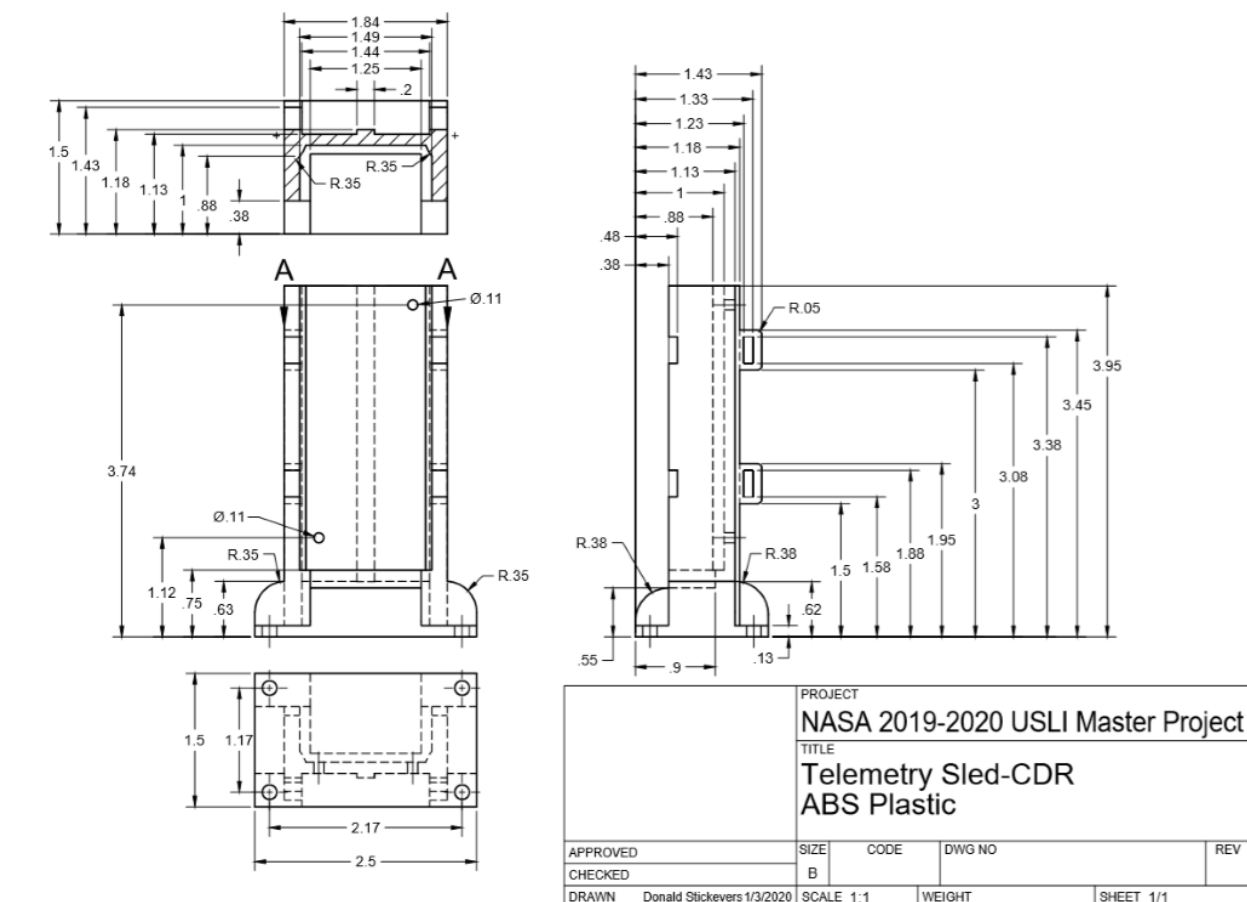


Figure 3.169: Dimensioned Telemetry Sled

These are the dimensions of the telemetry sled. They were chosen to help secure the transmitter in place in the sled better, as well as fit zip ties and bolts to retain the sled in the end plate.



*Figure 3.170: Telemetry Bay Assembly*

The telemetry bay assembly consists of the telemetry sled, which is 3D printed in the same piece as a plate to fit about halfway inside the nosecone, and a threaded rod attached to the metal tip of the nosecone. In order to account for the chance that the telemetry sled could have interfered with the bolts from the Payload bay, the position of the telemetry sled was moved to the top plate in the nose cone, attached to the lead screw end support mount. This allows for the payload rover to be retained as designed by their team. The lead screw passes through the plate as needed by the Payload team.

## 4 Payload Criteria

### 4.1 Tank Overview

The final design for the tank is shown below. Its chassis is made of machined plates of carbon fiber epoxied together and fitted geometrically using two custom made 6061 aluminum components. The integration of the carbon fiber and aluminum components are shown below. The drivetrain for the tank is treads driven by one motor on each side of the tank. On each side a motor is connected to one driver sprocket assembly which drives the connected idler sprocket assembly. The driving motor shafts are direct drive to the sprockets. The motor shafts go through the chassis walls and a shaft coupler and collar connect to the sprocket. The idler wheels have a similar assembly with an axle, the drivetrain will be discussed in detail in 4.2.2. The tank will also have a slot in the chassis for a matching key on the retention mounts for added stability and immobilization during flight in the radial direction. The sample collection system will be housed internally during flight and be deployed after exiting the payload bay. The storage unit will be rigidly fastened to the chassis of the tank and connected to the sample collection scoop via the collection motor.

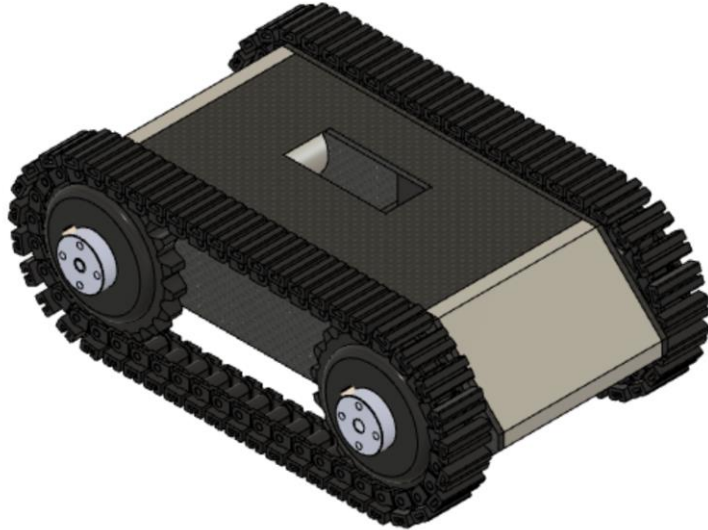


Figure 4-1: CDR Rover

### 4.2 Tank System Level Design

#### 4.2.1 Chassis

The chassis will be constructed using machined carbon fiber plates as well as 6061 aluminum. Carbon fiber plates will be ordered as stock and machined into the figure below and bolted into the connecting aluminum components. When machining carbon fiber all PPE must be

worn by the operator and all other non-operators must be cleared out of the facilities during production. An aluminum shell will be used to connect the plates together. The aluminum connecting component will be made using a mill. The custom-made aluminum piece shown below will be to each respective plate. If increased rigidity is needed to secure the carbon fiber plates together, we will use custom made angled brackets that we will create using a sheet metal bender and machining mill. Retention slots will be utilized to immobilize the rover in the radial direction during flight. There will be the male portion of the slot on the retention mounts and on the rover, there will be a matching female divot. The small matching divot will be on each side of the rover on the 6061 aluminum connecting components.

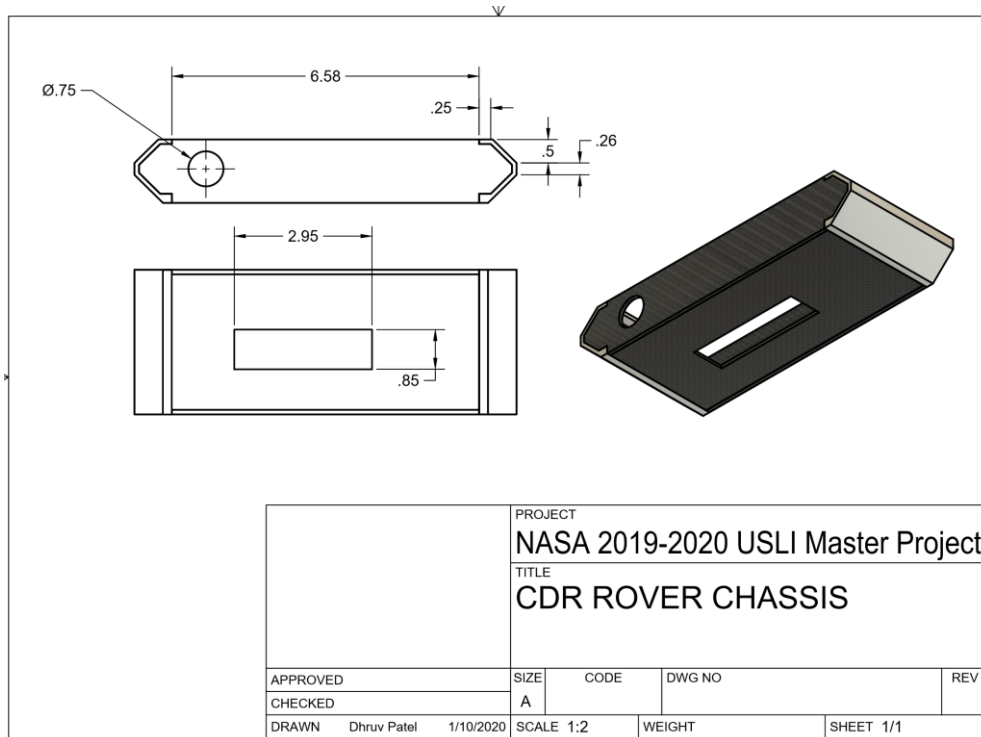


*Figure 4-2: CDR Rover Chassis*

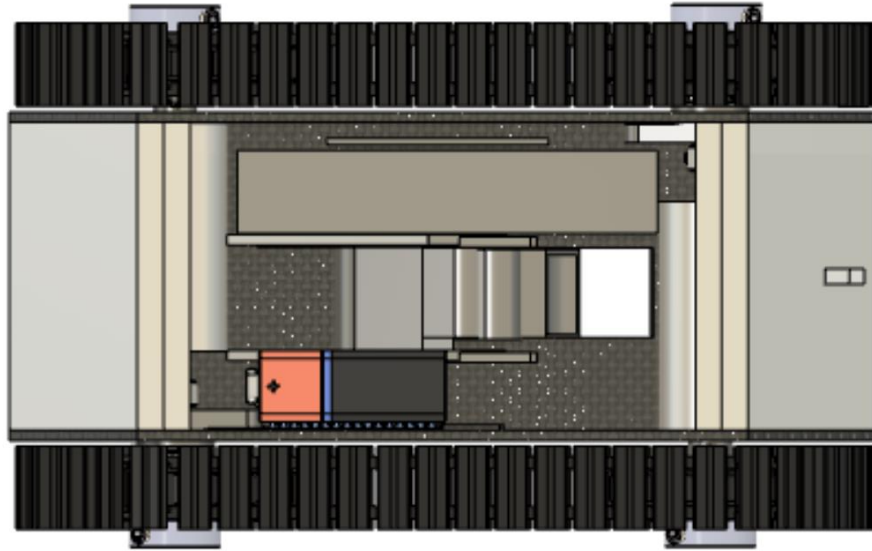


*Figure 4-3: CDR Rover Chassis Top View (Top plate hidden)*

#### **4.2.2 Drivetrain**

The drivetrain consists of treads with one motor on each side of the tank. Each side of the tank has one driver wheel with direct drive and one idler wheel. The driver sprocket assemblies include the motor shaft directly through a hole in the chassis going through the sprocket and attached by a shaft collar to the driver sprocket, and a shaft collar to restrict movement of the sprocket along the shaft. The idler sprocket assemblies for each side are as follows (and shown below), there is an axle through the chassis and connected to it inside the chassis is an axle set collar, a mounted flange bearing, the chassis wall, then a mounted sleeve ball bearing so the shaft can rotate while taking load, then the sprocket and finally a shaft collar identical to the one in the driver assembly. The sprockets are bolted to the shaft collars allowing the sprocket to move with the rotation of the shaft.

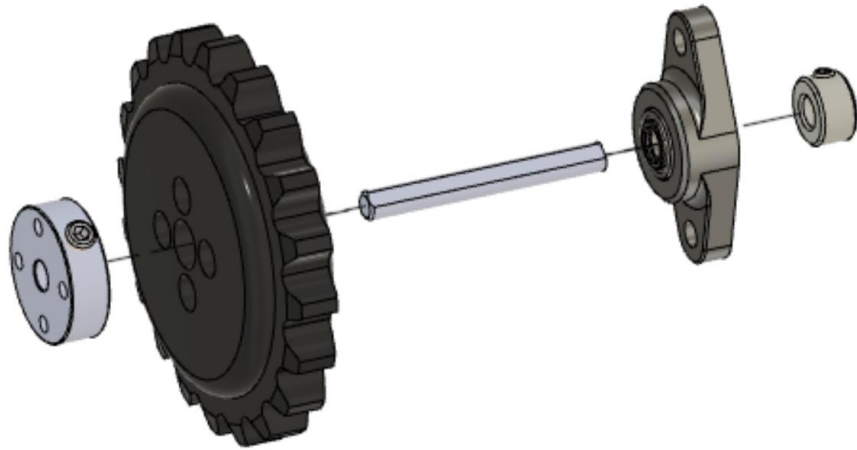


Figure 4-4: Tank Idler Axle Assembly

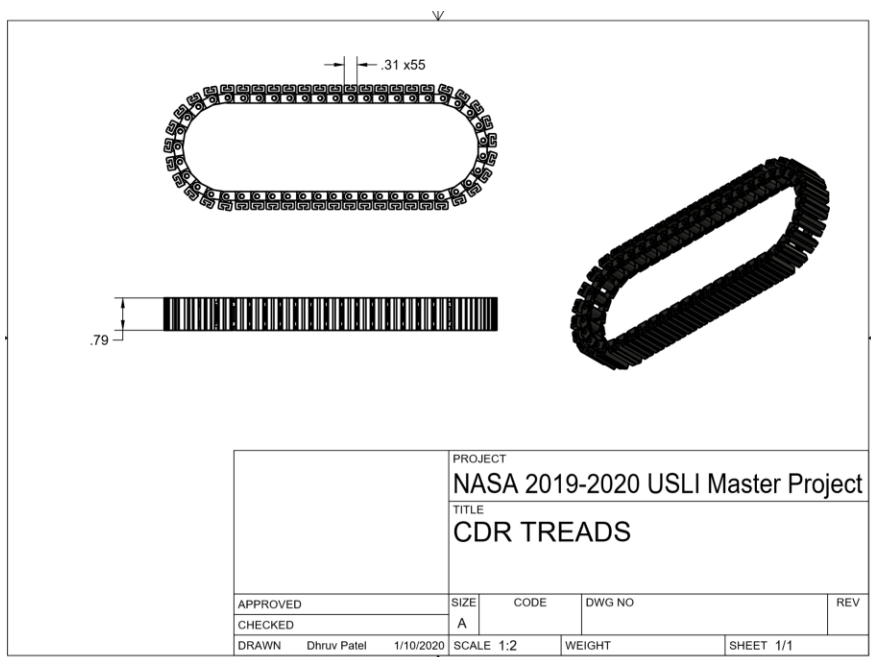


Figure 4-5: CDR Tank Treads

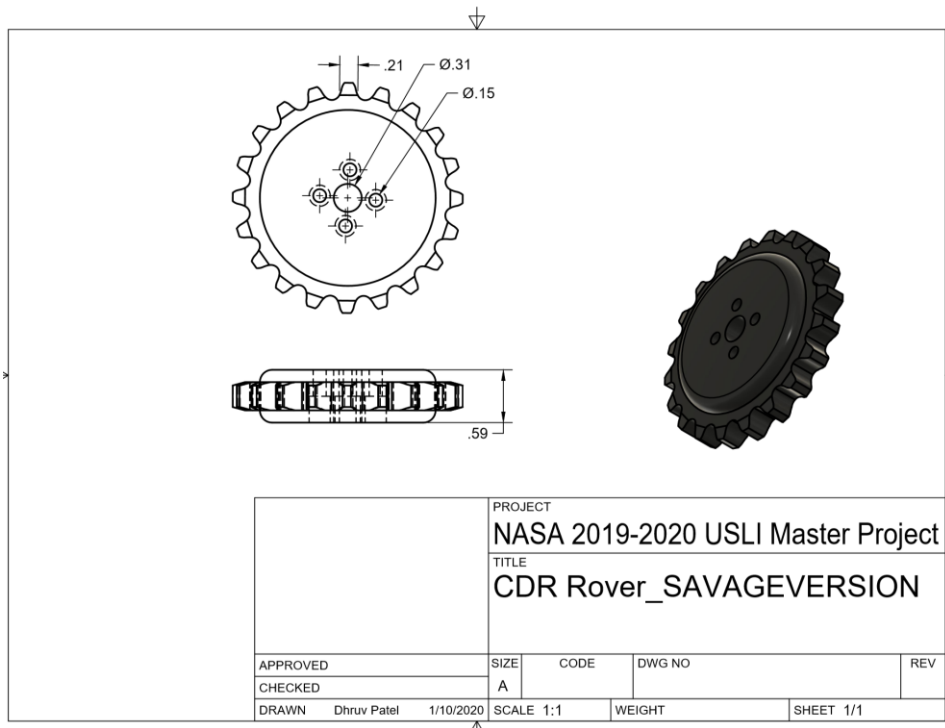


Figure 4-6: CDR Tank Sprocket

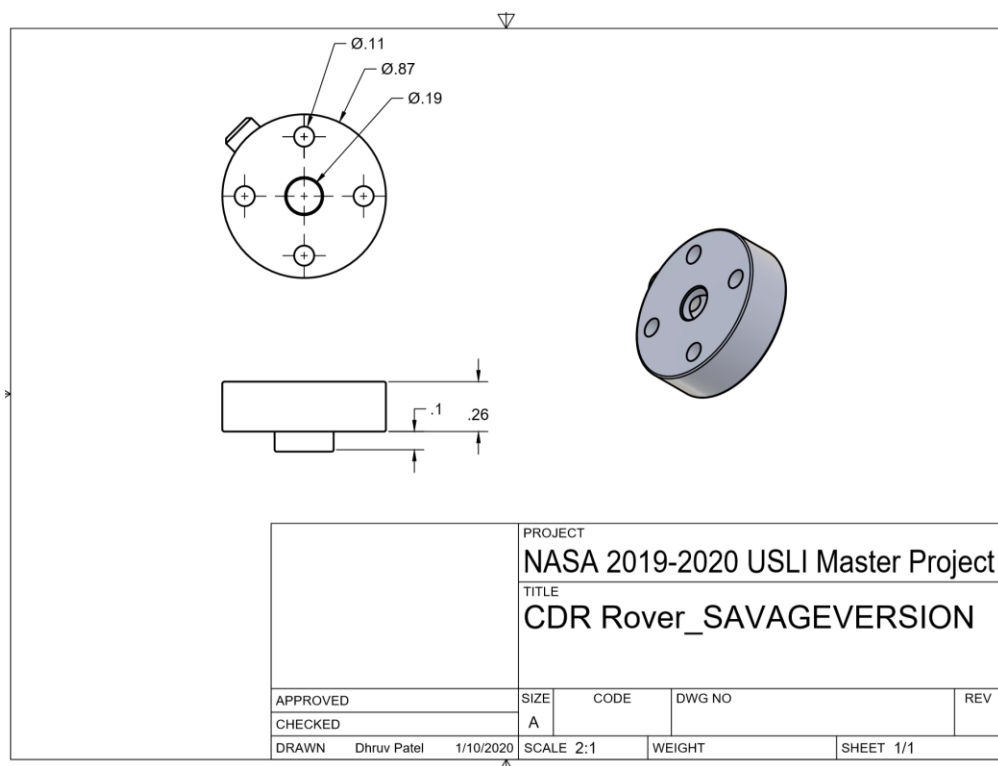


Figure 4-7: Tank Drive Axle Collar

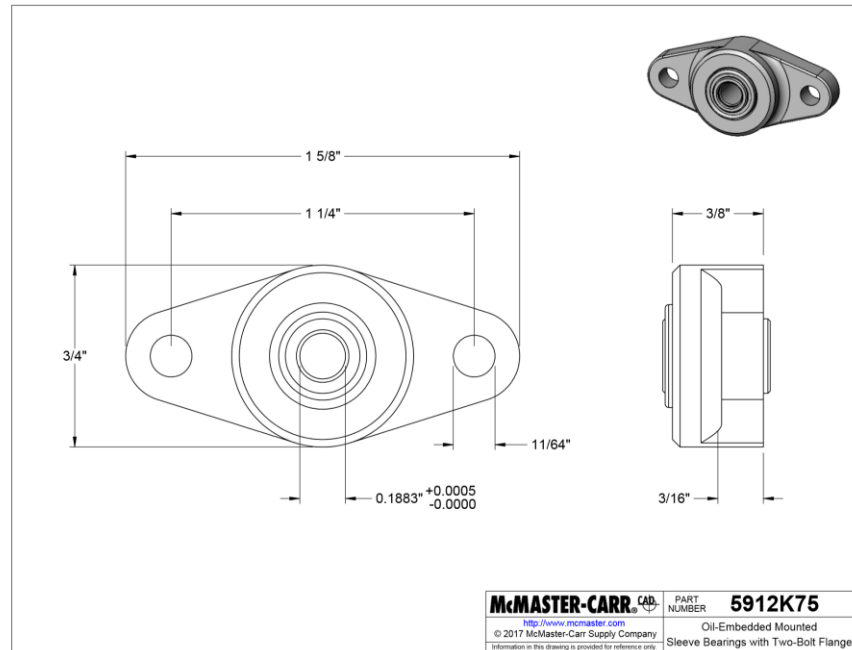


Figure 4-8: Tank Idler Axle Flanged Bearing

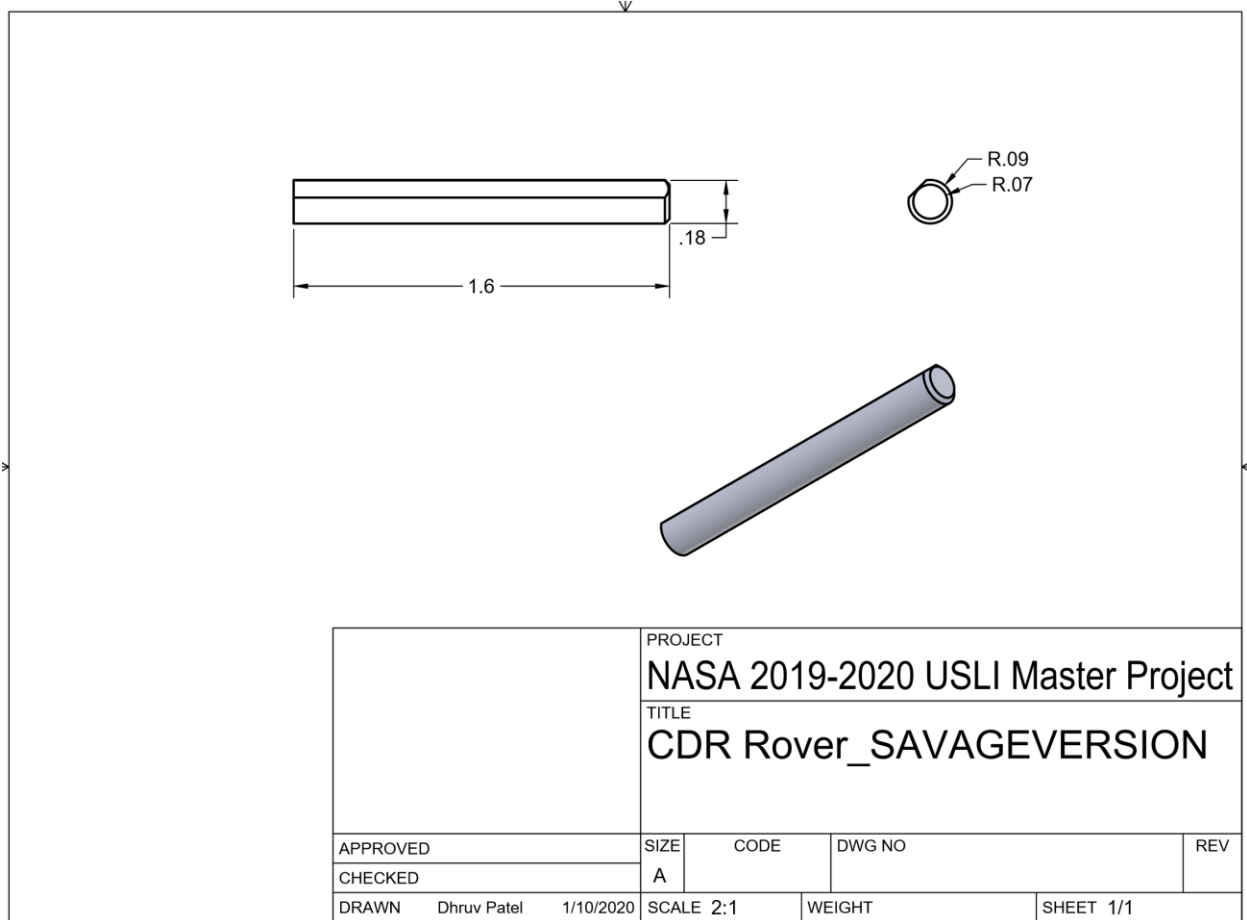
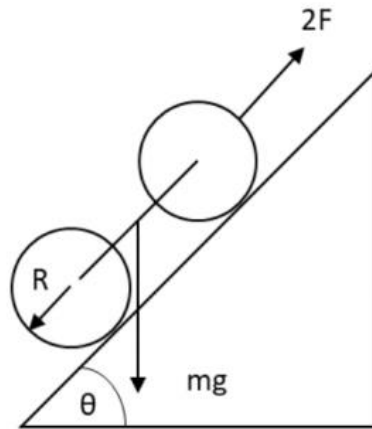


Figure 4-9: Tank Idler Axle

Torque requirement for the DC motor in the rover drivetrain is very simple to calculate. The model that was used for calculations is shown below.



The radius  $R$  is the pitch radius of the sprocket wheels that transmit torque from the motor to the threads. The force  $F$  is doubled because there are total of two motors that will be in the drivetrain

of the rover. The angle was chosen to be  $\theta = 45^\circ$  to simulate the rover going a 45 degree uphill and give some safety factor to calculations.

For the rover to be able to climb the ramp in our model, the following relationship needs to be satisfied

$$2F \geq mg \sin \theta$$

Thus, the minimum torque required is

$$T_{min} = \frac{mg \sin \theta R}{2\eta}$$

where  $m$  is the mass of the rover,  $g$  is the acceleration due to gravity, and  $\eta$  is the efficiency of the motor. After plugging in all the known variables, we get

$$T_{min} = 84oz \cdot in$$

Adding a safety factor of  $K = 3$  we need  $T_{required} = 252oz \cdot in$  of torque.

#### 4.2.3 Sample Collection Scoop

The sample collection system's operation is modeled below. Due to the sample being very lightweight and readily available for collection at surface level (no digging required), we can use 3D printed thermoplastic to create the scoop and sample collection container. This is 60 advantageous due to the complex geometry of the scoop which would be difficult to machine. The unit will then be bolted to the bottom of the chassis from the sample collection container. It will also be rigidly connected to the rover through the motor that's bolted to chassis, whose shaft will be engaged to scoop.

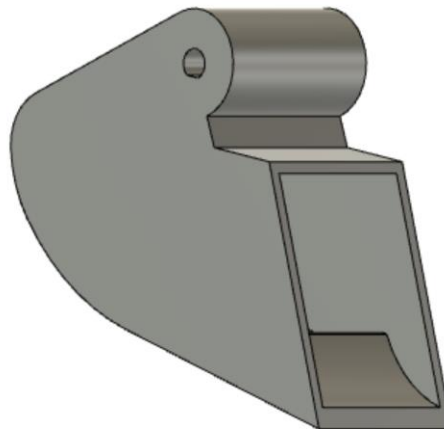


Figure 4-10: CDR Scoop

#### 4.2.4 Sample Collection Unit.

The sample collection container will also be made of thermoplastic due to strength requirements and ease of manufacturing. The volume of the collection unit was determined by the required

sample collection volume. The container will be rigidly bolted to the chassis walls and the container will be connected to the scoop allowing for stability of the scoop during flight.

## 4.3 Tank Electronics Design

### 4.3.1 Electrical Schematic and Block Diagram

Below is the electrical schematic for the rover. The Arduino Nano and FeatherWing Motor Controller will turn on once the NC microswitches are opened such that the circuit completes. This occurs when the rover exits the rocket since the microswitch is in contact with the edge of the rocket in the payload bay. The Arduino Nano is powered by a 9-volt battery and the FeatherWing by an Ovonic 2200mAh, 11.1-volt battery. The Ovonic 2200mAh, 11.1-volt battery is chosen because it provides us with enough power and is capable of fitting within our required dimensions. The XBee Transceiver will communicate motor control to the Arduino Nano through Hexadecimal, the Arduino Nano then converts this to micro python, as used by the FeatherWing Motor Controller, the Motor Controller then controls the motors as desired. The FeatherWing will control a NEMA 8 Stepper Motor for the scoop and two DC motors for the rover drive. The XBee on the rover will also send data to the DICU for it to display.

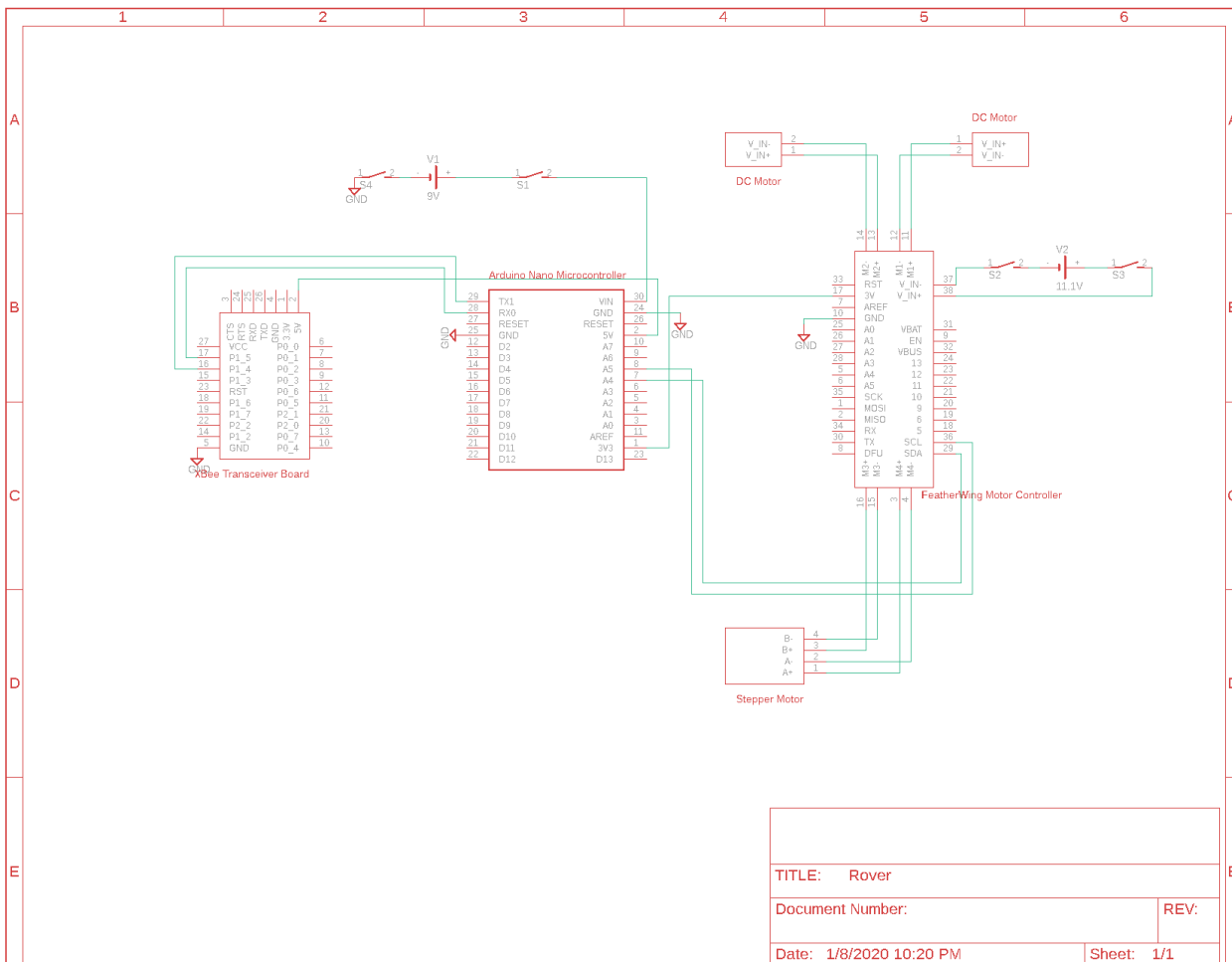


Figure 4-11: Electrical Schematic

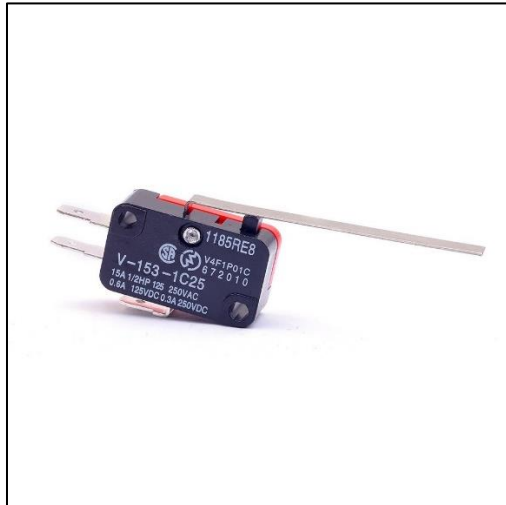


Figure 4-12: NC Micro Limit Switch

Below is the rover electronics block diagram. The Arduino Nano will transmit and receive data using the rover XBee to talk with the DICU XBee. Motor Control will be transmitted from the Arduino into the FeatherWing Motor Controller. This motor controller will in turn control the left driving DC motor, right driving DC motor, and the stepper motor. An Ovonic 2200mAh LiPo battery is used for the motors and a 9-volt battery averaging 500mAh is used for the Arduino Nano and its connections.

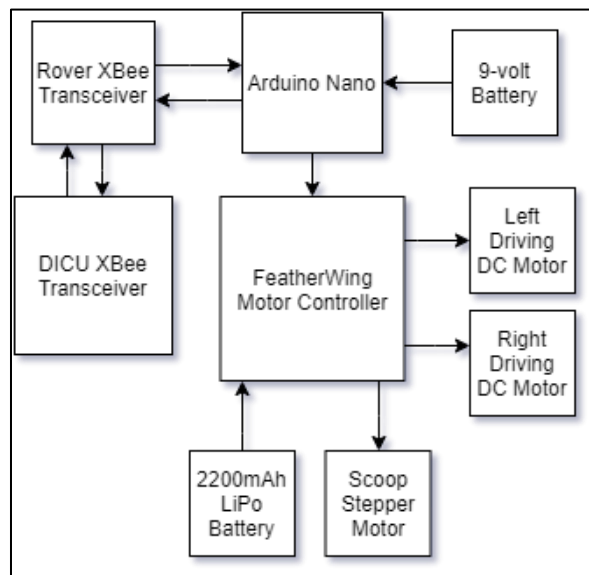


Figure 4-13: Rover Block Diagram

### 4.3.2 Microcontroller

On the rover we opt for an Arduino Nano. This was chosen primarily because of its low power consumption, small size and its reliability. Originally, we had planned to use a Raspberry Pi Zero, however this device presented issues for power and, even more importantly, was not reliable as it would crash seemingly randomly. The Arduino Nano is not as powerful as the Raspberry Pi Zero, yet this presents no issue because most computing will be performed by the DICU. The Arduino Nano also provides more than enough pins and computing power for our needs.

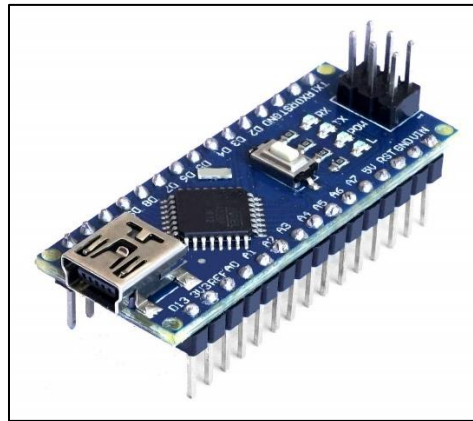


Figure 4-14: Arduino Nano

### 4.3.3 Motors

The motor for the drivetrain was chosen to be the 98 RPM Econ Gear Motor from Servo City. This motor was selected based on calculations given in Chapter 4.6.1 Lead Screw Assembly. Due to its high stall torque and good operating torque curve, it is a good choice for our application.



Figure 4-15: Drivetrain Motor

Voltage (Nominal)	12V
Voltage Range (Recommended)	6V - 18V
Speed (No Load)*	98 rpm
Current (No Load)*	0.10A
Current (Stall)*	3.8A
Torque (Stall)*	524.32 oz-in (37.76 kgf-cm)
Gear Ratio	100:1
Gear Material	Metal
Gearbox Style	Straight Cut Spur
Motor Type	DC
Output Shaft Diameter	4mm (0.1575")
Output Shaft Style	D-shaft
Output Shaft Support	Bushing
Electrical Connection	Male Spade Terminal
Operating Temperature	-10°C ~ +60°C
Mounting Screw Size	3mm
Product Weight	0.20lb (3.25oz)

Figure 4-16: Drivetrain Motor Specs

#### 4.3.4 Motor Controller

The FeatherWing motor controller is used for its size, low power consumption, and ability to easily and effectively control both stepper and typical dc motors. Additionally, the motor controller is cheap and can provide enough power for both stepper motors and drive motors with 1.2 amps per bridge on four bridges and can run motors from 4.5-volts to 13.5-volts. The FeatherWing's automatic thermal shutdown protection also provides additional safety measures.

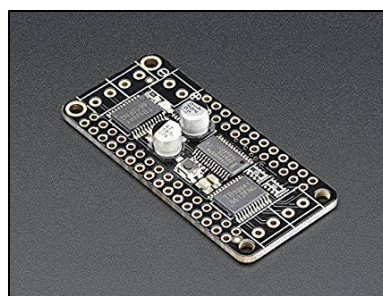


Figure 4-17: FeatherWing Motor Controller

#### 4.3.5 Communications

An XBee Series 2 with an RF output power of 2mW is used on the rover. Outdoor line of sight is up to 120 meters, which will be enough to connect with the DICU which controls the rover. The RF data rate is 250kbps which is an ample amount to deliver and receive all data required for us. This device works on a frequency of 2.4Ghz. DSSS is used where the direct-sequence modulation

makes the signal wider in bandwidth than the informational bandwidth, this primarily functions to reduce signal interference.



Figure 4-18: XBee Series 2

#### 4.3.6 Power Requirements

The FeatherWing Motor Controller will be required to drive the DC motors for 30 minutes and the Stepper Motor for 6 minutes, worst case scenario. We determine the driving motors require a 1900mAh battery as a minimum and the stepper motor power consumption is negligible. For power supply, we choose a 2200mAh LiPo battery rated at 11.1-volts. The calculations are as shown:

$$(1900\text{mA})(2 \text{ motors})(0.5\text{hr})=1900\text{mAh}$$

$$(600\text{mA})(0.1\text{hr})=60\text{mAh}$$



Figure 4-19: Ovonic 2200mAh Power Supply

On the Arduino Nano and XBee we will be using a 9-volt battery and assuming one hour runtime, which will consume 128.4mA over one hour. We then multiply this by 20% for battery uncertainty and determine a single 9-volt will more than suffice since 500mAh is much greater than 155mAh. Calculations shown below:

$$(128.4\text{mA})(1\text{hr})=128.4\text{mAh}$$

$$(128.4\text{mA})(1.2)=155\text{mAh}$$

#### 4.4 TEARS Overview

The tank exiting and reorientation system housed within the payload bay will be utilized to deploy the payload upon successful landing of the launch vehicle. This system consists of a bulkhead through which a connecting rod mounting assembly is attached. This connecting rod assembly mounts a fixed hub gear around which the reorientation assembly will rotate. The exiting mechanism for the payload is achieved through a linear exiting assembly mounted on the reorientation plate. The reorientation assembly comprises of a fixed hub gear and a reorientation plate that rotates relative to this gear. The linear exiting assembly consists of a lead screw that is rotated by a one-step gear reduction from a drive motor. Lead nuts are mounted on the front and rear retention plate for the payload. These lead nuts travel along the length of the lead screw as the lead screw is rotated. The lead screw runs through the nose cone shoulder into the hollow section of the nose cone to an end support assembly. The TEARS system with the payload are depicted below



Figure 4-20: TEARS side view with nose cone

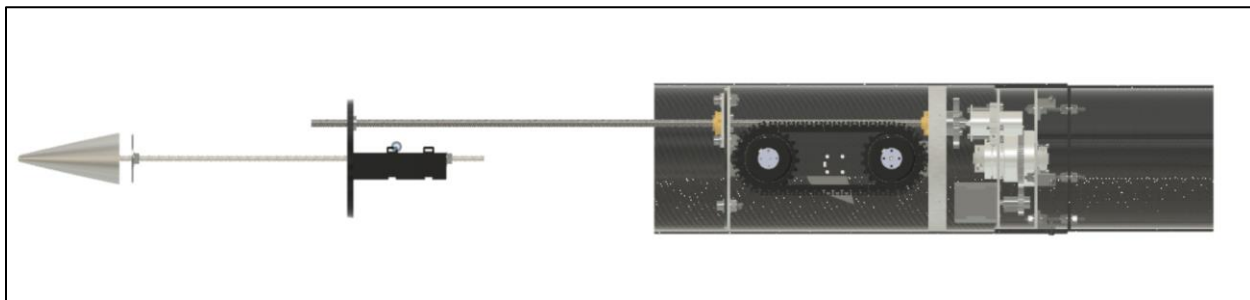


Figure 4-21: TEARS Side View

## 4.5 Reorientation

### 4.5.1 Connecting Rod Assembly

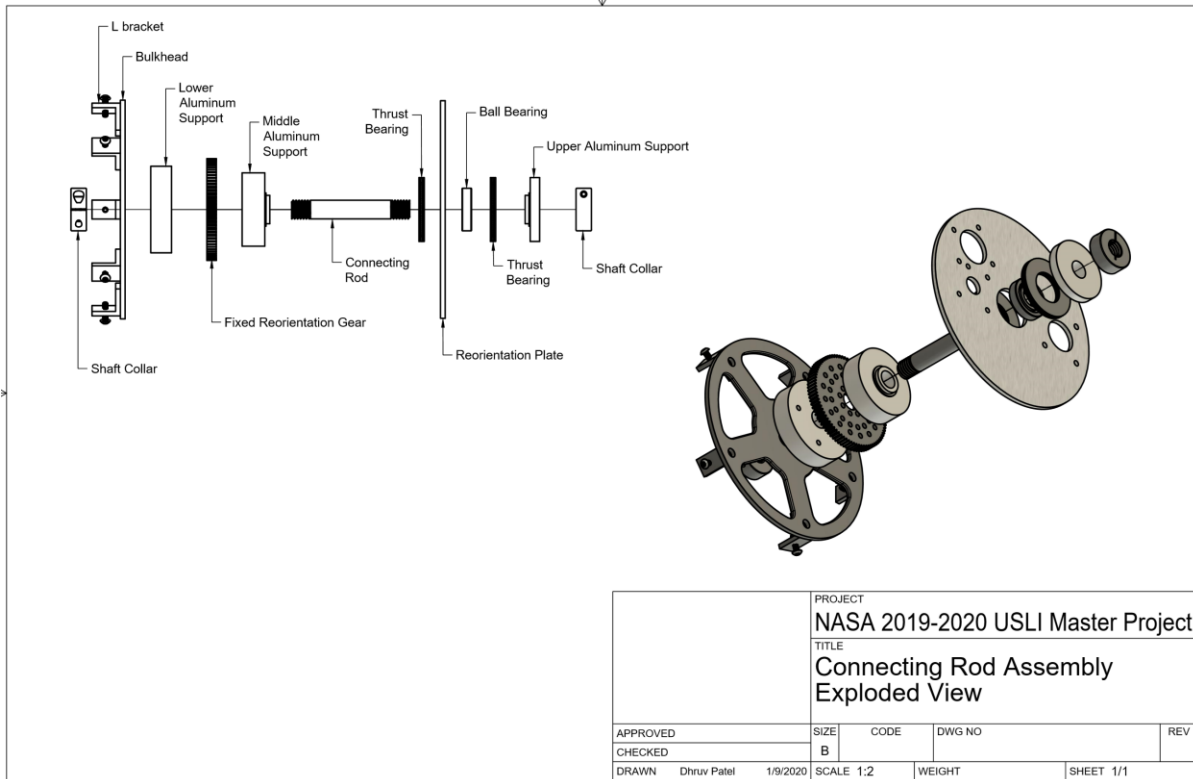


Figure 4-22: Connecting Rod Assembly Exploded View

The connecting rod serves as the fixed component of the reorientation assembly. The connecting rod is threaded on each end and has a smooth shaft in the middle. The shaft will be manufactured from purchased round aluminum stock and a CNC machine will be used to create the thread profile on each end of the rod.

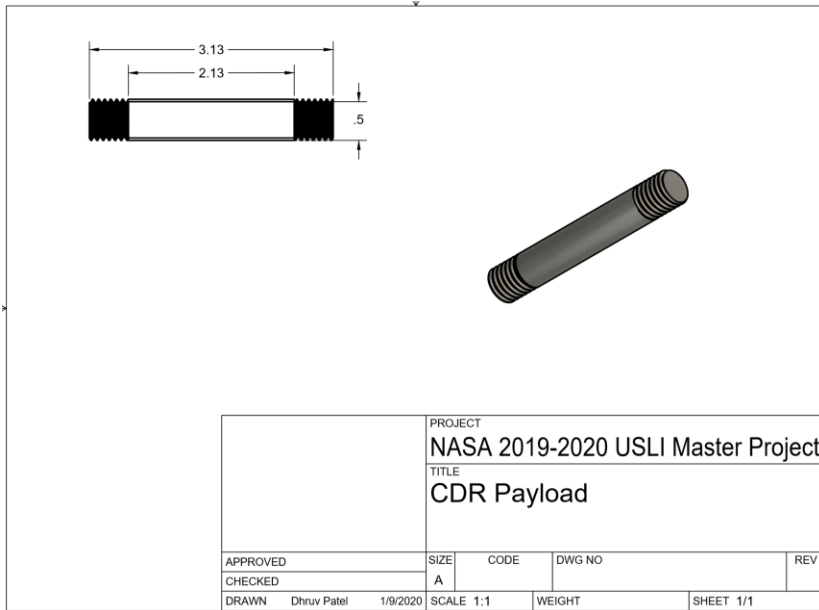


Figure 4-23: Connecting Rod

To prevent axial movement of the rod a threaded shaft collar (0.5' ID) is connected on each end. The shaft collars will be tightened using 8-32  $\frac{1}{2}$  in. screws .After the rod passes through the bulkhead, an aluminum support is mounted on the rod. This support serves as a spacer to allow for the mounting of the fixed hub gear at the appropriate height such that the pinion gear attached to the reorientation motor can mesh with it. Aluminum sheet will be purchased and used to machine the aluminum support.

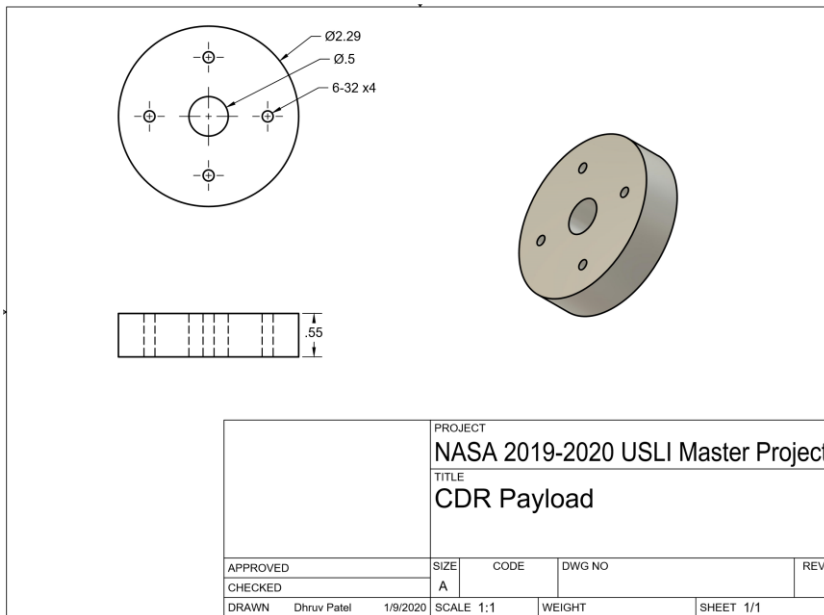


Figure 4-24: Lower Aluminum Support

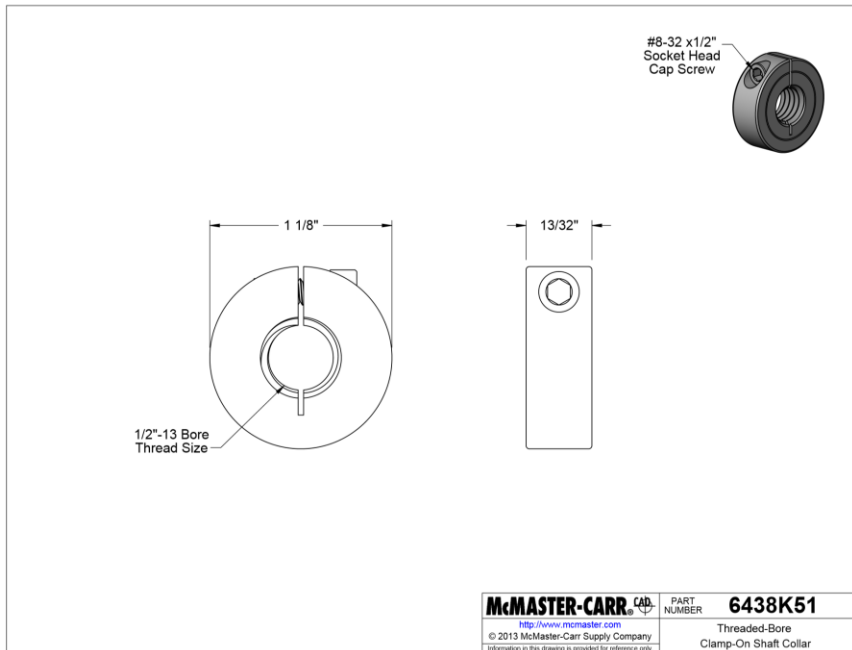


Figure 4-25: Connecting Rod Shaft Collar

The aluminum support also serves to improve the strength of our fixed system. A 84 tooth fixed hub gear with a pitch diameter of 2.625 in. is mounted on the rod following the lower aluminum support. The fixed hub gear has a mounting hole pattern through which two aluminum standoffs are connected from to the bulkhead. The aluminum standoffs are secured in place at the bulkhead and prevent the hub gear from rotation about the connecting rods axis. A middle aluminum support is mounted following the fixed hub gear. This middle aluminum support serves as a spacer and a structural support. Four holes will be drilled on the lower and middle aluminum supports. Aluminum rods will be attached through the drilled holes in the aluminum supports to the bulkhead. These rods serve to secure the aluminum supports with respect to the bulkhead

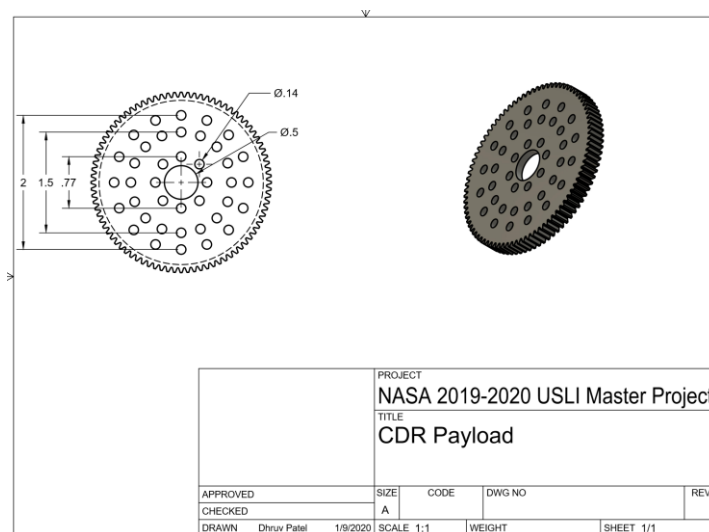


Figure 4-26: Fixed Reorientation Gear

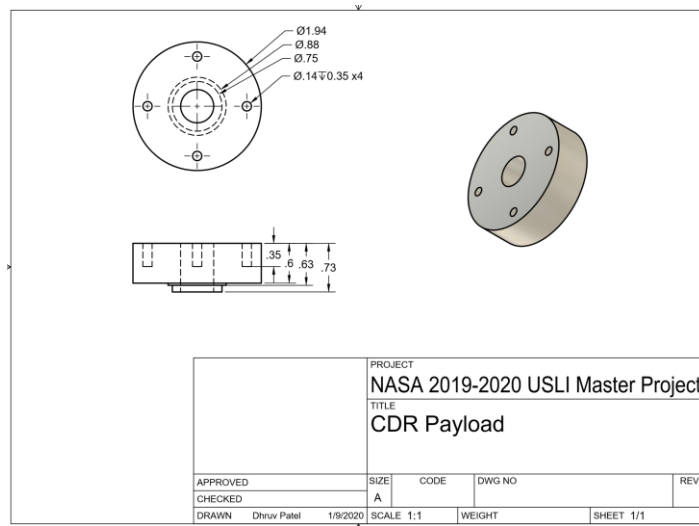


Figure 4-27: Middle Aluminum Support

The thrust bearings are mounted following the middle aluminum support. These thrust bearings help ease axial forces on the reorientation plate. The needle thrust bearing is mounted in between two washers. The bearing and washers are of the following dimensions.

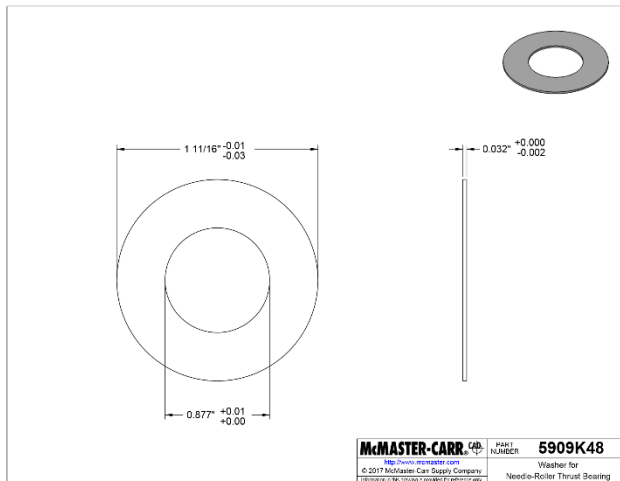


Figure 4-28: Connecting Rod Assembly Thrust Bearing Washer

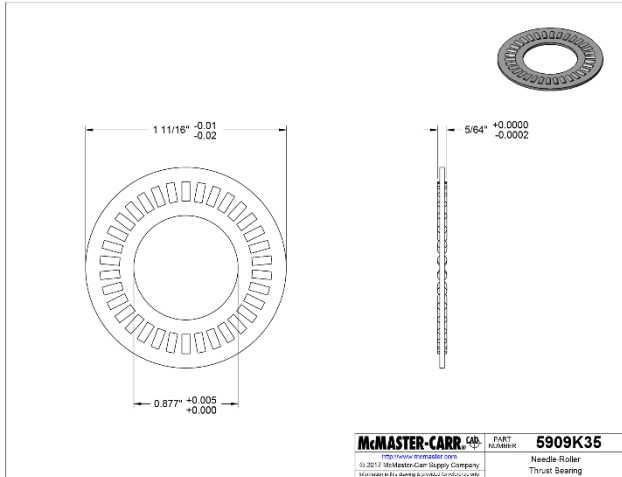


Figure 4-29: Connecting Rod Assembly Needler Bearing

Ball bearings are mounted after the thrust bearings. The reorientation plate is mounted on these ball bearings allowing for the system to rotate. The ball bearings also help with radial loads experienced by the system. Another set of thrust bearings is mounted after the reorientation plate. Incorporation of thrust bearings on each side of the reorientation plate reduces friction during rotation.

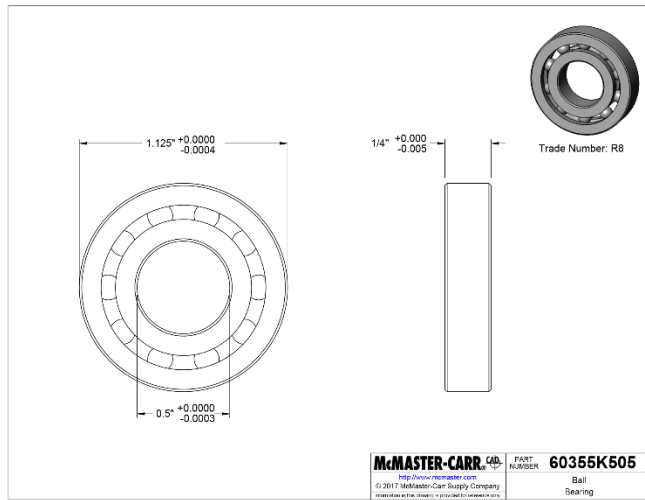


Figure 4-30: Connecting Rod Assembly Ball Bearing

A machined upper aluminum support is mounted after the thrust bearings to serve as a spacer. The shaft collar follows the upper aluminum support to prevent axial movement of the rod, and thus securing the assembly in place.

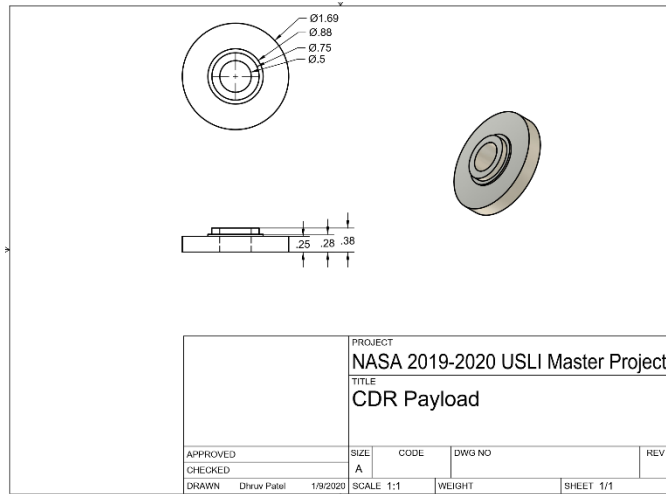


Figure 4-31: Connecting Rod Assembly Upper Aluminum Support

#### 4.5.2 Reorientation Plate

The payload reorientation is achieved by the means of a reorientation plate that rotates around the connecting rod assembly. The reorientation plate has the TEARS electronics and the lead screw assembly mounted on it. The reorientation plate will be made from 6061 Aluminum. The circular plate will be machined from purchased aluminum stock. The plate is 1/8 in. thick and has a diameter of 5.75 in. The reorientation motor is surface mounted on this plate with the shaft extending through the plate pointing towards the aft end of the payload bay. M3 x 0.5 mm thread, 12 mm screws are used to fasten the motor to the reorientation plate. The lead screw motor is mounted through the plate on end with the use of a 25 mm bore face tapped clamping hub. The clamping collar is tightened around the motor using 6-32 zinc plated socket head screws of 0.5 in. length. The clamping hub is mounted on the reorientation plate using four 6-32 socket head screws of 7/16 in. length. The aluminum standoff support structure for the lead screw is mounted close to the lead screw motor. The lead screw assembly mounts through the hole in the reorientation plate and the rectangular pattern bracket is mounted on top. The mounted parts on the reorientation plate and the mounting holes can be seen in the figures below.

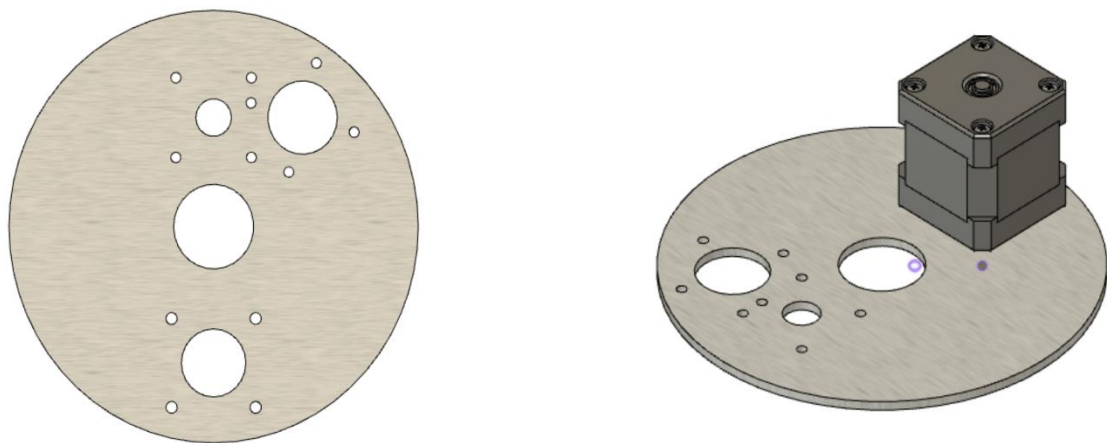


Figure 4-32: Reorientation Plate (left) and Reorientation Motor mounted (right)

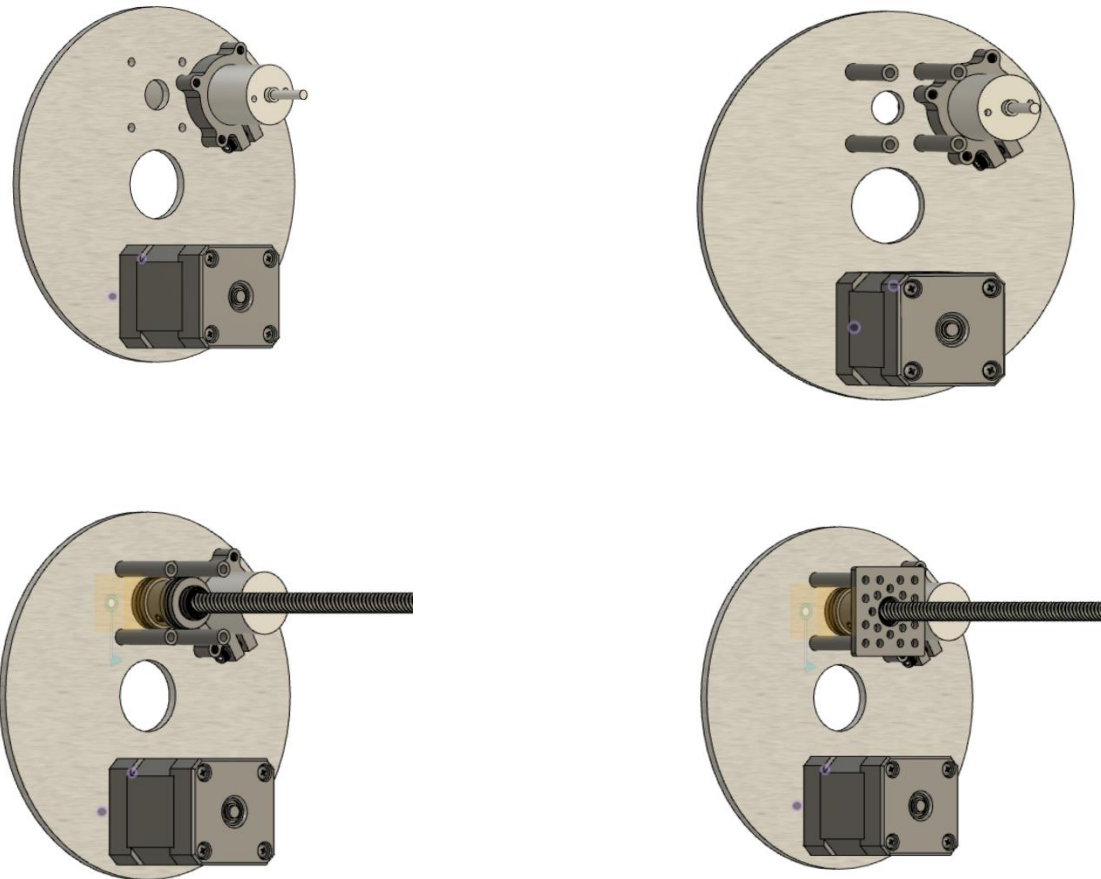


Figure 4-33: Reorientation Plate mounted components Lead screw motor (top left), aluminum standoffs (top right), lead screw assembly (bottom left), rectangular plate (bottom right).

The reorientation motor shaft has a shaft coupler attached to it that connects to a 32 teeth pinion gear with a 1 inch pitch diameter. This pinion gear will mesh with the fixed hub gear that is rigidly fixed to the connecting rod assembly. The entire reorientation plate will rotate around that fixed gear, thus rotating the assembly. The reorientation motor and its connection to the pinion gear is shown in figures below.

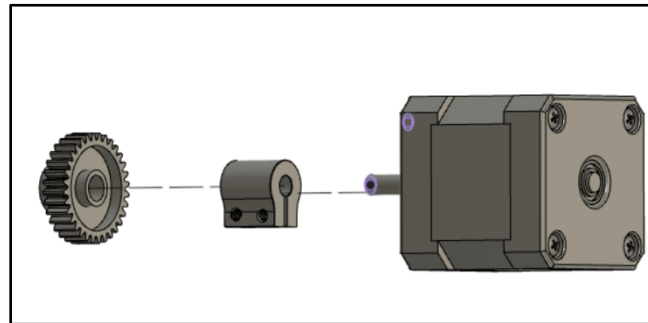


Figure 4-34: Reorientation Motor connection to pinion gear

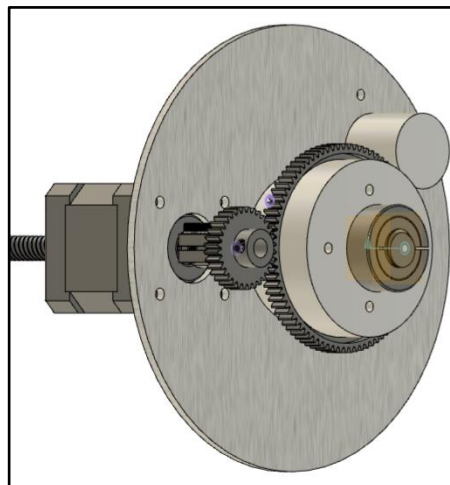


Figure 4-35: Reorientation Motor

pinion gear meshing with fixed hub gear

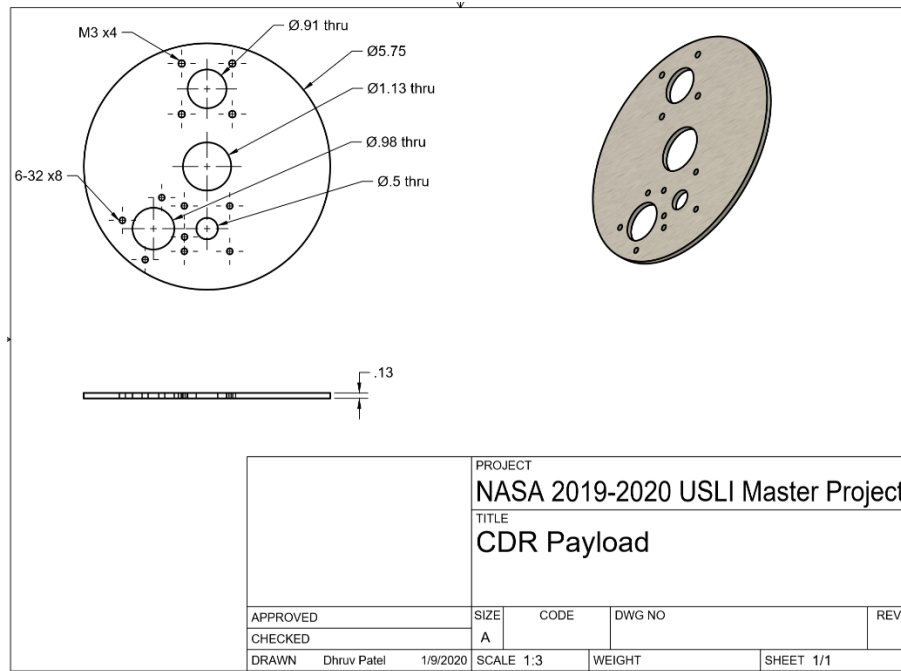


Figure 4-36: Reorientation Plate Drawing

The reorientation plate and the assembly will be rotated with the use of a single motor rotating around a centrally fixed hub gear. In order to pick the specific motor, the required motor torque had to be calculated. In order to perform this calculation the various loads on the reorientation plate had to be evaluated. The four major loads on the reorientation plate are the load of the lead screw assembly, the lead screw motor, the reorientation motor, and the reorientation plate itself. The mass value for the reorientation motor was estimated to be 6 oz. The total masses are shown below:

$$m_{\text{lead screw assembly}} = 220 \text{ oz} = 2.92 \text{ kg}$$

$$m_{\text{reorientation plate}} = 0.292 \text{ kg}$$

$$m_{\text{lead screw motor}} = 0.1 \text{ kg}$$

$$m_{\text{reorientation motor}} = 6 \text{ oz} = 0.17 \text{ kg}$$

These masses were represented as point masses on the reorientation plate and the moments of inertia for each corresponding mass with respect to the plate's rotation axis was calculated.

$$I = mR^2$$

$$I = \frac{1}{2}mR^2$$

The moments of inertia were calculated using the equations shown above. The lead screw assembly, the reorientation motor, and the lead screw motor were represented as point masses and equation 1 was used above. The reorientation plate was represented as a disk and equation 2 was used above to calculate the moment of inertia. The total moment of inertia was then calculated as shown below:

$$I_{total} = I_{reorientation\ plate} + I_{lead\ screw\ assembly} + I_{reorientation\ motor} \cdot I_{lead\ screw\ motor}$$

$$I_{total} = 0.02197 \text{ kg} * \text{m}^2$$

The following equation was then used to calculate the torque required for the motor to be used,

$$T = I\alpha$$

Where the angular acceleration of the plate,  $\alpha$ , was designated as  $5 \frac{\text{rad}}{\text{s}^2}$  since the reorientation should not happen too quickly. The required torque was converted to oz-in since generally motor manufacturer datasheets specified torque parameters in oz\*in.

$$T = 0.10985 \text{ N} * \text{m} = 15.56 \text{ oz} * \text{in}$$

Since the masses of smaller components were omitted in the estimation and frictional losses weren't accounted for, and only major loads were taken into consideration for the calculations, a factor of safety of 6 was assigned to the torque value. This resulted in a torque of

$$T_{FOS,6} = 6T = 93.36 \text{ oz} * \text{in}$$

This calculated torque value is applicable to a rotating assembly with direct motor drive attachment. Since our assembly uses a gear reduction in order to rotate, the required torque will be lower. In order to determine the required torque after gear reduction, the gearing ratio was first calculated as follows.

$$\text{Number of pinion teeth: } N_t = 32$$

$$\text{Number of hub gear teeth: } N_{hub} = 84$$

$$\text{Gear Ratio: } GR = \frac{84}{32} = 2.625$$

Using the calculated gear ratio, the required torque was calculated as follows:

$$T_{required} = \frac{T_{FOS,6}}{GR} = 35.57 \text{ oz} * \text{in}$$

Stress analysis was performed on the reorientation plate with forces during main parachute ejection. The acceleration experienced during main chute deployment is  $750 \text{ ft/s}^2$  and the reorientation plate will bear the weight of lead screw assembly, the reorientation motor, rover, and the nose cone during this event. The total weight that the reorientation plate is bearing is 8 lbs. This results in an applied force of 186 lbf. The stress simulation was performed using 250 lbf and resulting deformation and stress profile is shown in the figure below.

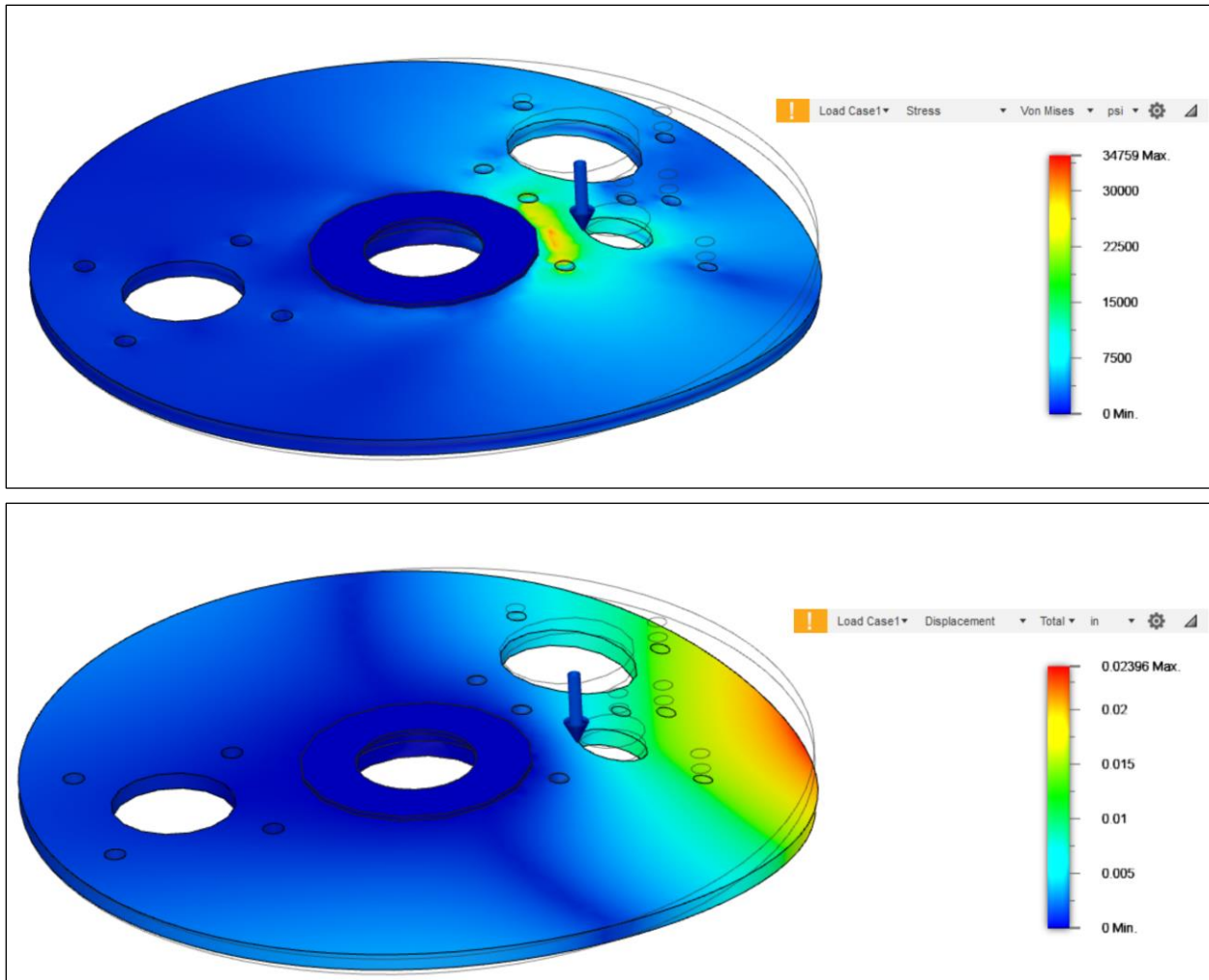


Figure 4-37: Reorientation Plate FEA stress profile (top) and deformation (bottom)

The max stress experienced by the plate is 34759 psi. The tensile yield strength of aluminum 6061 is 40000 psi and this yields a factor of safety of 1.15. The max deformation experienced under this stress is 0.02396 inches which is acceptable.

## 4.6 Tank Exiting

### 4.6.1 Lead Screw Assembly

The exiting of the rover is performed via a lead screw assembly, general overview of which is shown in Figure 4-38 below.



Figure 4-38: General Lead Screw Assembly

To reorient the entire rover along with the exiting mechanism, the lead screw and lead screw motor are both attached to the reorientation plate. As the plate rotates, so does the entire lead screw assembly. The reorientation plate is highlighted blue in the Figure 4-39 below.

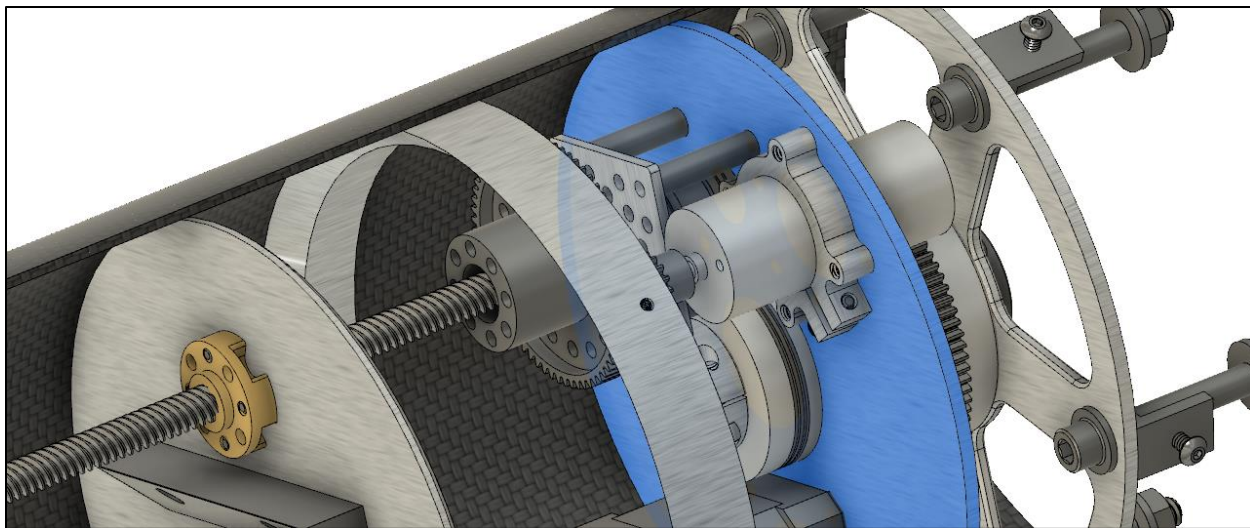


Figure 4-39: Exiting mechanism in relation to reorientation plate (shown in blue)

For clarity some of the components are removed, leaving only lead screw assembly and lead screw motor on the reorientation plate shown below.

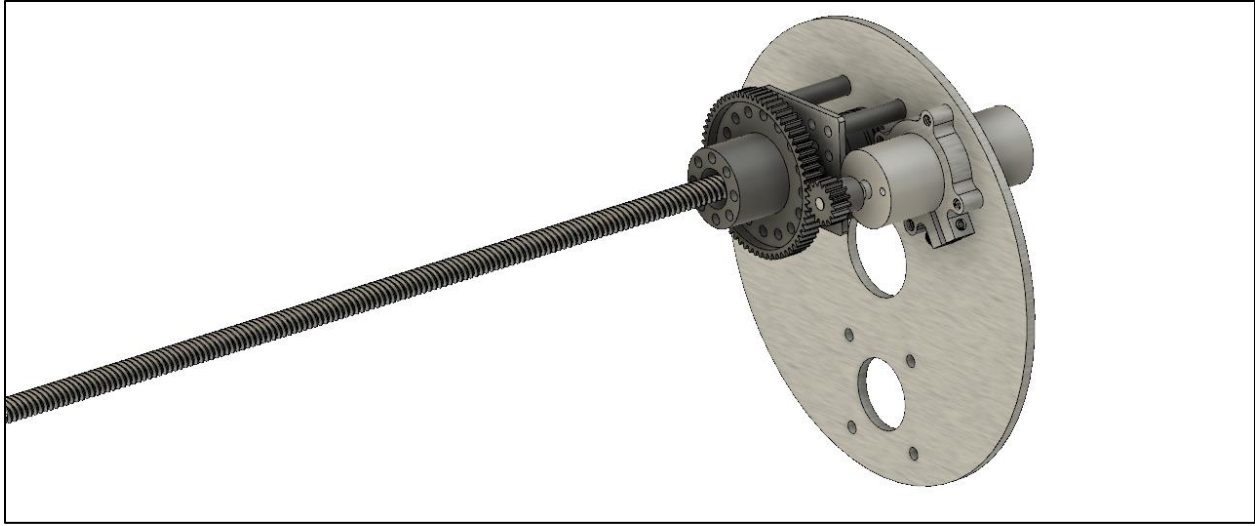


Figure 4-40: Lead screw components

The torque requirement for the DC motor to rotate the ACME thread is given by the equation below:

$$T = \frac{FD_p}{2} \left[ \frac{\cos \phi \tan \lambda + f}{\cos \phi - f \tan \lambda} \right]$$

where  $F$  is the force on the lead screw,  $D_p$  is the pitch diameter,  $f$  is the coefficient of friction between the nut and the screw,  $\phi$  is the thread angle,  $\lambda$  is the lead angle. The coefficient of friction for a well lubricated steel screw is  $f = 0.15$  which is a very conservative estimate. The thread angle and the lead are provided by the manufacturer of the part. The values are taken to be  $\phi = 14.5^\circ$  and  $L = 8mm$ . To find the lead angle, the following equation is used:

$$\begin{aligned} \tan \lambda &= \frac{L}{\pi D_p} \\ \lambda &= \tan^{-1} \left( \frac{L}{\pi D_p} \right) \end{aligned}$$

Thus, the torque requirement can be directly calculated by plugging in all the known values to yield the following result:

$$T = 0.96 \text{ lb} \cdot \text{in} = 15.39 \text{ oz} \cdot \text{in}$$

This is the minimum required torque for the application. Due to extreme importance of this particular mechanism it is crucial to include a safety factor of at least  $K = 3$ . Moreover, to prevent stalling the DC motor and draining too much current from the system it is necessary to choose the motor that will have sufficiently large stall torque. Both the motor and the lead screw are attached to the reorientation plate via 4 screws. The motor transmits torque to the screw via gear train amplifying torque in the process. The exploded view of this assembly is shown in the following figure.

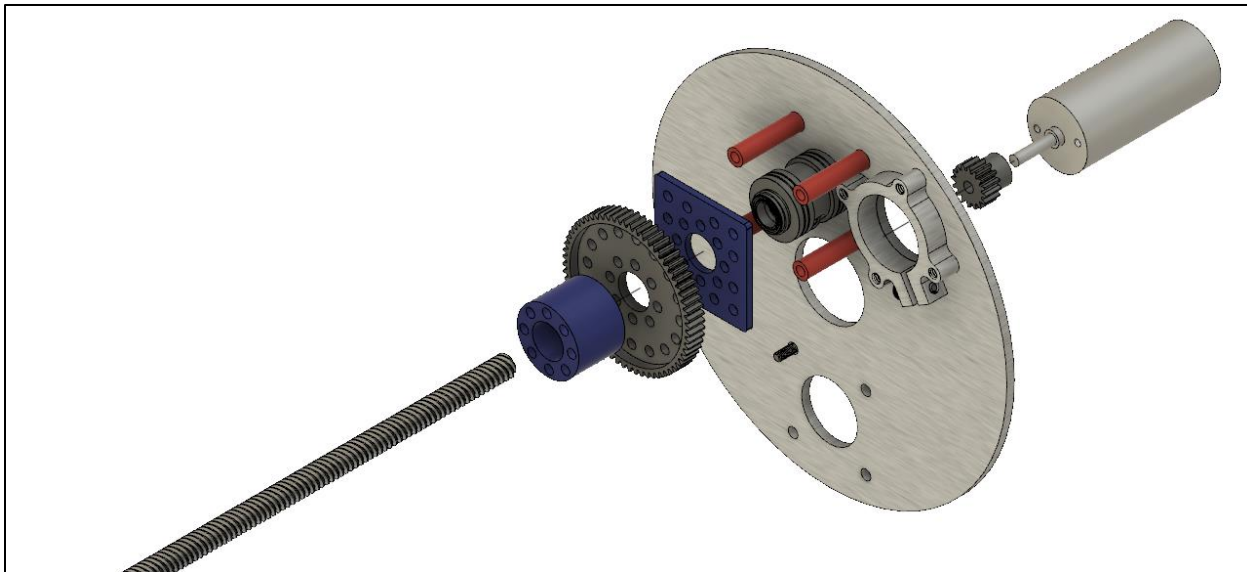


Figure 4-41: Lead screw assembly attachment points to the reorientation plate.

The large gear is attached to the lead screw via a screw hub shown in the figure above in blue. The aluminum standoffs shown in red are what keep the gear attached to the reorientation plate. The second purpose of these standoffs is to reinforce the leadscrew during the reorientation process. Four thrust bearings are what keep the lead screw in place and resist and axial load. Figure below shows the exploded view of the assembly.

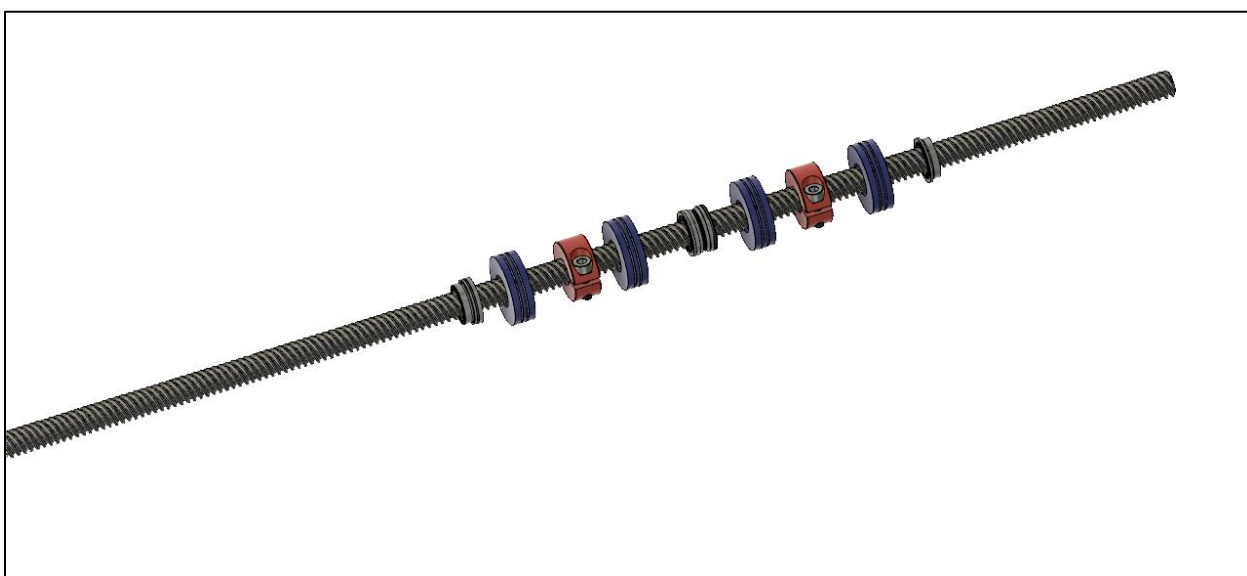


Figure 4-42: Lead screw bearings and clamping collar.

Thrust bearings are shown in blue. The parts in red are lead screw clamping collars which are what transmit the forces from the leadscrew to the bearings.

Lead nuts are what convert the lead screw rotation into linear motion of the exiting mechanism.

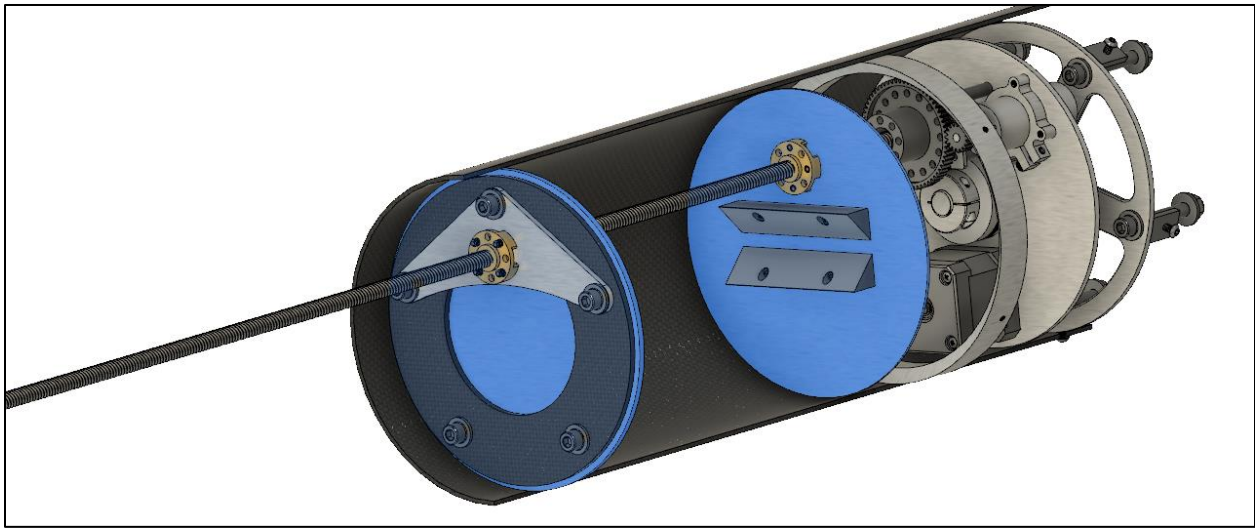


Figure 4-43: Lead nuts (shown in yellow) and retention plates (shown in blue)

As seen from the Figure 4-43 the lead nuts (shown in yellow) are attached to the retention plate via four screws.

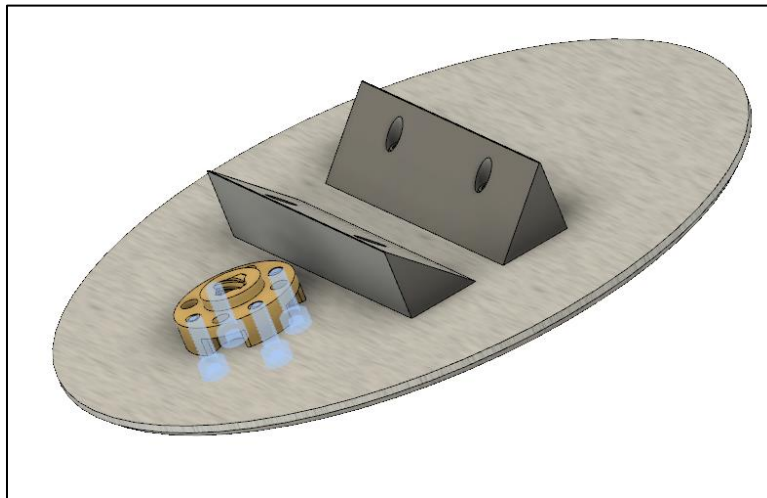


Figure 4-44: Retention Plate

The exiting mechanism in the deployed position is shown in the figure below.



*Figure 4-45: Exiting Mechanism in deployed position*

From this position the front retention plate lead nut is disengaged from the lead screw and the motor can be ran in reverse to increase the distance between plates. Thus, the rover can be successfully deployed.

#### 4.6.2 Support Collar

The support collar is added to reinforce the assembly from any axial and radial forces during flight. When rear retention plate is fully recessed into the airframe of the launch vehicle the collar will take on any load from the plate as shown in figures below. The support collar is highlighted in blue. As retention plate moves in deeper into the airframe it will hit against the collar at which point all the load is transferred to the airframe of the rocket.

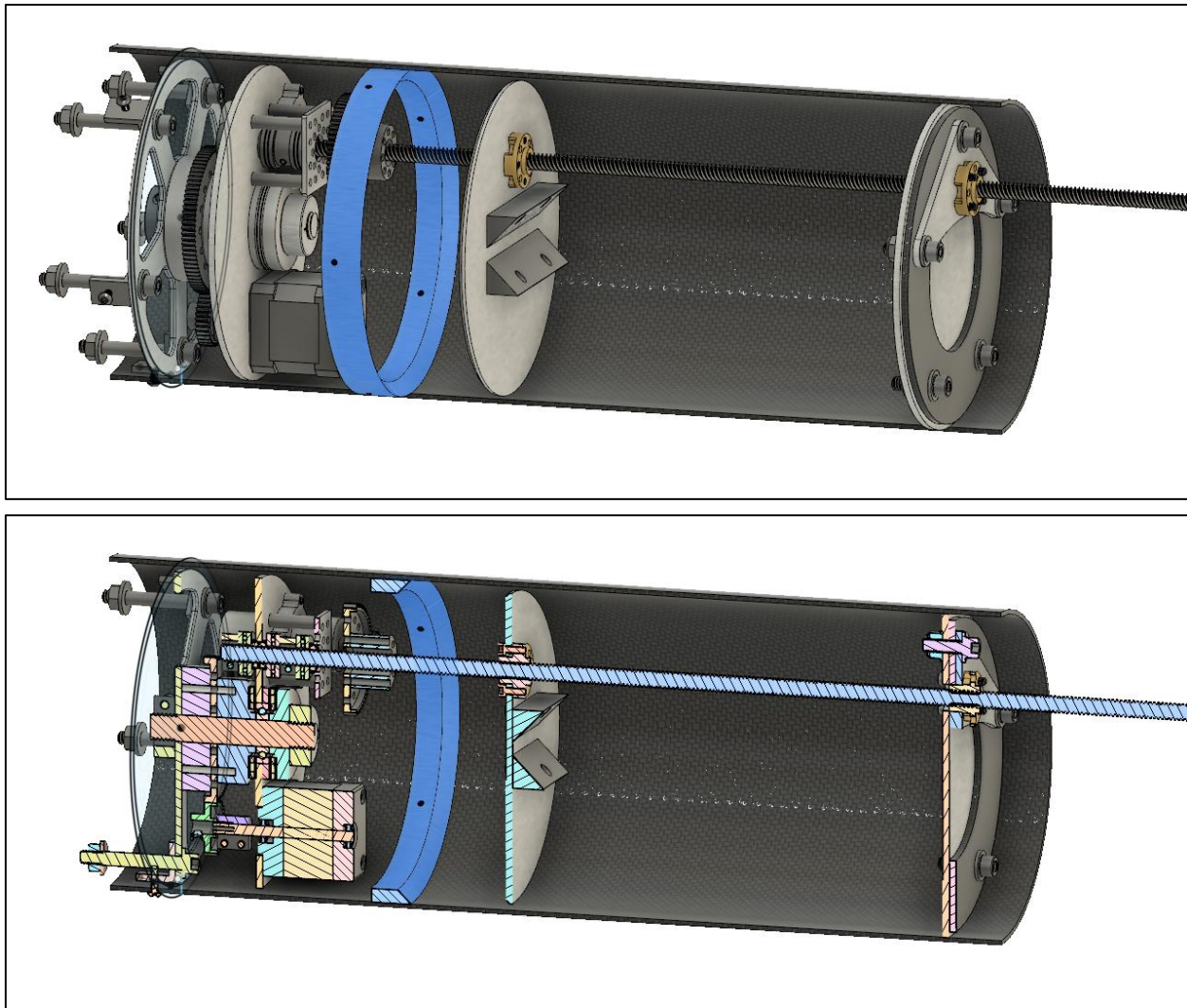
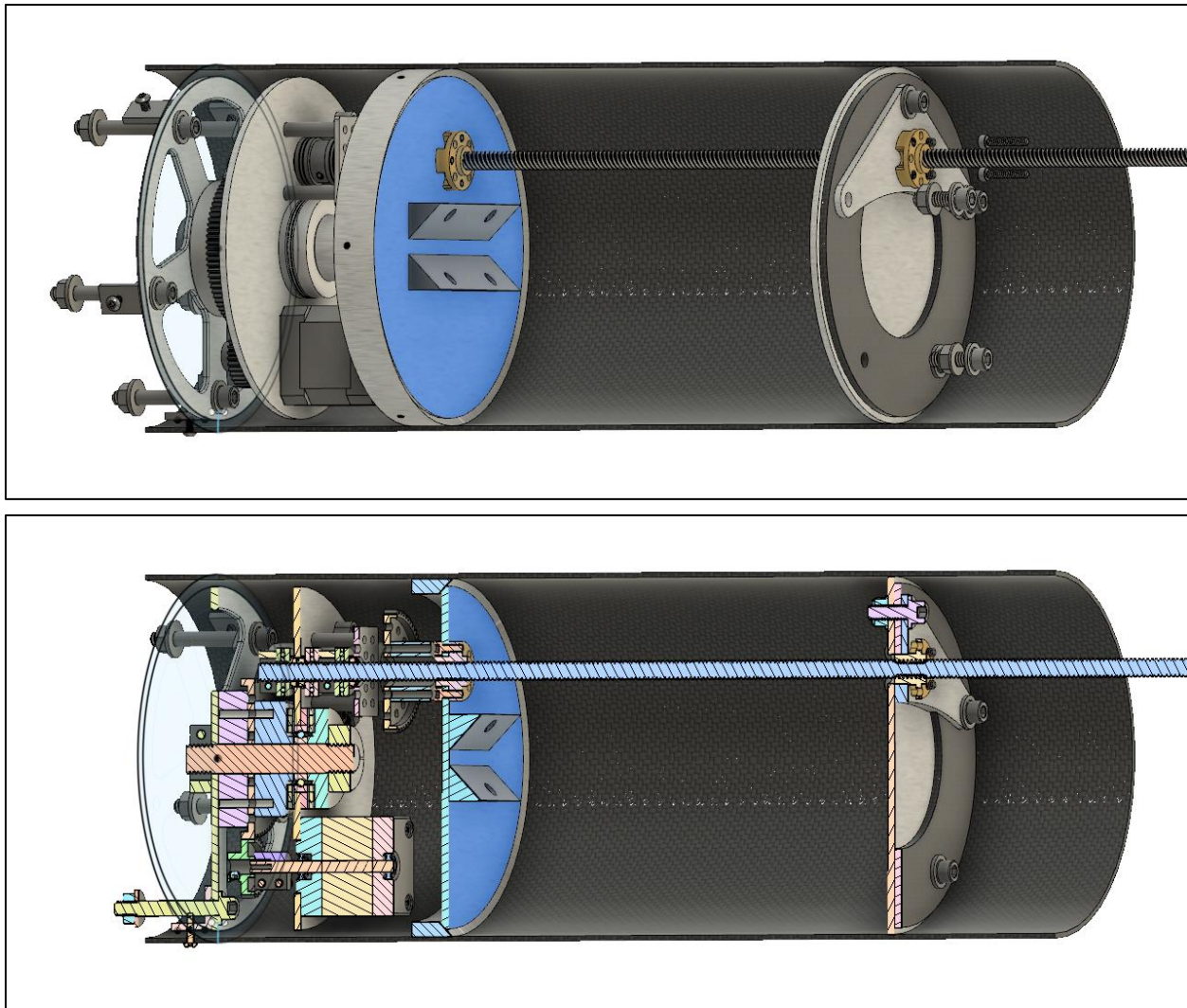


Figure 4-46: Regular and Section views of the retention plates and the support collar (shown in blue)



*Figure 4-47: Regular and section view of retention plate (shown in blue) and support collar.*

Support collar is attached directly to the airframe via bolts screwed directly from the outside of the launch vehicle. This ensures that all the load is transmitted directly to the carbon fiber airframe of the launch vehicle eliminating any stresses in the retention plates during the launch.

#### 4.6.3 Lead Screw End Support

Due to the length of the leadscrew, it is prudent to include some kind of support on its end to prevent it from vibrating during the flight. The following figure highlighted in blue the part of the mechanism that supports the leadscrew on its end.



Figure 4-48: Lead screw end support (shown in blue)

The 8mm lead screw will go through 9.5mm hole thus allowing some leeway during the assembly while keeping it from excessive vibration during flight. The figure below shows the section view of the nosecone.

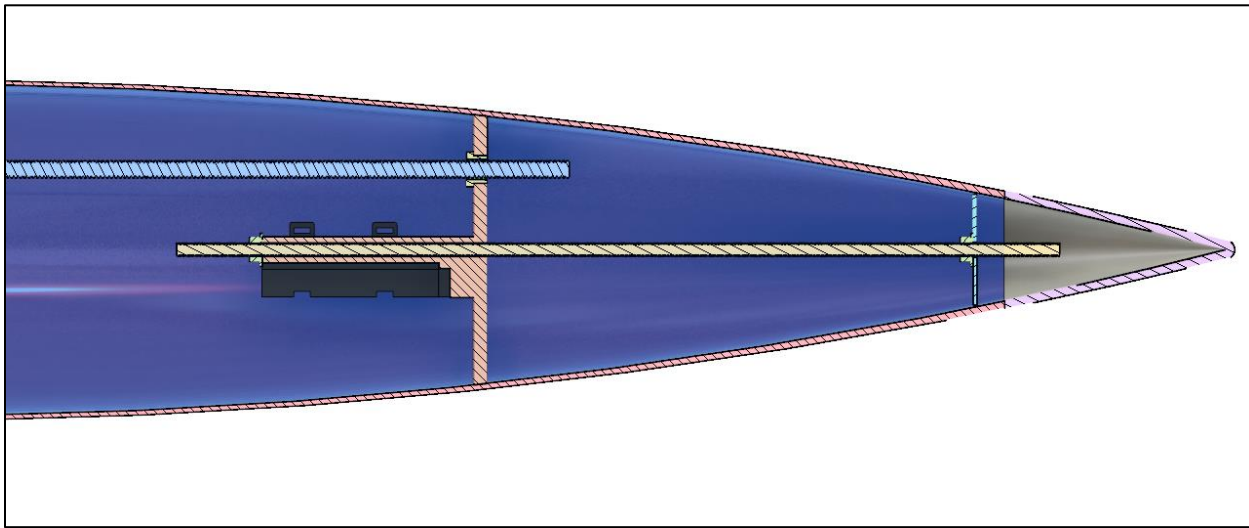


Figure 4-49: Nosecone section view.

This lead screw end support is integrated with the telemetry equipment in the nosecone. The entire sled is supported from the top of the nosecone by a screw which also acts to keep nosecone tip in place.

## 4.7 Tank Retention

The rover is held between two retention plates by the two triangular bodies on each plate. Figure below shows the bodies highlighted in blue.

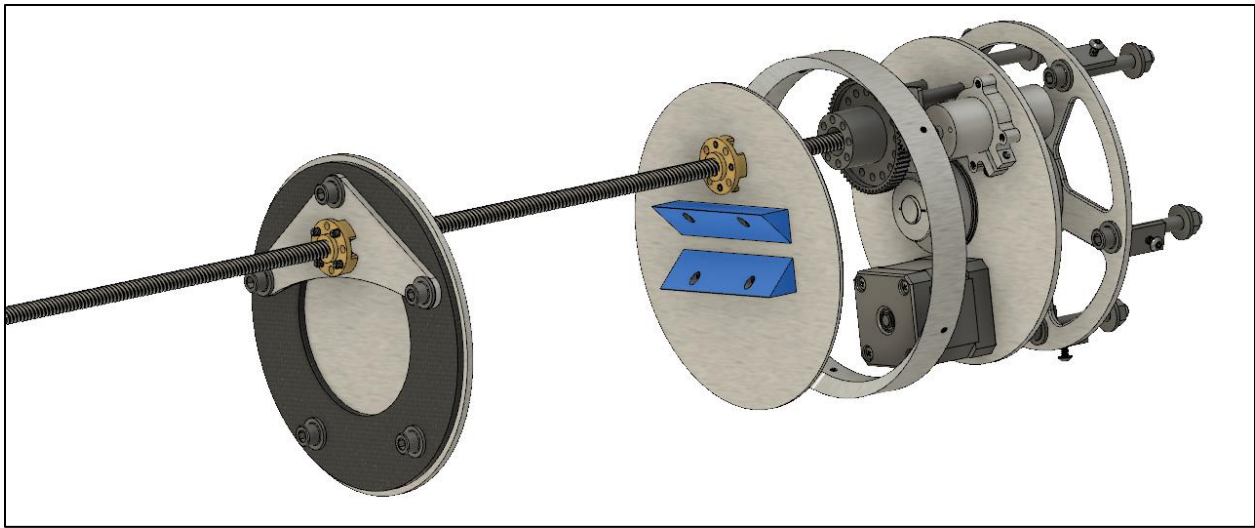
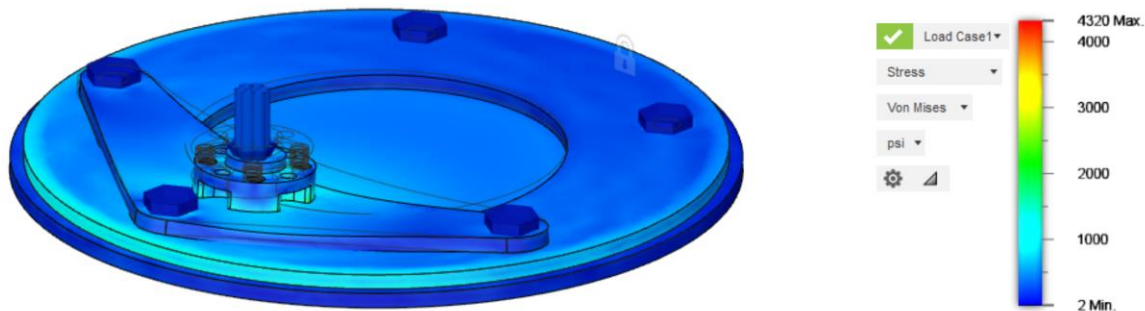
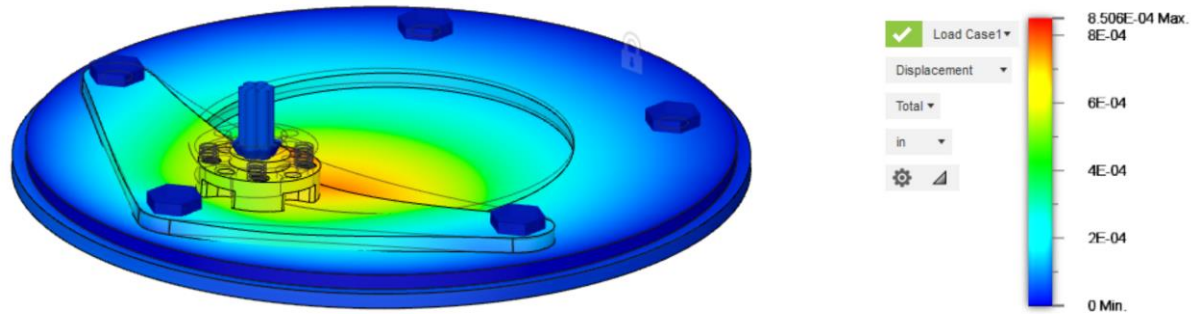


Figure 4-50: Tank retention mechanism (shown in blue)

The front and back of the tank chassis are the negative profile of the triangular bodies, thus preventing the rover from falling. As the distance between plates is increased during the deployment, the rover is slowly dropped to the ground. Each triangular retention mechanism is attached to the retention plates by two recessed screws. This mechanism only uses geometric constraints for retention, thus simplifying the entire assembly and eliminating any potential modes of failure.

FEA was performed on the front retention plate during deceleration of the payload bay. The payload bay decelerates at  $75 \text{ ft/s}^2$ . The lead nut on the front retention mount will carry the weight of the payload bay, which is 8.62 lbm. This results in a 20 lbf reaction force on the lead nut. The stress analysis was performed using a 50 lbf force directed on the brass lead nut. The resulting deformation and stress profile is shown in the figure below





*Figure 4-51: Front Retention Plate stress profile (top) and deformation (bottom)*

The max stress experienced on the front retention plate is 4320 psi with a max deformation of  $8.506 \times 10^{-4}$  inches, which is acceptable. The simulation resulted in a safety factor of 4.163.

## 4.8 Launch Vehicle Integration

### 4.8.1 Aft bulkhead and Coupler

The bulkhead is the base of the payload assembly. This bulkhead mounts the connecting rod that holds the entire payload assembly rigidly in place. The payload bay is connected to one end of the coupler of the avionics bay. After main parachute ejection the payload bay is tethered to the parachute via a shock cord attached on the coupler bulk plate. The bulkhead of the payload assembly will be attached to the airframe through a set of five L brackets that are fastened using  $\frac{1}{2}$  in. long 6032 black oxide alloy steel screws. The L brackets will be machined down to the required dimensions from purchased 90 degree angle 6061 aluminum stock. The dimensions of the L bracket are shown below:

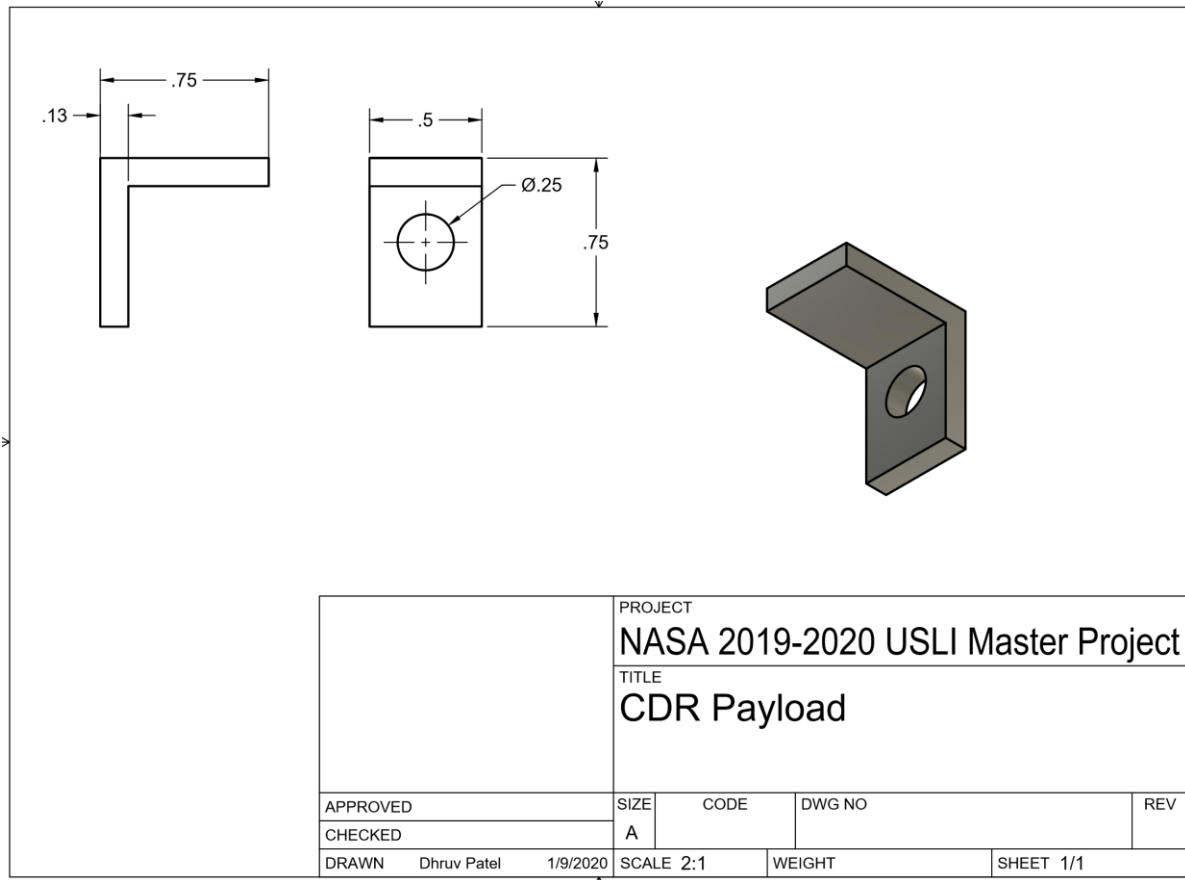


*Figure 4-52: L bracket Drawing*

The L brackets will be connected to the 1/8 in. thick bulkhead. The dimension of the bulkhead and the mounting hole pattern for the L brackets is shown in the figure below

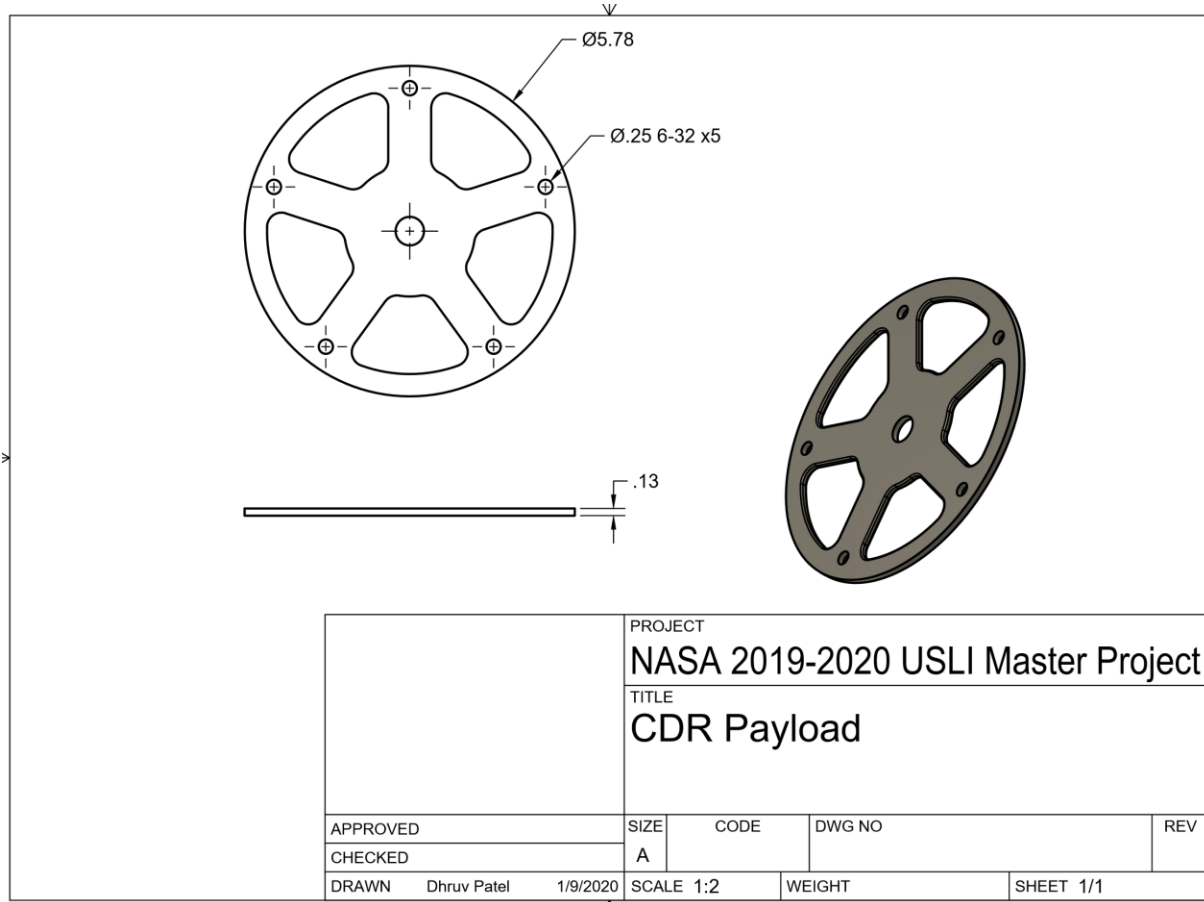


*Figure 4-53: Payload Bulkhead Drawing*

A threaded aluminum rod will run through the bulkhead and the L bracket to the coupler bulk plate to secure the payload bay. There will be threaded nuts on each side of the bulkhead to prevent the threaded rod from moving axially. The couple bulk plate will be epoxied to the airframe. The decision to use threaded aluminum rods was made as a form of redundancy. Since the payload bay bulkhead is a critical point of failure, it was deemed best to add a second retention mechanism for the payload bay in the event of failure of the L bracket screws that run through the airframe. During main parachute deployment if the L bracket screws shear off due to the parachute deployment forces, the aluminum rods will keep the payload bulkhead secure since it is connected to the epoxied coupler bulk plate.

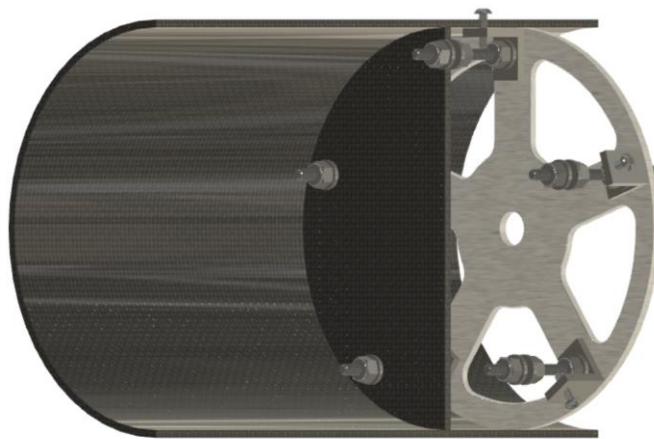
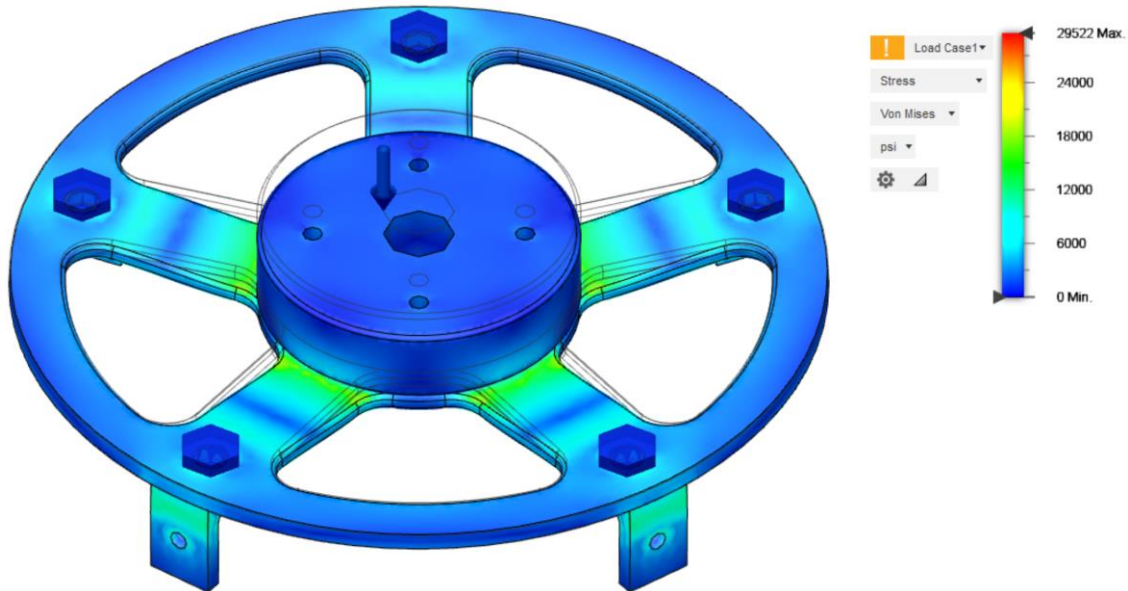


Figure 4-54: Reorientation Plate FEA stress profile (top) and deformation (bottom)

FEA analysis was conducted on the base bulkhead during the main parachute ejection. The acceleration experienced in that instance is  $750 \text{ ft/s}^2$ . The bulkhead has the mass of the payload bay supported on it during this event which is 12 lbm. Using these values a force of 279.5 lbf is acting on the bulkhead during main chute deployment. Stress analysis was performed using a 280 lbf acting on the center of the bulkhead. The resulting deformation and stress profile are shown in figures below. The max deformation for the bulkhead was 29522 psi and the max deformation was 0.012 in. The safety factor for the bulkhead is 1.351 based on the tensile strength for Aluminum 6061.



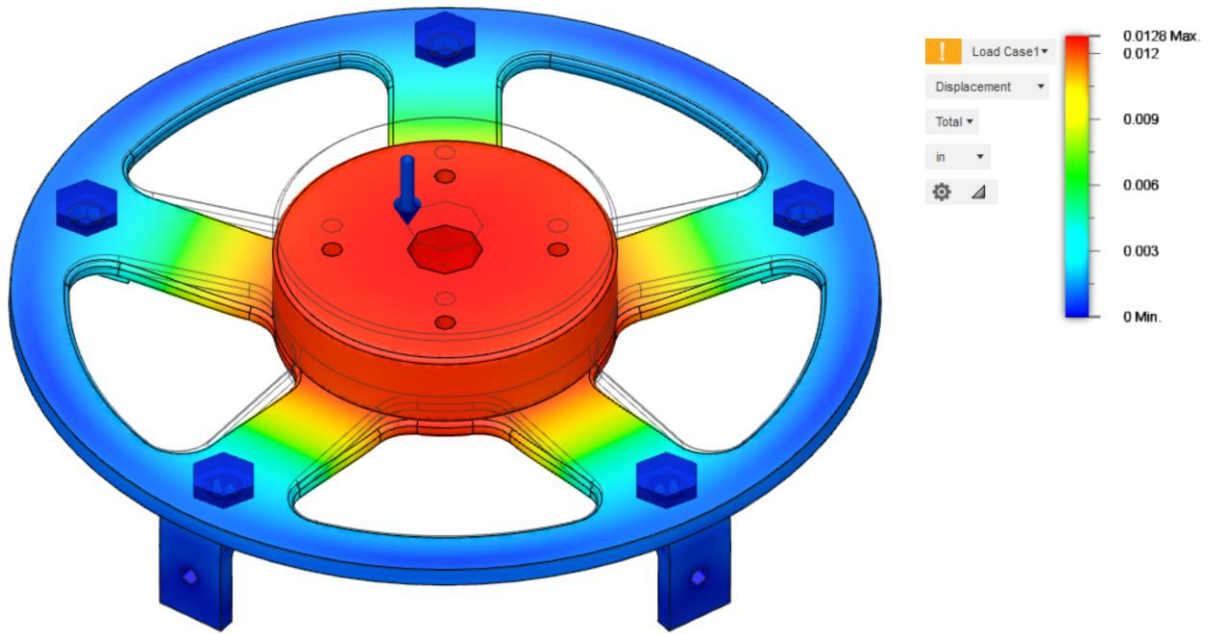


Figure 4-55: Payload Bulkhead FEA stress profile (top) and deformation (bottom)

#### 4.8.2 Nose Cone Integration

The payload front retention plate assembly is mechanically fastened on to a fiberglass centering ring that is epoxied on to the nose cone shoulder. The lead screw runs through this retention plate and centering ring into the hollow section of the nose cone. Due to a large unsupported length of the lead screw, an end support component was designed, the details of which were discussed in section 4.6.3. The telemetry bay that houses the GPS transmitter necessary for location recovery of the rocket is also attached to the same 3d printed end support structure. This integration of payload end support with the telemetry bay sled can be seen in the section analysis of the nose cone section of the rocket shown in the figure below:

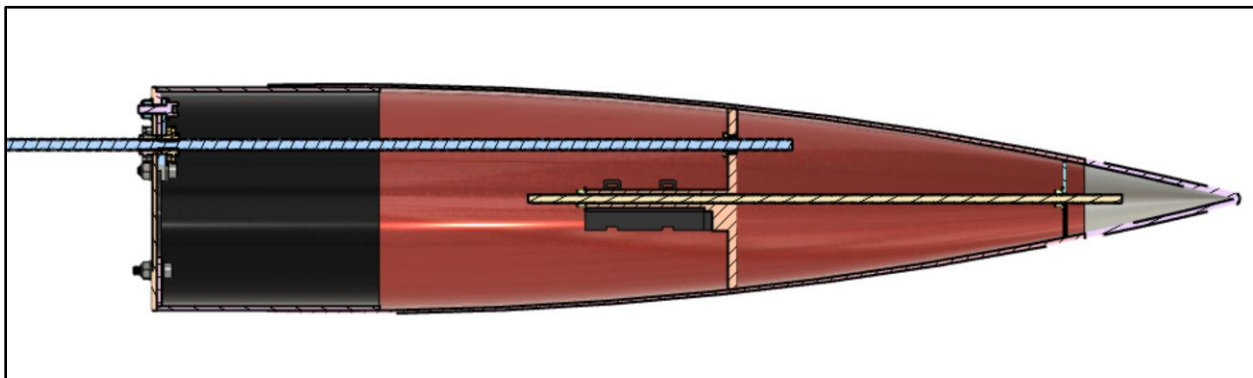


Figure 4-56: Nose Cone Payload Lead screw and Telemetry integration section view

The left most component is the front retention plate of the payload. The blue colored rod passing through is the lead screw. The orange colored component is the 3d printed end support housing. The yellow colored rod from the tip of the nose cone is the threaded aluminum rod that holds the 3d printed housing securely. The telemetry GPS and transmitter are mounted on the component that is colored black.

## 4.9 TEARS Electronics Design

### 4.9.1 Electrical Schematic and Block Diagram

In the electronics bay near the rover, we have the TEARS circuit, shown below. It is powered by two 9-volt batteries in parallel, this is fed through a step-up buck converter such that we can power the receiver with a 12-volt rating.

Whenever we press a button, the associated Normally Open Relay on the receiver will be closed and the circuit will be completed. Looking to the NO Relay under the supplied power, a voltage divider is used to power the circuit, the motor driver, and the stepper motor itself with 5-volts. We use one 555 timer to control the motor's rotation direction, IC2, and another to control the speed of the motor, IC1. A potentiometer, R1, is used to adjust the time constant and alter stepper motor speed according to our needs. This stepper motor driver will then in turn control the stepper motor. The following NO Relay will be used to reverse polarity going into the 555 timer via a momentary relay switch rated at 5-volts, accounted for with a voltage divider, allowing us to move the stepper in reverse. The third NO Relay will power the DC motor at 12-volts. The fourth NO Relay will reverse the polarity of the DC motor such that it can drive reverse via the 5-volt double pole double throw switching relay. This fourth NO Relay will also serve to switch the 555 timer's polarity such that the stepper motor will once again be able to drive forward through a 5-volt momentary relay switch. Lastly, as with the other circuits, a voltage divider is used to supply 5-volts for this fourth NO Relay. The LED indicators are 0.15 Watts and represent whether the stepper motor is turning in a reverse, D3, forward, D2, if power is being supplied, D1, or more specifically if IC1 is providing an output.

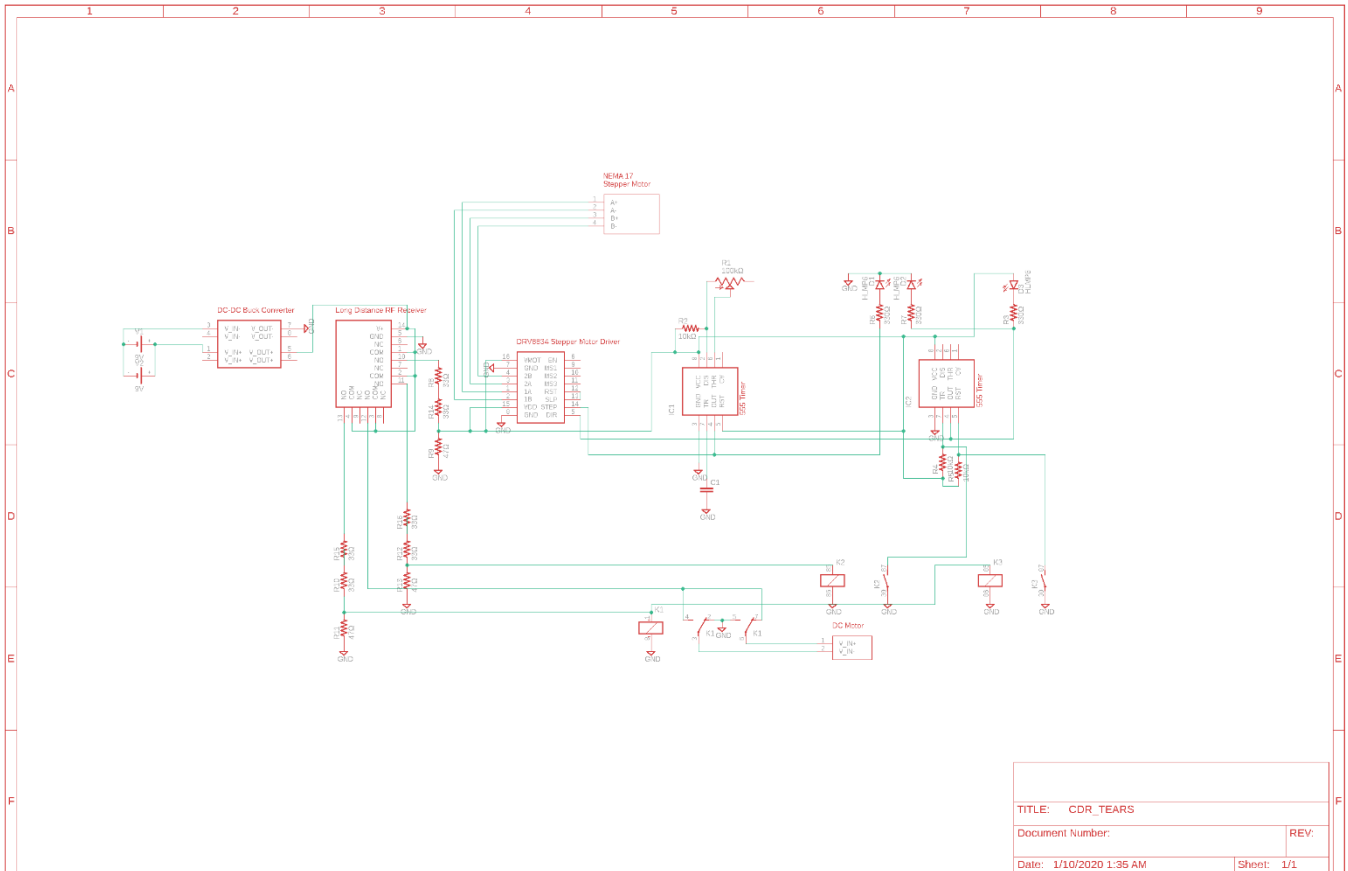


Figure 4-57: TEARS Electrical Schematic

Looking to the block diagram below, we can understand the circuit from a simpler view. The TEARS Receiver will be controlled via the Remote Control Transmitter, which is powered by a 12-volt battery. As mentioned above, the receiver is powered by two 9-volt batteries going through a step-up buck converter. The receiver itself powers the circuit which provides function generation to the A4988 Stepper Motor Driver which then controls the NEMA 17 Stepper Motor. The receiver also powers the DC Motor directly. Lastly, it powers the Relay switches which will control whether the DC Motor and NEMA 17 Stepper Motor function move in reverse or forwards.

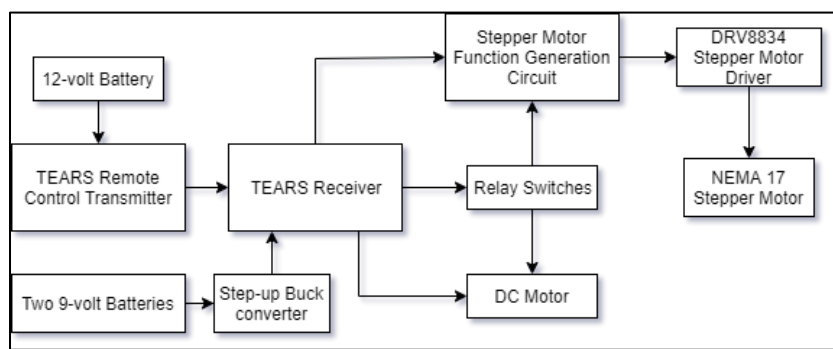


Figure 4-58: TEARS Block Diagram



Figure 4-59: DPDT Relay Switches

#### 4.9.2 Motors

The motor for reorientation was selected based on the torque requirements calculated in section 4.5.2. A stepper motor was selected since they offer high holding torque when current is applied and will prevent our system from rotating on its own during flight. The NEMA 17 bipolar stepper motor was selected with a step angle of 1.8 degrees and 62.3 oz-in of holding torque. The dynamic torque of the motor can be estimated at 70 percent of the holding torque which yields a value of 43.61 oz-in. This torque value is above the calculated required torque.

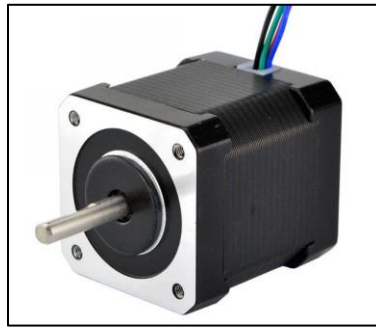


Figure 4-60: Reorientation NEMA 17 Stepper Motor

The motor for the leadscrew assembly was chosen to be 124 RPM Econ Gear Motor from Servo City. This motor was selected based on calculations given in Chapter 4.6.1 Lead Screw Assembly. Due to its high stall torque and good operating torque curve, it is a good choice for our application.



Figure 4-61: Lead Screw Motor

The table of specification for this motor is given below:

Voltage (Nominal)	12V
Voltage Range (Recommended)	6V - 18V
Speed (No Load)*	124 rpm
Current (No Load)*	0.10A
Current (Stall)*	3.8A
Torque (Stall)*	419.45 oz-in (30.20 kgf-cm)
Gear Ratio	78:1
Gear Material	Metal
Gearbox Style	Straight Cut Spur
Motor Type	DC
Output Shaft Diameter	4mm (0.1575")
Output Shaft Style	D-shaft
Output Shaft Support	Bushing
Electrical Connection	Male Spade Terminal
Operating Temperature	-10°C ~ +60°C
Mounting Screw Size	3mm
Product Weight	0.20lb (3.25oz)

#### 4.9.3 Motor Driver

The DRV8834 Stepper Motor Driver is used to control the stepper motor in our TEARS circuit. With maximum peak current as 2 amps per coil, and a maximum continuous current per coil of 1.5 amps, the A4988 will be able to safely direct current into our stepper motor rated at 0.85 amps. This is a low-voltage motor driver, capable of operating motors from 2.5-volts to 10-volts, we require a low-voltage motor driver due to our motor being rated at 5.3-volts. Additionally, it

provides safety features such as adjustable current limiting, overcurrent protection, and temperature protection.

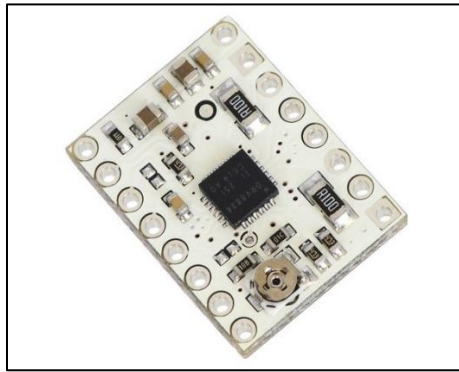


Figure 4-62: DRV8834 Stepper Motor Driver

#### 4.9.4 Communications Equipment

On the rocket will be a DC12V Relay Receiver Module, the receiver has ample relay switches to allow for remote control of TEARS. Off the rocket, we will use the RF Transmitter to connect to the receiver. The transmitter and receiver combo were chosen specifically for their ability to penetrate material and as such, signal penetration through the rocket shouldn't be an issue. We will be working at a frequency of 433MHz.



Figure 4-63: INSMA 4 Channel Transmitter and Receiver

#### 4.9.5 Power Requirements

Starting at the power supply, we use two 9-volt batteries. We determine this requirement from the following calculations. First, we look to the power requirements of the circuit. As we calculate the power requirements, we will use Watthours rather than mAh because a buck converter, which we will use in this circuit, exhausts power to generate a higher voltage. Here we have the power requirements of the motors.

$$(12V)(1.9A)(1.560\text{hrs})=0.57 \text{ Watthours}$$

$$(5.3V)(0.85A)(1.560\text{hrs})=0.112 \text{ Watthours}$$

Next, we consider the power requirements of the receiver.

$$(12V)(0.013A)(4\text{hrs})=0.624 \text{ Watthours}$$

Now we account for heat loss.

$$(12V)(1.9A)(360\text{hrs})=1.125 \text{ Watthours}$$

We then add this to get a total of 2.43Watthours. Next, we take 20% greater Watthours for uncertainty on of the 9-volt battery power supplies, which can vary. Lastly, from component consumption uncertainties, we take another 20% greater Watthours.

$$(1.2)(2.43\text{Watthours})=2.92 \text{ Watthours}$$

$$(1.2)(2.92\text{Watthours})=3.50 \text{ Watthours}$$

This will account for the circuit's total power requirements as other components are largely negligible in their power consumption. A Buck converter is used to change the supplied voltage from 9-volts to 12-volts, which is required by the receiver. Our buck converter's efficiency ranges from 80-95%. As such, we assume the worst efficiency as worst case. We look to a 9-volt batteries Watthours, which is about 4.5 Watthours, then multiply it by the efficiency of 80%.

$$(4.5\text{Watthours})(0.8)=3.6 \text{ Watthours}$$

The 3.50 Watthours requirement is too close to one 9-volt's Watthours for comfort. Thus, we use two 9-volt batteries.

## 4.10 DICU Electronics and Software Design

### 4.10.1 Software

For the DICU, we opted to have a software flowchart because it relies heavily on python programming. Below, we have the flowchart. The executable of the program is placed in the

`/etc/init.d"` folder of the Raspberry Pi such that upon system startup, the program will autorun. Initialization then occurs, libraries are imported, and variables are defined. We then check if a controller has been plugged in, if not then the program notifies no controller is plugged in and ends, if so then we continue. Two loops are then called to run concurrently.

On the right, we see the GUI loop for buttons, Tkinter is used for GUI. For buttons to work, Tkinter requires a call to its looping function which will continuously monitor whether the touchscreen has been touched and where it has been touched. If a button has been touched, then that button executes its associated command. The first button allows us to set the variable “done” equal to FALSE, the second button allows us to set it to TRUE, and the last button will send a series of pings to check connectivity with the rover.

On the left, we have rover control and GUI label data. Labels, as opposed to buttons, do not execute commands. First, we check if the variable “done” is equal to FALSE which it always is, then continue. Check if “transfer” is set to TRUE, if so then we continue, if not then keep checking until it is. The value of “transfer” is controlled by the other concurrent loop’s buttons, as mentioned above. Data is then imported from the rover and displayed on the GUI as a label. Next, we check if the controller has created an event, meaning has it changed any of its output values? If not then loop back to “`is 'done' == FALSE?`”, if so then continue. Check if the change is with the left joystick, if not then skip to the next if statement, if so, then map the coordinates from 0 to 255 on each motor and indicate whether reverse, forward, or stop. Display this information in a GUI label. On the next if statement we check if the controller’s hat, also known as arrow keys, has moved, if not then loop back to “`is 'done' == FALSE?`”, if so then format into (1) for scoop stepper motor forward or (2) for scoop stepper motor reverse. Send this to the rover and display the input as a GUI label.

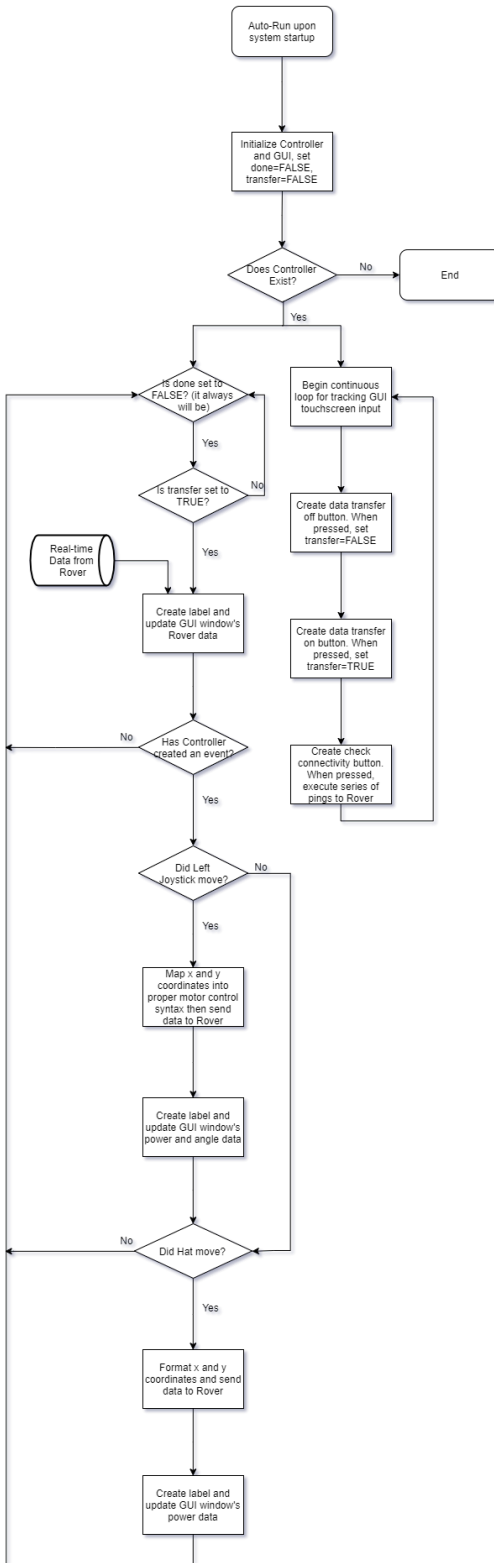


Figure 4-64: DICU Software Flowchart

#### 4.10.2 Electrical Schematic and Block Diagram

Below we have the circuit diagram for the DICU. It is powered by a 2200mAh Lithium Ion Battery at 5-volts. The TX and RX pins are connected to the XBee for communication.

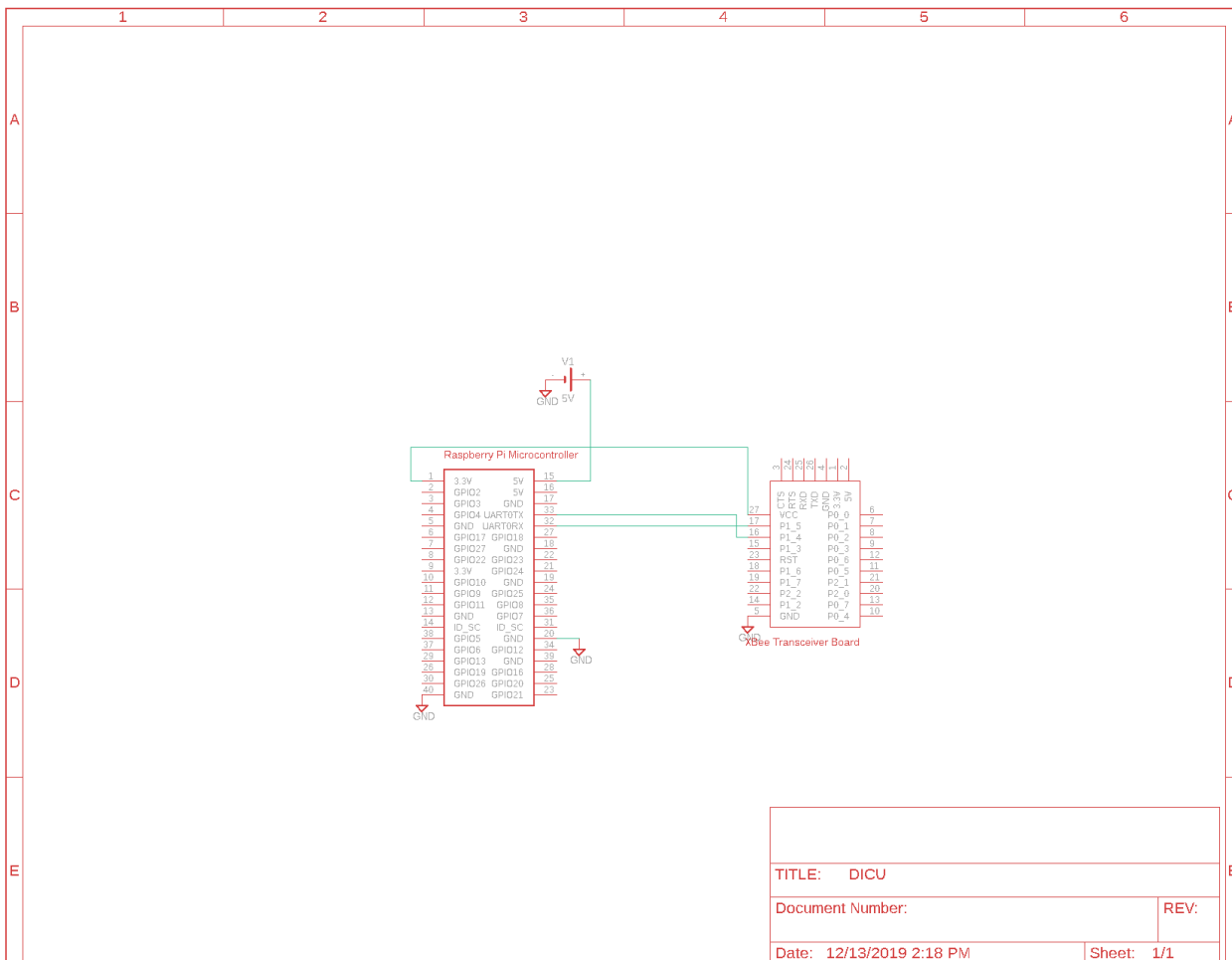


Figure 4-65: DICU Electrical Schematic

Here we have the block diagram for the DICU. A controller will be connected via USB into the Raspberry Pi. A Micro SD card will be used to store data. An LCD Touch Screen is connected via HDMI to display the GUI. As mentioned above, the Raspberry Pi is powered by a 22mAH Lithium Ion Battery at 5-volts and connected to the XBee. It will receive data from the rover's XBee as well as transmit data to the rover's XBee.

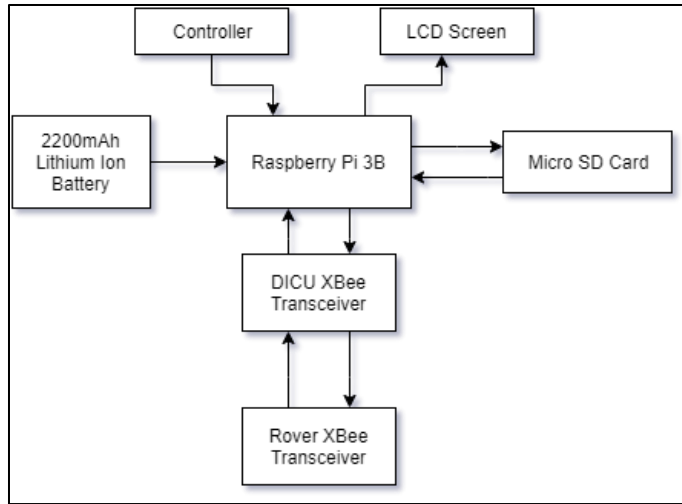


Figure 4-66: DICU Block Diagram



Figure 4-67: 7-inch DICU Display

#### 4.10.3 Microcontroller

A Raspberry Pi 3B is used on the DICU specifically because it is such a powerful microcontroller. The DICU will need to perform all calculations for the rover, due to the Arduino Nano being unable to match the computing power necessary for much of our calculations. Additionally, the DICU will be putting a GUI onto a 7-inch display. Arduino GUI's are not very clean, and Arduino's are not as powerful as Raspberry Pi's so displaying a clean GUI might be too hard a task. For the DICU, as mentioned earlier, battery requirements are no issue, thus the Raspberry Pi 3 B was chosen.



Figure 4-68: Raspberry Pi 3 B

#### 4.10.4 Communications Equipment

The DICU will host one XBee Series 2 with an RF output power of 2mW. Outdoor line of sight is up to 120 meters, more than ample to control the payload. The RF data rate is 250kbps which is an ample amount to deliver all data required for us. This device works on a frequency of 2.4Ghz. DSSS is used where the direct-sequence modulation makes the signal wider in bandwidth than the informational bandwidth, this primarily functions to reduce signal interference.



Figure 4-69: XBee Series 2

#### 4.10.5 Power Requirements

The Raspberry Pi will be supplied power via a 5-volt 2200mAh power supply. We assume 1 hour, the Raspberry Pi 3 B with display and XBee draws 1000mAh at 5-volts thus 1000mAh is required. We more than double this requirement simply because the size and weight are not significant factors since the DICU will not be on the rocket. The calculation is shown below:

$$(1\text{hr})(1000\text{mA})=1000\text{mAh}$$

Thus, with 2200mAh, we should be able to run the DICU for 2.2 hours:

$$(2200\text{mAh})/(1000\text{mA})=2.2 \text{ hours}$$



Figure 4-70: 2200mAh 5-volt Battery Pack

## 4.11 Payload Mass Total

The total component level mass estimate is shown in Table 4-1

Table 4 - I: Payload Mass Total

Part	Qty	Unit Mass (oz)	Total Mass (oz)	Total Mass (lb)
Bulkhead to Coupler Threaded Rod	3	0.076	0.229	0.0143
Bulkhead L bracket	4	1.313	5.251	0.3282
Bulkhead	1	10.221	10.221	0.6388
Lower Aluminum Support	1	3.909	3.909	0.2443
Connecting Rod (L)	1	1.682	1.682	0.1051
Reorientation Hub Gear	1	1.100	1.100	0.0688
Middle Aluminum Support (MAS)	1	2.182	2.182	0.1364
Reorientation Hub Gear screws (steel)	4	0.036	0.144	0.0090
Reorientation Needler Thrust Bearing	2	0.337	0.674	0.0421
Reorientation Thrust bearing washer	4	0.237	0.948	0.0593
Reorientation Ball Bearing	1	0.685	0.685	0.0428
Upper Reorientation Support	1	0.855	0.855	0.0535
Connecting Rod Shaft Collar (steel)	2	1.397	2.794	0.1746
Connecting Rod Shaft Collar Screw	2	0.071	0.142	0.0089
Reorientation Plate	1	9.043	9.043	0.2826
Reorientation Stepper Motor	1	12.350	12.350	0.7719
Reorientation Stepper Motor Screw	4	0.021	0.084	0.0053
Reorientation Motor Shaft Coupler	1	0.178	0.178	0.0111
Shaft Coupler Screws	2	0.039	0.078	0.0049
Reorientation Pinion Gear	1	0.800	0.800	0.0500
Reorientation Pinion Gear set screw	1	0.009	0.009	0.0006
TEARS long distance RF receiver	1	2.000	2.000	0.1250
Stepper Motor Driver	1	0.053	0.053	0.0033

555 Timer	2	0.067	0.134	0.0084
Diodes	3	0.020	0.060	0.0038
DPDT Relay	4	0.170	0.680	0.0425
Step up Voltage Regulator	3	0.265	0.794	0.0496
TEARS 9v battery	2	1.587	3.175	0.1984
Limit Switch	1	0.133	0.133	0.0083
DC to DC buck converter (?)	1	0.260	0.260	0.0163
Protoboard	1	0.260	0.260	0.0163
LS Motor	1	3.225	3.225	0.2016
LS Motor Clamping Hub	1	0.450	0.450	0.0281
LS Motor Clamping Hub Screw	4	0.050	0.200	0.0125
LS Motor Clamping Hub Collar Screw	1	0.046	0.046	0.0029
LS Motor Pinion Gear	1	0.250	0.250	0.0156
LS Motor Pinion Gear set screw	1	0.009	0.009	0.0006
Lead Screw 8 mm	1	7.800	7.800	0.4875
LS Clamping Collar	2	0.170	0.340	0.0213
LS Clamping Collar Screw	2	0.032	0.065	0.0040
LS Thrust Bearings	3	0.405	1.215	0.0759
LS Flanged Ball Bearing	2	0.060	0.119	0.0074
LS Aluminum Standoffs	4	0.055	0.220	0.0138
LS Aluminum Standoff Screws	8	0.043	0.344	0.0215
LS Aluminum Pattern Bracket	1	0.200	0.200	0.0125
LS Hub Gear	1	0.550	0.550	0.0344
LS Hub Gear Barrel Clamping Hub	1	0.560	0.560	0.0350
LS Hub Gear Barrel Clamping Hub Screw	4	0.046	0.184	0.0115
8 mm LS Nut	2	0.900	1.800	0.1125
LS Nut mounting screw	8	0.042	0.336	0.0210
Support Collar	1	2.656	2.656	0.1660
Rear Retention Plate	1	9.928	9.928	0.6205
Rover Chassis front and rear plates	2	1.332	2.663	0.1664
Rover chassis side and bottom plates	1	4.123	4.123	0.2577
Tread Sprockets	4	1.320	5.280	0.3300
Tread Links	110	0.044	4.840	0.3025
Rover Scoop (ABS)	1	0.231	0.231	0.0144
Sample Collection Unit (SCU) side wall (ABS)	2	0.102	0.204	0.0128
SCU Container (ABS)	1	0.235	0.235	0.0147
SCU Container and side wall mount	2	0.050	0.100	0.0063
SCU Mount screw	8	0.050	0.400	0.0250
SCU scoop motor	1	2.110	2.110	0.1319
SCU scoop motor screws	4	0.003	0.014	0.0009
Rover Drive Motors	2	3.250	6.500	0.4063

Rover Drive Motor Mounting Screw	4	0.020	0.080	0.0050
Drive Motor set screw shaft collar	2	0.091	0.182	0.0114
Rover Bogey Sprocket Axle set collar	4	0.116	0.466	0.0291
Rover Bogey Sprocket Axle	2	0.700	1.400	0.0875
Bogey Sprocket Flanged bearing	4	0.028	0.112	0.0070
LiPO Battery	1	6.702	6.702	0.4189
9V battery	1	1.587	1.587	0.0992
Arduino Nano	1	1.600	1.600	0.1000
Xbee Module	1	0.640	0.640	0.0400
Xbee Adapter	1	0.320	0.320	0.0200
Featherwing Motor Controller	1	0.160	0.160	0.0100
Relay for rover	4	0.170	0.680	0.0425
Protoboard	1	0.260	0.260	0.0163
Front Retention Plate	1	5.474	5.474	0.3422
Rover Retention Blocks	4	0.779	3.116	0.1947
Nose Cone Threaded Rod	1	0.077	0.077	0.0048
Lead Screw Nose Cone End Support Assembly	1	1.361	1.361	0.0851
End Support Assembly Flanged Bearing	2	0.060	0.119	0.0074
Centering Ring Extension	1	1.100	1.100	0.0688
<b>Total</b>				8.6687

## 5 Safety

### 5.1 Pre – Field Subsystem Preparation

This section describes the pre-field procedures and checklists necessary to complete a safe and effective mission. Each team, Navigation and Recovery (NAR), Structures, Aerospace and Propulsion (SAP), and Payload (PAY) section includes a list of required personnel and equipment, instructions on how to assemble each sub-system within their system, and procedures on how to safely pack their complete system for transport.

### 5.2 Master Material Checklist

Each team has a required materials checklist as well as procedures to ensure all components are in good condition and are packed safely for travel.

#### 5.2.1 Structure, Aerodynamics, and Propulsion

##### Materials

- Nose cone
- Payload bay
- Avionics bay

- VDS cannister
- VDS Battery
- Propulsion bay
- Motor retainer
- Couplers
- AeroTech L1420RP motor
- Grease
- Flange screws
- Epoxy sealer
- Launch pad
- Rail
- E-matches

### **Packing inspection**

- Inspect fins for chipping or damage
- Inspect epoxy fillets for cracking
- Inspect bays and couplers for cracking, delamination, and zippering
- Inspect nose cone for deformation or chipping
- Inspect motor retainer for damage or bending
- Ensure all bays fit together securely
- Ensure there are no shear pins left inside the frame
- Keep igniters/starters, BP & motor reloads in separate, anti-static & approved metal magazines.
- Keep reloads sealed in their original packaging to avoid losing parts and exposing propellant to the elements.
- Make sure all battery leads & contacts are covered.
- Store all electronics in cushioned anti-static packaging until ready to use.
- Clearly mark with industry-standard placarding all packages containing flammable or hazardous material so it can be quickly identified in an emergency.
- Ensure that all boxes & shipping containers are restrained during transportation to & from the launch site.
  - Any excessive room between coupler and body tube can lead to instability and vibration while too tight of a fit can lead to failure to eject during recovery.
  - Motor will only be handled by NAR/TRA certified members in order to comply with the safety regulation.
  - Improper storage of black powder, motors, and starters can lead to contamination or even premature ignition.
  - Failure to properly store electronics can cause shorts, sparks and accidental discharges during storage & transportation.
  - Failure to properly restrain boxes and containers while being transported can lead to damaged materials as well as dangerous situations in the event of an accident.

### **Ensure all batteries are charged**

- a) VDS Battery
- b) Telemetry Sled Battery
- c) Avionics Battery
- d) Rover Battery
- e) TEARS Battery

### **5.2.2                  Navigation and Recovery**

#### **Materials**

- Avionic Tube
- Avionic Sled
- End Plates
- Retention Bulk plates
- Recovery Harness Mounts
- Hex Nuts
- Threaded Rods
- Washers
- Main Parachute
- Drogue Parachute
- Shock Cords
- Quicklinks
- Charge Wells
- Pistons
- Electric Matches
- Altimeters
- GPS Transmitter/Receiver
- Batteries
- Black Powder
- Wiring
- Avionics Bay Arming Switch
- Aluminum Foil
- Shear Pins
- Zip Ties
- Packing Hook

#### **Packing inspection**

- Ensure all hex nuts are tightened and all threaded rods are secure.
- Inspect threaded rods for chipping.
- Inspect avionic sled for damages such as bending or damage due to the threaded rods.
- Check the end plates and avionic tube for bending or other damages.
- Inspect the shock cords and parachutes for tearing.

- Inspect electronics for damages and ensure they are operational.
- Ensure all batteries are charged.

### **5.2.3 Payload**

#### **Materials**

- Lead Screw
- Bulkhead Assembly
- Reorientation plate assembly
- Lead Screw Support assembly
- Retention Plate and mounts
- Rover
- Remote Control
- Batteries (and charging components)

#### **Packing inspection**

- Inspect lead screw for bending or damage.
- Inspect Bulkhead and reorientation plate for bending or damage.
- Ensure all nuts, screws and bolts are tightened.
- Inspect retention system for chips, bending or damage
- Inspect that the rover drivetrain is attached and that the chain is in good condition.
- Inspect the sample collector and collection bay for chips or damage and that the sample collection scoop is housed internally so it is not damaged during travel.
- Inspect the chassis for damage.
- Check the remote control and electronics for functionality.
- Ensure all batteries are charged

### **5.2.4 Miscellaneous.**

- Nitrile gloves
- Precision flathead screw driver
- Garbage bags
- Safety glasses
- Respirators
- Fire extinguisher
- First aid kit
- All necessary spare batteries and chargers.

#### **1. Pre-Flight Safety Inspection checklists**

This section describes the pre-flight procedures and checklists necessary to complete a safe and effective mission. All procedures to completely assemble each system, inspect the assembled

rocket, and possible troubleshooting will be included. A post launch safety inspection will be done prior to starting the ground mission and deployment of the payload.

## **2.1 Navigation and Recovery Pre-Flight Checklist**

### **List of required personnel and equipment**

*Required Personnel* - Team lead, Team Captain, Safety Officer, NAR team.

*Required Equipment* -

- i. Drogue Parachute
- ii. Main Parachute
- iii. Packing Hook
- iv. Altimeters
- v. GPS Transmitter/Receiver
- vi. Arming Switch
- vii. Allen Key or screwdriver
- viii. Zip Ties
- ix. 9V Batteries
- x. LiPo Battery
- xi. Voltmeter
- xii. Nylon screws

*Required PPE* - Safety Glasses

### **NAR Checklist,**

#### **Parachute System,**

- a) Fold the parachute properly. Ensure the steps in the parachute manual are closely followed.
- b) Ensure the shroud lines are stored properly and no lines are wrapped around the parachute.
- c) Ensure the parachute is properly stored in the parachute deployment compartment. If necessary, use the packing hook to ensure the parachute is tightly folded.
- d) Repeat step 2 a) to c) if necessary until smooth ejection and deployment of the parachute can be ensured.
- e) Properly stow the parachute bags for safe transport to the launch site.

**Avionics Bay,**

- a) Ensure the altimeters, mechanical arming switch, and 9V batteries are secure and that all zip ties used in their security are tightened.
- b) Ensure that the nylon screws securing the altimeters are tightened.
- c) Ensure there are no loose wiring connections.
- d) Check that the batteries are charged with a voltmeter.
- e) Test the altimeters by turning the arming switch into the ON position, waiting for the arming sequence sound, and turning the switch into the OFF position.
- f) Check to make sure the aluminum foil wrapped around the inside of the avionic tube will protect the altimeters from false trigger due to RF signals.
- g) Ensure the avionics bay is sealed and all nuts are tightened.
- h) Make sure all shear pins are tightened and securely in place.

**Telemetry Bay,**

- a) Ensure zip ties and nylon screws securing the electronics are tightened.
- b) Plug the LiPo battery into the GPS transmitter
- c) Turn on the receiver and hold the configuration button to lock in the base altitude of the transmitter.
- d) Make sure the GPS transmitter is sending data packets to the receiver by reading the coordinates and verifying them using a locational program such as Google Earth or MotionX. Be sure to keep this program available for use when the rocket is to be located.
- e) Ensure all hex nuts are tightened and bulkheads are secure.

Signature      of      Safety      Officer,      Team      Lead,      NAR      team,

---

## **2.2 Structures, Aerodynamics, and Propulsion Pre-Flight Checklist**

### **List of required personnel and equipment**

Required Personnel - NAR/TAR certified mentor, Team lead, Team Captain, Safety Officer, SAP team.

*Required Equipment -*

- i. Nose cone

- ii-Payload bay
- iii-Avionics bay
- iv-VDS cannister
- v-Propulsion bay

*Required PPE - Safety Glasses*

### **Body Assembly**

- i. Inspect fins for chipping or damage
- ii. Inspect fins for chipping or damage
- iii. Inspect epoxy fillets for cracking
- iv. Inspect bays and couplers for cracking, delamination, and zippering
- v. Inspect nose cone for deformation or chipping
- vi. Inspect motor retainer for damage or bending
- vii. Inspect all shear pin holes and threads for damage
- viii. Inspect all electronic sleds for damage or shorts
- ix. Inspect 3.7V and 7.4V batteries are charged and capable of outputting full power
- x. Inspect for loose, disconnected, or damaged wires
- xi. Inspect, upload, and test the diagnostic code for Teensy 4.0, 9DoF, BMP280 and HS-5585MH
- xii. Inspect, reupload, and test flight code
- xiii. VDS MECHANICAL

### **Motor Assembly**

- a)- Safety officer verifies that the proper PPE is worn by all team members.  
Motor preparation must be handled by NAR/TRA certified members to comply with the safety regulation. Failure to comply with the safety requirement might result in catastrophic vehicle and or personal damage.
- b)- Use the epoxy putty to seal all surfaces and O-rings.
- c)- Epoxy the two grains. Align the cores. Slide liner over epoxied grains
- d)- Install nozzle into the real end of the liner and stand assembly on nozzle. Ensure nozzle rear is seated on the liner.
- e)- Place seal disk o-ring into the groove in the forward seal disk. Install the seal disk into the open end of the motor liner until seated and flush.
- f)- Slide the motor casing over the motor lining.
- g)- Seal the o-ring against the forward case end until it mates with the forward seal disk.
- h)- Thread the forward closure assembly into the forward end of the motor case by hand until it is seated against the case.

Signature of Safety Officer, Team Lead, SAP team, NAR/TAR certified mentor

---

### **2.2.1 Launch Pad Pre-Flight Checklist**

- i. Clear area of all flammable material
- ii. Ensure the ground is firm and level before setting up launch pad
- iii. Set up launch pad with rail at least 1500ft away from any occupied building and 300ft from any personnel
- iv. Ensure there is no more than 20° of tilt to the launch pad as unstable take off could negatively impact flight
- v. Have predesignated team members carefully carry the launch vehicle to the launch pad
- vi. Carefully slide launch vehicle onto rail, ensuring co-linearity
- vii. Make sure the vehicle can slide freely along the entire length of the rail.
- viii. Set launch vehicle upright with rail, ensuring that it is not applying any force to the fins
- ix. Turn the avionics bay arming switch into the ON position with a screwdriver or Allen key and ensure the altimeters are on by waiting for the arming sequence sound.

NOTICE- Failure to remove flammable material can lead to injury and potential property damage.

NOTICE- Improper handling of launch vehicle can lead to dropping which could result in damage to the vehicle as well as injury to personnel handling said vehicle.

NOTICE- If vehicle is not co-linear or is obstructed from moving along the rail, rail exit failure may occur which could lead to severe damage to the vehicle and injury to all bystanders.

Signature of Safety Officer, Team Lead, SAP team, NAR/TAR certified mentor

---

### **2.3 Payload Pre-Flight Checklist**

#### **List of required personnel and equipment**

*Required Personnel - Team lead, Team Captain, Safety Officer, PAY team.*

*Required Equipment -*

- i. TEARS
- ii. Rover
- iii. Electronic remote controller,
- iv. Batteries

*Required PPE - Safety Glasses*

**TEARS system,**

- a)- Inspect TEARS to ensure the lead screw has not bent or been damaged.
- b)- Test TEARS to ensure functionality by rotating lead screw and rotating reorientation plate remotely using the remote control.
- c)- Ensure retention mounts and mounting system are installed correctly by inserting the rover into TEARS and inspecting immobilization of the rover in the axial and radial directions.
- d) Ensure that the retention mounts are securely fastened to the retention plate.
- e)- Re-tighten any necessary screws, nuts or bolts.
- f)- Ensure all batteries are fully charged.

Signature      of      Safety      Officer,      Team      Lead,      PAY      team,

---

**Rover System,**

- a)- Inspect that the rover's belt and drivetrain are assembled correctly and verify functionality using the remote control.
- b)- Test the sample collection system using the remote control to ensure functionality.
- c)- Test the powering on when sensing light capabilities of the rover. Put the rover in the dark and ensure the rover is able to power on autonomously when sensing light.
- d)- Test all remote data acquisition such as battery levels, distance traveled, etc.
- e)- Re-tighten any necessary screws, nuts or bolts.
- f)- Re-charge all batteries after testing is completed.

Signature      of      Safety      Officer,      Team      Lead,      PAY      team,

---

## **2.4 Inspection of Assembled rocket**

- a)- Inspect air frame for any holes, chips, scratches or damage.
- b)- Inspect fins for any holes, chips, scratches or damage.
- c)- Inspect nose cone for any chips, scratches or damage.
- d)- Inspect rail for any bending, damage, or obstructions.
- e)-Inspect launch pad and surrounding area for any potential hazards or obstructions.
- f)-Ensure all team members and spectators are a safe distance (300ft) from the launch area.

Signature of Safety Officer, Team Lead, NAR/TAR certified mentor

---

## **2.5 Igniter Installation and Disarm Procedures**

*Required Personnel-* NAR/TAR certified mentor, Safety Officer

*Required Materials-* Vehicle, Igniter, Launch Pad

*Required PPE-* safety glasses

- i. Ensure launch area is clear of personnel
- ii. Insert igniter all the way into the motor cap
- iii. Move required distance away from launch area

NOTICE- Igniters should be kept away from all batteries, sparks, and open flames to prevent accidental firing.

NOTICE- If motor fails to ignite go to troubleshooting section.

Signature of Safety Officer, Team Lead, NAR/TAR certified mentor

---

## **2.6 Post launch safety inspection**

- i. Inspect fins for cracking or chipping
- ii. Inspect body tube for cracking, zippering, or delamination
- iii. Inspect nosecone for damage
- iv. Inspect motor retainer and centering rings for deformation
- v. Inspect epoxy fillets for cracking or flaking
- vi. Inspect electrical sleds for damage
- vii. Inspect couplers and shear pin holes for damage
- viii. Inspect all threaded rods, lead screws, and bolts for thread damage
- ix. Inspect shock cords and parachutes for tearing and deformation

- x. Inspect end plates, parachute ejection pistons, shock cords, shock cord mounts, charge wells, and parachutes for corrosion due to black powder charges
- xi. Inspect electronics for damages
- xii. Ensure unused black powder charges are removed carefully by the NAR mentor using the applicable PPE.

Signature of Safety Officer, Team Lead, NAR/TAR certified mentor

---

## 2.7 Troubleshooting

Potential Launch/Assembly Issue	Potential Solution
Unable to have positive control of the electronic remote switches	Return launch vehicle to preparation area. Off load each section and ensure all the circuit is connected correctly. Verify that the battery is in good working condition. Remount the launch vehicle and try again according to all relevant safety checklists and procedures.
Folded parachute appears to have discrepancy due to improperly folding. This causes main or drogue parachute to be unable to properly fit in the bay.	Unfold the parachute by repeating the recovery preparation step 2. Verify the newly folded parachute can be ejective freely.
L type motor installed incorrectly.	Reassemble the motor again using instructions from kit with help from NAR certified mentor according to all relevant safety checklists and procedures.
Launch Vehicle lands more than 2500 ft radius from launch pad in personal property	Inform NASA RSO and wait for instructions on how to retrieve vehicle.
Motor fails to ignite	DO NOT approach rocket if igniter fails for at least 60 seconds. Hang fire could lead to severe injury to personnel that approach prematurely. Contact safety officer. While wearing safety glasses, attempt to visually determine the cause of misfire. If only a minor connection issue, reattach to motor cap. If unable to visibly determine cause of error, remove igniter from motor making sure not to have hands directly under the rocket nor the rocket tail pointed at any handlers. Install backup igniter and reset rocket.
Altimeter failure to arm	Disarm all active charges. Remove rocket from rail and bring back to assembly table. Check for faulty battery. If not battery remove faulty ejection charge and replace with backup ejection charge and e-match using ejection charge assembly procedure. NOTICE- when dealing with BP make sure to wear safety glasses and nitrile gloves, and ensure those dealing with it are grounded. Premature ignition of ejection charges can lead to serious bodily harm as well as damage to equipment.

GPS fails to turn on or read coordinates.	Remove GPS transmitter from rocket and check for faulty battery. If battery is not faulty, turn the transmitter and receiver off and on again. Hold the configuration button on the receiver to re-lock altitude and wait for coordinates to be obtained again up to about 15 minutes. If this does not work, plug the receiver into a computer and follow the GPS instruction manual to set up alternative ground station using a computer.

Table : Troubleshooting

## 2. Hazard Analysis

Potential hazards can cause serious injury, death and mission failure. These hazards are mitigated using the Risk Assessment code (RAC) created by Industrial Safety Bastion Technologies. The definitions are shown in the tables below and are helpful in effectively mitigating potential hazards.

Probability	Severity			
	1 Catastrophic	2 Critical	3 Marginal	4 Negligible
A- Frequent	1A	2A	3A	4A
B- Probable	1B	2B	3B	4B
C- Occasional	1C	2C	3C	4C
D- Remote	1D	2D	3D	4D
E- Improbable	1E	2E	3E	4E

Table : Risk Assessment Code (RAC)



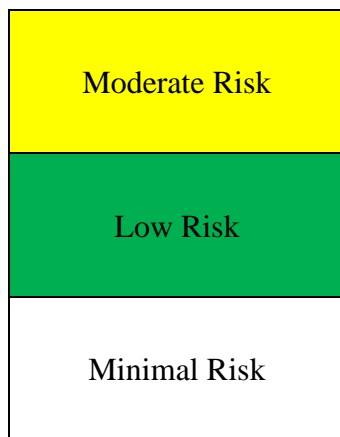


Table : Risk Level Color Code Scheme

Description	Personal Safety and Health	Facility/Equipment	Environmental
<b>1-Catastrophic</b>	Loss of life or a permanent disabling injury	Loss of facility, systems of associated hardware.	Irreversible severe environmental damage that violates law and regulation.
<b>2-Critical</b>	Severe injury of occupational related illness.	Major damage to facilities, systems, or equipment.	Reversible environmental damage causing a violation of law or regulation.
<b>3-Marginal</b>	Minor injury or occupational related illness.	Minor damage to facilities, systems, or equipment.	Mitigable environmental damage without violation of law or regulation where restoration activities can be accomplished.
<b>4-Negligible</b>	First aid injury or related occupational related illness.	Minimal damage to facilities, systems, or equipment.	Minimal environmental damage not violating law or regulation.

Table : Definitions of Severity

### **3.1 Personal Protective Equipment (PPE)**

Required personal protective equipment has been defined in the tables below. All team members must follow the guides below as well as read relevant MSDS before working with hazardous materials, chemicals, or using heavy machinery and power tools. Warnings will be issued for non-compliance that will lead to termination if repeated.

<b>Task: Working with Hazardous Chemicals or Materials</b>		
<b>Potential Hazard</b>	<b>PPE Required</b>	<b>Risk Mitigation</b>
<b>Eye Irritation/Damage</b>	<b>Safety Goggles</b>	Read and understand the MSDS. Wear goggles to prevent contact between chemical particulate and eyes. Wear disposable gloves to lessen the chances of one attempting to touch their eyes while working, as one may otherwise be required to use an eye wash station.
<b>Respiratory Infection/Damage</b>	<b>Facemask/Respirator</b>	Read and understand the MSDS. Wear some sort of face apparatus that will lessen the risk of fibers or particulate from entering bodily airways, as inhalation of such can cause infections and/or permanent damage to the respiratory system. Use of epoxy or sanding/cutting of fiberglass, for example, should only be done in a well-ventilated area, in addition to already utilizing the required PPE.
		Read and understand the MSDS. Prevent prolonged contact with chemicals such as epoxy. Use soap and hot water to immediately wash the areas

<b>Skin Irritation/Damage</b>	<b>Gloves</b>	that have been in contact with such chemicals. Gloves must be used whenever there is a threat of skin irritation from a chemical or material, as would be noted on the MSDS.
-------------------------------	---------------	--

Table : PPE Required for Hazardous Chemicals and Materials

<b>Task: Using Power Tools or Heavy Machinery</b>		
<b>Potential Hazard</b>	<b>PPE Required</b>	<b>Risk Mitigation</b>
<b>Eye Irritation/Damage</b>	<b>Safety Goggles</b>	Use goggles to prevent machining chips from making contact with the eyes. Do not work alone when handling heavy machinery or power tools. Only qualified personnel may operate certain heavy machinery in the machine shop.
<b>Respiratory Infection/Damage</b>	<b>Facemask/Respirator</b>	For general safety practice when using power tools, wear a respirator to avoid inhalation (and possible subsequent respiratory damage) of dangerous materials.
<b>Bodily Injury</b>	<b>Proper Attire</b>	Wear short sleeve shirts with no loose jewelry or hair to prevent the tool from catching on loose clothes/items. For the same reason of catching, do not wear gloves. Do not work alone when handling either the power tools or heavy machinery

Table : PPE for using Power Tools and Heavy Machinery

<b>Task: Handling Black Powder</b>		
<b>Potential Hazard</b>	<b>PPE Required</b>	<b>Risk Mitigation</b>

<b>Eye Irritation/Damage</b>	<b>Safety Goggles</b>	Wear PPE properly prior to work. Only NAR/ TRA certified mentor will handle the black powder.
<b>Respiratory Infection/Damage</b>	<b>Facemask/Respirator</b>	Wear PPE properly prior to work. Only NAR/ TRA certified mentor will handle the black powder.
<b>Bodily Injury</b>	<b>Gloves, Safety Goggles, Inflammable Cloth</b>	Wear PPE properly prior to work. Only NAR/ TRA certified mentor will be in charge of handling and storing the black powder. Ensure that the black powder is isolated from any source of ignition.

Table :PPE for Handling Black Powder

### 3.2 Personnel Hazard Analysis and Mitigation

<b>Personnel Hazard</b>	<b>Causes</b>	<b>Effects</b>	<b>Pre RA C</b>	<b>Mitigation</b>	<b>Verification Plan</b>	<b>Post RA C</b>
Unignited ejection charges ignites pre-assembly.	Improper storage or handling of black powder such as overheating, vulnerability to static, vibration, or exposure to flame.	Potential explosion or fire. Injury or death to team members or nearby spectators.	1A	Black Powder will be stored in non-static / non-flammable containers away from any potential heat sources and will be kept with the NAR certified mentors at all times.	Only NAR certified members will be allowed to handle all black powder. All team members will still be required to read all black powder related MSDS and safety procedures.	1E
Unignited ejection charges after recovery.	Ejection charges don't fully ignite at programmed altitudes, leaving partially unignited black powder	Charges might ignite unexpectedly during the recovery process of the vehicle, causing serious injury or death to team members	1B	The NAR/TRA certified mentor will inspect the launched vehicle prior to the recovery process by the NAR team members. If unignited black powder are found, the launched vehicle will be removed from the field and transported, with caution, to designated area off the field where the	Launch Operations procedure provides detailed instruction on how to recover vehicle which includes inspection of unignited ejection charges.	1E

				leftover charges will be properly removed and disposed from the vehicle. To ensure the safety of the all personnel, the switches will be turned off during the inspection.		
Team members are injured while working in Stony Brook machine shops.	Team members do not follow machine shop safety rules, do not comply with relevant MSDS, or wear appropriate PPE.	Team members are physically injured by mills, lathes, drills, CNC, etc. Serious injury or death may occur from high powered machinery.	1B	All team members will sign the safety agreements which includes the Stony-Brook machine shop safety rules that they must abide by. Also all team members working in shop must take and pass a semester long machine shop class, MEC 225.	All team members will sign the safety agreements and pass MEC 225, a semester long machine shop class before they are allowed to fabricate. Any violations of machine shop rules will immediately result in ejection of the person from this project	1E
Team members inhale epoxy fumes, while gluing together parts or inhale fibers of hazardous materials such as fiberglass.	Failure to wear proper PPE, like face mask, and gloves and failing to properly use chemical per MSDS. Not working in a ventilated area.	Epoxy fumes can cause skin irritation, oral toxicity, allergic reaction, nausea, headaches, etc. Fiberglass fibers can cause respiratory infection or permanent damage.	1A	Team members will be required to sign the safety agreement which mandates proper PPE (fumes protective face mask) is worn at all times during working with epoxy.	Team member violation in particulate or chemical PPE will be given a warning and repeated violation will result in termination from the project. Team members will work in ventilated work environments.	1D
Team members get injured while using hand held power tools outside of Stony Brook machine shop like drills, electric hacksaws, etc.	Team members do not follow safety agreement rules like not having an assistant while using hand held power tools drills. Not wearing protective gear like safety glasses, gloves, masks and proper clothing	Team members physically injured by drills. These are high powered machinery that can cause serious injury or death.	1A	All team members will sign the safety agreements which includes hand held power tools safety rules that they must abide by.	All team members will sign the safety agreements. Any violations of safety agreement will result in warning and repeated offence will result in termination from team.	1D
Team members get shocked while working with electronics components.	Working with electronics component while being wet, improper short circuiting, etc. can lead to team members getting shocked even	Low voltage shocks can result in serious electric burns and trauma, while high voltage shocks can lead to serious injury and death.	1A	All members must take a semester long practical electronics course, MEC 220 before they are allowed to work with electronics. In addition, the safety agreement which details proper handling of	Any violation of MEC 220 or safety agreement rules will result in warning and repeated offence will result in immediate termination from project.	1E

	while working with low voltages.			electronic equipment must be signed by all team members. In addition, all power must be switched off before modification of any circuitry.		
Battery explosion at high temperature causes injury to team members and nearby spectators.	Not inspecting alkaline batteries for damage, leaks, or proper voltage output before installation	Battery explosion will destroy the bay it is housed, vehicle airframe and the broken pieces of ABS and blue tube will be projectiles causing serious injuries to nearby members and spectators. Also alkaline batteries contain potassium hydroxide that may cause skin burns.	2B	Batteries will be tested for damage, leaks and voltage output each time it is installed in electronics circuit during ground testing and test flights	Safety officer will check batteries properly with approved voltmeters and purchase new batteries if the battery output is under 9V.	2D
Main parachute fails to deploy.	Improper installation of the parachute, discrepancies such as tangled lines, cut, burn in the parachute shroud lines and canopy.	The rocket will free fall and crash land, potentially causing serious injury or death to the team or spectators as well as catastrophic damage to the rocket.	1B	Ensure the proper folding and installation of the parachutes for both the main and the drogue parachutes. Properly verify that the parachutes are free from discrepancies.	Safety Officers and the NAR team will verify the status of the parachute prior to the launch and before leaving for the launch site. The verification process will strictly follow the recovery preparation checklist.	1E
Rocket dropped (inert)	Improper handling of rocket while being transported	Structural integrity may be compromised and/or internal framework and components may be damaged. Additionally, personnel may be injured if around the site of the accident	2C	Taking care when transporting the rocket as well as designing the rocket to withstand a certain degree of impulse when hitting the ground will greatly reduce potential issues.	Supports as well as close supervision when dealing with the assembly of the rocket will be utilized and only certain predetermined team members will be in charge of carrying large and or heavy components	2E
Rocket dropped (live)	Improper handling of rocket while being transported	Similar damage may be incurred with the added danger that a powder explosion may occur which would could significantly injure someone as well as damage the internal equipment.	1C	Taking care when transporting the rocket as well as designing the rocket to withstand a certain degree of impulse when hitting the ground will greatly reduce potential issues.	A minimum of three predetermined team members are required to move the live rocket to the stand.	1E

### 3.3. Failure Modes and Effects Analysis

#### Structures, Aerodynamics and Propulsion (SAP) FMEA

Failure Mode	Causes	Effects	Pre RA C	Mitigation	Verification Plan	Post RA C
Drag system does not function properly during launch.	Drag system could be inaccurately adjusting roll, or fins may not be turning synchronously	The vehicle's flight trajectory will be altered, and apogee may not be reached.	2A	Extensive testing of the launch vehicle avionics along with the VDS to ensure that the system functions as expected.	The drag system will only be used if there is a high success rate during full-scale testing.	2D
Drag system does not deploy properly during launch.	Malfunctions could occur in the electronical system or software programming	The vehicle will overshoot the target apogee and flight trajectory might be altered.	3A	Extensive testing of the launch vehicle avionics along with the VDS to ensure that the system deploys as expected	The drag system will only be deployed if there is a high success rate during full scale testing.	3D
Motor mount fails to keep motor in place.	The motor could push upwards into the body of the rocket and damage internal components located above the moto	Upward thrust vector is off centered, trajectory path is compromise, apogee may not be reached, catastrophic failure possible.	1D	The motor mount is tested before flight to ensure it can withstand the forces during flight. It will also be inspected during assembly to determine whether it was installed correctly	An assembly checklist will be followed, and full-scale testing will verify this.	1E
Fins fracture during flight due to normal in-flight forces.	Fins are sheared off due to incorrect epoxy choice or method of installation.	The vehicle trajectory will be drastically altered and become unstable	2D	Fin fillets and adhesive attachment points are inspected for fractures before and after flight.	Simulations will verify the structural integrity of the fins before testing. Assembly checklist will include inspecting the fins.	2E
Airframe fails during launch and in-flight.	The forces during flight exceed those that can be handled by the airframe material.	The launch vehicle breaks apart during flight resulting in catastrophic failure.	1D	The vehicle will be designed with the appropriate materials to handle the stress in-flight.	Simulations along with full-scale test flights will verify that the airframe can withstand launch and flight forces.	1E
Airframe buckles at landing due to impact.	Recovery system is not properly sized or fails to deploy all together.	Airframe breaks and becomes unusable resulting in mission failure.	1D	The vehicle will be designed to survive landing forces and the recovery system will be sized correctly and implemented such	Doing hand calculations along with computer simulations for descent velocity will provide the data required to choose materials and	1E

				that it will deploy successfully.	parachutes that are appropriate for the rocket to survive recovery	
Bulkheads fail during recovery due to shock of parachutes opening.	Bulkheads are incorrectly epoxied to the frame, and/or connection is too weak to withstand shock cord forces.	Airframe becomes projectile, endangering bystanders as well as resulting in significant damage to the airframe.	1C	The epoxy fillets will be inspected for any damage both before and after launch and threaded rods will also be utilized to distribute force.	Through stress testing and thorough inspections for epoxy cracking or galling of threaded rods, the retention system will be designed to mitigate any chance of bulkhead failure.	1E
Delamination of carbon fiber elements	Excessive heating	Airframe becomes weakened inviting increased chance of buckling	2D	Carbon fiber components will be stored away from all heating elements or open flames.	Extensive checks will be made pre-flight for any delamination that may compromise structural integrity	2E
Zippering	Recovery lines pulling through the edge of the body tube.	Serious airframe damage resulting in possible failure of mission	2D	Airframe will be constructed out of wound carbon fiber which strongly resists zippering.	Extensive checks will be made pre-flight for any zippering that may compromise structural integrity	2E
Coupler failure due to shear	In flight forces exceed shear strength of chosen coupler	Premature breakup of airframe resulting in loss of launch vehicle and potential bystander injury due to ballistic landing	1C	Couplers will be chosen that are properly sized and of strong material (ie. fiberglass) for the airframe and which will be purchased from a reputable vendor	FEA will be conducted on the couplers to determine what size and strength is necessary.	1E
Shear pins fail to break	Improperly sized black powder charges or shear pins that are too robust	Failure to eject bays and chutes will result in a ballistic landing which endangers bystanders and destroys launch vehicle	1C	A backup charge that is larger than the initial charge will be included so that if the first charge fails, the second will be able to break the shear pins	Hand calculations as well as computer generated calculations will be performed to properly size the black powder charges, with the secondary charges having a safety factor applied to ensure success	1D
Non uniform actuation of VDS blades	Discrepancy in the fabrication of VDS	Non uniform actuation can lead to non-uniform drag which will turn the rocket leading to a lower apogee at best and a ballistic threat at worst	1C	The VDS system will be designed such that all the blades will actuate uniformly	In house fabricated parts will be checked by at least three people for accuracy and extensive tests will be done before flight to make sure that the blades actuate uniformly	1E

Failure of threaded rods in tension	Rods are improperly sized	Bays could be compromised and could break apart in flight	1C	The threaded rods will be sized such that their tensile strength is enough to withstand tension forces	Calculations and tests will be performed to determine the proper size of the threaded rods	IE
Failure of threaded rods through stripping of threads	Rod thread count is insufficient or there are not enough threads engaged	Bays could be compromised and could break apart in flight	1C	The threaded rods will be sized such that their thread count is high enough to withstand forces on them	Calculations and tests will be performed to determine the proper size of the threaded rods	IE

## Navigation and Recovery (NAR) FMEA

Failure Mode	Causes	Effects	Pre RA C	Mitigation	Verification Plan	Post RA C
Unignited ejection charges ignites preassembly.	Improper handling of black powder, such as storing in a container, allowing it to be vulnerable to static, storing in heated conditions, too much vibration during travel, etc	Explosion of ejection charges and possibly engine causing possible harm to surrounding people and damage to property.	1C	Allowing only NAR certified personnel to handle the motor and black powder, abiding by the safety agreement. Storage containers must not create static and be located in facilities at relatively low temperatures	The NAR mentor will handle the purchase, sizing, storage, and installation of the motor and black powder charges. Regardless, all team members must read the MSDS of black powder.	1D
Premature separation due to drag forces	Incorrectly sized main and drogue shear pins are sheared due to larger drag forces generated by lower section of the vehicle relative to the upper section, causing separation after motor burn out.	Parachutes deployed before apogee will withstand excess forces while the rocket travels at high speed, ripping apart the body of the rocket and causing catastrophic failure.	1B	Shear pins must be placed and sized correctly for the drogue and main parachutes.	Simulations and calculations of the launch related to drag caused by fins and other such systems will be carried out in order to determine the forces the shear pins must be able to handle. Thus, the correct shear pin configuration can be ascertained. Ground and sub-scale tests will further verify this.	1C
Premature deployment due to unwanted altimeter triggering	RF signals from tracking electronics triggers altimeters.	Parachutes deployed before apogee will withstand excess forces while the rocket travels at high speed, ripping apart the body of the rocket and causing catastrophic failure.	1C	The avionics bay that houses the altimeters will be physically separated from the tracking electronics and aluminum foil shall line the inside of the avionics tube to	During ground tests, the system as a whole will be turned on in order to determine if the aluminum foil serves its purpose in blocking the RF signals that could	IE

				create a Faraday cage that will block RF signals that may trigger the altimeters.	trigger the altimeters.	
Premature separation due pressure differential	Incorrectly sized and distributed altimeter pressure portholes cause uneven pressure in the altimeter and trigger it prematurely.	Parachutes deployed before apogee will withstand excess forces while the rocket travels at high speed, ripping apart the body of the rocket and causing catastrophic failure.	1A	Pressure portholes for avionics bays will be researched for correct sizing and be spaced evenly in the avionics bay to minimize the pressure differential.	Air pressure relief holes will be checked for their size, and the subscale flight tests will be able to demonstrate if they are spaced and sized correctly.	1D
Vehicle is not tracked after certain altitude is reached.	The tracking electronics wiring comes loose due to launch vibrations, or RF signals are too weak for the ground receiver due to heavy cloud obstructions.	Vehicle cannot be found if GPS tracking fails, may drift too far, or take too long to land due to overshoot.	2C	The GPS tracking system circuit can be tied down with cable ties or other fasteners in order to prevent the wiring from coming loose.	The tracking electronics can be tested on the ground if the wiring will come loose with a mechanical shaker, which can simulate the vibrations of the rocket during flight.	2D

## Payload (PAY) FMEA

Failure Mode	Causes	Effects	Pre RA C	Mitigation	Verification Plan	Post RA C
Payload becomes loose in payload bay.	Payload mounting system does not immobilize rover during flight.	Payload is damaged, not able to exit payload bay properly due to not utilizing TEARS correctly, and can disrupt projected flight path.	2D	Payload will be mounted in x,y and z direction using geometric fit, pins, and lead screws.	Rover mounting will be tested during Full scale test flight.	2E
TEARS or the payload breaks during landing	Impact with the ground causes stress within the components of TEARS or the rover that cause them to fracture.	Rover and/or TEARS catastrophically fails and the mission cannot be completed.	1D	TEARS and the Rover will be reinforced with heavy duty mounting plates that will withstand projected impact forces.	Rover and TEARS strength and ability to withstand impact forces will be tested during full scale test flight.	1E
Wires controlling TEARS and the rover become disconnected	Forces during flight or landing cause wires to become disconnected that	TEARS or the Rover are not damaged but not able to complete the mission, due to inability to either	1C	All electronics will be soldered in place and encased in a heat shield. Electrical retention	Ability of the electronic connections to stay wired correctly will	1D

during flight or landing.	control any aspect of TEARS or the rover including but not limited to the raspberry pi, transponder, receiver, or battery connections.	receive, send, process information or become disconnected from the power supply.		tape as an extra measure will also be applied before launch.	be tested in the full scale test flight	
Driver battery becomes disconnected due to motion during launch or landing.	Battery's movement is not restricted in all planes and shifts during flight enough to disconnect from hardware.	Payload is not able to complete mission due to absence of power.	1B	The battery to power the payload and TEARS will be mounted so movement is restricted in all directions to ensure it does not shift or become disconnected during the mission.	Battery mounting will be tested during the full scale test flight.	1D
TEARS lead screw becomes bent or damaged during flight or landing.	A large impact force during landing or excess loading during flight bends the lead screw.	TEARS is unable to deploy the payload and the mission cannot be completed.	1B	A mounting block with a bushing in the nose cone shoulder will take part of the load to reduce the risk of bending.	Full scale test launch will verify the lead screw can withstand flight and landing forces without bending.	1D

### 3.4 Safety and Environment

#### Hazards to Environment

Hazards to Environment	Causes	Effects	Pre RA C	Mitigation	Verification Plan	Post RA C
Unignited ejection charges ignites preassembly.	Improper handling of black powder, such as storing in a container, allowing it to be vulnerable to static, storing in heated conditions, too much vibration during travel, etc	Explosion of ejection charges and possibly engine causing fires, damage to property, launch fields, other team's launch vehicles, etc.	1C	Only NAR certified personnel will handle the motor and black powder, abiding by the safety agreement. Storage containers must not create static and be located in facilities at relatively low temperatures.	The NAR mentor will handle the purchase, sizing, storage, and installation of the motor and black powder charges. Regardless, all team members must read the MSDS of black powder. Any repeated offenses will result in termination from the project.	1D
Unintended ejection of	Not assembling the launch vehicle	Components like brackets, fasteners, and other parts of	3A	All team members are responsible for taking precaution in	Root cause analysis is in place to avoid such disasters. If	3D

pollutants from vehicle.	appropriately; leaving components loose within the rocket body may cause them to be ejected into the environment during flight	mechanical packaging that come off during flight would become ground rubble, polluting the environment.		ensuring that no loose components are left within the rocket body. Team members will also follow comprehensive checklists pre-field and pre-flight to ensure correct assembly to avoid such cases.	root cause points to certain team members violating procedures, they will be given a warning and instructed in how to correct these actions in the future. Repeated offenses will lead to termination from the project.	
Team members leave shop/launch fields unorganized, don't clean up/take out trash/chips from mill/lathes, waste material, etc	Team members don't follow instructions to clean up after launch/ fabrication.	Leaving trash behind in fabrication shop/launch field pollutes the local environment and jeopardizes Seawolves' commitment to sustainability and a pollution-free work environment.	2B	Team members are required to follow the clean-up instructions that address these hazards.	Team members are required to sign the safety agreement. Any violations will result in a warning, and repeated offence will result in termination from the project	2D

### 3.5 Hazards from the Environment

Hazards from the Environment	Causes	Effects	Pre RA C	Mitigation	Verification Plan	Post RA C
Launch vehicle/electronics become damaged due to rain/wet ground landings	Water sensitive part of the vehicle like the airframe, motor and the electronics come in contact with water.	The payload or avionics electronics may be damaged and structural integrity of the airframe will be compromised due to epoxy, circuits, and the like being damaged due to water vulnerability.	2C	The mechanical packaging must be designed to adequately seal electronics from wet environments. In addition, epoxy must be used sparingly and in sequestered locations to reduce chance of exposure. Tests and launches will not be performed in heavy rain.	The packaging of the electronics will be tested on the ground and during launches. If such tests occur during light rain, the parts will be inspected for damage, and changes will be made to design if there are such signs.	2E
Team members are required to sign the safety	( ) is temperature sensitive and components may	A malfunctioning altimeter may jeopardize the entire	2A	All altimeters will be kept in temperature	All altimeters will be periodically tested in different	2D

agreement. Any violations will result in a warning, and repeated offence will result in termination from the project	be damaged if kept in very cold/warm temperatures for extended periods of time	recovery of the vehicle, permanently damaging the payload and the vehicle. Altimeters are expensive, and replacing damaged ones would strain the budget		controlled environments, within the range specified by the manufacturer (not deviating far from 23 degrees Celsius).	pressures and temperatures to ensure they are working. Members who are responsible for handling altimeters will be responsible to replace it if damaged.	
Premature separation due pressure differential due to high winds/gusts of wind	Incorrectly sized and distributed altimeter pressure portholes cause uneven pressure in the altimeter and trigger it prematurely.	Vehicle deploys parachutes before reaching apogee. Kevlar shock cords damage the airframe by slicing through it	1A	Port holes will be correctly distributed evenly on the altimeter bay to minimize pressure differential. No protrusion will be placed in front of the parachutes to create artificial pressure differentials	Vent holes sizing calculations is done to accurately size pressure port holes according to altimeter manuals. Full scale flight tests will further verify this	1D
Launch vehicle, parachutes, payload become damaged due to drifting too far from 2500 ft requirement.	Parachutes are not size properly leading to excessive drift beyond 2500 ft. Vehicle is launched in wind speed over 20 mph.	Launch vehicle, parachutes, payload become damaged as it comes in contact with trees, unapproved terrains outside of launch field.	2B	Parachutes are sized and simulated using multiple methods for different wind speeds up to and including 20 mph.	Full scale flight tests will further verify this	2E
High wind speeds cause inaccurate readings from altimeter(s)	High winds inhibit airflow into the avionics bay.	Altimeter cannot accurately determine pressure differences, potentially causes premature deployment.	3B	Appropriate number and size of pressure relief holes will be drilled into the airframe	Subscale and full scale flight test data will verify whether the winds have a great effect on altimeter readings.	3D

## 6 Project Plan

### 6.1 Testing

#### Airframe Testing

##### *Complete Rocket Center of Mass and Weight Testing*

This test is to ensure that the actual mass and center of gravity match up with the estimated values that had been used in calculations for stability and apogee. If there is discrepancy between the actual values and the values being used for calculations it could lead to an inaccurate apogee and or unstable flight.

Materials being tested: fully assembled rocket

Success criteria: The fully assembled rocket should not have more than 5% difference in weight and cg from the calculated values in order to maintain a reasonable apogee and stable flight.

Materials being used in test: rope, spring scale

**Procedure:**

1. Make sure all personnel working on test are wearing appropriate PPE
1. Take assembled rocket and place on level table with stands so as to make sure that it is completely horizontal
2. Mark out where the center of mass should be according to calculations on the outside of the rocket
3. Loop the rope around the body of the rocket starting on the marked center of gravity
4. Attach the spring scale to the other end of the rope and lift
5. Adjust the rope as necessary in order to find the true center of gravity
6. Make a mark on the outside of the rocket where the actual center of gravity is located
7. Write down the recorded weight of the rocket
8. measure the distance between the projected center of gravity and the actual
9. Calculate whether or not this falls within the 5% allowable difference

**Result:** Test has yet to be conducted.

*Bulkplate Security Test*

This test is conducted to see if the bulkplate retention system is strong enough to withstand the impulse of the in-flight forces produced by the motor.

Materials being tested: a mock bay made out of excess body tube material that has a bulkplate retention system that is an accurate analog to the one used in the actual rocket

Success criteria: The mock bay must be able to withstand 675lbf applied in compression to the bulkplates which simulates the forces experienced during takeoff multiplied by a safety factor of 1.5.

Materials being used in test: Hydraulic press

**Procedure:**

1. Make sure all testers are wearing appropriate PPE
2. Place mock bay on testing plane
3. Make sure all personnel are a safe distance away from the hydraulic press before turning it on
4. Begin a compression test on the mock bay, bringing the applied force up to a maximum of 675lbf
5. Once the machine is turned off, remove the mock bay and inspect it for damage (ie. cracking of epoxy or galling of threaded rods)

**Result:** Test has yet to be conducted.

*Airframe Impact Test*

In order to determine if the airframe is strong enough to withstand landing impact this test is implemented.

Materials being tested: nose cone, payload bay, avionics bay, booster bay

Success criteria: The separate bays must maintain structural integrity as well as protect all internal components after simulated impact.

**Procedure:**

1. All involved personnel will wear necessary PPE
1. The separate bays will be brought up to a height above ground level that will simulate kinetic energy at touchdown during a regular flight
2. The landing area will be cleared of personnel as well as any obstructions and will be comprised of loosely packed earth to simulate actual field drop zone

3. From there the bays will be systematically oriented as they would be during descent and dropped

4. After each bay is dropped it will be retrieved and inspected for damage

Results: Test has yet to be conducted.

#### *Fullscale Avionics Ground Ejection Test*

Ensure the drogue and main deployment mechanism works: including the parachutes, shock cords, pistons, e-matches, etc. Check if the shear pins break due to the overpressurization and the pistons pushing against the bulkplates. Ensure the sections separate while not damaging any of the fittings, pistons, bulkplates, shock cords, or parachutes.

Materials Tested: Deployment Mechanism

Success Criteria: The rocket deploys the parachutes and separates into three sections while doing no damage to the components in the process.

Procedure: This procedure is very similar to a true launch procedure.

1. The launch vehicle will be loaded with the avionics equipment.
2. The assembly will be placed on a launch pad testing rig.
3. The drogue ejection charge will be connected to an external battery connected to a manual arming switch.
4. The switch will then be moved into the ON position, which would then activate the drogue charge.
5. The switch will be turned off.
6. Repeat steps 3-5 for the main charge.

Results: Test has yet to be conducted.

#### *Electronics Endurance Test*

Ensure all the electronics from the Navigation and Recovery, Payload and Propulsion teams can endure and withstand being on the launch pad for at least sixty minutes without losing any functionality.

Materials Tested: The functionality of the electronics after being on the launch pad for a full hour.

Success Criteria: Electronics will not lose any degree of functionality after integrated vehicle is mounted on the launch pad

Procedure:

1. The fully integrated vehicle must be mounted on the launch pad and all of the avionics from the different subsystem teams must be turned on.
2. After a sixty-minute period, the electronic functions will be terminated by the each of their respective sub team and tested for functionality.
3. Any system that fails the test is required to have its respective subsystem team make any and all necessary design changes in order for the test to be passed in the future.

Results: Test has yet to be performed.

#### *GPS Transmitter Location Test*

Ensure the transmitter works as intended and parameters are set correctly. The transmitter should work out to a range of at least one mile and be able to read coordinates of a moving target.

#### Materials Tested: GPS Transmitter/Receiver

Success Criteria: The GPS receiver reads out the coordinates of the transmitter for the duration and then guides the user of the receiver to the transmitter.

Procedure:

1. Equip one individual with the GPS transmitter and the other with the receiver.
2. Turn the transmitter and receiver on and wait until GPS lock has been achieved.
3. Ensure the coordinates of the GPS transmitter are correct by using a location program on a cell phone, such as MotionX.
4. Move the transmitter 1-6 miles away from the receiver and obstruct line of sight so GPS coordinates are required for locating the transmitter. Simulate the transmitter being inside the nosecone of the rocket by covering it.
5. Use the coordinates displayed on the receiver to find the transmitter by plugging the coordinates into a location program like MotionX.

Results: Test has yet to be conducted.

#### Demonstrations

##### *Full Scale Flight*

A full-scale flight is required by section 2.18.1 of the handbook which will be performed using the final design of the launch vehicle complete with payload.

Success criteria:

1. Recovery system operates properly as designed allowing the rocket to fall without incurring damage
2. Flight data is recorded using onboard altimeters and gps
3. The rocket is fully ballasted

Results: Demonstration has yet to be completed

##### *Payload Demonstration Flight*

A demonstration of the payload designed to fly in the launch vehicle is required by handbook section 2.18.2 and so will be performed prior to the deadline.

Success criteria:

1. Flight is smooth with all recovery systems functioning properly
2. Payload is retained until ready to be deployed
3. Payload is retained properly and functions as designed

Procedure: follow flight and payload operation checklist

Results: Demonstration has yet to be completed.

## 6.2 Requirement Compliance

Item ID	Verification Method	Verification Plan
<b>General Requirements</b>		
1.1	Inspection	Stony Brook University Rocket team consist exclusively of

		students who are working on this project as part of their senior design. All work will be completed by students with the exception of motor assembly and handling of black powder ejection charges.
1.2	Demonstration	The project plan is constantly being updated and discussed during team bi-weekly meetings to ensure that all project milestones, personal assignments, events and checklists are followed.
1.3	Inspection	Every team member will be asked about their citizenship status and a list of foreign nationals is to be submitted to NASA by PDR.
1.4	Inspection	A list of all team members and adult educators attending launch week activities is going to be submitted to NASA by CDR.
1.5	Demonstration	Every educational outreach event will be documented following STEM Engagement Activity Report template provided by NASA.
1.6	Demonstration	Social media accounts will be established and links will be delivered to NASA by October 25 <sup>th</sup> .
1.7	Inspection	Team lead will send all the deliverables to the NASA team by the deadline and verify it with confirmation email from NASA project management team.
1.8	Inspection	All deliverables will be converted to PDF format before submission to NASA.
1.9	Inspection	Every report will have table of contents including major sections and their respective sub-sections.

1.10	Inspection	Every report will have page numbers at the bottom of each page.
1.11	Demonstration	All equipment to have successful video teleconference will be demonstrated during Kickoff video session.
1.12	Demonstration	The launch vehicle will utilize launch pads provided by Student Launch's launch services provider.
1.13	Inspection	The team has identified a mentor who meets all the requirements in the Proposal.
<b>Vehicle Requirements</b>		
2.1	Demonstration Testing Analysis	The launch vehicle will reach the target altitude by careful selection of motor, control of vehicle's mass, and overall shape of the rocket. The vehicle will be analyzed using OpenRocket simulations and tested during Vehicle Demonstration Flight.
2.2	Analysis	The target altitude will be identified based on the collected data from simulations and launch vehicle design.
2.3	Demonstration	One commercially available altimeter will be set aside for recording official altitude purposes
2.4	Demonstration Test	The launch vehicle will be designed to ensure it can be reused and launched on the same day.
2.5	Demonstration	The launch vehicle will have 3 independent sections.
2.5.1	Demonstration	Coupler/airframe shoulders will be 6 inches in length.
2.5.2	Demonstration	The nosecone shoulder will be 6 inches in length.
2.6	Demonstration Testing	The launch vehicle will be designed to ensure that it can be assembled in under 2 hours. The assembly time will be

		timed during Vehicle Demonstration Flight.
2.7	Demonstration Testing	Appropriate battery and the overall launch vehicle design is going to be chosen to remain in launch-ready configuration for at least 2 hours.
2.8	Demonstration	Standard 12-volt DC firing system is going to be utilized.
2.9	Demonstration	All electronics will be housed internally and only launch services provider equipment will be used to initiate launch.
2.10	Inspection	The motor certified by NAR and TRA will be used.
2.10.1	Inspection	The final motor selection is going to be declared by CDR.
2.10.2	Inspection	Any motor changes after CDR will be approved by NASA Range Safety Officer.
2.11	Demonstration	Launch vehicle motor will be a single stage motor.
2.12	Inspection	The motor will be L-class or lower.
2.13	Inspection	The launch vehicle will have no pressure vessels.
2.14	Analysis	The launch vehicle will be analyzed with OpenRocket software to ensure that the static stability margin is at least 2.0.
2.15	Inspection	Any protuberance will be located aft of the burnout CG.
2.16	Analysis	OpenRocket software will be used to determine exit velocity.
2.17	Demonstration	Subscale model launches have been scheduled to take place before December 1 <sup>st</sup> .
2.17.1	Demonstration	Subscale model will be an exact scaled down shape of the launch vehicle with the same corresponding CG and CP.
2.17.2	Demonstration	Subscale model will be equipped with altimeter.
2.17.3	Demonstration	Subscale model will be a newly built vehicle.

2.17.4	Demonstration	Subscale model launch will be documented and flysheet information will be included in CDR report.
2.18.1	Demonstration	Vehicle Demonstration Flight will be performed to ensure that all the full-scale vehicle criteria are met.
2.18.2	Demonstration	Payload will be launched and recovered in the full-scale launch vehicle to ensure that all payload criteria are met.
2.19	Demonstration	FRR Addendum will be submitted if NASA-required Vehicle Demonstration Re-flight will take place after the FRR deadline.
2.20	Demonstration	Team contact information will be written on the rocket airframe.
2.21	Demonstration	All Lithium Polymer batteries will be enclosed in protective cases and brightly colored.
2.22	Demonstration	The launch vehicles will not utilize prohibited techniques outlined by NASA in section 2.22.
<b>Recovery System Requirements</b>		
3.1	Demonstration Testing	The launch vehicle will deploy its drogue parachute at apogee and the main parachute will be deployed later at the set altitude.
3.1.1	Demonstration Testing	The main parachute deployment altitude will be above 500 feet.
3.1.2	Demonstration Testing	The drogue parachute will be deployed within 2 seconds of reaching apogee.
3.1.3	Inspection	Motor will not be ejected.
3.2	Testing	Ground ejection tests will take place before subscale and full-scale launches.
3.3	Demonstration	Parachutes will be chosen to ensure that each independent section of the launch vehicle

		will have kinetic energy at landing under 75 ft-lbf.
3.4	Inspection	The launch vehicle will have a redundant altimeter.
3.5	Inspection	Each altimeter will have an independent power supply.
3.6	Inspection	Each altimeter will be armed with a dedicated mechanical switch accessible from the exterior of the rocket airframe.
3.7	Inspection	Each arming switch have a locking mechanism.
3.8	Inspection	Recovery and payload bay will be independent sections and have a separate electrical circuits.
3.9	Inspection	Removable shear pins will be used for all parachutes.
3.10	Testing Analysis	Delayed main parachute deployment will limit the drift of the launch vehicle to 2,500 ft radius.
3.11	Testing Analysis	Descent time will be timed during full-scale test flights and estimated in MATLAB.
3.12	Inspection	Tracking device will be attached to the vehicle.
3.12.1	Inspection	Payload will be attached with a tracking device.
3.12.2	Inspection	All tracking devices will be inspected before the official flight.
3.13	Inspection Testing	All recovery system electronics will be properly shielded. Recovery system altimeter will be located in a separate compartment.
<b>Payload Experiment Requirements</b>		
4.1	N/A	N/A
4.2	Demonstration	Payload will be designed that is capable being launched in a high power rocket, landing safely, and recovering simulated lunar ice from one of

		several locations on the surface of the launch field.
4.3.1	Inspection	All hardware will be housed inside the launch vehicle airframe.
4.3.2	Demonstration	The rover will recover sample material from one of the five recovery areas.
4.3.3	Demonstration	The recovered ice sample will be at least 10 milliliters.
4.3.4	Demonstration	The rover will safely store and transport recovered material 10 feet away from the recovery area.
4.3.5	Inspection	Team will abide by all FAA and NAR rules and regulations.
4.3.6	Inspection	Payload will utilize no black power or other energetics.
4.3.7	Inspection Testing	Payload will be securely attached to the launch vehicle until deployment. No excessive shear pins will be used in payload deployment mechanism.
4.4	N/A	N/A
<b>Safety Requirements</b>		
5.1	Inspection	Safety checklist will be generated by our team's safety officer and will be included in the FRR report. This checklist will be used during the LRR and any other launch day operations.
5.2	Inspection	Our team safety officer is Jonathan Sossover. Donald Stickevers is deputy safety officer.
5.3.1	Inspection	The safety officer will monitor all team activities with an emphasis on safety.
5.3.2	Demonstration	Safety officer will implement procedures and checklists to be used during construction, assembly, launch and recovery.
5.3.3	Demonstration	Safety office will keep detailed records of team's hazard

		analyses, failure modes analyses, procedures, and MSDS/chemical inventory data.
5.3.4	Demonstration	Safety office will assist in the writing and development of the team's hazard analyses, failure modes analyses, and procedures.
5.4	Demonstration	Team will abide by all the rules and regulations of the local rocketry club RSO.
5.5	Inspection	Team will abide by all rules set forth by the FAA.

### 6.2.1 Vehicle Derived Requirements

Description	Verification Method	Verification Plan
Vehicle must be able to utilize VDS system independent of ground control.	Analysis Testing	The VDS system will be designed and coded to be able to actuate on its own and will be tested to ensure this function
VDS system must be a closed loop that can actively make adjustments to drag based off of data gathered in flight.	Testing	The system will be coded such that it can actively stabilize the rocket. Testing will be done to fine tune this system and ensure that it works for the actual flight
VDS system must allow for uniform actuation of blades.	Analysis	A VDS system will be designed such that all of the blades are actuated at the same time from the same central actuating disk to ensure uniform actuation

### 6.2.2 Navigation and Recovery Derived Requirements

Description	Verification Method	Verification Plan
The telemetry bay will not interfere with payload deployment.	Inspection	The Recovery team will work closely with the Payload team in order to ensure their designs work in conjunction with one another.
The electronic tracking equipment will not have its	Inspection Testing	The telemetry bay will not be surrounded in metal or be housed in a section of airframe

signals blocked by sections of the rocket.		or nosecone that is made of carbon fiber or is painted with metallic paint, which would block RF signals of the GPS transmitter. Ground tests and test flights will also verify the transmission of RF signals to the ground receiver.
The electronic tracking equipment will send data to a ground receiver, which will not receive interference from other electronics tracking equipment on other rockets.	Inspection Testing	The tracking system will be connected or coded in such a way that the receiver in use by the SBU team only receives data from the proper GPS tracking device.
The parachutes will not only be deployed by the expansion of hot gases alone but will be assisted by a mechanical ejection mechanism as well.	Inspection Testing	Parachute deployment will be assisted by pistons that will push the parachutes out of their respective bays. Ground testing and flight tests will ensure the system works.
The parachutes will not be adversely affected by hot ejection gases.	Inspection	The parachutes will be protected by an object or device as nylon parachutes are susceptible to burning or melting.

### 6.3 Budget

The component wise cost of each subsystem is shown in the table below. The travel costs were estimated based on lodging and car rental prices found online.

Structures						
Part Name	Vendor	Part Number	Quantity	Unit Price	Total Price	
Motor Retainer	Madcow	RA75	1	\$48.75	\$48.75	
RocketPoxy	Madcow	G5000-RP-PNT	1	\$26.24	\$26.24	
Tube Coupler	Madcow	FC60-120-BLA	2	\$45.00	\$90.00	
Centering Ring	Madcow	FCR6075	3	\$7.50	\$22.50	
Nose Cone	Madcow	FWNC60	1	\$112.46	\$112.46	
Bulkplate	Madcow	FCB60-BLK	8	\$6.75	\$54.00	
Rail Buttons	Madcow	RB-PACK-1515	1	\$5.96	\$5.96	
Motor Tube	Madcow	FT30-STD-220-NAT	1	\$27.75	\$27.75	
Airframe Tubing	DragonPlate	FDPBT-DIA*6x48	2	\$302.25	\$604.50	
Total Shipping						\$355.82

Total	\$1,347.98
-------	------------

VDS Components				
Part Name	Unit Mass	Quantity	Unit Price	Price Subtotal
Blades	0.076	3		
Rails	0.032	3	26	78
Carriage	0.035	3	67.3	201.9
Baseplate	0.25	1		
Motor	0.14	1	65	65
808 cam	0.0625	2		
Camera Battery	0.035	2	7.89	15.78
3D housing	0.24	1		
Plates	0.25	2		
Links	0.004	3		
VDS Battery	0.05	1	11.28	11.28
Teensy	0.02	1	19.95	
Teensy Battery	0.02	1	6.49	6.49
Actuating plate	0.06	1		
Barometric Pressure Sensor	0.01	1	9.95	9.95
Radial Bearing	0.025	1	11	11
Thrust Bearing	0.02	2	10	20
threaded rods	0.06	3	3.7	11.1
U-bolt	0.12	1	1.56	1.56
Nuts & Bolts	0.05	1		
More nuts + bolts	0.1	1		
Shaft	0.02	1		
Misc Electronics	0.05	1		
9DoF Sensor	0.02	1	15.95	15.95
Motor Securing Plate	0.1	1		
Fiberglass Outer ring (bulkhead)	0.069	1		
<b>Total</b>				<b>448.01</b>

Recovery and Navigation				
Part Name	Description	Unit Cost	Quantity	Cost
StratologgerCF Altimeter (2 needed)	Altimeters	\$ -	2	\$ -
U-Bolt with Mount Plate, Zinc-Plated Steel	1/4"-20 Thread Size, 1" ID	\$ 0.78	2	\$ 1.56
BRB900 GPS Transmitter	GPS Transmitter with LIPO	\$ 393.00	1	\$ 393.00
Iris Ultra 96" Standard Parachute - 50lbs @ 20fps	Main Parachute	\$ 348.15	1	\$ 348.15
24" Elliptical Parachute - 2.2lb @ 20fps	Drogue Parachute	\$ 64.00	1	\$ 64.00

Steel Thin Nylon-Insert Locknut Grade 8		\$ 8.79	1	\$ 8.79
High-Strength Steel Threaded Rod	1/4"-20 6" Long	\$ 6.17	2	\$ 12.34
ACDelco 9 Volt Batteries		\$ -	2	\$ -
2 gram Black Powder Charge Wells, PVC		\$ 3.28	2	\$ 6.56
Blue Tube Coupler	Coupler/Avionic Bay Tube	\$ 21.35	1	\$ 21.35
21" Nomex Blanket - 6" Airframe		\$ 27.00	2	\$ -
Nylon Shear Pins	20 pack	\$ 5.56	1	\$ 5.56
USB data transfer kit		\$ 24.95	1	\$ 24.95
Altimeter Mounting hardware		\$ 3.83	3	\$ 11.49
30' x 7/16" Kevlar 2 Loop Shock Cord		\$ 46.00	1	\$ 46.00
20' x 7/16" Kevlar 3 Loop Shock Cord		\$ 54.00	1	\$ 54.00
Electronics Rotary Switch		\$ 10.33	1	\$ 10.33
8" 120LB BLACK CABLE TIES		\$ 8.96	1	\$ 8.96
Dual Altimeter Wiring Kit		\$ 25.50	2	\$ 51.00
FIREWIRE MINI INITIATOR		-	2	-
Aluminum Split Lock Washer	For Number 8 Screw Size	\$ 3.82	1	\$ 3.82
Aluminum Hex Nut	8-32 Thread Size	\$ 4.44	1	\$ 4.44
Aluminum Threaded Rod	8-32 Thread Size	\$ 15.20	1	\$ 15.20
4-40 Tap and Drill Set		\$ 7.70	1	\$ 7.70
18-8 Stainless Steel Washer	For 1/4" Screw Size	\$ 3.37	1	\$ 3.37
Quicklink, Zinc-Plated Steel		\$ 1.89	2	\$ 3.78
<b>Total Components Cost</b>				<b>\$ 1,106.35</b>

Rover				
Part Name	Description	Unit Cost	Quantity	Cost
9V Batteries	Used for Arduino Nano	\$ 10.99	1	\$ 10.99
11.1 V 2200 mAH LIPO battery	For rover motors and DICU	\$ 17.99	3	\$ 53.97
98 RPM Gear Motor	Rover drivetrain motor	\$ 14.99	2	\$ 29.98
Drive Motor Mounting Screws (M3 x 0.5mm)	Mounting Motor	\$ 3.20	1	\$ 3.20
Drive Motor Set Screw Shaft Collar	Motor Shaft Collar	\$ 2.11	2	\$ 4.22
NEMA 8 Stepper Motor	Sample Collection motor	\$ 17.95	1	\$ 17.95
Stepper Motor mounting screw	Fastener	\$ 5.17	1	\$ 5.17
Pitsco Tank Tread Kit	Tread Assembly for Rover	\$ 99.95	1	\$ 99.95
Bogey Sprocket Wheels Flanged Bearing	Drive assembly for Rover	\$ 2.89	2	\$ 5.78
Sample Collection Unit side wall mounts	Mount for SCU walls attachment	\$ 5.90	1	\$ 5.90
Arduino Nano	Microcontroller for Rover	\$ 6.78	1	\$ 6.78
Raspberry Pi 3 B	For DICU control	\$ 48.99	1	\$ 48.99
Xbee Module	Rover and DICU data transmission	\$ 26.95	2	\$ 53.90
Xbee Adapter	For Xbee Module	\$ 13.99	2	\$ 27.98

FeatherWing Motor Controller	Rover and scoop motor control	\$ 22.05	1	\$ 22.05
7 inch Touchscreen Monitor	For DICU display	\$ 49.99	1	\$ 49.99
Carbon Fiber Sheet	For Rover Chassis	\$ 25.00	1	\$ 25.00
<b>Total</b>				<b>\$ 471.80</b>

### TEARS

Part Name	Description	Unit Cost	Quantity	Cost
98 ft Remote Control Kit	Receiver on TEARS	\$ 16.69	1	\$ 16.69
124 RPM Gear Motor	Lead Screw Motor	\$ 14.99	1	\$ 14.99
NEMA 17 Stepper Motor	Reorientation Motor	\$ 11.37	1	\$ 11.37
NEMA 17 Shaft Coupler (625050)	Stepper Motor Coupler	\$ 4.99	1	\$ 1.00
A4988 Stepper	Stepper Motor Driver	\$ 7.49	1	\$ 7.49
NEMA 17 Screw	Stepper Motor Fastener	\$ 3.20	1	\$ 3.20
8 mm Lead Screw (37.4")	For Exiting	\$ 20.99	1	\$ 20.99
Aluminum Sheet	For plates, and mounts	\$ 27.95	2	\$ 55.90
Lead Screw Clamping Collar	Fastener and Screws for TEARS	\$ 4.99	2	\$ 9.98
Lead Screw Clamping Collar Screw: M3 ( x 0.5 mm) 10 mm length	Fastener and Screws for TEARS	\$ 5.56	1	\$ 5.56
Lead Screw Thrust bearings (6655K15)	Exiting system bearing	\$ 4.63	3	\$ 13.89
Lead Screw Ball Bearing	Exiting system bearing	\$ 3.49	3	\$ 10.47
1/2 " - 12 mm Hole Reducer	For LS ball bearing	\$ 2.49	1	\$ 2.49
6-32 Thread 1/4" Round Aluminum Standoffs (633128)	Fastener TEARS	\$ 2.09	1	\$ 2.09
LS Aluminum Spacer 1" (633170)	Fastener TEARS	\$ 1.89	1	\$ 1.89
Aluminum Standoff Screw (98164A443)	Fastener TEARS	\$ 6.40	1	\$ 6.40
Aluminum Pattern Bracket	Strengthening LS assembly	\$ 1.49	1	\$ 1.49
Barrell Clamping Hub (Clamping to hub gear)	Fastener and Screws for TEARS	\$ 6.99	1	\$ 6.99
Clamping Hub Collar Screw (6-32 x 0.375" socket head)	Fastener and Screws for TEARS	\$ 1.99	1	\$ 1.99
Clamping hub and hub gear screw (6-32 x 5/16" socket head)	Fastener and Screws for TEARS	\$ 1.99	1	\$ 1.99
Lead Screw hub gear (64 teeth, 2 inch pitch diameter)	Exiting Mechanism Gear	\$ 12.99	1	\$ 12.99
Lead Screw pinion gear (4mm bore, 16 teeth, 0.5 inch pitch diameter)	Exiting Mechanism Gear	\$ 7.99	1	\$ 7.99
Lead Screw Nut (8mm 4 start)	For Exiting	\$ 7.99	2	\$ 15.98
Lead Screw Nut fastening screw (6 - 32 7/16" socket head)	Fastener and Screws for TEARS	\$ 1.99	1	\$ 1.99
25 mm Face Tapped Clamping Hub (LS motor)	Fastener and Screws for TEARS	\$ 6.99	1	\$ 6.99
25 mm Clamping Hub collar screw(6-32 x 0.5" socket head screw)	Fastener and Screws for TEARS	\$ 1.99	1	\$ 1.99
25mm Clamping Hub mounting screw (6-32 x 9/16" socket head)	Fastener and Screws for TEARS	\$ 1.99	1	\$ 1.99
Round Aluminum Stock 12" Long	Connecting Rod Assembly	\$ 11.06	1	\$ 11.06
Reorientation Fixed Gear (84 teeth, 2.625 inch pitch diameter)	Reorientation Mechanism Gear	\$ 12.99	1	\$ 12.99
Reorientation Pinion Gear (32 teeth, 1 inch pitch diameter)	Reorientation Mechanism Gear	\$ 7.99	1	\$ 7.99
Pinion Gear Set Screw	Reorientation Mechanism Gear	\$ 10.50	1	\$ 10.50

Needle Roller Thrust Bearing for 7/8" shaft diameter (1 - 11/16" OD)	Reorientation System Bearings	\$ 4.66	2	\$ 9.32
0.032" Thick Washer for 7/8" Shaft Diameter Needle-Roller Thrust Bearing	Washer for bearings	\$ 2.48	2	\$ 4.96
Ball bearing for 1/2" shaft diameter	Reorientation system bearings	\$ 6.27	2	\$ 12.54
Threaded Shaft Collar for 1/2"-13	Fastener and Screws for TEARS	\$ 11.96	1	\$ 11.96
Threaded Shaft Collar Screw (8-32 x 1/2" socket head cap screw)	Fastener and Screws for TEARS	\$ 6.88	1	\$ 6.88
Aluminum L bracket stock (1 ft length)	Fastener for base of TEARS	\$ 2.53	1	\$ 2.53
<b>Total</b>				<b>\$ 337.51</b>

Miscellaneous				
Part Name	Description	Unit Cost	Quantity	Cost
Transistor Set		\$ 8.98	1	\$ 8.98
Limit Switches		\$ 7.39	1	\$ 7.39
DPDT Relay Switches		\$ 1.75	5	\$ 8.75
Diode Set		\$ 7.99	1	\$ 7.99
12 V Step up Voltage Regulator		\$ 13.95	1	\$ 13.95
Solder Sucker		\$ 9.89	1	\$ 9.89
PCB Prototype Boards		\$ 11.99	1	\$ 11.99
<b>Total</b>				<b>\$ 68.94</b>
<b>Total Cost of Payload</b>				<b>\$ 878.25</b>

Team Expenses	
Expense	Amount
Structures	\$1347.98
VDS	\$448.01
Navigation and Recovery	\$1106.35
Payload	\$878.25
L1420RP Motors	\$1,356.63
<b>Total</b>	<b>\$5137.22</b>

Travel Expenses	
Expense	Amount
Vehicle demonstration car rental	\$125.00
Payload demonstration car rental	\$125.00
Competition travel car rental	\$625.00
Competition lodging costs	\$450.00
<b>Total</b>	<b>\$1325.00</b>

Team Expenses	
Expense	Amount
Team component cost	\$5137.22
Travel Expenses	\$1325.00
<b>Total</b>	<b>\$6462.22</b>

## 6.4 Funding

To successfully complete the project, the team will require \$6462.22 as outlined by the proposed team budget. The funding sources for the project are outlined below for the team to meet the required budget.

### Stony Brook Engineering Department

The College of Engineering and Applied Sciences (CEAS) at Stony Brook University has allocated \$280 per student for senior design projects. The team has 13 members, all of which have access to CEAS senior design funding. This leads to a total of \$3640 for the team. The team expects to receive \$1500 in funding from sponsorship obtained through CEAS as well.

### AIAA Fundraisers

The Stony Brook University team will perform fundraisers with the AIAA club on campus to raise funds for the project. The outline fundraising events and dates are shown in Table below

Fundraising Event	Event Date	Anticipated Amount
Krispy Kreme Fundraiser	1/29/20	\$ 400.00
Bake Sale	2/5/20	\$ 200.00
Krispy Kreme Fundraiser	2/19/20	\$ 400.00
<b>Total</b>		<b>\$1000.00</b>

### Online Crowdfunding Campaign

The team will host a crowdfunding campaign on Go Fund Me with collaboration from the AIAA club. This crowdfunding campaign will run from February to March. The team expects to raise \$500 from the fundraising.

### Team Donations

The team received \$500 in donation from an stony brook university alumni.

The total funding for the team is shown in Table below

Funding Source	Amount
CEAS Senior Design	\$ 3640
CEAS sponsorship	\$ 500
<b>AIAA Fundraisers</b>	<b>\$ 1500.00</b>

Go Fund Me crowdfunding	\$ 500.00
Team Donations	\$ 500.00
<b>Total</b>	<b>\$6540.00</b>

The teams proposed budget is \$6462.22 and the expecting total funding is \$6540.00. Based on the current funding plan the team will have \$77.34 over the proposed budget.

## 6.5 Timeline

Our team has divided the project into five main phases. In the first proposal phase our team will focus on idea generation and determining team structure. PDR phase mainly consist of creating a design that meets all the general, vehicle, and payload requirements of the competition. CDR phase ensures that the previously created design is ready to fabricate. If it is not ready, necessary changes to the design are made to meet fabrication criterion. FRR phase tests vehicle and payload readiness for the competition. And finally, the Launch Phase mainly consist of Student Launch competition week and post launch assessment review. A detailed project timeline is shown in the following figure.

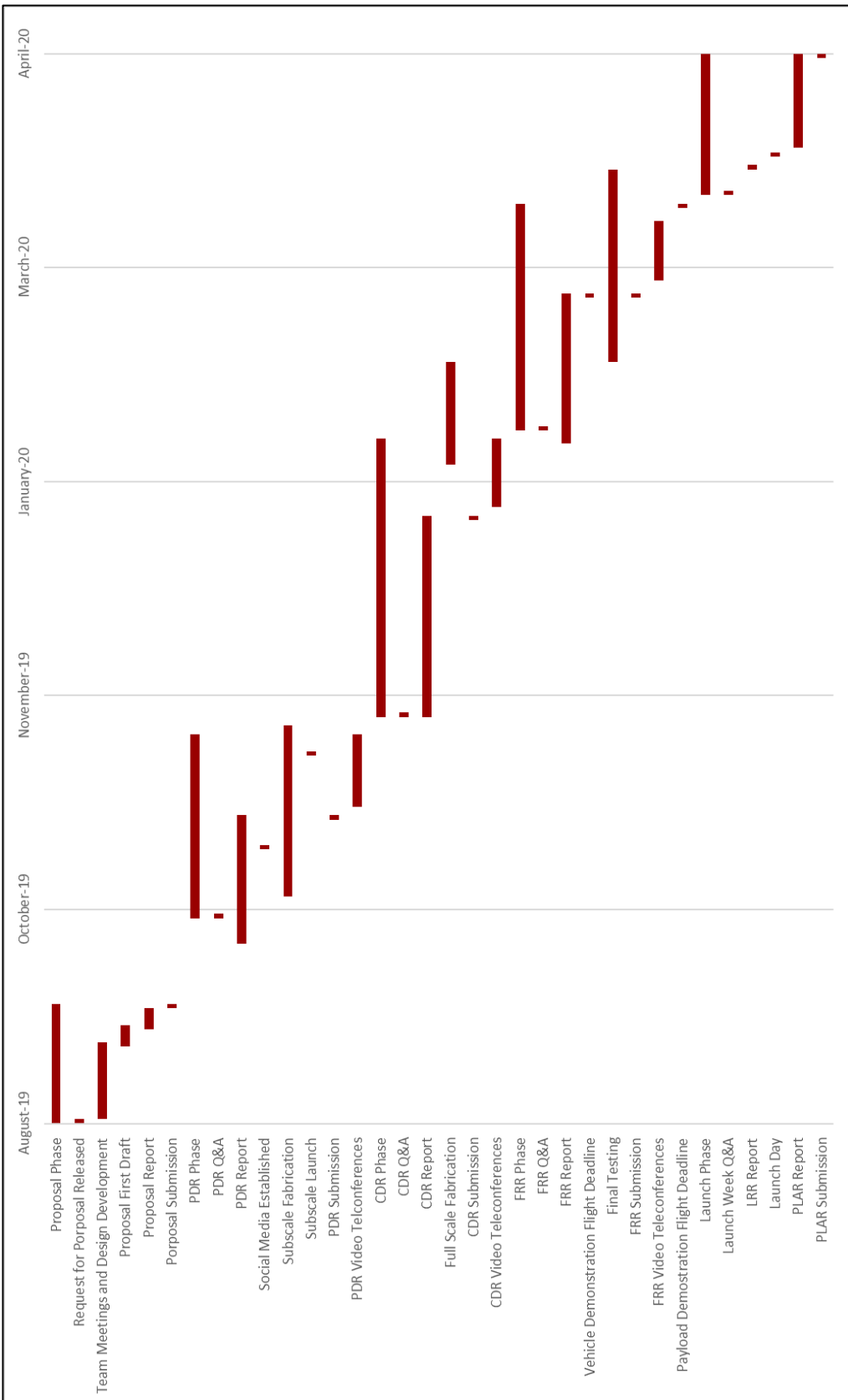


Figure 6.1: Project Gantt Chart